JÚLIO CEZAR MÁRIO CHAUL

TAXONOMIA DE BESOUROS PSELAPHINAE (COLEOPTERA: STAPHYLINIDAE): DESCRIÇÕES DE NOVAS ESPÉCIES E POSICIONAMENTO FILOGENÉTICO DA FAUNA CRETÁCICA EM RELAÇÃO À MODERNA

VIÇOSA - MINAS GERAIS

2024

JÚLIO CEZAR MÁRIO CHAUL

TAXONOMIA DE BESOUROS PSELAPHINAE (COLEOPTERA: STAPHYLINIDAE): DESCRIÇÕES DE NOVAS ESPÉCIES E POSICIONAMENTO FILOGENÉTICO DA FAUNA CRETÁCICA EM RELAÇÃO À MODERNA

Tese apresentada à Universidade Federal de Viçosa, como parte das exigências do Programa de Pós-Graduação em Ecologia, para obtenção do título de *Doctor Scientiae*.

Orientador: Cristiano Lopes Andrade

VIÇOSA - MINAS GERAIS

2024

Ficha catalográfica elaborada pela Biblioteca Central da Universidade Federal de Viçosa - Campus Viçosa

T
C497t
2024

Chaul, Júlio Cézar Mário, 1989-
Taxonomia de besouros Pselaphinae (Coleoptera: Staphylinidae): descrições de novas espécies e posicionamento filogenético da fauna cretácica em relação à moderna / Júlio Cézar Mário Chaul. – Viçosa, MG, 2024.
1 tese eletrônica (175 f.): il. (algumas color.).

Texto em português e inglês.
Inclui apêndice.
Orientador: Cristiano Lopes Andrade.
Tese (doutorado) - Universidade Federal de Viçosa, Departamento de Biologia Geral, 2024.
Inclui bibliografia.
DOI: https://doi.org/10.47328/ufvbbt.2024.316
Modo de acesso: World Wide Web.

1. Besouros - Classificação. 2. Paleontologia - Cretáceo. 3. Biodiversidade. 4. Serapilheira. 5. Insetos florestais. 6. Análise clástica. I. Andrade, Cristiano Lopes, 1980-. II. Universidade Federal de Viçosa. Departamento de Biologia Geral. Programa de Pós-Graduação em Ecologia. III. Título.

CDD 22. ed. 595.7642

Bibliotecário(a) responsável: Alice Regina Pinto Pires CRB-6/2523

JÚLIO CEZAR MÁRIO CHAUL

TAXONOMIA DE BESOUROS PSELAPHINAE (COLEOPTERA: STAPHYLINIDAE): DESCRIÇÕES DE NOVAS ESPÉCIES E POSICIONAMENTO FILOGENÉTICO DA FAUNA CRETÁCICA EM RELAÇÃO À MODERNA

Tese apresentada à Universidade Federal de Viçosa, como parte das exigências do Programa de Pós-Graduação em Ecologia, para obtenção do título de *Doctor Scientiae*.

APROVADO: 23 de fevereiro de 2024

Documento assinado digitalmente
gov.br
JULIO CEZAR MARIO CHAUL
Data: 31/07/2024 10:38:16-0300
Verifique em https://validar.iti.gov.br

Júlio Cezar Mário Chaul
Autor

Documento assinado digitalmente
gov.br
CRISTIANO LOPES ANDRADE
Data: 31/07/2024 11:28:03-0300
Verifique em https://validar.iti.gov.br

Cristiano Lopes Andrade
Orientador

DEDICATÓRIA

A todos os meus professores, formais e informais, que fizeram possível este trabalho.

AGRADECIMENTOS

O presente trabalho foi realizado com apoio da Coordenação de Aperfeiçoamento de Pessoal de Nível Superior – Brasil (CAPES) - Código de Financiamento 001. As agências de fomento Conselho Nacional de Desenvolvimento Científico e Tecnológico (CNPq) e Fundação de Amparo à Pesquisa do Estado de Minas Gerais (FAPEMIG) também financiaram partes do projeto e na formação acadêmica do autor.

RESUMO

CHAUL, Júlio Cezar Mário, D.Sc. Universidade Federal de Viçosa, fevereiro de 2024. **Taxonomia de besouros Pselaphinae (Coleoptera: Staphylinidae): descrições de novas espécies e posicionamento filogenético da fauna cretácica em relação à moderna**. Orientador: Cristiano Lopes Andrade.

Recentemente, as descrições de várias espécies de artrópodes provenientes do âmbar de Kachin, Myanmar, um sítio do Cretáceo (Cenomaniano inferior, 98.79 ± 0.62 milhões de anos), têm modificado significativamente a compreensão da história evolutiva destes táxons. Apesar de existirem muitos outros sítios fossilíferos do Cretáceo, nenhum se compara ao de Kachin em termos de diversidade e da qualidade das preservações. Pselaphinae, uma das mais diversas subfamílias de Staphylinidae, com mais de dez mil espécies descritas, apenas começou a ter sua fauna cretácica descrita na década passada. Uma pequena parte destes fósseis são provenientes de âmbar Espanhol (Albiano) e a maior parte é de âmbar de Kachin. Esta tese tem como foco os besouros pselafíneos cretácicos, com ênfase para os fósseis de Kachin. No capítulo I, a fauna de pselafíneos cretácicos é completamente revisada em uma sinopse, quatro espécies fósseis são descritas, uma delas em um novo gênero, ferramentas de identificação das espécies foram produzidas e um adendo à filogenia vigente foi feito através da inclusão das novas espécies. Nos capítulos II e III, espécies viventes são descritas; suas descrições serviram como base para estudar caracteres importantes que foram utilizados no quarto capítulo, compondo um banco de dados morfológicos. O capítulo IV, o último da tese, apresenta uma nova proposta filogenética resultante de um robusto banco de dados morfológicos gerado a partir do estudo de dezenas de espécies fósseis e centenas de espécies viventes. Novas relações de parentesco entre os pselafíneos cretácicos e os viventes são propostas, com destaque para uma maior proximidade filogenética da maior parte das espécies cretácicas entre si do que que previamente era suposto. Espera-se que as descrições e hipóteses filogenéticas desta tese impulsionem novos estudos em Taxonomia e Sistemática desta expressiva subfamília.

Palavras-chave: Cretáceo; besouros estafilinídeos; diversidade; fauna de serapilheira

ABSTRACT

CHAUL, Júlio Cezar Mário, D.Sc. Universidade Federal de Viçosa, February 2024. **Taxonomy of Pselaphinae beetles (Coleoptera: Staphylinidae): descriptions of new species and phylogenectic placement of the Cretaceous fauna in relation to the modern taxa.** Advisor: Cristiano Lopes Andrade.

The recent descriptions of hundreds of fossil species of arthropods included in amber from Kachin, Myanmar, a Cretaceous site (Lower Cenomanian, 98.79 ± 0.62 million years of age), have significantly modified the understanding of the evolutionary history of these taxa. Although there are many other Cretaceous fossil sites, none stands to Kachin in terms of the diversity and quality of the preservations. Pselaphinae, one of the most diverse Staphylinidae subfamilies, having more than ten thousand described species, only began to have its Cretaceous representatives described in the past decade. A small part of these fossils comes from Spanish amber (Albian) and the majority comes from Kachin amber. This thesis focused on Cretaceous pselaphines, with an emphasis on the Kachin fauna. In chapter I, the Cretaceous pselaphine fauna is completely reviewed in a synopsis, four fossil species are described, one of them in a new genus, species identification tools were produced and an addendum to the current phylogeny was made by including the new species to it. In chapters II and III, living species are described; their descriptions were the basis to the study important characters that were later used in the fourth chapter, which generated a morphological databank. Chapter IV, the last of the thesis, presents a new phylogenetic hypothesis that was generated from a robust morphological database constructed through the examination of dozens of fossils and hundreds of living species. Novel kin relationships between Cretaceous and living lineages are proposed, with highlight for the greater affinities of the majority of the Cretaceous lineages between themselves than previously thought. Hopefully the descriptions and phylogenetic hypotheses presented in this thesis will stimulate new studies in Taxonomy and Systematics of this expressive subfamily.

Keywords: Cretaceous; staphylinid beetles; diversity; litter fauna

SUMÁRIO

I. INTRODUÇÃO GERAL

A subfamília Pselaphinae Latreille, 1802 (Coleoptera: Staphylinidae) Pselaphinae é a segunda mais diversa subfamília de Staphylinidae, com aproximadamente 10.000 espécies descritas (Parker, 2016a; Yin et al., 2017). Possuem distribuição global e sua grande diversidade e abundância nas florestas tropicais, bem como as relações de simbiose de muitas de suas espécies com espécies de formigas (ocasionalmente também com cupins) (Parker, 2016b) os tornam organismos de grande interesse biológico. Apesar disso, estudos ecológicos e etológicos sobre a subfamília são escassos (Sakchoowong et al., 2008; Schomann et al., 2008; Psomas et al., 2017).

Dentro de Staphylinidae, os Pselaphinae fazem parte do grupo Omaliinae de subfamílias, sendo irmãos da subfamília monogenérica Protopslaphinae (Newton & Thayer, 1995). Os Pselaphinae se diferenciam das demais subfamílias por apresentarem (i) três tarsômeros, (ii) uma sensila apical no palpômero maxilar 4 e (iii) um padrão de fóveas corporais (Chandler, 2001). A subfamília está dividida em seis supertribos: Batrisitae, Clavigeritae, Euplectitae, Faronitae, Goniaceritae e Pselaphitae, sendo que Faronitae é irmã de todas as demais, que são denominadas em conjunto como "higher Pselaphinae" (ou "pselaphíneos superiores", em uma tradução livre) (Newton & Thayer, 1995). Os Faronitae apresentam algumas características plesiomórficas, como: (i) *habitus* alongado, dorsoventralmente achatado, e com mobilidade do abdomen relativamente alta; (ii) antenas sem clava apical; (iii) retenção de fóveas na superfície elitral para além das fóveas basais; (iv) tarsômero 2 curto, não maior que 2x o tarsômero 1; e (v) garras pretarsais pares e similares em desenvolvimento. Nas outras cinco supertribos, as características diagnóticas são mais variáveis, mas no geral possuem: (i) corpo mais fusionado, muitas vezes dorsoventralmente amplo; (ii) antenas não clavadas, geralmente de três segmentos; (iii) fóveas elitrais apenas na base do élitro, nunca na superfície elitral; (iv) tarsômero 2 alongado, maior que 2x o tarsômero 1; e (v) garras pretarsais variáveis, podendo ser pares de tamanhos similares, de tamanhos desiguais, ou únicas (Chandler, 2001) (Figura 1).

Em níveis de espécie e gênero, a exceção do Neotrópico e Afrotrópico (regiões biogeográficas de acordo com Morrone & Ebach, 2022), pode-se considerar que a taxonomia das espécies Pselaphinae dos últimos anos tem se desenvolvido relativamente bem. A fauna Paleártica e Neártica são relativamente bem estudadas, com trabalhos sendo constantemente

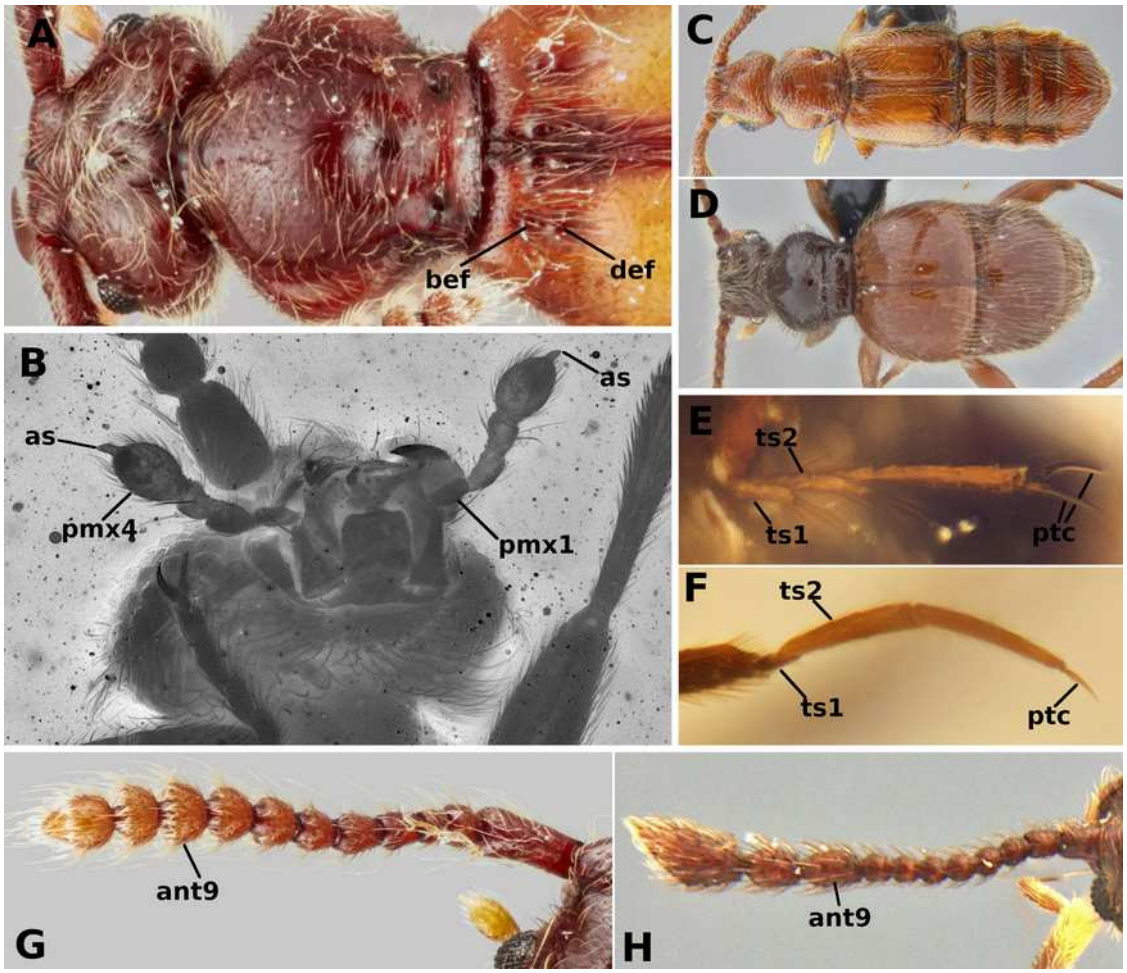

Figura 1. Caracteres diagnósticos de Pselaphinae. **A**, *Sagola poortmani* Park & Carlton, 2014 (Faronitae), o padrão de fóveas corporais pode ser observado (fóveas pronotais e elitrais visíveis); no élitro, tanto fóveas basais (**bef**) quanto fóveas discais (**def**) estão presentes. **B**, Faronitae, fóssil de âmbar "birmanês" não descrito em visão dorsal da cabeça evidenciando o quarto palpômero maxilar (**pmx4**) com sensila apical (**as**). **C**, *Tuberoplectus* sp. (Euplectitae), *habitus* alongado, margens laterais subparalelas, plesiomórfico para a subfamília, presente em Faronitae e alguns Euplectitae. **D**, *Arthmius* sp. (Batrisitae), *habitus* globoso, derivado e presente em várias linhagens de "higher Pselaphinae". **E** e **F,** comparação dos tamanhos relativos dos tarsômeros (**ts**) entre Faronitae e dos "higher Pselaphinae" (imagens de espécies fósseis descritas no Capítulo 1) e comparação das garras pretarsais (**ptc**) pares e simples. **G** e **H**, comparação das antenas sem clava de Faronitae e com clava apical dos "higher Pselaphinae", o antenômero 9 (**ant9**) é consideralmente maior do que o 8 em H.

publicados (e.g. Chandler & Caterino, 2011; Hlaváč et al., 2014; Owens & Carlton, 2016; Caterino & Vasquéz-Vélez, 2017). Na região Australiana, o trabalho seminal de Chandler (2001) representa não somente um grande avanço para aquele continente, mas também a base teórica para os estudos em outras regiões biogeográficas. Na região Oriental, as dezenas de recentes

contribuições de Zi-Wei Yin (e.g. Yin e Li, 2015; Yin & Cuccodoro, 2016; Yin & Shen, 2020; Yin, 2023) representam um grande avanço para a taxonomia da subfamília. Na região Neotropical, a taxonomia das espécies nativas desenvolveu-se, em sua maioria, entre a segunda metade do século XIX e a primeira metade do século XX, em trabalhos clássicos sobre a subfamília (naquele momento, ainda considerada uma família, Pselaphidae) (Reitter, 1885; Raffray, 1908; Park, 1942; Park, 1952). Contudo, nas últimas décadas, poucos estudos taxonômicos foram produzidos, em sua maioria descrições isoladas (e.g. Oliveira & Fonseca , 1998; Cuccodoro et al., 2012; Asenjo et al., 2017), e, apenas em raros casos, estes foram de caráter revisional mais abrangente, como revisões genéricas ou tribais (Vásques-Vélez, 2016). Em relação às hierarquias taxonômicas mais altas, há uma série de questões pendentes. No nível de supertribos, a classificação atual da subfamília foi estabelecida por Newton & Thayer (1995), que dividiu a subfamília em seis supertribos, como explicado acima. Contudo, Parker (2016a) apresenta pela primeira vez uma filogenia molecular e morfológica em que questiona a monofilia de algumas supertribos (e até mesmo de algumas tribos). As definições de tribos foram dadas em sua maioria pelos autores clássicos (e.g. Raffray, 1908; Park, 1942) e podem representar, em maioria, grupos monofiléticos. As relações de parentesco entre os gêneros dentro de cada tribo são amplamente desconhecidas, salvo algumas exceções (e.g. Parker & Grimaldi, 2014; Hlaváč et al., 2021).

Fósseis de Pselaphinae preservados em âmbar

O estudo dos fósseis ainda é incipiente em Pselaphinae. Contudo, a última década viu sugir uma série de trabalhos que descreveram espécies cretácicas preservadas em âmbar e que abriram caminho para se compreender a evolução da subfamília. Os Pselaphinae preservados em âmbar são conhecidos de seis sítios de épocas muito distintas, os dois mais antigos sendo do período Cretáceo. São eles, do mais antigo para o mais recente: âmbar espanhol (Cretáceo, Albiano, duas espécies descritas); âmbar “birmanês” de Kachin (Cretáceo, Cenomaniano, onze espécies descritas, sem contar as novas espécies descritas nesta tese); âmbar indiano de Cambay (Eoceno, Ypresiano, duas espécies); âmbar Báltico (Eoceno, Lutetiano, com 36 espécies descritas), âmbar mexicano e dominicano (Mioceno, ambos do Burdigaliano, apenas uma espécies descrita de âmbar mexicano e nenhuma formalmente descrita de âmbar dominicano) (Figura 2) (Schaufuss,

1890; Newton & Chandler, 1989; Chatzimanolis & Engel, 2013; Peris et al., 2014; Parker & Grimaldi, 2014; Parker, 2016a; Yin et al., 2017; Yin et al., 2019a; Yin et al., 2019b; Yin & Cai, 2021; Yin et al., 2021; Yin et al., 2022; Parker, 2022).

Dentre os vários sítios cretácicos de âmbar que possuem inclusões de artrópodes, os fósseis do norte de Myanmar (antiga Birmânia), estado de Kachin, são os que apresentam a maior riqueza de espécies. O âmbar de Kachin é datado do Cretáceo médio, da idade Cenomaniana, com 98.79 ± 0.62 milhões de anos de idade (Shi et al., 2012). A quantidade de espécies descritas de artrópodes até 2016 era de 587 espécies (Guo et al., 2017), um número já amplamente superado, dadas as numerosas publicações de descrições de espécies que ocorreram na última década. O foco principal desta tese foi compreender como as espécies fósseis preservadas no âmbar de Kachin se relacionam com a fauna moderna.

Material estudado e questões éticas concernentes à origem dos fósseis

A Coleção Entomológia do Laboratório de Coleoptera da Universidade Federal de Viçosa (CELC; Evenhuis, 2024) possui uma coleção com mais de 300 espécies de Pselaphinae da fauna brasileira de diversas localidades, mas principalmente dos estados de Minas Gerais, Espírito Santos, Bahia e Amazonas. Também há na coleção em torno de 100 espécies da fauna australiana. O estudo dos espécimes depositados na CELC foi a base primária para a realização desta tese. Os fósseis estudados na tese são da coleção particular do autor, contudo, todos os espécimes propostos como tipos para as novas espécies serão doados à CELC.

Conflitos político-militares de Myanmar dos anos recentes motivaram a publicação de uma carta da Sociedade de Paleontologia de Vertebrados dos Estados Unidos da América, a SVP, em que a instituição dá diretrizes para os editores de periódicos científicos, solicitando uma moratória na publicação de quaisquer espécimes fósseis adquiridos de fontes em Myanmar após junho de 2017 (Rayfield et al., 2020; Theodor et al., 2021). As cartas motivaram respostas por alguns estudiosos de âmbar “birmanês”, que propuseram alternativas, além de terem apontado inconsistências na argumentação da SVP (Haug, J. et al., 2020; Shi et al., 2021). A posição da CELC em relação a esta questão ética da origem do âmbar está em acordo com os últimos autores, de modo que o material tipo proveniente da tese será depositado permanente nesta coleção.

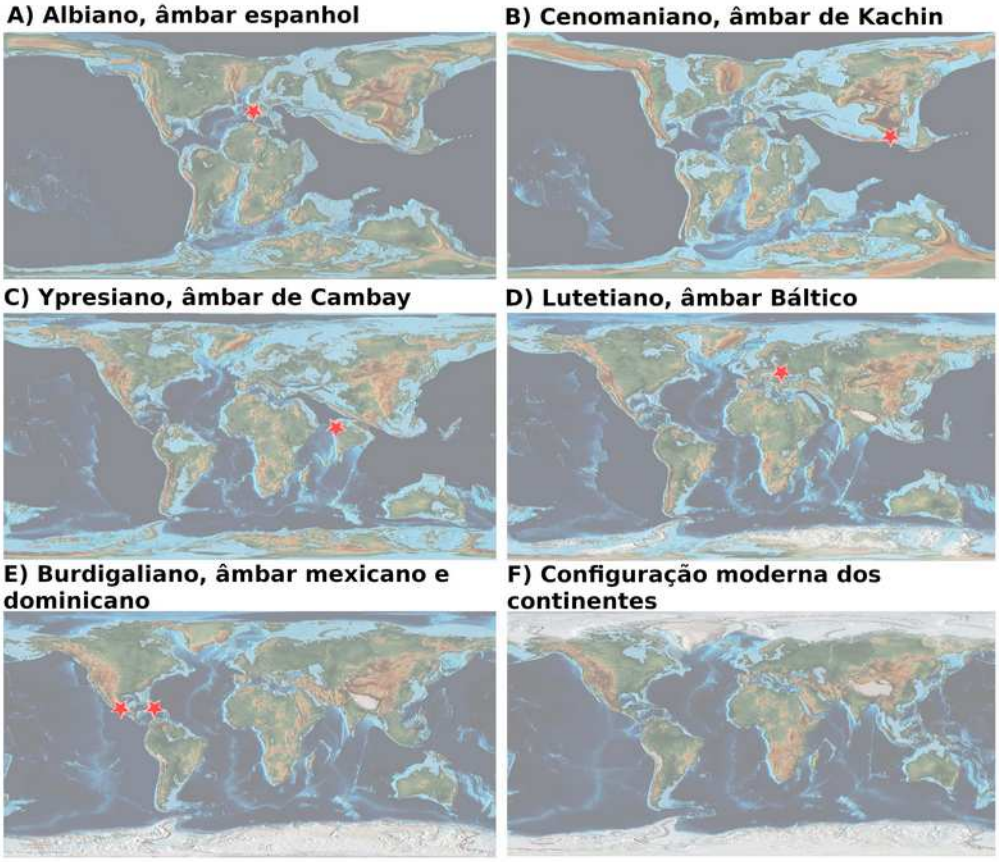

Figura 2. Paleomapas da configuração da Terra durante o momento de formação de cada sítio fossilífero de âmbar. O ponto rosa indica a localidade aproximada de cada sítio. Retirado de PALEOMAP PaleoAtlas for GPlates, por Christopher Scotese (imagens dos paleomapas disponíveis em https://www.earthbyte.org/paleomap-paleoatlas-for-gplates/).

JUSTIFICATIVA

Pela grande diversidade, abundância e ampla distribuição global, Pselaphinae se torna um táxon de particular interesse a ser estudado do ponto de vista ecológico. Sua recorrente relação com as formigas, um dos artrópodes com maior importância ecológica, abre portas para estuos comportamentais e evolutivos. Por fim, a presença de fósseis de Pselaphinae em diversos sítios possibilita estudos evolutivos e biogeográficos. Todos estes estudos em diversas sub-áreas da biologia apenas podem ser desenvolvidos estando apoiados em uma sólida base taxonômica e filogenética, a qual ainda não está consolidada, a despeito dos inúmeros esforços conduzidos recentemente entre os autores que se dedicam à subfamília. No estudo da sistemática de um dado

táxon, a inclusão das linhagens fósseis é de grande auxílio na compreensão dos caminhos evolutivos que determinam a fauna vivente daquele táxon. As descrições de espécies e refinamento filogenético deste trabalho, com enfoque nas linhagens fósseis mais antigas conhecidas de Pselaphinae, servem ao propósito de consolidação de uma sólida e estável Taxonomia e Sistemática para Pselaphinae e de elucidar os caminhos evolutivos que determinaram a distribuição e diversidade das tribos atuais.

OBJETIVOS

(i) Compilar em um artigo de sinópse todo o conhecimento dos fósseis do Cretáceo de Pselaphinae descritos até o momento;
(ii) Examinar o máximo de espécies fósseis e viventes atráves do estudo físico de espécimes depositados em coleção, ou através de imagens e descrições da literatura, em busca de compilar uma lista de caracteres morfológicos relevantes para o estudo da subfamília;
(iii) Descrever eventuais espécies novas de fósseis examinadas;
(iv) Descrever eventuais espécies novas viventes examinadas;
(v) Produzir uma nova hipótese filogenética para os Pselaphinae que contemple de maneira mais abrangente as espécies extintas do Cretáceo;
(vi) Responder às perguntas: os fósseis cretácicos de Pselaphinae são uma ou várias linhagens? Há evidências robustas para classificar estas linhagens como grupos "stem" de tribos modernas da subfamília? Ou, alternativamente, elas representariam linhagens totalmente perdidas e não proximamente relacionadas aos elementos discerníveis da fauna moderna?

RESULTADOS

A tese contém quatro capítulos, todos sob a forma de artigo científico. O Capítulo I foi submetido à revista *Cretaceous Research*, o Capítulo II está publicado na revista *Zootaxa*, o Capítulo III está na fase final do processo de revisão da revista *Studies on Neotropical Fauna and Environment* (já revisado, correções enviadas ao editor dia 25 de janeiro de 2024) e o Capítulo IV ainda está em fase de refinamento, tanto das análises quanto da escrita e será submetido após a

conclusão da tese (Capítulo IV). Abaixo é apresentada uma descrição de cada capítulo:

Capítulo 1: “Taxonomy and Systematics of Pselaphinae beetles (Coleoptera: Staphylinidae) preserved in Cretaceous Amber”. **Explicação**: O primeiro capítulo teve por objetivo descrever quatro novas espécies de Pselaphinae preservadas em âmbar “birmanês”, uma delas em um novo gênero. Além disso, foi apresentada uma sinopse de todas as espécies da fauna cretácica de Pselaphinae descritas até então, chaves de identificação para todas as espécies e um adendo à filogenia vigente de Parker (2016a), em que se acrescentou as espécies descritas na matrix morfológica existente para inseri-las em uma filogenia. **Importância**: O trabalho uniformizou o conhecimento acerca das espécies cretácicas por meio das diagnoses revisadas de todas as espécies, ressaltando caracteres que se demonstraram mais fortes ao longo do tempo e apontando outros que, a princípio, poderiam parecer importantes, mas se mostraram pouco informativos. Além disso, aumentou significativamente a fauna (quatro novas para um total de 11 espécies descritas), descrevendo o primeiro Faronitae para o âmbar “birmanês” (uma espécie já havia sido descrita de âmbar Espanhol). O Capítulo I consistiu no primeiro esforço da tese e demonstrou a necessidade de se produzir uma matriz com mais caracteres morfológicos, algo que veio a ser feito posteriormente no desenvolvimento da tese, no último capítulo.

Capítulo 2: “First record of Mayetiini (Coleoptera: Staphylinidae: Pselaphinae) from Brazil, with the description of a new macropterous and macrophthalmic species of *Mayetia* Mulsant & Rey, 1875”. **Explicação**: Neste trabalho se registrou pela primeira vez o gênero *Mayetia* e a tribo Mayetiini para o Brasil com a descrição da espécie *Mayetia atlantica* Chaul & Lopes-Andrade, uma espécie macroftálmica e macróptera, características incomuns para o gênero. **Importância**: O gênero, que é parte da supertribo Euplectitae, à primeira vista parece ter características plesiomórficas para os "higher Pselaphinae", devido à aparência geral do corpo (alongado e relativamente achatado dorsoventralmente). Entretanto, em detalhe, é repleto de autapomorfias, possuindo as mandíbulas e complexo labio-maxilar muito derivados e distintos das demais tribos da subfamília. O estudo pormenorizado dessas estruturas permitiu acrescentar diversos caracteres (ou estados de caracteres) ao banco de dados morfológicos que alimentou a matriz construída para o Capítulo IV. Além disso, o gênero *Mayetia* contém as espécies que estão entre os menores

coleópteros (certamente as menores em Pselaphinae), o que tornou desafiadora a descrição da nova espécie, sendo necessário amplo uso de técnicas de microscopia e dissecção dos espécimes. Os métodos utilizados para a descrição de *M. atlantica* foram amplamente aplicados durante o estudo das demais espécies da CELC a fim de produzir um banco de dados morfológicos.

Capítulo 3: "A new species of *Metopiellus* Raffray (Coleoptera: Staphylinidae: Pselaphinae) from the Atlantic Forest of Brazil, with keys to species of the genus and to the genera of Metopiasini". **Explicação**: Neste capítulo se descreveu a nova espécie para a Mata Altântica, *Metopiellus emavieirae**, que pertence a um gênero sulamericano contendo, após este trabalho, um total de sete espécies: três descritas entre o fim do século XIX e a primeira metade do século XX e outras três descritas recentemente, entre 2017 e 2023. O gênero é parte de Metopiasini, uma tribo que parece ser composta por espécies mirmecófilas (Parker, 2016b). A espécie descrita é a maior do gênero e figura entre os maiores Pselaphinae (espécies com mais de 3 mm).
Morfologicamente, a espécie mais próxima da nova espécie é justamente a que ocorre mais distante geograficamente, *M. guanano* Fiorentino, Tocora & Ramirez, da Colômbia. Chaves de identificação para os gêneros de Metopiasini e uma chave atualizada para as espécies de *Metopiellus* foram produzidas. A tribo, que atualmente é restrita ao Neotrópico, ocorre também no âmbar Báltico, do Eoceno europeu, o que torna complexa a explicação da evolução da tribo, uma questão paleobiogeográfica discutida no trabalho. **Importância**: Ambas as espécies descritas nos Capítulos II e III são Euplectitae. Contudo, são extremamente diferentes. Isto é devido à polifilia da supertribo, sendo que muitas das tribos que a compõem são apenas distantemente relacionadas (o caso entre Mayetiini e Metopiasini) (Parker, 2016a, Yin et al., 2017; Yin et al., 2019b). Por esta razão, o estudo pormenorizado desta espécie, necessário para que se realizasse sua descrição, resultou na descoberta de caracteres morfológicos bem diferentes daqueles descobertos no Capítulo II. Em termos de tamanho, esta espécie é parte dos maiores Pselaphinae, no extremo oposto de *Mayetia atlantica*. A nova espécie e a espécie colombiana acima citada só podem ser separadas facilmente através dos caracteres sexuais secundários dos machos e de sua genitália. Em relação às fêmeas, exclusivamente, as espécies são extremamente similares, diferenciando-se apenas por tamanho corporal e proporções de alguns escleritos.

Capítulo 4: “Phylogenetic placement of Cretaceous Pselaphinae (Coleoptera: Staphylinidae)”. **Explicação**: Neste capítulo foi proposta uma nova hipótese filogenética para os Pselaphinae, com ênfase nas espécies fósseis do Cretáceo “birmanês”, baseada em uma análise de parcimônia de uma matriz morfológica de 154 caracteres. Trata-se do estudo filogenético mais abrangente para Pselaphinae do Cretáceo até o presente. Os resultados dessa nova proposta filogenética diferem das filogenias prévias em vários aspectos. Dentre eles, o mais importante foi sugerir uma maior proximidade dos gêneros cretácicos entre si do que com tribos viventes, com poucas exceções. Uma discussão foi feita para argumentar sobre a necessidade de uma ampla matriz de caracteres em busca de uma melhor resolução para as relações dos Pselaphinae extintos com a fauna moderna. **Importância**: Este capítulo concentra os maiores esforços da tese. Todo o processo de busca por caracteres entre as dezenas de espécies (descritas e não descritas) fósseis e centenas de espécies viventes foram sintetizados na matriz morfológica que é apresentada no capítulo. A lista de caracteres consiste em um grande avanço aos trabalhos prévios que examinaram em torno de um terço do número de caracteres estudado no capítulo. A partir desta proposta, e considerando as limitações do trabalho que são explicitadas no texto, será possível avançar com mais facilidade em direção à construção de uma abrangente filogenia, a qual contemple tanto a diversidade fóssil quanto a vivente.

REFERÊNCIAS

Asenjo, A., Ferreira, R.L., Zampaulo, R.D.A., 2017. Description of *Metopiellus painensis* sp. nov. (Coleoptera, Staphylinidae), first troglobitic Pselaphinae from Brazil. Zootaxa, 4269 (1), 115–123.

https://doi.org/10.11646/zootaxa.4269.1.5

Caterino, M., Vásquez-Vélez, L., 2017. A revision of *Prespelea* Park (Staphylinidae, Pselaphinae).ZooKeys, 685, 105–130.

https://doi.org/10.3897/zookeys.685.13811

Chandler, D.S., 2001. Biology, morphology and systematics of the ant-like litter beetles of Australia (Coleoptera: Staphylinidae: Pselaphinae). Associated Publishers, Gainsville, Florida: Mem. Entomol. Int., Vol. 15.

Chandler, D., Caterino, M., 2011. A taxonomic revision of the New World genus *Oropodes* Casey (Coleoptera, Staphylinidae, Pselaphinae). ZooKeys, 147, 25–477.

https://doi.org/10.3897/zookeys.147.2072

Chatzimanolis, S., Engel, M., 2013. The fauna of Staphylininae in Dominican amber (Coleoptera: Staphylinidae), Annals of Carnegie Museum, 81 (4), 281–294.

https://doi.org/10.2992/007.081.0401

Cuccodoro, G., Kurbatov, S., Oliveira, L., Fonseca, M., 2012. On the Genus *Paragoniastes* Comellini, 1979, with Description of a New Species from Ilhéus, Brazil (Coleoptera, Staphylinidae, Pselaphinae). Psyche, 2012, 1–6.

https://doi.org/10.1155/2012/561352

Evenhuis, N.L., 2024. The insect and spider collections of the world website. Available from: http://hbs.bishopmuseum.org/codens/ (acessado 22 Janeiro de 2024)

Guo, M., Xing, L., Wang, B., Zhang, W., Wang, S., Shi, A. & Bai, M., 2017. A catalogue of Bur mite inclusions. Zoological Systematics, 42 (3), 249–379.
https://doi.org/10.11865/zs.201715

Haug, J.T., Azar, D., Ross, A., Szwedo, J., Wang, B., Arillo, A., Baranov, V., Bechteler, J., Beutel, R., Blagoderov, V., Delclòs, Haug, C., *et al*., 2020. Comment on the letter of the Society of Vertebrate Paleontology (SVP) dated April 21, 2020 regarding “Fossils from conflict zones and reproducibility of fossil- based scientific data”: Myanmar amber. Paläontologische Zeitschrift, 94, 431–437.

https://doi.org/10.1007/s12542/s12542-019-00503-9

Hlaváč, P., Baňař, P., Parker, J., 2014. Endogean and cavernicolous Coleoptera of the Balkans. XIV. Melledobythus bilandzijae, new genus and species of cavernicolous Bythinini (Staphylinidae: Pselaphinae) from the Island Mljet, Croatia. Zootaxa, 3835 (4), 564 – 572.
http://dx.doi.org/10.11646/zootaxa.3835.4.7

Hlaváč, P., Parker, J., Maruyama, M., Fikáček, M., 2021. Diversification of myrmecophilous Clavigeritae beetles (Coleoptera: Staphylinidae: Pselaphinae) and their radiation in New Caledonia. Systematic Entomology, 46, 422–452. https://doi.org/10.1111/syen.12469

Morrone, J.J., Ebach, M.C., 2022. Toward a terrestrial biogeographical regionalisation of the world: historical notes, characterisation and area nomenclature. Australian Systematic Botany, 35 (3), 89–126.

https://doi.org/10.1071/SB22002

Newton, A.F., Chandler, D.S., 1989. World catalog of the genera of Pselaphidae (Coleoptera). Fieldiana, Zoology (New Series), 53, 1–93.

Newton, A., Thayer, M., 1995. Protopselaphinae new subfamily for *Protopselaphus* new genus from Malaysia, with a phylogenetic analysis and review of the Omaliine Group of Staphylinidae including Pselaphidae (Coleoptera). Biology, Phylogeny, and Classification of Coleoptera: Papers Celebrating the 80th Birthday of Roy A. Crowson (ed. by J. Pakaluk and A. Ślipiński), 221–320. Muzeum i Instytut Zoologii PAN, Warszawa.

Oliveira, H., Fonseca, C., 1998. Descrição de duas espécies novas de Pselaphinae (Coleoptera: Staphylinidae) da Amazônia Central brasileira. Acta Amazonica, 28 (1), 93–100.

Owens, B., Carlton, C., 2016. Revision of *Eutyphlus* LeConte (Coleoptera: Staphylinidae: Pselaphinae), with description of a new species and phylogenetic placement within the tribe Trichonychini. The Coleopterists Bulletin, 70 (1), 1–29.

Park, O., 1942. A study in Neotropical Pselaphidae. Northwestern University Studies in the Biological Sciences and Medicine. Northwestern University, Evanston and Chicago, 1, 1, 403 pp.

Park, O., 1952. A revisional study of Neotropical Pselaphid beetles. Part Two.The Chicago Academy of Sciences, 54–148.

Parker, J., Grimaldi, D.A., 2014. Specialized myrmecophily at the ecological dawn of modern ants. Current Biology, Current Biology, 24, 2428–2434.

https://doi.org/10.1016/j.cub.2014.08.068

Parker, J., 2016a. Emergence of a superradiation: pselaphine rove beetles in midCretaceous amber from Myanmar and their evolutionary implications. Systematic Entomology, 41, 541–566.

https://doi.org/10.1111/syen.12173

Parker, J., 2016b. Myrmecophily in beetles (Coleoptera): Evolutionary patterns and biological mechanisms. Myrmecological News, 22, 65–108.

https://doi.org/10.25849/myrmecol.news_022:065

Parker, J., 2022. Transitional morphology and Afrotropical affinity of a bythinoplectine rove beetle from the early Eocene of India (Coleoptera: Staphylinidae: Pselaphinae). Palaeoentomology, 005 (5), 452–460.

https://doi.org/10.11646/palaeoentomology.5.5.6

Peris, D., Chatzimanolis, S., Delclòs, X., 2014. Diversity of rove beetles (Coleoptera: Staphylinidae) in Early Cretaceous Spanish amber. Cretaceous Research, 48, 85–95.

https://doi.org/10.1016/j.cretres.2013.11.008

Psomas, E., Holdsworth, S., Eggleton, P., 2017. Ant diversity as a direct and indirect driver of pselaphine rove beetle (Coleoptera: Staphylinidae) functional diversity in tropical rain forests, Sabah, Malaysian Borneo. Journal of Morphology, 279 (7), 981–996. https://doi.org/10.1002/jmor.20828

Raffray, A., 1908. Coleoptera. Fam. Pselaphidae. In Wytsmann P., editor. Genera Insectorum, 64th fascicule, Rome, 487 pp.

Rayfield, E.J., Theodor, J.M., Polly, P.D., 2020. Fossils from conflict zones and reproducibility of fossil-based scientific data. Society of Vertebrate Paleontology (SVP), letter, 21 April 2020. Available from: https://vertpaleo.org/wp-content/uploads/2021/01/SVP-Letter-to-Editors-FINAL.pdf (accessed 20 June 2023).

Reitter, E., 1885. Abbildungen und Bemerkungen zu wenig gekannten selaphiden-Gattungen mit Beschreibungen neuer Arten. Dtsch. Entomol. Zeitschrift. 29: 333–339, pls.2–3.

Schaufuss, L.W., 1890. System-Schema Der Pselaphiden, ein Blick in die Vorzeit, in die Gegenwart und in die Zukunft. Tijdschrift voor Entomologie, 33, 101–162.

Sakchoowong, W., Jaitrong, W., Ogata, K., Nomura, S., Chanpaisaeng, J., 2008. Diversity of soil-litter insects: comparison of the pselaphine beetles (Coleoptera: Staphylinidae: Pselaphinae) and the ground ants (Hymenoptera: Formicidae). Thai Journal of Agricultural Science, 41 (1–2), 11–18. https://doi.org/www.thaiagj.org

Schomann, A., Afflerbach, K., Betz, O., 2008. Predatory behaviour of some Central European pselaphine beetles (Coleoptera: Staphylinidae: Pselaphinae) with descriptions of relevant morphological features of their heads. European Journal of Entomology, 105, 889–907.

Shi, G., Grimaldi, D.A., Harlow, G.E., Wang, J., Wang, J., Yang, M., Lei, W., Li, Q., Li, X., 2012. Age constraint on Burmese amber based on UePb dating of zircons. Cretaceous Research, 37, 155–163. https://doi.org/10.1016/j.cretres.2012.03.014

Shi, C., Cai, H.H., Jiang, R.X., Wang, S., Engel, M.S., Yuan, J., Bai, M., Yang, D., Long, C.L., Zhao, Z.T., Zhang, D.X., Zhang, X.C., Peng, H., Wang, Y.D., Spicer, R.A., 2021. Balance scientific and ethical concerns to achieve a nuanced perspective on ‘blood amber’. Nature Ecology and Evolution, 5, 705–706. https://doi.org/10.1016/j.cub.2022.06.086

Theodor, J.M., Lewis, M.E., Rayfield, E.J., 2021. Amber specimens acquired from Myanmar fol lowing military coup. Society of Vertebrate Paleontology (SVP), letter, 14 June 2021. Ac cessed via: https://vertpaleo.org/wp-content/uploads/2021/06/SVP-Letter-to-paleontological-community-on-Myanmar-Amber_FINAL.pdf

Vásques-Vélez, L., 2016. Revision of the genus *Pselaphomorphus* Motschulsky, 1855 (Staphylinidae, Pselaphinae: Jubini). Zootaxa, 4107 (1), 001–048. http://doi.org/10.11646/zootaxa.4107.1.1

Yin, Z.-W., Li, L.-Z., 2015. New and little known species of the genus *Songius* (Coleoptera: Staphylinidae: Pselaphinae) in China. Zootaxa, 3905 (2), 293–300. http://dx.doi.org/10.11646/zootaxa.3905.2.10

Yin, Z.-W., Cuccodoro, G., 2016. *Colilodion schulzi* sp. n. (Coleoptera: Staphylinidae: Pselaphi nae) from Palawan, the Philippines, with habitus photographs and a revised key to all

Colilodion species. Revue suisse de Zoologie, 123 (1), 153–158.

Yin, Z.-W., Parker, J., Cai, C.-Y., Huang, D.-Y., Li, L.-Z., 2017. A new stem bythinine in Creta ceous Burmese amber and early evolution of specialized predatory behaviour in pselaphine rove beetles (Coleoptera: Staphylinidae). Journal of Systematic Palaeontology [volume and issue information and pagination were assigned in 2018 as follows: 16 (7), 531–541]. https://doi.org/10.1080/14772019.2017.1313790.

Yin, Z.-W., Kurbatov, S., Cuccodoro, G., Cai, C.-Y., 2019a. *Cretobrachygluta* gen. nov., the first and oldest Brachyglutini in mid-Cretaceous amber from Myanmar (Coleoptera: Staphylinidae: Pselaphinae). Acta Entomologica Musei Nationalis Pragae, 59, 101–106. https://doi.org/10.2478/aemnp-2019-0008

Yin, Z.-W., Chandler, D., Cai, C.-Y., 2019b. *Priscaplectus* gen. nov. and two new species in mid-Cretaceous amber from Myanmar (Coleoptera: Staphylinidae: Pselaphinae). Cretaceous Research, 103, 104174. https://doi.org/10.1016/j.cretres.2019.07.004

Yin, Z.-W., Shen, Q., 2020. Fifteen new species of *Sathytes* Westwood from China (Coleoptera, Staphylinidae, Pselaphinae), with an updated checklist of world species. European Journal of Taxonomy, 722, 37–74. https://doi.org/10.5852/ejt.2020.722.1133

Yin, Z.-W., Cai, C.-Y., 2021. A new Brachyglutini from mid-Cretaceous amber of northern Myanmar (Coleoptera: Staphylinidae: Pselaphinae). Cretaceous Research, 124, 104807. https://doi.org/10.1016/j.cretres.2021.104807

Yin, Z.-W., Zhao, Q.-H., Cai, C.-Y., 2021. *Megabythinus* gen. nov., a new stem-group Pselaphi nae from mid-Cretaceous Myanmar amber (Coleoptera, Staphylinidae). Cretaceous Re search, 125, 104879. https://doi.org/10.1016/j.cretres.2021.104879

Yin, Z.-W., Tihelka, E., Lozano-Fernandez, J., Cai, C-Y., 2022. The first fossil Hybocephalini (Coleoptera: Staphylinidae: Pselaphinae) from the middle Eocene of Europe and its evolu tionary and biogeographic implications. Arthropod Systematics & Phylogeny, 80, 279–294. https://doi.org/10.3897/asp.80.e82644

Yin, Z.-W., 2023. Range extension and male description of a rare clavigerite beetle in China (Coleoptera: Staphylinidae: Pselaphinae). Zootaxa, 5357 (4), 595–600. https://doi.org/10.11646/zootaxa.5357.4.7

II. CAPÍTULO 1

SYNOPSIS OF THE CRETACEOUS PSELAPHINAE (COLEOPTERA: STAPHYLINIDAE), WITH THE DESCRIPTION OF A NEW GENUS AND FOUR NEW SPECIES FROM MID-CRETACEOUS BURMESE AMBER

Este manuscrito não deve ser considerado como publicação válida para fins de nomenclatura zoológica, em acordo com as normas do Código Internacional de Nomenclatura Zoológica de 1999 (Capítulo 3, Artigos 8.2 e 8.3).

Artigo submetido à revista Palaeoentomology em julho de 2024, com a autoria de Júlio Cezar Mário Chaul; Isadora Gerheim de Vasconcellos Moreira & Cristiano Lopes-Andrade.

Synopsis of the Cretaceous Pselaphinae (Coleoptera: Staphylinidae), with the description of a new genus and four new species from mid-Cretaceous Burmese amber.

Júlio Cezar Mário Chaul; Isadora Gerheim; Cristiano Lopes-Andrade.

Corresponding author: Júlio Cezar Mário Chaul, Pós-Graduação em Ecologia, Departamento de Biologia Geral, Universidade Federal de Viçosa, 36570-900, Viçosa, Minas Gerais, Brazil. email: juliocchaul@gmail.com

ABSTRACT

In the past decade, the Pselaphinae rove beetles have gained their first Cretaceous unequivocal members with the description of eleven species belonging to nine genera, preserved either in Spanish or Burmese amber. Although still in its infancy, the taxonomy of the Cretaceous pselaphines have already revealed a considerable morphological and phylogenetic diversity. Here we increment this diversity with the following new descriptions of Burmese amber taxa: †*Burmalogasa perisi* **gen. et sp. nov.**, †*Boreotethys caii* **sp. nov.**, †*Cretobythus parkeri* **sp. nov.**, and †*Cretobythus yini* **sp. nov.** We provide a complementary description for *Boreotethys grimaldii* Parker based on an additional specimen determined by us as belonging to that species. We revise the diagnosis of all previously described species, proposing a new set of characters useful in separating the Cretaceous pselaphines. A traditional dichotomous key and a multi-entry, interactive online-based key of all described Cretaceous pselaphines are presented. Additionally, we add the newly described species to the previously published phylogenetic framework of Pselaphinae.

Keywords: rove beetles; Taxonomy; leaf-litter; Paleoentomology.

1. INTRODUCTION

A global mass resin production and burial occurred during the Cretaceous Resin Interval (Delclòs et al., 2023). In recent years, fossils recovered as inclusions in many of these resin deposits have yielded many paleoentomological discoveries that have greatly contributed to uncovering the evolutionary history of insects (e.g., Pérez-de la Fuente et al., 2011; Engel et al., 2016; Mey et al., 2017; Yin et al., 2018; Pérez-de la Fuente et al., 2019). Most of these discoveries come from the mid-Cretaceous (early Cenomanian, 98.79 ± 0.62 Ma) amber deposits from the Kachin state, Myanmar (Grimaldi et al., 2002; Shi et al. 2012). Coleoptera are among the most species-rich taxa found in these sites, along with Diptera and Hymenoptera (Guo et al. 2017), but precise quantification is impossible because the total amber extraction of Kachin is not catalogued (Peris, 2020). Staphylinidae, the largest family of beetles (Parker, 2016), is the most abundant Coleoptera among Cretaceous ambers (Peris and Rust, 2019). The descriptions of these beetles sometimes have an outstanding quality, due to excellent preservation amber inclusions and the use of modern imaging techniques, allowing the long-extinct Cretaceous lineages to be satisfactorily compared to their extant relatives in the finest levels of morphological detail (Yin et al., 2019; Yin and Zhou, 2020), even in cases of minute species (Yin and Cai, 2019; Li et al., 2023).

Within the Staphylinidae, the Omaliine group of subfamilies (Newton and Thayer, 1995) has recently gained the description of many fossil members, including several Dasycerinae species (Yin et al., 2021a), two species of the enigmatic Protopselaphinae (Liu et al., 2020 a; 2020b), and several fossil Pselaphinae (Peris, 2014; Parker, 2016; Yin, 2017; Yin 2019a, Yin 2019b; Yin and Cai, 2021, Yin et al., 2021b). Pselaphinae is the second-largest subfamily of staphylinids (Newton and Chandler, 1989; Parker, 2016). Overviews of the subfamily systematics are available (Chandler, 2001; Parker, 2016; Yin et al., 2017). Pselaphinae have been divided by morphology-based taxonomy into six supertribes:

Faronitae, Euplectitae, Batrisitae, Goniaceritae, Pselaphitae, and Clavigeritae, these latter five forming a large clade, usually called the “higher Pselaphinae”. Recently, a partitioned analysis of combined morphology and molecular data resulted in a phylogeny confirming the sister relationship between the Faronitae and the higher Pselaphinae and demonstrating polyphiletism of some of the supertribes within the higher Pselaphinae (Parker, 2016).

Cenozoic pselaphines are long known from Baltic amber (Schaufuss, 1890) and are, at least tentatively, assigned to extant tribes (Newton and Chandler, 1989). Mesozoic pselaphines, on the other hand, started to be described recently, as mentioned above, and their link to the modern fauna, although sometimes proposed, is much less clear. In 2014, two species in two genera, †*Cretasonoma corinformibus* Peris, Chatzimanolis and Delclòs, 2014 and †*Penarhytus tenebris* Peris, Chatzimanolis and Delclòs, 2014, were described based on specimens from the Albian Spanish amber. All subsequent descriptions are from Cenomanian Burmese amber, as follows: †*Boreotethys arctopteryx* Parker, 2016, †*Boreotethys grimaldii* Parker, 2016, and †*Protrichonyx rafifrons* Parker, 2016; †*Cretobythus excavatus* Yin, Parker, Cai, Huang and Li, 2017; †*Cretobrachygluta laurasiensis* Yin, Kurbatov, Cuccodoro and Cai, 2019; †*Priscaplectus carinatus* Yin, Chandler and Cai, 2019 and †*P. grandiceps* Yin, Chandler and Cai, 2019; †*Burmagluta rougemonti* Yin and Cai, 2021; and †*Megabythinus spinitibialis* Yin, Zhao and Cai, 2021. The affinities of †*Cretasonoma*, †*Cretobrachygluta* and †*Burmagluta* to modern groups are reasonably established, the first being interpreted as stem Faronitae (Peris et al., 2014; Parker, 2016) and the other two assumed to be stem lineages of Brachyglutini, showing that at least one modern tribe was unequivocally already present by mid-Cretaceous (Yin et al., 2019; Yin and Cai, 2021). The relationships of the other five genera are more obscure: three of them, †*Boreotethys*, †*Cretobythus*, and †*Megabythinus* are thought to be stem lineages of the Bythinini, while the other two, †*Protrichonyx* and †*Priscaplectus* arise from a great polytomy amidst various lineages of Euplectitae, a

supertribe that is almost certainly polyphyletic within the higher Pselaphinae clade (Parker, 2016; Yin et al., 2019). Parkwer (2016) makes a detailed argument for the relationship between *Boreotethys* and modern Bythini, but while they share trraits, the are also a considerable amount of differences.

Here we **(i)** describe four new species and one new genus of Cretaceous Pselaphinae from Burmese amber; **(ii)** supplement the diagnosis of all Cretaceous species; **(iii)** assign the new species to the existing phylogenetic framework of Pselaphinae; and **(iv)** provide a dichotomous key and an online-based, multi-entry interactive key as identification tools.

2. MATERIAL AND METHODS

2.1. Repository institution, fossil preparation and imaging

All specimens are deposited in the Entomological Collection of the Coleoptera Laboratory (CELC), at the Universidade Federal de Viçosa, Minas Gerais, Brazil (Evenhuis, 2024). Fossils were purchased from sellers that confirmed their provenance from mines around Myitkyina, Kachin state, Myanmar. Ambers from this locality are early Cenomanian in origin (98.79 ± 0.62 Ma, Shi et al., 2012). In order to make facets to enhance visualization, the stones were sanded in a series of gradually finer sandpapers (300 up to 3000 grit). After that, the facets were gently rubed in a soft cloth embeeded with polishing paste. Facets were made to allow various views of each specimen. The resulting specimen, usually very small amber pieces with the inclusions, were given unique identifier numbers, provenance labels, and are maintained isolated within a plastic bags in the drawers of the dry collection. Stereomicroscope images were made in a Leica S8 APO or a Zeiss Stereo Discovery V20. Other images were made in an Olympus CX40 microscope or under the epifluorescence component of an Olympus BX60 microscope.

Images were stacked in Zerene software. Resulting stacked images were edited in GIMP and figures were composed in that software as well (Kimball and Mattis, 1996). Whenever needed, scale bars were added through ImageJ software (Schneider et al., 2012). Additional images for each species not shown in the plates can be found at the Xper3 multi-entry key (see below).

2.2. Morphological terminology and measurements

We followed Chandler (2001), with the modifications proposed in Parker (2016) and selected modifications proposed in other recent publications which scrutinized anatomically a couple of Pselaphinae species (Jałoszyński, et al., 2020; Beutel, et al., 2021; Jałoszyński, et al., 2022, Luo et al., 2021a; Luo et al., 2021b; Luo et al., 2022). The effort to include all these modifications in this work, matching all morphological information of previous publications on fossil species to the new proposed terminology, is outside the scope of our work. We noticed that some structures have been called differently (e.g. apical pseudosegment *versus* apical palpal cone *versus* apical sensilla) and that different structures received the same acronyms (e.g. “s” for *spur* and also for *sternite*, “pc” for *procoxa* and for *paranotal carina*) in different publications. These inconsistencies can cause confusion and diminish image and description intelligibility in the long term. Here, whenever there was such an issue, we chose for one of the terms and its corresponding acronym, trying to maintain one of the two conflicting names and/or acronyms and only suggesting new ones occasionally (e. g. we used *pretarsal claw*, ptc, instead of “*tarsal claw*”, following Lawrence et al., 2011). Whenever we gave an acronym to a structure which combines two structures that already have acronyms, we combined the acronyms of these two to form the new one (e.g. “antbc” for *antennal tubercle*, given that “an” stands for *antenna* and “tbc” for *tubercle*). This approach has the onus of creating longer acronyms that at first look tiresome and a "pollutant" to the figures. However, it avoids acronym similarity and as the reader gets used to the method

reading them in the images becomes more intuitive. We wrote the acronyms always in low case. Regarding foveation pattern, we followed strictly Chandler (2001), without any changes to the acronyms, as those are well-established in the literature. Terms and abbreviations are given in the figure legends.

We were conservative to establish the presence of foveae in the descriptions due to the difficulty of clearly and undoubtedly seeing them, as pointed by Parker (2016). In the descriptions, we cited only the foveae which are "likely present", and in Table 1 a more complete attempt to map the foveae of the species was made. In Table 1 (only scored the specimens which were physically examined, the remaining Burmese species were scored in the Supplementary material 1, Foveation tab), *absent fovea* (“0” in the table) was coded when the region expected to contain a fovea was clearly exposed and did not have any signs of having it; *likely absent fovea* (“1”) was coded when no fovea was observed in a region, but conditions of observation were not exceptional (e.g. dark regions or wrinkle/dried out cuticle); *likely present fovea* (“2”) was coded when there was signs of the foveae, but the pit itself could not be clearly or completely seen (e.g. when there was a tiny bubble right in front of the expected position of the fovea, but the immediate surrounding appear to form a depression, or when a pit was observed, but overall preservation was bad so that the fovea could be artifactual); *present fovea* (“3”) was coded when the pit was clearly observed. Whenever a region expected to have fovea was entirely obscured (e.g. blocked by large debris or bubbles) we coded it as *impossible to determine* (“-”). The names for the foveae used in the descriptions are exactly as in Chandler (2001), except for the meso- and metasternal foveae, which have been changed to meso- and metaventrital, respectively, and their abbreviations have been adapted as well (e.g. from "**lmsf**, latero mesosternal foveae" to **lmsvf**, latero mesoventrital foveae"). The names and abbreviations adopted are as follows (whenever tha name of the fovea does not explicitly link it to the sclerite it is on, we named the sclerite in brackets): **ff**, frontal fovea; **vf**, vertexal foveae; **aldf**, anterolateral discal foveae (pronotum); **ldf**, lateral discal foveae

(pronotum); **maf**, medial antebasal fovea (pronotum); **laf**, lateral antebasal foveae (pronotum); **iblf**, inner basolateral foveae (pronotum); **oblf**, outer basolateral foveae (pronotum); **apsf**, antero prosternal foveae; **lpcf**, lateral procoxal foveae (prosternum); **mpcf**, medial procoxal fovea (prosternum); **pef**, proepimeral foveae; **sef**, subbasal elytral foveae; **bef**, basal elytral foveae; **shef**, subhumeral elytral foveae; **def**, discal elytral foveae; ppf, preppectal foveae; **mmvf**, median mesoventrital fovea; **almvf**, anterolateral mesoventrital foveae; **lmsvf**, lateral mesoventrital foveae; **pmcf**, promesocoxal foveae (mesoventrite); **lmcf**, lateral mesocoxal foveae (metaventrite); **mmtvf**, median metaventrital fovea; **lmtvf**, lateral metaventrital foveae; **ptf**, paratergal foveae (tergite); **mbf**, mediobasal foveae (tergite and sternite); **blf**, basolateral foveae (sternite).

We tried to take as many measurements as possible (56 measurements, Supplementary material 1, Measurements tab), but presented under each species descriptions only the ones we could extract from all examined fossils and were considered determinant in revealing each species diagnostic dimensions. They were (presented in an anteroposterior axis of the body):

- Head length (**HL**),
- Antenna total length taken *in situ* (**ANL**),
- Antennal total length as a sum of antennomeres lengths (**ANLs**),
- Maxillary palp size as a sum of the lengths of maxillary palpomeres 2–4 (**MXPL**),
- Compound eye length (**CEL**),
- Pronotum anterior width (**PRAW**),
- Pronotum maximum width (**PRW**),
- Pronotum posterior width (**PRPW**),
- Pronotal length (**PRL**), the maximum length of the pronotum medially,
- Elytral length (**ELL**), the maximum length of the elytra medially,

- Abdomen length (**ABL**), taken preferreably in dorsal view, the longest length from the posterior end of ELL to the posteriormost point of tVIII,
- Hind leg length (**HLL**),
- Total length taken *in situ*, ideally from anterior clypeal margin to posterior point of tergite VIII (**TL**),
- Total length as a sum of HL, PRL, ELL and ABL (**TLs**).

We wrote the measurements abbreviations always in upper case to contrast with the structures' acronyms which are in low case.

2.3. Multi-entry key

Apart from the dichotomous key presented below, an interactive multi-entry key was made in the Xper3.fr online platform (Ung et al., 2010; Vignes-Lebbe et al., 2017; Kerner et al., 2021). The key is accessed in the browser and works by choosing among the list of characters that can be compared to the user's specimen. Then, states are presented, the user choose the best match accordingly, and click on the top green button. Each chosen character has the potential to eliminate impossible candidate species, making progressively short the list of possible species. Ideally the user will remain with a single species, which should then be compared to the keyed specimen in detail (using the descriptions and images of that species). The key can be accessed here:

http://www.xper3.fr/xper3GeneratedFiles/publish/identification/-4517313894653082321/mkey.html

2.4. Phylogenetic analysis

To test the phylogenetic placement of the new species, we performed a parsimony analysis for the morphological (with and without molecular constraint) and a Bayesian analysis for the partitioned data (morphology and molecular combined). We augmented the most updated morphological matrix provided by Yin et al. (2019) with data on the new species, an addditional †*Boreotethys grimaldii* specimen, and †*Protopselaphus thayeri* Liu, Tihelka and Cai, 2020 (Supplementary material 1, Matrix table). The molecular constraint was made by forcing some clades to be grouped together, based on the molecular tree available in Parker (2016). We subdivided the molecular tree in eight small clades instead of using the entire tree, allowing the new species to be placed in a more inclusive position (the eight clades are informed in Supplementary material 2). All parameters were the same as described in detail in Parker (2016) and Yin et al (2017), and for the parsimony analysis we also set the random seed as zero and the space for 25000 trees in memory. The parsimony analysis was performed on TNT v.1.5 no taxon limit (Goloboff, Farris and Nixon 2008) and the Bayesian analysis on MrBayes 3.2.6 through the CIPRES Science Gateway (Miller et al. 2010).

3. RESULTS

3.1. List of Cretaceous Pselaphinae species

†*Boreotethys arctopteryx* Parker, 2016 (Myanmar, Cenomanian)

†*Boreotethys grimaldii* Parker, 2016 (Myanmar, Cenomanian)

†*Boreotethys caii* Chaul and Lopes-Andrade **sp. nov.** (Myanmar, Cenomanian)

†*Burmagluta rougemonti* Yin and Cai, 2021 (Myanmar, Cenomanian)

†*Burmalogasa perisi* Chaul and Lopes-Andrade **gen. et sp. nov.** (Myanmar, Cenomanian)

†*Cretasonoma corinformibus* Peris, Chatzimanolis and Delclòs, 2014 (Spain, Albian)

†*Cretobrachygluta laurasiensis* Yin, Kurbatov, Cuccodoro and Cai, 2019 (Myanmar, Cenomanian)

†*Cretobythus excavatus* Yin, Parker, Cai, Huang and Li, 2017 (Myanmar, Cenomanian)

†*Cretobythus parkeri* Chaul and Lopes-Andrade **sp. nov.** (Myanmar, Cenomanian)

†*Cretobythus yini* Chaul and Lopes-Andrade **sp. nov.** (Myanmar, Cenomanian)

†*Megabythinus spinitibialis* Yin, Zhao and Cai, 2021 (Myanmar, Cenomanian)

†*Penarhytus tenebris* Peris, Chatzimanolis and Delclòs, 2014 (Spain, Albian)

†*Priscaplectus carinatus* Yin, Chandler and Cai, 2019 (Myanmar, Cenomanian)

†*Priscaplectus grandiceps* Yin, Chandler and Cai, 2019 (Myanmar, Cenomanian)

†*Protrichonyx rafifrons* Parker, 2016 (Myanmar, Cenomanian)

3.2. Systematic paleontology of the Cretaceous Pselaphinae

Order **Coleoptera** Linnaeus, 1758

Family **Staphylinidae** Latreille, 1802

Subfamily **Pselaphinae** Latreille, 1802

Supertribe **Faronitae**

Tribe *Incertae sedis*

†*Cretasonoma* Peris, Chatzimanolis and Delclòs, 2014

Type species. †*Cretasonoma corinformibus* Peris, Chatzimanolis and Delclòs, 2014.

Diagnosis. Antennae: length not greater than half the body length; scape almost twice as long as pedicel; antennomeres gradually increasing in size from 3 to 11, not forming a club. Antennal tubercles separated by sulcus, interantennal ridge absent. Compound eyes relatively large. Pronotum wider than long. Elytra more than twice as long as pronotum. Tarsomere 2 only slightly longer than tarsomere 1; pretarsal claws composed of two equally-sized, well-developed claws.

†*Cretasonoma corinformibus* Peris, Chatzimanolis and Delclòs, 2014

(Fig.13)

Type locality. Spain, amber from Peñacerrada I and El Soplao deposits, Albian.

Diagnosis. As for the genus.

Comments. The species has been described based on six specimens, with the holotype (MCNA-8654) and some of the paratypes (MCNA-13254, CES-433.1, and MCNA-14265) being in a good state of preservation. There are differences in the body proportions of the specimens of the type series, meaning that some could be other species. For example, the holotype and some paratypes have broader heads and pronota than paratype CES-433-1, and paratype MCNA-14265 is comparatively larger. Overall, the available images of the specimens are a bit dark, with pilosity, body cavities, carinae or foveae difficult to ascertain. Epifluorescence microscopy could probably reveal those traits in most of the specimens (Fu et al., 2021). There are further Cretaceous Faronitae other than †*C. corimformibus* and †*Burmalogasa perisi* **gen. et sp. nov.** (described below) awaiting formal description (Parker, 2016; personal observation). A better characterization of some details of †*C. corimformibus* will be of great importance in the comparison between it and the Burmese fauna, especially considering that the Spanish and Burmese sites do have congeneric occurrences (e.g. the genus †*Kachinus* Chatzimanolis, Engel and Newton, 2010, Scydmaeninae).

†*Burmalogasa* Chaul and Lopes-Andrade **gen. nov.**

Type species. †*Burmalogasa perisi* sp. nov. by monotypy.

Diagnosis. Body appearing subparallel. Antennae: scape twice as long as pedicel; antennomeres gradu

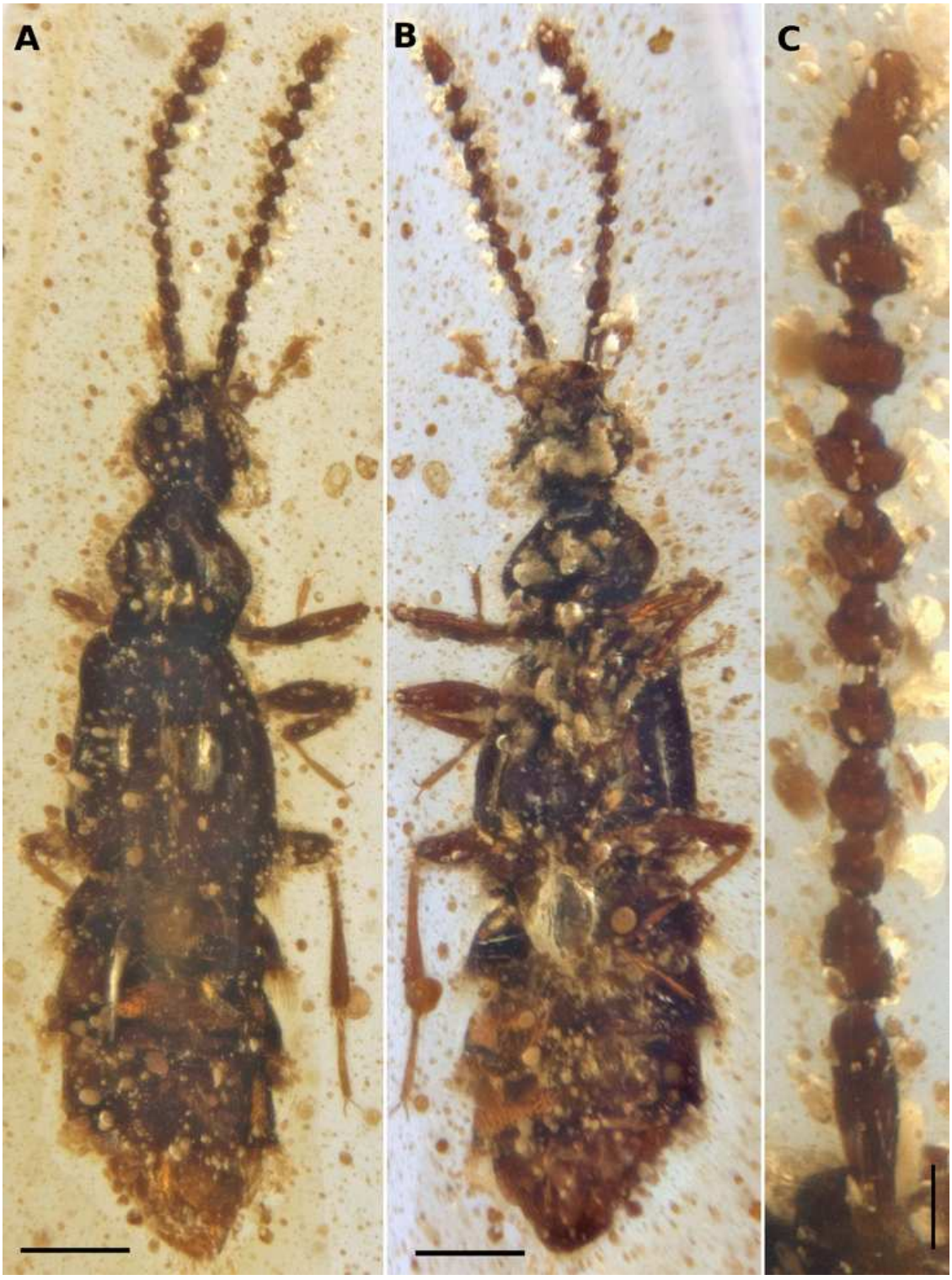

Fig. 1. *Burmalogasa perisi* **gen. et sp. nov.** holotype (UFV-LABECOL-010429). **A**, *habitus*, dorsal view; **B**, *habitus*, ventral; **C**, right antenna. Scale bars are 0.2 mm (A and B); 0.1 mm (C).

ally increasing in size from antennomere 3 to 11, not forming a club. Maxillary palpomere not greatly enlarged. In dorsal view of head, interantennal ridge absent; antennal tubercles distinct, with a narrow medial sulcus in between them. Pronotum longer than wide; with a medial to posteromedial cavity; without carinae; lateral surfaces slightly lowered in relation to medial surface. Both basal and discal elytra foveae present. Tarsomere 2 at most twice as long as tarsomere 1 (discounting ventral lobes); and much smaller than half tarsomere 3; pretarsal claws of two equally-sized, well-developed claws.

Description. **Body.** Head slightly narrower than pronotum, pronotum slightly narrower than elytra, and elytra slightly narrower than abdomen. Proportions: pronotum about 1.2x as wide as head; elytra about 1.4x as wide as pronotum; tergite 5 (broader in abdomen) about 1.1x as wide as elytra; elytra 1.5x as long as pronotum; abdomen almost 1.5x as long as elytra; legs and antennae not conspicuously long, metafemur length about as much as pronotal width and antennal length smaller than half the body length (or smaller than the summed lengths of elytra and pronotum). **Head.** In dorsal view, cephalic capsule overal round. Antennal tubercles prominent, separated by an interantennal sulcus (an indentation of the frons). Interantennal sulcus fused posteriorly to a shallow, much broader, frontovertexal cavity. Compound eyes relatively large, with relatively coarse ommatidia. Ocular-mandibular carinae present, small and thin. Vertexal foveae present. Gular region and labrum mostly obscured/unaccesible. Mandibles robust, blade-like; inner margin likely edentate; apical tooth large and acute. Maxillary palpomere 1 small, but not minute, not much smaller than maxillary palpommere 2, both palpomeres 1 and 2 roughly cylindrical and gradually thickenning to apex; palpomere 3 thicker and smaller than palpomere 2; palpomere 4 fusiform, its apical sensilla small with trucate tip. Antennae with antennomeres 3 to 11 gradually increasing in width; scape relatively long. **Pronotum**. Widest at mid-length; with one medial to posteromedial cavity; lateral foveae likely present, medial foveae; lateral portions lowered from central, larger surface, forming "pronotal wings". **Elytra**. Basal and discal foveae present; a pair of shallow discal sulci. Humeri well-marked. Posterolateral clefts. **Legs**. Metacoxae jux-

taposed. Tarsomere 2 not much larger than tarsomere 1; tarsomere 2 ventrally lobed, both apicoventrally lobed. Pretarsal claws subequal, robust, basally mildly lobate. **Abdomen**. Tergite VI the broadest and longest. Posterolateral tergite corners in dorsal view indented laterally, so that lateral abdominal margins are stair-like, dense patches of setae project from these corners. Paratergites distinct on segments IV to VII. Tergites VII and VIII strongly converging.

Etymology. The name is a combination of Burma, the former name of Myanmar, and *Logasa*, due to the resemblance between the extant Australian species *Logasa newtoni* Kang, Chandler and Park, 2019 and the genotype of the new genus.

Comments. Differences in the diagnosis between †*Cretasonoma* and †*Burmalogasa* are somewhat subtle and could be considered as regular intrageneric variation. Nevertheless, we decided to describe the new genus as there are some morphological differences and the two genera are temporally and spatially separated: †*Cretasonoma* being from early Albian Spanish sites and †*Burmalogasa* being from an early Cenomanian Burmese site. Therefore, the two are separates by at least 10 million years in time. The seas between the two sites in those periods were shallow and not perennial, so landbridges between them were probably available (Delclos et al., 2023). When more material of both genera are found, it will be easier to refine the morphological boundaries between the two.

†*Burmalogasa perisi* Chaul and Lopes-Andrade **sp. nov.**

(Figs. 1, 2, and 13)

Type material. Holotype (UFV-LABECOL-010429) is housed in CELC.

Type locality. Myanmar: Kachin, Hukawng Valley, early Cenomanian (age 98.79 ± 0.62 Ma).

Measurements. ANL 0.63, ANLs 0.64, MXPL 0.144, HL 0.21, CEL 0.074, PRL 0.285, PRW 0.275, ELL 0.43, ELW 0.38, ABL 0.7, HLL 0.81, TLr 1.625, TLs 1.625.

Diagnosis. As for the genus plus the following. Head in dorsal view from occipital constriction to an

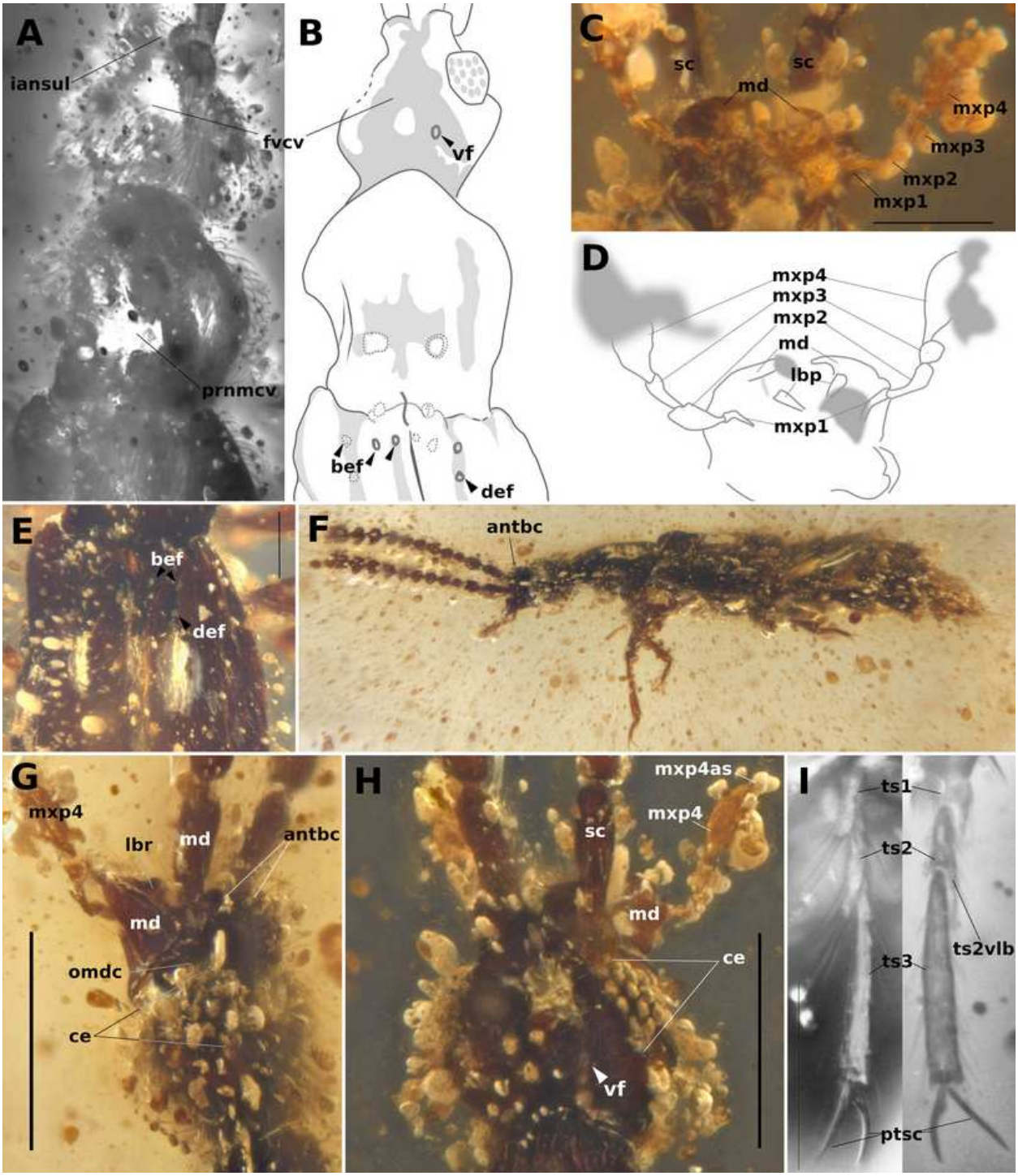

Fig. 2. †*Burmalogasa perisi* **gen. et sp. nov.** holotype (UFV-LABECOL-010429). **A**, dorsum of head and pronotum under epifluorescent light; **B**, drawing of a similar view as in A; **C**, mouthparts in ventral view; **D** drawing of a similar view as in C; **E**, elytra; **F**, *habitus* in profile; **G**, detail of head in lateral view; **H**, detail of head in dorsal view; **I**, hindleg tarsi under regular light (left leg, lateral view) and under epifluorescent light

(right leg, dorsal view). Scale bars: 0.1 mm (C); 0.2 mm (G, H). Abbreviations: **antbc**, antennal tubercle; **bef**, basal elytral fovea; **ce**, compound eye; **def**, discal elytral fovea; **fvcv**, frontovertexal cavity; **iansul**, interantennal sulcus; **lbp**, labial palp; **lbr**, labrum; **md**, mandible; **mxp (1, 2, 3, and 4)**, maxillary palpomeres; **mxp4as**, maxillary 4 apical sensilla; **oanr**, ocular antennal ridge; **ocp**, occiput; **ocpvlc**, occipital-vertexal longitudinal carina; **omdc**, ocular-mandibular carina; **prnmcv**, pronotal medial cavity; **ptsc**, pretarsal claw; **sc**, scape (antennomere 1); **ts (1, 2, and 3)**, tarsomeres; **ts2vlb**, tarsomere 2 ventral lobe; **vf**, vertexal fovea.

tennal tubercles, roughly round. Compound eyes only mildly bulging from head's surface. Maxillary palpomere 4 slightly narrower than scape and considerably less volumous than it; more than twice as large as palpomere 3. Pedicel conspicuously longer than wide; antennomere 3 about half as long as pedicel; apical antennomere cone-shaped. Body setation dense and lanuginose.

Description. As for the genus, with the following additions. **Pilosity**. Dense, filiform, recurved setae across the body; longer setae posterior to the eye, and at the posterolateral corners of the abdominal tergites. **Sculpturing**. Surfaces of body appear to be mostly smooth. **Coloration**. Apparently brown, with palpi, legs, antennae, and tip of abdomen lighter. **Head**. Cephalic capsule overal round (dorsal view of the body, cephalic capsule slightly tilted ventrally). Cavity on frontovertexal region continuous to interantennal frons sulcus, shallow, possibly triangular or V-shaped and having a pair of vertexal foveae at its posterior ends. Vertexal foveae at the level of the posterior limits of compound eyes. Vertexal medial protuberance (mild tumulus), posterior to frontovertexal cavity, likely present. Antennal scape as long as antennomeres 3 to 5 together; antennomere 3 the smallest, followed by gradually larger antennomeres, except that antennomere 5 appears to be slightly smaller than fourth; antennomere 11 cone-shaped; antennomeres 10 and 9 transverse, "flying saucer" shaped. **Thorax**. Metaventrite elongate, distance between meso- and metacoxae about twice as long as that of pro- and mesocoxae. **Foveation pattern**. Foveae which are more evident (but see Table 1): vertexal (one pair, large); basal elytral (two or

three pairs); discal elytral (at least one pair); lateral procoxae (one pair).

Sex. Undetermined.

Preservation. Holotype overall nicely preserved, apparently with minimal dessication, torsion, and distentions. The specimen is homogeneously surrounded by very small particles of debris, which make visualization much harder.

Etymology. The specific epithet is in honor of the paleontologist David Peris. The name was created by adding the singular Latin genitive case suffix -i to the last name of a male person. The orthography of an eponym is unchangeable and does not depend on the generic name for which the epithet is used.

Supertribe *Incertae Sedis*

Tribe *Incertae Sedis*

†***Penarhytus*** Peris, Chatzimanolis and Delclòs, 2014

Type species. †*Penarhytus tenebris* Peris, Chatzimanolis and Delclòs, 2014.

Diagnosis. Antennal scape slightly longer than pedicel; apical three antennomeres clearly forming a club. Frons without deep excavation. Eyes relatively large. Palpomere 4 not greatly enlarged, smaller than pedicel. Pronotum wider than long (transverse). Putative absence of antebasal (transverse) or medial (longitudinal) sulci on the pronotum. Elytral discal foveae absent. Tarsomere 2 not much longer than 1. Tarsomere 3 longer than 1 and 2 combined; tarsomere 2 ventrally lobate; pretarsal claws composed of a main, larger claw and a secondary, reduced one. In dorsal view, abdomen shorter than elytra.

Comments. In addition to the traits discussed in Parker (2016), †*Penarhytus* is an intriguing taxon among Cretaceous pselaphines for combining unequally-sized pretarsal claws (a common trait of the higher Pselaphinae) and short tarsomere 2 in relation to tarsomere 3 (a common trait of the Faronitae). Such combination is not seen in extant lineages of pselaphines.

†***Penarhytus tenebris*** Peris, Chatzimanolis and Delclòs, 2014

(Fig. 13)

Type locality. Spain, amber from Peñacerrada I, early Albian.

Diagnosis. As for the genus.

Comments. The unique known specimen of †*Penarhytus tenebris* is embeeded in clear amber, with fungal hyphae (or a similar debris, cotton fiber-like) obscuring mainly its dorsal view. The specimen itself is nicelly preserved, with apparent well-conserved cuticle (not dehydrated and wrinkled) and without evident body distortions. The images of the specimen, however, are too dark, so that minor details cannot be ascertained. The use of epifluorescence (Fu et al., 2021) could yield important morphological information from the holotype and potentialy better place the species in the subfamily phylogeny.

Supertribe **Euplectitae** Streubel, 1839

Tribe *Incertae sedis*

†***Priscaplectus*** Yin, Chandler and Cai, 2019

Type species. †*Priscaplectus grandiceps* Yin, Chandler and Cai, 2019.

Diagnosis. Antennae with apical three atennomeres slightly enlarged, loosely forming a club; antennomere 11 the most enlarged, without an apical notch. Maxillary palps relatively reduced. Head subquadrate or subrectangular from interantennal ridge to vertexal posterior margin (occipital constriction). Frontovertexal area excavated. Median section of vertex raised, forming a vertexal tubercle. Interantennal ridge well-defined. Antennal tubercles notches present. Ocular-antennal ridge present. Pronotum wider than long or as wide as long; anterolateral corners strongly marked; disc carinated, lat-

eral longitudinal carinae spans the entire pronotal length; median and lateral antebasal foveae on pronotum present. Tarsomere 2 much larger than tarsomere 1 and a bit smaller than tarsomere 3; meso- and metatarsi having a single pretarsal claw; protarsi with pretarsus having a larger and a smaller ("accessory") claws.

Comments. †*Priscaplectus* exibits a very unique combination of characters when compared to other Cretaceous genera. Despite this, it shares intriguing features with †*Boreothethys*, †*Cretobythus* and †*Protrichonyx* (see under *Priscapectus grandiceps* notes and in the Discussion).

†*Priscaplectus carinatus* Yin, Chandler and Cai, 2019

(Fig. 13)

Type locality. Myanmar: Kachin, Hukawng Valley, early Cenomanian (age 98.79 ± 0.62 Ma).

Diagnosis. Having the genus diagnosis plus the following. Antennal tubercles notches large and deep. Pronotal, medially to the pair of complete lateral carinae, with a pair of anteromedial carinae restricted to the pronotal anterior half. Elytra with two pairs of strongly marked carinae across their entire length.

Comments. The species is known for two specimens, one putative male and another of undetermined sex, and is one of the most impressive Cretaceous pselaphines. The holotype is exceptionally preserved and has been imaged in extreme detail with a combination of regular steromicroscopy, epifluorescence microscopy and confocal fluorescent microcopy, which together reveal a great amount of details that make possible to compare it to any extant and extinct pselaphine species.

†*Priscaplectus grandiceps* Yin, Chandler and Cai, 2019

(Fig. 13)

Type locality. Myanmar: Kachin, Hukawng Valley, early Cenomanian (age 98.79 ± 0.62 Ma).

Diagnosis. With the genus diagnosis plus the following. Vertex elongate. Eyes closer to mouthparts

than to occiput. Pair of pronotal anteromedial carinae on the anterior half of the pronotum absent. Only a single pair of elytral discal carinae that do not reach the elytral posterior margin.

Comments. The species has been described based on 10 specimens, five males, three females and two of undetermined sex. It shares with †*Boreotethys grimaldii* the notched ocular-mandibular carina (**omdcn**), which was called postantennal notch in the original description, (Fig.6, A in Yin et al., 2019, here called antennal tubercle notch and abbreviated as **antbcn**). However, the antennal tubercle notches are here interpreted according to Yin et al. (2017) and not Yin et al. (2019); therefore, *P. grandiceps* has both **omdcn** and **antbcn**. It is not clear whether †*P. carinatus* presents **omdcn**. †*Priscaplectus* also shares with †*Boreotethys* the paired pretarsal claws in the protarsi and single in the meso- and metatarsi. These two characters are very unusual in modern *taxa* and indicate a relationship of †*Priscapletus* to †*Boreotethys* (see Discussion for more characters shared between some of the Cretaceous genera).

Supertribe **Euplectitae** Streubel, 1839

Tribe *Incertae sedis*

†*Protrichonyx* Parker, 2016

Type species. †*Protrichonyx rafifrons* Parker, 2016.

Diagnosis. Antennae with apical three antennomere forming a loosely defined club; apical antennomere (XI) apically notched. Interantennal ridge straight. Antennal tubercles notches present. Frotovertexal area with deep excavation. Excavation posteriorly delimited by (or "closed" by) a thick transversal ridge (likely entirely vertexal). Posterolateral margins of the head posterad the eyes straight and oblique. Ocular-antennal ridge present. Pronotum longer than wide; its lateral margins relatively straight and slightly diverging posteriorly; lateral longitudinal carinae likely present, restricted to the

pronotal posterior half; posteromedial cavity present; putative absence of medioposterior longitudinal sulci and of antebasal sulcus. Tarsomere 2 much longer than tarsomere 1 and of similar length to tarsomere 3; meso- and metatarsi likely having a single pretarsal claw (at most with very reduced, unspotted, "acessory" claws) and protarsi having a larger and a smaller acessory pretarsal claws.

†*Protrichonyx rafifrons* Parker, 2016

(Fig. 13)

Type locality. Myanmar: Kachin, Hukawng Valley, early Cenomanian (age 98.79 ± 0.62 Ma).

Comments. The amber piece of the holotype, the only known individual of the species so far, has a transversal fracture at about the posterior level of the elytra which does not affecct visualization so much. The cuticle appears to have some degree of wrinkling, especially ventrally. Also, some appendages are detaching or are bronken (palpomeres, legs and antennae), indicating the specimen suffered significant stretching. Because of that, †*Protrichonyx rafifrons* is a challenging fossil to be studied. Regular stereomicroscope images of the specimen are very dark, however epifluorescence images reveals quite a lot of extra details. †*Protrichonyx rafifrons* is intriguingly similar to one species of †*Cretobythus*, †*C. parkeri* (see notes under that species below). The preservation conditions of †*P. rafifrons* are not ideal and new material could allow a reevaluation of the generic limits between it and †*Cretobythus*.

Supertribe **Goniaceritae** Reitter, 1882

Tribe **Brachyglutini** Raffray, 1904

†*Cretobrachygluta* Yin, Kurbatov, Cuccodoro and Cai, 2019

Type species. †*Cretobrachygluta laurasiensis* Yin, Kurbatov, Cuccodoro and Cai, 2019.

Diagnosis. Antennae apical three antennomeres forming relatively distinct club; antennomere 11 apical internal surface broadly concave (notched). Palpomere 4 relatively small, less than twice as large as palpomere 3; maxillary palpomere 4 apical sensilla conspicuous. Frotovertexal area without excavation. Interantennal ridge barely formed; antennal tubercles low. Antennal tubercles notches absent. Vertexal foveae small, nude. Compound eyes large. Ocular-antennal ridge absent. Gular ridge present, broad, with a pair of gular foveae posterior to it. Pronotum antebasal sulcus present, with small, nude median and lateral antebasal foveae. Pronotum without carinae or conspicuous cavities. Elytral discal striae absent. Trochanters short. Metacoxae contiguous. Tarsomere 2 much longer than tarsomere 1 and a bit shorter than tarsomere 3; tarsi each with a single pretarsal claw. Abdominal tergite IV clearly longer than tergite V.

†*Cretobrachygluta laurasiensis* Yin, Kurbatov, Cuccodoro and Cai, 2019

(Fig. 13)

Type locality. Myanmar: Kachin, Hukawng Valley, early Cenomanian (age 98.79 ± 0.62 Ma).

Diagnosis. As for the genus.

Comments. The termed "ocular-mandibular carina" in the original publication (Fig.2 D of Yin et al., 2019) is here considered an "ocular-clypeal carina". The carina is not paired and does not seem to touch or end at the mandible insertions as in, for example, *Batriscydmaenus tishechkini* Parker and Owens, 2018. Instead, it is a single, arched carina that originates in the anteromedial part of the compound eye perimeter and runs across the clypeus to the other compound eye. Such carina is seen in some extant taxa (e.g. *Mayetia atlantica* Chaul and Lopes-Andrade, 2022).

†***Burmagluta*** Yin and Cai, 2021

Type species. †*Burmagluta rougemonti* Yin and Cai, 2021.

Diagnosis. Body large (around 3 mm). Antennal scape barely longer than pedicel; apical three antennomeres loosely forming a club. Maxillary palpomere 4 more than twice as large as palpomere 3, with apical sensilla conspicuously large. Interantennal ridge absent; antennal tubercles very prominent, frons squeezed in between them, not clearly forming a sulcus since the tubercles are considerably separated; antennal tubercles notches absent. Frontovertexal surface without excavation. Compound eyes ventrolaterally positioned, vetrally and only slightly posteriorly positioned in relation to antennal tubercles. Ocular-antennal ridge absent. Pronotum longitudinal lateral sulci and antebasal sulcus distinct; surfaces laterad the longitudinal sulci in a slightly lowered level in relation to medial surface. Metacoxae contiguous. Tarsomere 2 much longer than tarsomere 1 and much shorter than tarsomere 3; pretarsal claws composed of a main, long claw and a secondary, reduced claw.

Comments. Similar morphology to that of the head and pronotum of †*Burmagluta* occurs in extant species, but not among the known Cretaceous genera. The antennal tubercles in †*Burmagluta* roughly resemble those of †*Burmalogasa*. However in the latter the tubercles are very approximated and the frons is narrowly inserted in between them, forming a sulcus. The pronotum of †*Cretobrachygluta* resembles that of †*Burmagluta*, but in the latter the divisions are more strongly marked. The shape of the head and pronotum of †*Cretobythus*, †*Protrichonyx*, and †*Priscaplectus* are radically different from that of †*Burmagluta*.

Fig. 3. †*Boreotethys grimaldii* (UFV-LABECOL-009191). **A**, *Habitus*, dorsal view; **B**, *habitus*, ventral; **C**, habitus, lateral view. Scale bars: 0.2 mm (A, B). Abbreviations: **ce**, compound eye; **mxp**, maxillary palpomeres.

†*Burmagluta rougemonti* Yin and Cai, 2021

(Fig. 13)

Type locality. Myanmar: Kachin, Hukawng Valley, early Cenomanian (age 98.79 ± 0.62 Ma).

Diagnosis. As for the genus.

Tribe **Bythinini** Raffray, 1890

†***Boreotethys*** Parker, 2016

Type species. †*Boreotethys grimaldii* Parker, 2016.

Diagnosis. Body dorsoventrally flattened. Antennae with apical three antennomeres forming a club, sometimes distinct, sometimes loosely-formed. Palpomere 4 large, easily larger than twice the size of palpomere 3 and thicker than scape. Interantennal ridge not greatly elevated. Antennal tubercles notches possibly absent. Frontovertexal area without excavation. Ocular-antennal ridge absent. Vertexal transversal thick ridge absent. Medial, longitudinal carina at occipital constriction likely absent. Pronotal discal cavities and carinae likely absent; antebasal sulcus absent. Metacoxae contiguous or narrowly separated. Tarsomere 2 much larger than 1 and smaller, subequal, or longer than tarsomere 3; pretarsal claws single or paired with one main claw and one reduced ("acessory") at least on protarsi.

Comments. Parker (2016) makes an argument for the relationship of †*Boreotethys* to Bythinini, listing the similarities and differences between the extinct genus and the extant tribe. They share the elongate scape (sometimes the elongate pedicel too), gular tubercles in male, a single claw in the pretarsus (at most with a very reduced second claw). Moreover, they share a large maxillary palp, the most obvious feature linking both groups. However, many Bythinininii, in detail, have a very distinc fourth maxillary palpomere, with a strongly constricted base (stalked), which is not the case in †*Boreotethys*. The differences between †*Boreotethys* and Bythinini are the dorsoventrally flattened body in †*Boreotethys* versus globular body in bythinines, the tarsomere 2 being smaller than the tarsomere 3 in †*Boreotethys* while

it is the opposite in bythinines, and the adjacent metacoxae in †*Boreotethys* versus the widely separated metacoxae in bythinines. The compression of the body is even more evident in the new specimen of †*B. grimaldii,* that has a facet more correctly aligned to reveal the lateral view of the body (Fig.3C) than in the holotype, in which the view is ventrolateral (Figure 3, D and E, of Parker, 2016). Moreover, the ocular-mandibular notch shared between †*Boreotethys* and †*Priscaplectus* is very intriguing and could suggest a closer affinity between these two very distinct Cretaceous genera than between each of them to any Modern lineage. On balance, we suspect that †*Boreotethys* might not be related to Bythinini at all, but that must be tested phylogenetic in another work, since that characters of the matrix of Parker (2016), replicated here, do not contain a few of the characters pointed as differences between them.

†*Boreotethys arctopteryx* Parker, 2016

(Fig.14)

Type locality. Myanmar: Kachin, Hukawng Valley, early Cenomanian (age 98.79 ± 0.62 Ma).

Diagnosis. With the genus diagnosis and the following. Body densely setose. Scape and antennomere 2 approximately equal in length. Eyes not particularly prominent laterally. Lateral margins of head anterior to occipital constriction mildly and gradually diverging anteriorly until meeting the posteriormost perimeter of the compound eye; occipital constriction width about 0.9x as broad as width of head just posterior to the eyes. Pronotum wider than long. Pronotal cavities (mediobasal and laterobasal) possibly artifactual. Legs thickened, particularly femur. Pretarsal claws single.

Comments. Most of the holotype's characters are inaccesible because the specimen is surrounded by bubbles. The head shape is a key trait to separate this species from the others in the genus.

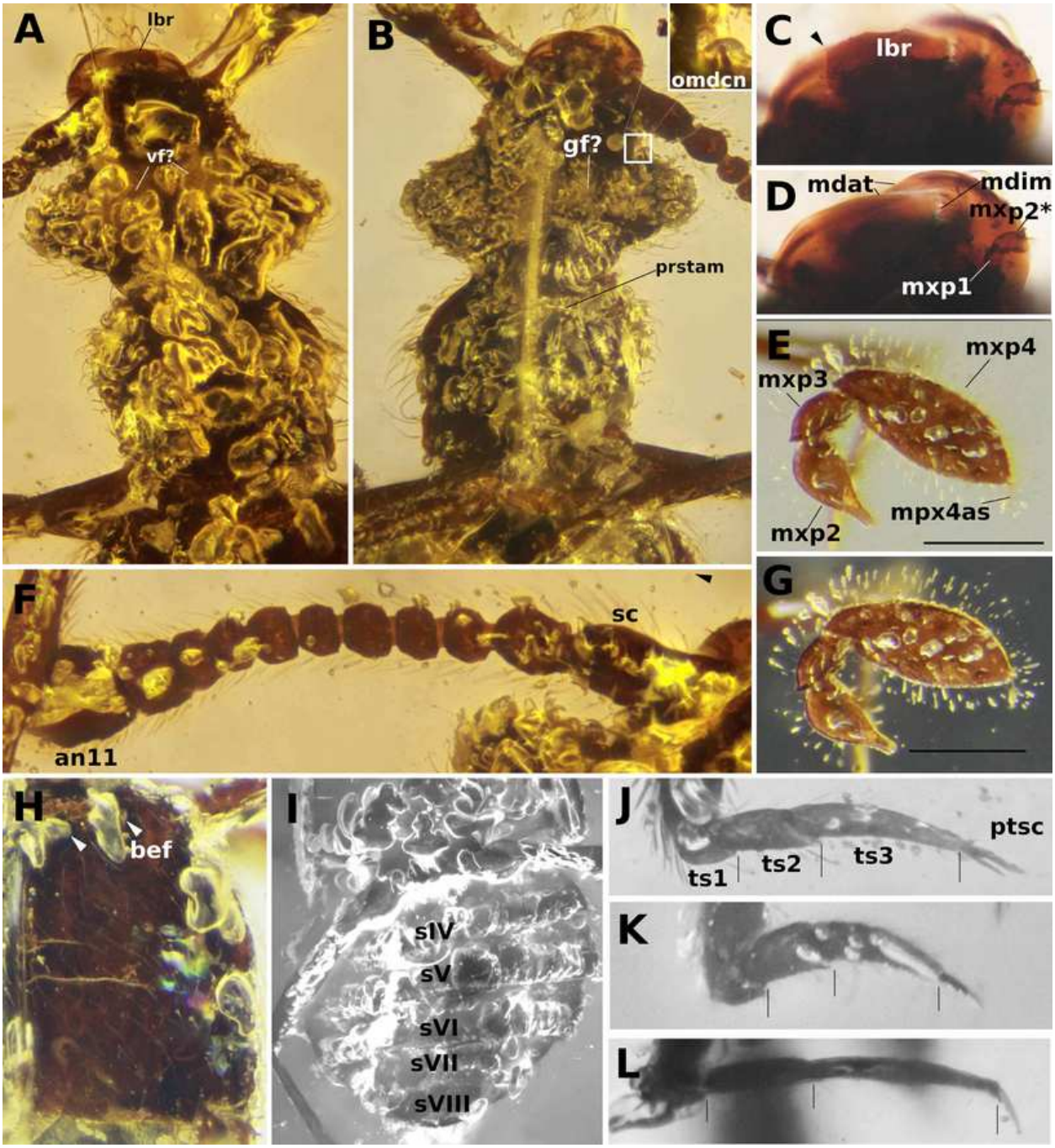

Fig. 4. †*Boreotethys grimaldii* (UFV-LABECOL-009191). **A** and **B**, head and pronotum in dorsal and ventral views, respectively; **C** and **D**, ventral view of the mouthparts in two different focal planes, C evincing labrum and D evincing mandible and broken palp; **E** and **G**, broken left palpomere in light and dark backgrounds, respectively; **H**, detail of right elytrum; **I**, ventral view of posterior metaventrite and abdominal sternites; **J**, **K** and **L**, tarsi of foreleg, midleg and hindleg, respectively. Scale bars in E and G are 0.1 mm. Abbreviations: **an** (1-11),

antennomere; **bef**, basal elytral fovea; **gf**, gular fovea; **lbr**, labrum; **md**, mandible; **mdat**, mandible apical tooth; **mdim**, mandible inner margin; **mx**, maxilla; **mxp** (1, 2, 3, and 4), maxillary palpomeres; **mxp4as**, maxillary 4 apical sensilla; **omdcn**, ocular-mandibular carina notch; **prstam**, prosternal anterior margin; **ptsc**, pretarsal claw; **s** (III-VIII), abdominal sternites 3 to 8; **sc**, scape (antennomere 1); **ts** (1, 2, and 3), tarsomeres; **vf**, vertexal fovea.

†***Boreotethys grimaldii*** Parker, 2016

(Figs. 3, 4, 14)

Type locality. Myanmar: Kachin, Hukawng Valley, early Cenomanian (age 98.79 ± 0.62 Ma).

Diagnosis. With the genus diagnosis and the following. Ocular-mandibular carinae present, notched. Scape clearly longer than antennomere 2. Eyes strongly prominent laterally. Lateral margins of head, anterior to occipital constriction, strongly diverging anteriorly until meeting the posteriormost perimeter of the compound eye; occipital constriction about 0.75x as wide as width of head just posterior to the eyes. Pronotum wider than long, lacking carinae and cavities. Pretarsal claws single in the meso- and metatarsi and composed of a long claw and an acessory claw in the protarsus.

Examined material. Myanmar: Kachin, Hukawng Valley, Cenomanian deposit (age 98.79 ± 0.62 Ma) [UFV-LABECOL-009191, housed in CELC].

Measurements. ANLr 0.45, ANLs 0.525, MXPL 0.325, HL 0.22, CEL 0.07, PRL 0.22, PRW 0.26, ELL 0.33, ELW 0.455, ABL 0.39, HLL 0.84, TLr 1.26, TLs 1.16.

Preservation. There are many small bubbles adjacent to the body, dorsally concentrated on the head and pronotum, ventrally widespread. Apart from that, the specimen does not seem to have suffered distortion or desiccation. One of its maxillary palps has broken at the level of palpomere 2, but the broken part is next to the legs in the amber matrix.

Notes. Specimen UFV-LABECOL-009191 is very likely conspecific to †*Boreotethys grimaldii*. There

are, however, a few obscured characters in UFV-LABECOL-009191, or in the holotype of †*Boreotethys grimaldii*, or in both, which made it impossible to undoubtfully match them (Fig. 14). The most notable difference between the two, is the overall size, the holotype being slightly smaller. Assuming they were conspecifics, and that some characters are better exposed in the specimen UFV-LABECOL-009191 than in the holotype, the following characters are added to the description of †*Boreotethys grimaldii*: **1**, labral distal margin corners and medial section with minute spines/protrusions (Fig. 4, C); **2**, mandible apical tooth curved, well-developed, inner margin with minute teeth or serration (Fig. 4, D); **3**, left maxillary palp broken off from the specimen (Fig. 3, A and B and Fig. 4, E and G), the palpomeres 1 and base of palpomere 2 remained in the body (Fig. 4, D). Despite that, the shape of the maxillary palp can be fully seen and matches that of holotype's (Fig. 4, D, E and G and Fig. 3, G of Parker, 2016); **4**, the ventral morphology of the head of the holotype was partly photographed and drawn (Fig.3, E and G, respectively, in Parker, 2016). The drawing shows a single, medial gular tubercle and, anterior to it, a pair of larger tubercles. This pair of tubercles protruding as low triangles are likely the basal sclerites of the maxillae, likely the cardo and basistipes (as seen in Fig.3, E of Parker, 2016 and similar to what is seen in †*Cretobythus yini*, Fig.12, D, mx). The specimen UFV-LABECOL-009191 does not provide a good lateral view, ideal to confirm the morphology of these structures, but we strongly suspect that the paired tubercles originally postulated (Fig.3, G of Parker, 2016) were a misinterpretation of the protruded maxillae; **5**, the notched ocular-mandibular carina has been confirmed in UFV-LABECOL-009191. This peculiar trait is shared only with †*Priscaplectus grandiceps* (see Notes of that species); **6**, pretarsal claws in foreleg are bifurcated, unequally developed, those on mid and hindlegs appear to be simple, also similar to †*Priscaplectus* species; **7**, strong backlighting revealed a internal structure beneath sternite VIII, which is likely the aedeagus, indicating specimen UFV-LABECOL-009191 is a male.

†***Boreotethys caii*** Chaul and Lopes-Andrade **sp. nov.**

(Figs. 5, 6, 14)

Type material. Holotype, unique specimen identifier UFV-LABECOL-010376, housed at CELC.

Type locality. Myanmar: Kachin, Hukawng Valley, early Cenomanian (age 98.79 ± 0.62 Ma).

Fig. 5. †*Boreotethys caii* **sp. nov.**, holotype (UFV-LABECOL-010376). **A**, *Habitus*, dorsal view; **B**, *habitus*, ventral; **C**, detail of the right antenna. Scale bars: 0.5 mm (A, B).

Measurements. ANLr 0.58, ANLs 0.674, MXPL 0.268, HL 0.285, CEL 0.095, PRL 0.22, PRW 0.255, ELL 0.42, ELW 0.46, ABL 0.27, HLL 1.12, TLr 1.26, TLs 1.195.

Diagnosis. With the genus diagnosis and the following. Scape very long, about 3x as long as pedicel. Head immediately anterior to eyes strongly narrowed. Antennae with apical three segments forming a distinct club. Legs relatively elongate. Pretarsal claws composed of a single long claw in all legs, accessory claws apparently absent.

Description. **Pilosity**. Filiform, suberect setae cover the body, aparently uniformily, not particularly dense. Setae vary in size in different parts, very short on the legs, medium-sized on the antennae, and longer elsewhere. **Sculpturing**. Surfaces of body appear to be mostly smooth. **Coloration**. Apparently homogeneously light brown, with palpi, and legs lighter than the main body. **Head**. In dorsal view, cephalic capsule long and narrow anterad the eyes; the anterior end (the anterior clypeal margin) strongly convex; immediately posterad the eyes, head 1.6x as broad as the width at the antennal level, but lateral margins from eyes to occiput converge strongly to an occipital constriction as narrow as the anterior section of the head. Antennal tubercles low and not linked by a transversal interantennal ridge; the antennal tubercles seem to gradually low down to the level of the forns posteriorly up to the eye level, but medially to them and not forming an ocular-antennal ridge. Compound eyes strongly protruding laterally, with about 50 ommatidia. Frontovertexal surface of difficult visualization due to bubbles, apparently without large cavities, only having vertexal foveae (all features uncertain). In lateral view, a carina in front of the eye might represent the pair of ocular-mandibular carinae or the single ocular-clypeal arched carina, difficult to confirm due to a limited lateral view of the head. Ventral surface of head difficult to describe due to a fracture; large cavities absent, gular tubercle likely absent, gular foveae likely present, small. Mandibles relatively robust, forming a flatenned blade; outer surfaces curved, inner margin with various small teeth; apical teeth not visible in right mandible; left mandible

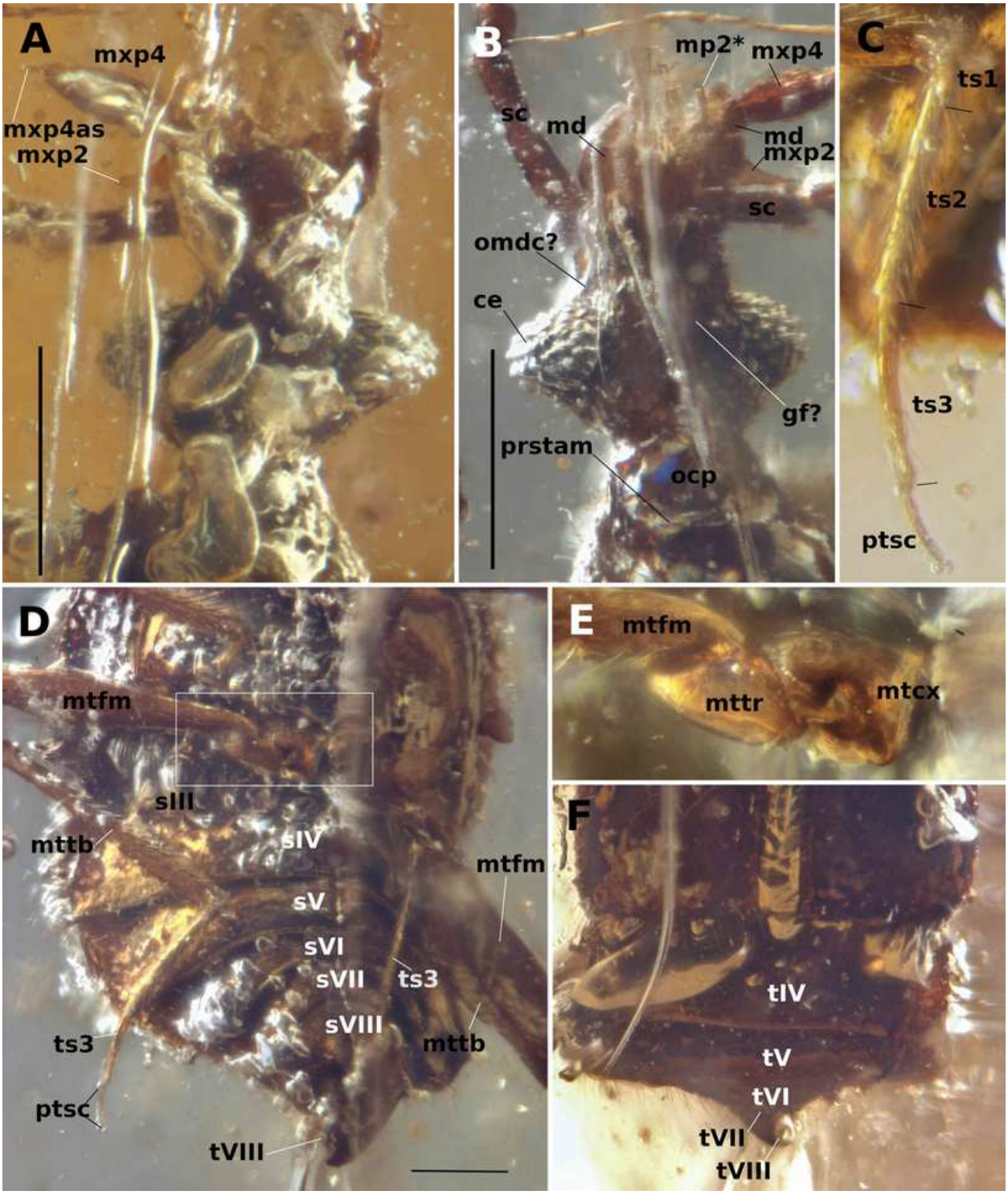

Fig. 6. †*Boreotethys caii* **sp. nov.**, holotype (UFV-LABECOL-010376). Scale bars: 0.2 mm (A, B); 0.1 mm (D). Abbreviations: **ce**, compound eye; **gf**, gular fovea; **md**, mandible; **mtcx**, metacoxa; **mtfm**, metafemur; **mttb**, metatibia; **mttr**, metatrochanter; **mxp (2 and 4)**, maxillary palpomeres; **mxp4as**, maxillary 4 apical sensilla;

ocp, occiput; **omdc**, ocular-mandibular carina; **prstam**, prosternum anterior margin; **ptsc**, pretarsal claw; **s (III-VIII)**, abdominal sternites 3 to 8; **sc**, scape (antennomere 1); **t (IV-VIII)**, abdominal tergites 3 to 8; **ts (1, 2, and 3)**, tarsomeres.

apex broken. Labrum not seen, although the view for its expected position is free (possibly lost). Mentum and labial palps not visible. Maxillary palp well developed; only left palp remains, broken, but the broken part is next to the head; palpomere 1 not visible; palpomere 2 anterior half cylindrical and thin, posterior half drastically enlarged; palpomere 3 not seen; palpomere 4 fusiform, its apical sensilla small. Antennae with very long scape, about as long as antennomeres 2 to 5 together; pedicel subquadrate, but slightly inflated laterally; antennomeres 3 to 8 subequal; antennomeres 9 to 11 forming a very distinct club, with 9 and 10 being trapezoidal, and 11 fusiform. **Pronotum**. Broadest at a level slightly anterior to midlength, its maximum width about 0.7x the maximum elytra width; slightly wider than long; its posterior width 0.82x the maximum width; and its anterior width (at the occipiput-pronotal articulation/foramen) 0.45x the maximum width. Anterior margins almost straight up to widest level; posterior to widest level, margins mildly convex and converging. Pronotal carinae and cavities apparently absent; antebasal sulcus likely absent; presence of lateral and medial antebasal foveae hard to confirm. **Elytra**. Bell-shaped, lateral margins diverging at the anterior third and subparallel from second third to posterior end. Sutural stria conspicuous; discal carinae absent; at least one pair of basal elytral foveae present, from which a pair of discal sulci arise and follow posterad up to the end of the anterior third; marginal striae likely present; subhumeral foveae not confirmed; elytral posterolateral cleft absent. Hind wings not visible. **Legs**. Legs somewhat elongate; femora strong, thick medially and not particularly long; tibiae and tarsi thin and long; pretarsal claw single and relatively long. Spines, tubercles or protrusions, usually interpreted as male sexual secondary characters, absent on all legs. Metacoxae mildly projected posteroventrally, juxtaposed. Tarsomere 2 much larger than tarsomere 1

and subequal to tarsomere 3. **Abdomen**. In dorsal view tergites IV and V subparallel and as broad as elytra; tergites converge from VI to VIII; tergite VIII "hood-like"; a tergite IX could be present below the middle portion of tergite VIII. Relative lengths of tergites in relation to one another difficult to ascertain, as abdomen is considerably curved, but tergites IV and V appear to be subequal and the longest. Paratergites visible in segments IV and V; sternites progressively smaller from VI to VIII, their distal margins concave, being strongly concave in sternite VI. Division between tergites and sternites strongly marked. **Foveation pattern**. Foveae which are more evident (but see Table 1): vertexal (one pair, large); gular (a pair?); basal elytral (at least one pair).

Sex. Undetermined.

Preservation. Body dessication, torsion or wrinkling is minimal, but other artifacts makes the examination of the holotype extremely challenging. The anterior section of head has suffered considerable damage: the apex of the left mandible is broken, labrum has presumably been lost, right maxillary palp has been completely lost, and the left one is broken, but the broken part is close to the head in the amber matrix. There are a lot of bubbles adjacent to the surfaces of the body, what prevents a complete description of several important details. A fracture goes along the whole main longitudinal axis of the body in ventral view, causing mirroring.

Comments. †*Boreotethys caii* is very different from †*B. arctopteryx* and †*B. grimaldii* in the species level to a point that congenericity between it and the two could be questioned. Even though †*B. caii* could well be described in a different genus, the holotype preservation was not ideal to allow a satisfactorily generic description. We assumed a conservative approach at the generic level and attributed the new species to the genus it fit the most. We believe the generic boundaries between the Cretaceous pselaphine genera are likely to be considerably reinterpreted, and †*B. caii* is probably one of the species that would suffer generic change. At the species level, though, the peculiarities of †*B. caii* are enough to allow that newly found conspecific specimens to be readly matched to it and, therefore, the species

description is justified.

Etymology. Named in honor of the prolific paleontologist and coleopterist Chen-Yang Cai. The name was created by adding the singular Latin genitive case suffix -i to the last name of a male person. The orthography of an eponym is unchangeable and does not depend on the generic name for which the epithet is used.

†***Cretobythus*** Yin, Parker and Cai, 2017

Type species. †*Cretobythus excavatus* Yin, Parker, Cai, Huang and Li, 2017.

Diagnosis. Body dorsoventrally flattened. Antennae with apical three antennomeres forming a club, sometimes loosely-formed. Maxillary palpomere 4 large, sometimes enormous. Frontovertexal areae with deep excavation that is delimited laterally by the ocular-antennal ridges and anteriorly by the interantennal ridge; excavation is not delimited posteriorly, where it becomes gradually shallower until it is leveled to the posterior vertexal surface. Interantennal ridge well-developed. Antennal tubercles notches present. Ocular-antennal ridges well-developed. Medial, longitudinal carina at the occipital constriction present. Pronotal lateral longitudinal carinae present, restricted to the posterior half; posteromedial carina present, sometimes inconspicuous; posteromedial and posterolateral cavities present; antebasal sulcus absent. Metacoxae contiguous or slightly separated. Tarsomere 2 much larger than 1 and shorter or subequal to tarsomeres 3. Pretarsal claws, apparently in all legs, composed of a main, developed claw plus a secondary, reduced one (sometimes extremely, "seta-like").

†***Cretobythus excavatus*** Yin, Parker, Cai, Huang and Li, 2017

(Fig. 14)

Fig. 7. †*Cretobythus parkeri* sp. nov. holotype (UFV-LABECOL-009897). **A**, *Habitus*, dorsal view; **B**, *habitus*, ventral (detail of profemoral apical spines); **C**, habitus, lateral view. Scale bars: 0.2 mm.

Type locality. Myanmar: Kachin, Hukawng Valley, early Cenomanian (age 98.79 ± 0.62 Ma).

Diagnosis. With the genus diagnosis and the following. Head in dorsal view, from vertex to interantennal ridge, subtrapezoidal. Apical antennomere round, without notch; antennomere 10 transverse; antennal club loosely formed. Eyes relatively large, much larger than palpomere 3; laterally directed. Maxillary palpomere 4 large and ovoid.

†***Cretobythus parkeri*** Chaul and Lopes-Andrade **sp. nov.**

(Figs. 7-10, 14)

Type material. Holotype, unique specimen identifier UFV-LABECOL-009897, housed at CELC. (Figs. 7, 8 and 14). Paratype, unique specimen identifier UFV-LABECOL-009218, housed at CELC (Figs. 9, 10, and 14).

Type locality. Myanmar: Kachin, Hukawng Valley, early Cenomanian (age 98.79 ± 0.62 Ma).

Measurements. ANLr 0.45 (0.4), ANLs 0.465 (0.44), MXPL 0.215 (0.24), HL 0.195 (0.16), CEL 0.07 (0.07), PRL 0.23 (0.205), PRW 0.19 (0.225), ELL 0.34 (0.31), ELW 0.35 (0.43), ABL 0.38 (0.44), HLL 0.78 (0.71), TLr 1.16 (1.19), TLs 1.145 (1.115) (paratype measurements in brackets).

Diagnosis. With the genus diagnosis and the following. Head in dorsal view, from vertex to interantennal ridge, subtrapezoidal; in lateral view, head not narrowed at the eye level; interantennal ridge straight. Apical antennomere cylindrical/fusiform, slightly constricted at mid-length, notched apically in the holotype on the inner-ventral portion of the apex; antennomere 10 subquadrate. Maxillary palpomere 4 in the paratype basal and inner surfaces angulate in relation to each other, outer surface evenly curved (holotype's might be compressed due to a crack in the sclerite). Pronotum about as long as wide or slightly longer than wide. Protibia outer surface crenulate. Pretarsal claws composed of a

main, developed claw plus a secondary, very reduced one (secondary claw seen on foreleg of the holotype and middle leg of the paratype).

Description. **Pilosity**. Filiform setae cover the body, relatively dense but not easily seen without proper illumination. Setae on the antennae and legs, small, suberect; dorsally on the head, pronotum, elytra, and on abdominal tergites, recurved and slightly raised; on meso- and metaventrites and abdominal sternites, setae smaller, decumbent to appressed. Setation in paratype harder to ascertain due to preservation, but most likely in accordance to holotype's. **Sculpturing**. Surfaces

of body appear to be mostly smooth. Piligerous punctae relatively dense across the dorsal surfaces of the head in the paratype. **Coloration**. Apparently reddish brown, with maxillary palpi, legs and antennae lighter than the main body. Paratype having the main body darker, but might be a result of preservation. **Head**. In dorsal view, ocular-antennal ridges slightly concave, sub-parallel in relation to each other or, at most, mildly converging anteriorly up to the antennal tubercles; ocular-antennal ridges in right angle with interantennal ridge; interantennal ridge straight in dorsal view (slightly concave in anterior view). Antennal tubercles notched. Head just posterior to the eyes about 1.8x wider than at the level of interantennal ridge. Posterior to the eyes, lateral margins strongly converging to occipital constriction (head immediately posterior to the eyes 1.6x as wide as occipital constriction in the holotype). Compound eye medium sized (having approximately 40 ommatidia), larger than maxillary palpomere 3, but smaller than maxillary palpomere 4, facing anterolaterally. Longitudinal median occipital constriction carina present,more developed posteriorly, on the occiput surface, and fading at the vertexal surface. Frontovertexal area with strong heart-shaped excavation, broadest and shallower posteriorly, funneling and deepening anteriorly to immediately below the midpoint of the antennal ridge; vertexal foveae at the posterior end of the excavation, with a patch of fine setae surrounding them.

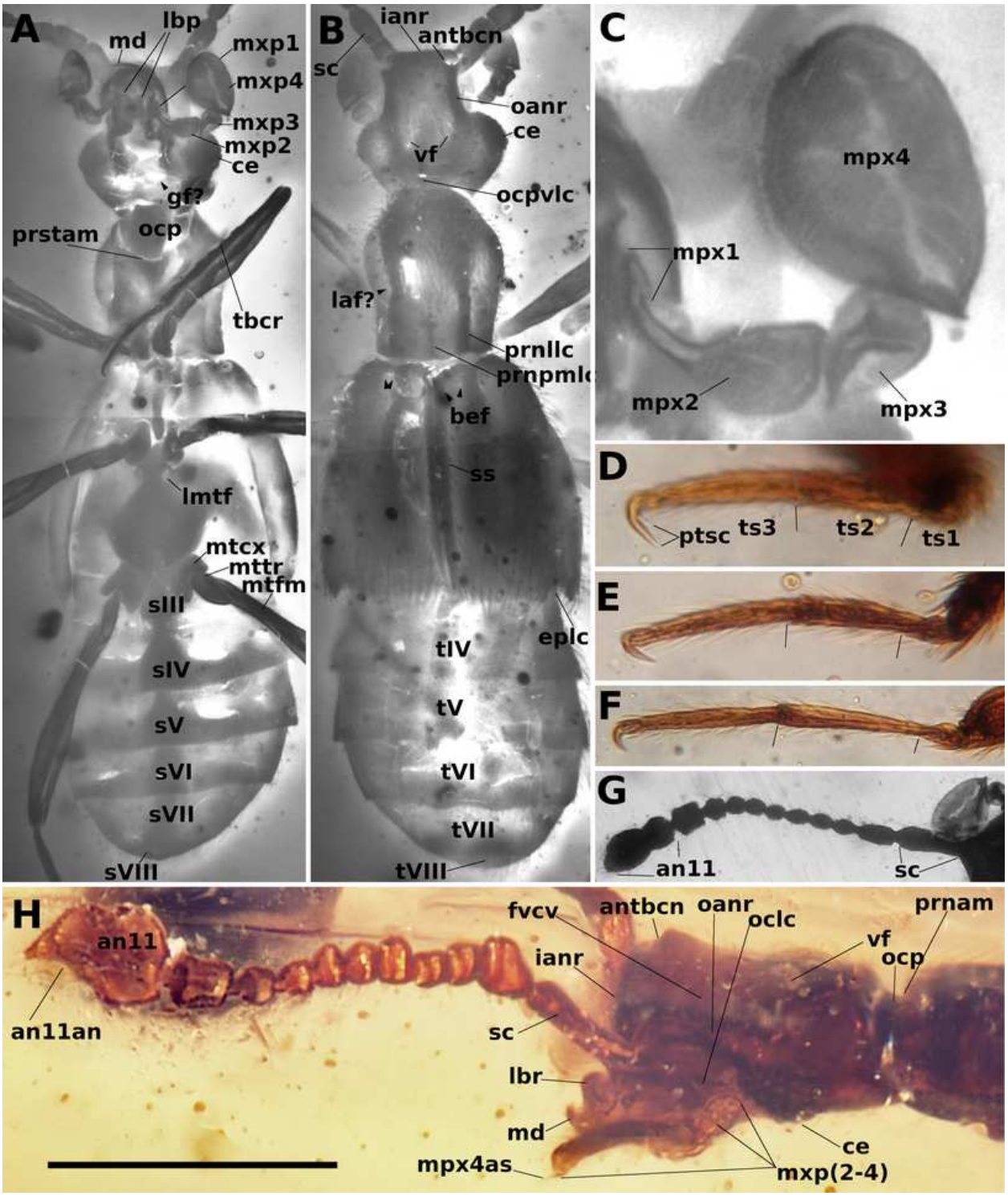

Fig. 8. †*Cretobythus parkeri* **sp. nov.** holotype (UFV-LABECOL-009897). **A** and **B**, body under fluorescent light, ventral and dorsal, respectively; **C**, ventral view of left maxillary palp; **D**, **E** and **F**, tarsi of foreleg, midleg and hindleg, respectively; **G**, detail of left antenna; **H**, detail of head in lateral view. Scale bar: 0.2 mm (H). Ab-

breviations: **an (11)**, antennomere; **an11an**, antennomere 11 apical notch; **antbcn**, antennal tubercle notch; **bef**, basal elytral fovea; **ce**, compound eye; **eplc**, elytral posterolateral cleft; **fvcv**, frontovertexal cavity; **gf**, gular fovea; **ianr**, interantennal ridge; **laf**, lateral antebasal fovea; **lbp**, labial palp; **lbr**, labrum; **lmtf**, lateral metaventrite fovea; **md**, mandible; **mtcx**, metacoxa; **mtfm**, metafemur; **mttr**, metatrochanter; **mxp (1, 2, 3, and 4)**, maxillary palpomeres; **mxp4as**, maxillary 4 apical sensilla; **oanr**, ocular antennal ridge; **ocp**, occiput; **ocpvlc**, occipital-vertexal longitudinal carina; **oclc**, ocular-clypeal carina; **prnllc**, pronotal lateral longitudinal carina; **prnam**, pronotal anterior margin; **prnpmlc**, pronotal posteromedial longitudinal carina; **prstam**, prosternum anterior margin; **ptsc**, pretarsal claw; **s (III-VIII)**, abdominal sternites 3 to 8; **sc**, scape (antennomere 1); **ss**, sutural stria; **t (IV-VIII)**, abdominal tergites 4 to 8; **tbcr**, tibial crenulation; **ts (1, 2, and 3)**, tarsomeres; **vf**, vertexal fovea.

In lateral view, compound eyes connected to antennal tubercles by an ocular-antennal ridge; ocular-clypeal carina present, contouring the head from eye to eye across the anterior clypeal margin; surface from interantennal ridge to anterior clypeal margin steep, almost straight; labrum small, but robust. Head without strong dorsoventral constriction at any level; greatest cephalic capsule depth at the interantennal ridge level. Ventral surface of head damaged, with a very large cavity, part of which seems artifactual; gular fovea likely present, posterior to the cavity; gular tubercle likely absent. Outer margins of mandible evenly curved; apical tooth long. Maxillary palps with first palpomere very small; second palpomere elongate, basally cylindrical, strongly clubbed and anteriorly curved; palpomere 3 subtrapezoidal, about the size of the club of palpomere 2; palpomere 4 the largest, somewhat ovoid, with oblique base; in the paratype its basal and inner surfaces are conspicuously angled (the two palpomeres 4 of each specimen of the type series appear to have sufferred crushing); maxillary palpomere 4 apical sensilla small, thin and elongate. Labial palp visible in the holotype, about as long as basal half (the stalk) of maxillary palpomere 2. Scape moderately elongate, about as long as antennomeres 2 and 3 together; antennomeres 3 to 8 about the same size; antennomeres 9 to 11 forming a club; antennomere 10

roughly subquadrate, as long as wide or longer than wide; apical antennomere twice as long as wide, cylindrical, with notched apex ventromedially. In the holotype, in lateral view, antennomeres 5 to 7 of left antenna are slightly offset from the main axis of the antenna (could be artifactual). **Pronotum**. Pronotum overall bell-shaped, broadest at a level anterior to midlength, its maximum width slightly more than half elytra width; slightly longer than wide (not in the paratype, but could be artifactual); its posterior width is 0.84x the maximum width; and its anterior width (at the occipiput-pronotal articulation/foramen) 0.52x the maximum width. Anterior margin evenly curving to lateral margins, which are mildly concave and converging posterior to pronotal midlength. Pronotal lateral longitudinal carinae distinct, thick (more like ridges); mediobasal carina weak, barely seen (well-marked in the paratype, but small); cavity in between longitudinal carinae deep and large, restricted to posterior half of pronotum; cavities lateral to the longitudinal carinae shallower and elongate, reaching anterior half of pronotum. Antebasal sulcus absent. Lateral antebasal foveae within the medial cavity, mesad the pronotal longitudinal carinae (maybe a second par is present laterad them). **Elytra**. Elytra lateral margins convex and diverging up to second third, mildly converging at the posterior third; marginal striae conspicuous; discal striae poorly-marked, low and thick, separating anteriorly the basal elytral fovea. Basal elytral foveae, four pairs. Elytral posterolateral lobe and cleft evident. Hind wings present (not visible in the paratype). **Legs**. Femora and tibiae thicker apically; profemur with a pair of low spines on the medioapical surface; meso- and metafemora mildly clavate. Tibial outer surfaces crenulate at distal to mid-length, strongly marked on the fore leg. Longer spines, tubercles or protrusions, usually interpreted as sexual secondary characters, absent on all legs. First tarsomere very small when compared to the others; second and third subequal in length. Pretarsal claws paired, composed of a developed claw and a minute, seta-like acessory claw. Pro- and mesocoxae juxtaposed; metacoxae can be slightly separated (difficult to ascertain); metacoxae conspicuously projected posteroventrally.

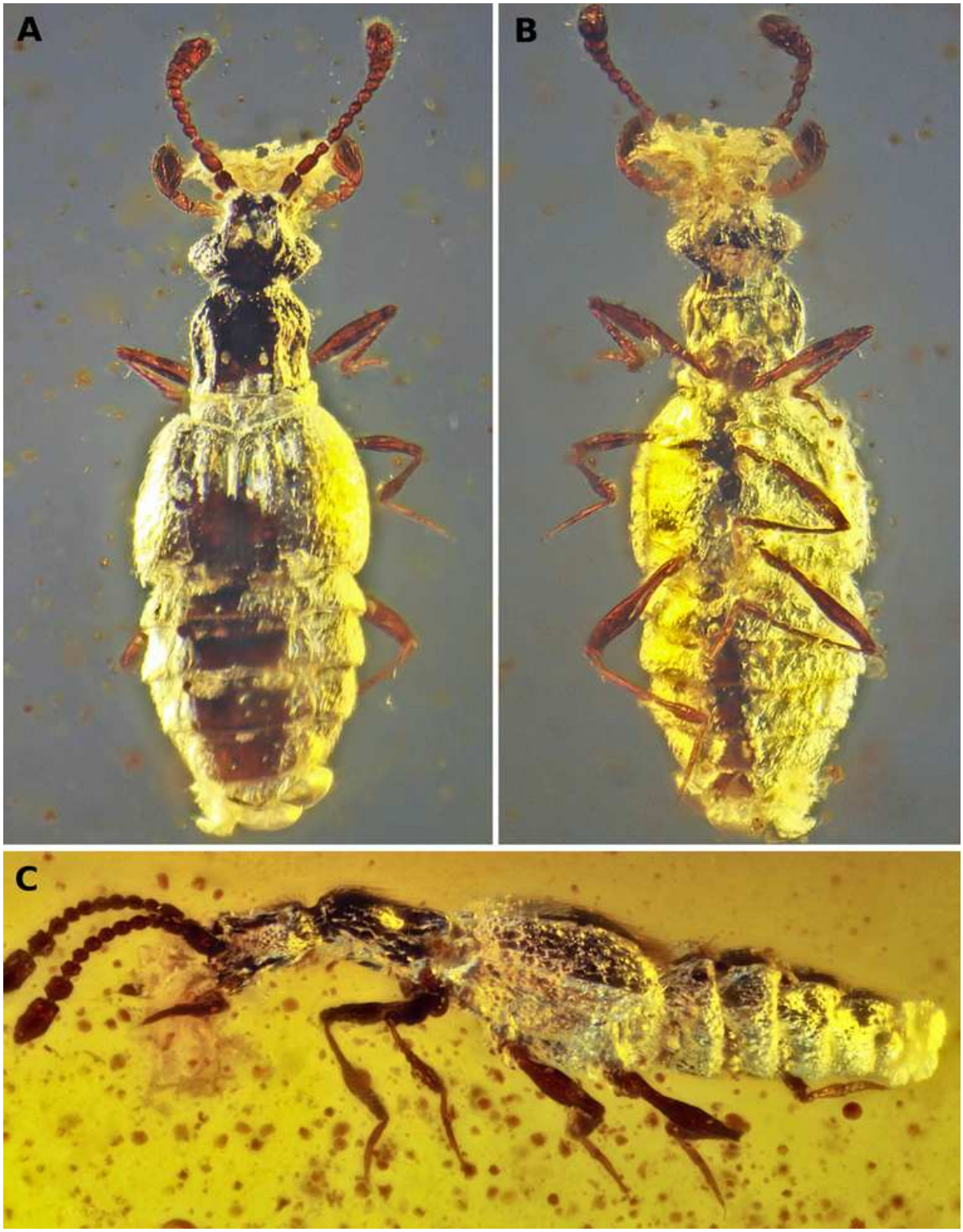

Fig. 9. †*Cretobythus parkeri* **sp. nov.** paratype (UFV-LABECOL-009218). **A**, *Habitus*, dorsal view; **B**, *habitus*, ventral; **C**, habitus, lateral view.

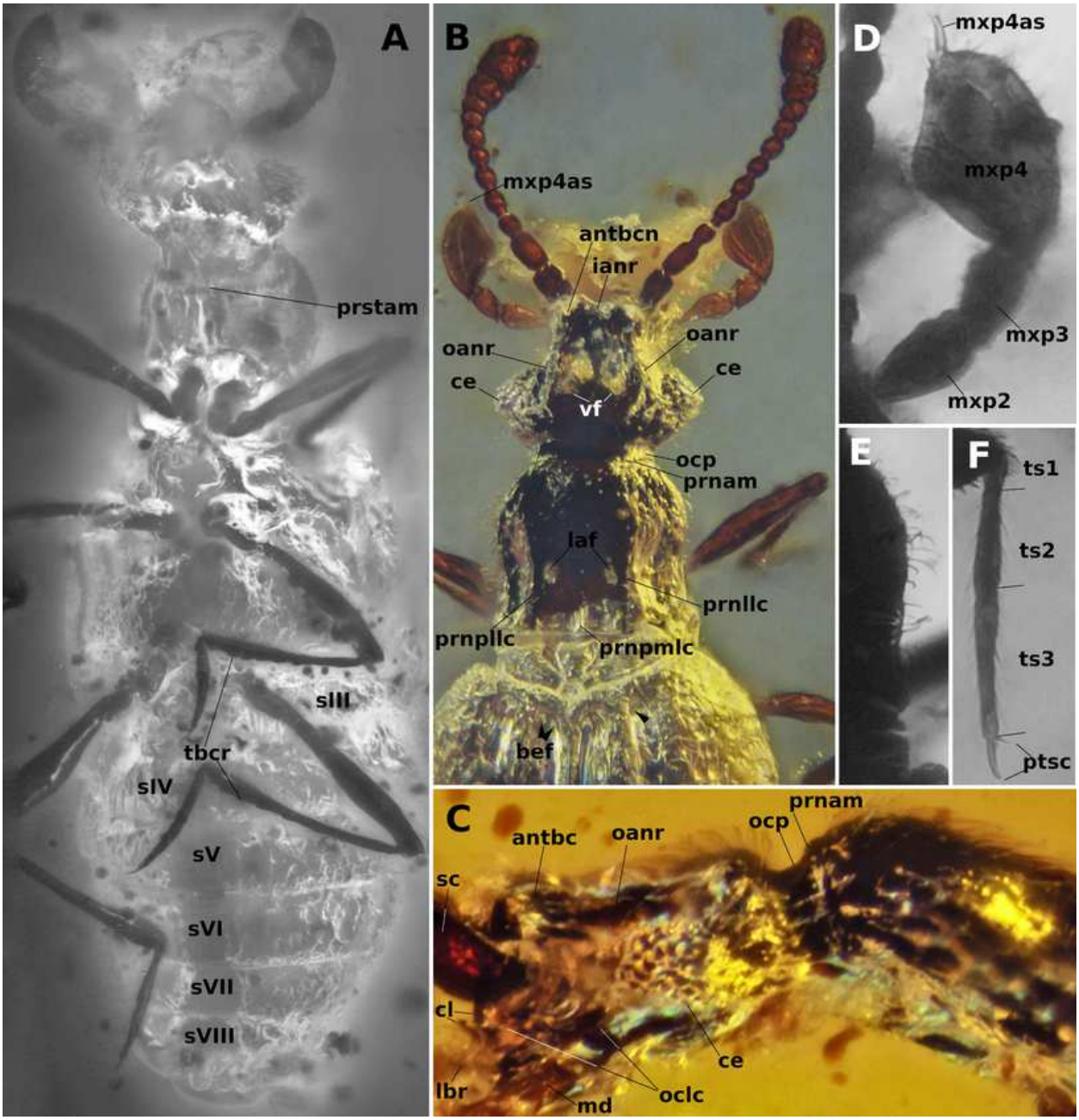

Fig. 10. †*Cretobythus parkeri* **sp. nov.** paratype (UFV-LABECOL-009218). **A**, ventral view of the body under fluorescent light; **B**, detail of the dorsum of the pronotum and head; **C**, detail of head in lateral view; **D**, detail of left maxillary palp in ventral view; **E**, lateral margin of the pronotum evincing pilosity; **F**, detail of right meso-tarsus. Abbreviations: **antbc**, antennal tubercle; **antbcn**, antennal tubercle notch; **bef**, basal elytral fovea; **ce**, compound eye; **cl**, clypeus; **ianr**, interantennal ridge; **laf**, lateral antebasal fovea; **lbr**, labrum; **md**, mandible; **mxp** (1, 2, 3, and 4), maxillary palpomeres; **mxp4as**, maxillary 4 apical sensilla; **oanr**, ocular antennal ridge;

ocp, occiput; **oclc**, ocular-clypeal carina; **prnam**, pronotal anterior margin; **prnllc**, pronotal lateral longitudinal carina; **prnpmlc**, pronotal posteromedial longitudinal carina; **prstam**, prosternum anterior margin; **ptsc**, pretarsal claw; **s** (III-VIII), abdominal sternites 3 to 8; **tbcr**, tibial crenulation; **ts** (1, 2, and 3), tarsomeres; **vf**, vertexal fovea.

Abdomen. Tergites IV to VI strongly concave in the holotype, likely artifactual. Lateral margins convex, diverging from tergite IV to V and then converging from VI to VIII. Tergite V the widest, slightly narrower than elytra; tergite lengths from IV to VII subequal; VIII the smallest. Paratergites distinct from segment IV to VII, relatively thick, the pair on tergite V about 0.4x the entire width. **Foveation pattern**. Foveae which are more evident (but see Table 1): vertexal (one pair, large); gular (a single?); lateral antebasal (likely two pairs, in relation to the pronotal longitudinal carinae, the lateral pair is more evident than the medial); basal elytral (four pairs, small); lateral metaventrital (one pair).

Sex. Undetermined for both holotype and paratype.

Preservation. Holotype overall greatly preserved, with wrinkled cuticle ventrally on the head and prothorax, and apparently some crushing to the maxillary palps. Apex of antennomere 11 of left antenna has been sanded off during the making of an additional facet to reveal the head in anterior view (an image made of this facet is available in the multi-entry key). Paratype with mildly desiccated/wrinkled surfaces. Both apical maxillary palpomeres appear to be dorsoventrally compressed, but slightly better preserved than in the holotype. There is a diffuse whitish debris blocking the view of the mouthparts and clypeus (maybe secreted by the beetle). In most of elytra and lateral portions of the abdomen the amber matrix has slightly detached from the surfaces of the specimen forming a silvery cast that has the specimen shape, but is considerably larger (real size of specimen can be seen with difficulty through the cast).

Notes. †*Cretobythus parkeri* shares intriguing similarities with †*Protrichonyx rafifrons*, namely: the

notched apical antennomere, the anterolateral orientation of the eyes, the antennal tubercles notches, pronotal lateral carinae (mild in †*Protrichonyx*), and medial pronotal cavity. Some characters, however, guarantee they are not conspecifics: the transversal vertexal ridge of †*P. rafifrons* and absent in †*C. parkeri*, the denser pilosity in †*P. rafifrons*, the metatrochanter process present in †*P. rafifrons* and apparently absent in †*C. parkeri*, and the overall size, with †*P. rafifrons* larger than †*C. parkeri*. †*Protrichonyx rafifrons* has been described based on a badly preserved specimen. Considering the newly described species of †*Cretobythus* described in this paper and the new genus diagnosis, the boundaries between †*Protrichonyx* and †*Cretobythus* might be revealed blurred when new material of †*P. rafifrons* is found.

Etymology. The specific epithet is in honor of the British biologist and staphylinologist Joseph Parker. The name was created by adding the singular Latin genitive case suffix -i to the last name of a male person. The orthography of an eponym is unchangeable and does not depend on the generic name for which the epithet is used.

†*Cretobythus yini* Chaul and Lopes-Andrade sp. nov.

(Figs. 11, 12, 14)

Type material. Holotype, unique specimen identifier UFV-LABECOL-009210, housed at CELC.

Type locality. Myanmar: Kachin, Hukawng Valley, early Cenomanian (age 98.79 ± 0.62 Ma).

Holotype measurements. ANLr 0.45, ANLs 0.445, MXPL 0.32, HL 0.2, CEL 0.05, PRL 0.2, PRW 0.22, ELL 0.3, ELW 0.44, ABL 0.34, HLL 0.86, TLr 1.1, TLs 1.04.

Diagnosis. With the genus diagnosis and the following. Head in dorsal view, from vertex to interantennal ridge, subquadrate. Apical antennomere round, without notch; antennomere 10 slightly wider than long. In lateral view, head strongly narrowed at the eye level. Maxillary palpomere 4 inner and basal

surfaces angled. Interantennal ridge straight. Occiput relatively narrow. Pronotum about as long as wide. Protibial outer surface not crenulate.

Description. Pilosity. Dense filiform, thin setae covering the body, giving a lanuginose overall appearance. Setae on the antennae and legs suberect; on the maxillary palps suberect to erect (a few setae having a curved tip, likely artifactual); recurved, flexuous, and decumbent to semidecumbent setae dorsally and ventrally on head, pronotal disc, elytra, and abdominal tergites. Ventrally on thorax and on abdominal sternites, setae appearing not as abundant as on each corresponding tergite. **Sculpturing.** Surfaces of body appear to be mostly smooth. Anterior pronotum may be mildly punctate, elytra and abdominal tergites smooth to at most shagreenate. **Coloration.** Apparently brown, with palpi, legs and antennae possibly reddish brown. **Head.** In dorsal view, subquadrate from occipital constriction to interantennal ridge (excluding eyes); margins posterior to the eyes strongly curving to an almost straight vertexal margin; occipital constriction relatively narrow (head width immediately posterior to the eyes 2.4x occipital constriction width); margins anterior to the eyes until antennal tubercles notches (=edges of ocular-antennal ridges) mildly concave; interantennal ridge roughly straight. Head just posterad the eyes about 1.3x as wide as interantennal ridge. Longitudinal median occipital carina present. Frons and vertex with strong excavation, triangular or heart-shaped, broadest posteriorly, funneling anteriorly to below the midpoint of antennal ridge; vertexal foveae likely present at the posterior end of the excavation, covered by dense patch of surrounding setae. Eyes small, strongly bulging, about as large as third maxillary palpomere; each with approximately 30–40 small ommatidia. Antennal tubercles notches distinct. In lateral view, cephalic capsule strongly narrowed or constricted at eye level, broadened anterior to it at the interantennal ridge level (greatest head depth), and posterior to it at the vertexal level (only mildly broadened), this narrowing or constriction makes head profile roughly hourglass-shaped; surface from interantennal ridge to anterior clypeal margin oblique, forming a ridge just anterior to the convex-anterior clypeal margin. In ventral view, converging margins from eyes to maxillae bases angled or car-

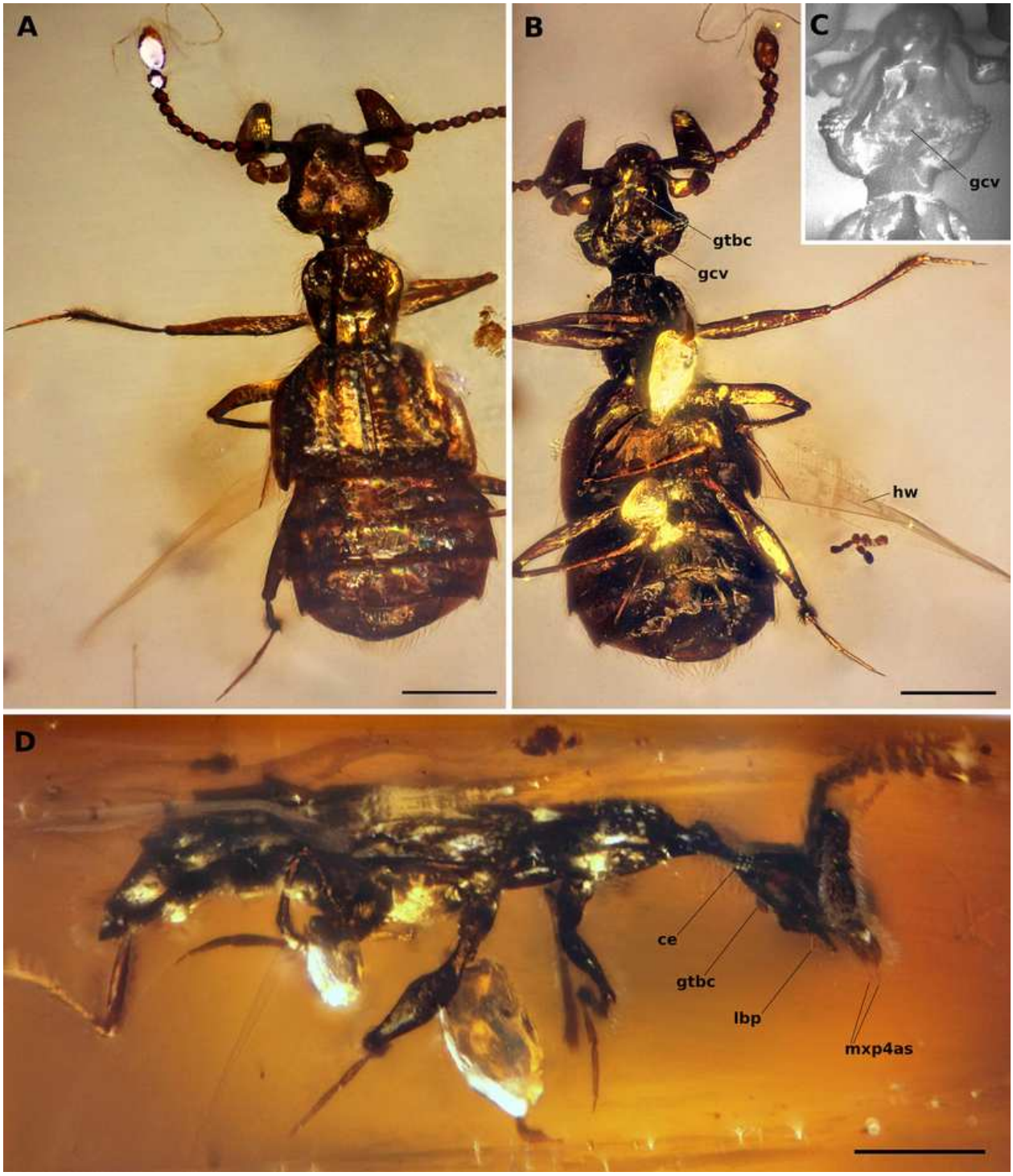

Fig. 11. †*Cretobythus yini* **sp. nov.** holotype (UFV-LABECOL-0009210). **A**, *Habitus*, dorsal view; **B**, *habitus*, ventral; **C**,detail of ventral view of the head under fluorescent light; **D**, habitus, lateral view. Scale bars: 0.2 mm (A, B, D). Abbreviations: **ce**, compound eye; **gcv**, gular cavity; **gtbc**, gular tubercle; **hw**, hind wing; **lbp**, labial palp; **mxp4as**, maxillary 4 apical sensilla.

inated (in this view, the ocular-antennal ridges seen as shelf-like projections behind margins). Outer margins of mandibles evenly curved; no other aspect of mandible morphology was visible. Labrum about 3x wider than long; lateral margins convex, slightly diverging from clypeo-labral articulation to apex; apicolateral corners sharply angled, distal margin straight to mildly convex, with a pair of minute teeth medially (likely dentiform setae). First maxillary palpomere very small, cone-shaped; second palpomere long, basally cylindrical, strongly clubbed posterior to its midlength, its apical half somewhat quadrate/blocky; third palpomere trapezoidal, about the size of the apical club of the preceding palpomere; apical palpomere greatly enlarged, somewhat cone-shaped, with oblique rather than flat base; its apical sensilla ("apical pseudosegment" or "palpal cone") very small, much longer than wide, truncate apically. In lateral view, bases of maxillae protruding as a pair of low triangles; immediately posterior to the oral cavity, a single, median tube-like tubercle is present. Posterior to the tubercle there is a large cavity (seen in ventral view) which presumably harbor the gular fovea/foveae. Ventral surface of head with long and flexuous setae concentrated around the cavity and with smaller and denser setae surrounding the inner border of the cavity. Labial palpomere 2 (the longest) is slightly longer and thicker than apical sensilla of maxillary palpomere 4. Antenna with scape moderately elongate, about as along as antennomeres 2 and 3 together; antennomeres 3 to 8 about the same size; antennomeres 9 to 11 forming a club; antennomere 10 transverse, clearly wider than long; apical antennomere 1.25x as long as wide, oval, without a notched apex ventromedially. **Pronotum**. Broadest at anterior third; as wide as half elytral width and about as wide as head at eye level (eyes not included). Pronotum about as long as wide; posterior width 0.8x the maximum width; anterior articulation area with occiput about 0.4x the maximum pronotal width; anterior pronotal margin evenly curving to the lateral margins, which are more or less straight and converging posteriorly until the posterolateral corners; posterior margin slightly convex; right lateral margin crenulate at mid third (could be artifactual); posteromedial longitudinal carina weak; lateral longitudinal carinae strongly marked from posterior margin to about

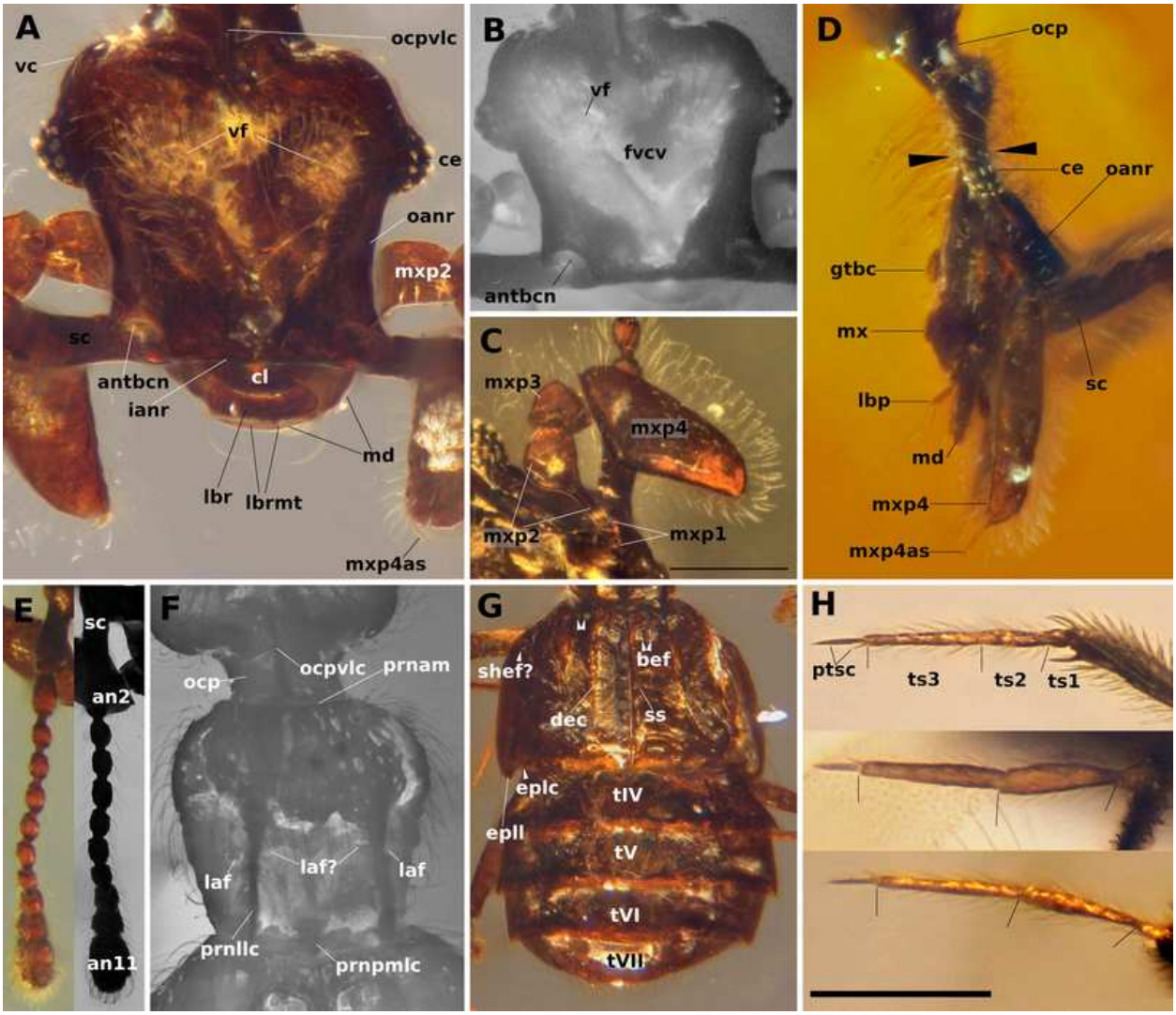

Fig. 12. †*Cretobythus yini* **sp. nov.** holotype (UFV-LABECOL-0009210). **A**, dorsal view of head ; **B**, frontovertexal area (cavity) under fluorescent light; **C**, detail of right maxillary palp in ventral view; **D**, lateral view of head; **E**, Detail of right antenna (left image from stereomicroscope, right from light microscope evincing thickened setae on antennomere 11 apex); **F**, detail of pronotum under fluorescent light; **G**, elytra and abdominal tergites; **H**, tarsi, from top to bottom: foreleg, midleg and hindleg. Scale bar: 0.1 mm (H). Abbreviations: **an (2, 11)**, antennomere; **antbcn**, antennal tubercle notch; **bef**, basal elytral fovea; **ce**, compound eye; **cl**, clypeus; **dec**, discal elytral carina or ridge; **eplc**, elytral posterolateral cleft; **epll**, elytral posterolateral lobe; **fvcv**, fronto-vertexal cavity; **gtbc**, gular tubercle; **ianr**, interantennal ridge; **laf**, lateral antebasal fovea; **lbp**, labial palp; **lbr**, labrum; **lbrmt**, labral medial teeth on labral distal margin; **md**, mandible; **mxp (1, 2, 3, and 4)**, maxillary

palpomeres; **mxp4as**, maxillary 4 apical sensilla; **oanr**, ocular antennal ridge; **ocp**, occiput; **ocpvlc**, occipital-vertexal longitudinal carina; **prnam**, pronotal anterior margin; **prnllc**, pronotal lateral longitudinal carina; **prnpmlc**, pronotal posteromedial longitudinal carina; **ptsc**, pretarsal claw; **sc**, scape (antennomere 1); **shef**, sub-humeral elytral fovea; **ss**, sutural stria; **t (IV-VII)**, abdominal tergites 4 to 7; **ts (1, 2, and 3)**, tarsomeres; **vf**, ver-texal fovea.

mid-length of pronotal disc; single, large discal cavity in between the lateral longitudinal carinae and a pair of smaller cavities laterally to the carinae; without antebasal sulcus.

Elytra. Lateral margins diverging on the anterior third, and being more or less straight to slightly diver-gent posterior to that, forming a lobe between the lateral and apical (posterior) margins; lobe followed medially by an elytral posterolateral cleft; apical elytral margins straight to mildly concave; one pair of discal carinae marked from base to about midlength; sutural striae present; marginal striae not evident; four pairs of basal elytral foveae, two between the discal carinae and the sutural striae, and two laterally to the discal carinae. Hind wings normally

developed. **Legs**. Spines or protrusions absent on all legs. Tibiae, particularly pro- and metatibiae curved and somewhat thicker apically, their outer surfaces even. First tarsomere very small when com-pared to the others; second and third subequal in length. Pretarsal claws each with a pair of one devel-oped claw and one minute, seta-like claw. Pro-, meso- and metacoxae juxtaposed; metacoxae with pos-terodorsal projections. **Abdomen**. Lateral margins convex, diverging from tergite IV to V and then converging from tergites VI to VIII; tergite V being the widest, slightly broader than elytra. Length of tergites from IV to VII subequal. Paratergites evident, the pair on tergite V about 0.4x the entire width (tergite plus paratergites); on the other segments, paratergites relatively smaller. Tergite VIII small, convex.

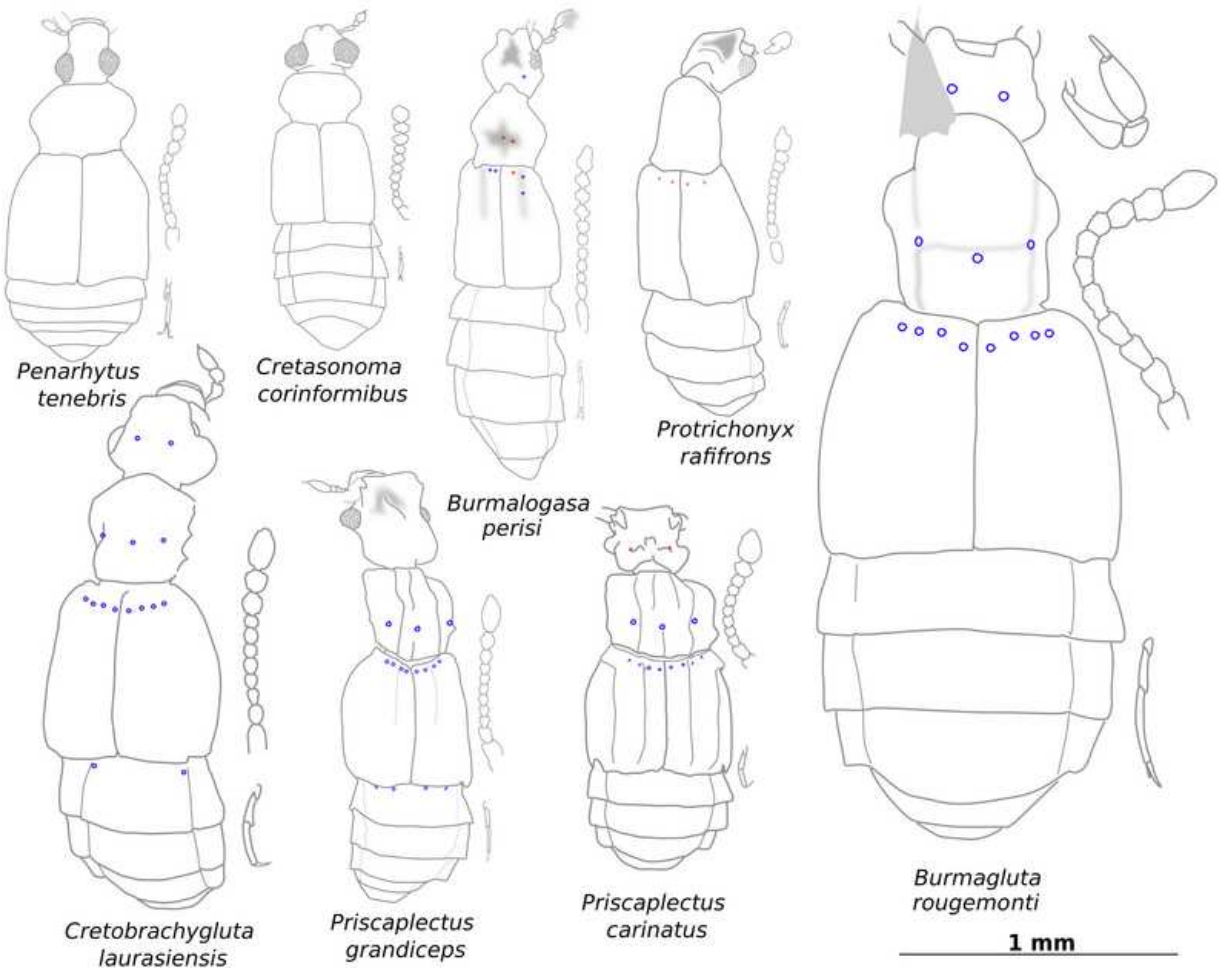

Fig. 13. Habitus of the Cretaceous Pselaphinae with detail of antenna and tarsus next (right side) of each species. Figure in the same scale as Fig.14.

Foveation pattern. Most evident foveae (but see Table 1): vertexal (one pair, large); gular (presumably within the enormous gular cavity); lateral antebasal (two pairs, one pair at each side of the pronotal longitudinal carinae); basoelytral (four pairs, small); lateral mesocoxal (one pair).

Sex. Undetermined, but the presence of a gular tubercle suggests it is a male.

Preservation. Specimen included in a roughly triangular piece and has excellent preservation. Ventral prothorax appears to have suffered some compression, with uneven or slightly wrinkled surfaces. The apex of the right hind wing and the dorsum of antennomeres 10 and 11 of the left antenna have been

sanded off during preparation. It has a piece of a leaf and other botanical and arthropod remains and unidentified debris as syninclusions.

Notes. †*Cretobythus yini* is unique among the Cretaceous species due to its cephalic capsule strong afunilation at the eye level. Excellent preserved specimens, such as the holotype of †*C. yini*, allow not only the almost completely understanding of their morphology, but also give clues on morphological aspects of other fossil species without specimens with an equally satisfactorily preservation. For example, the clear view of the ventral surface of the head of †*C. yini* allowed us to reinterpret the ventral morphology of †*B. grimaldii* (see in comments under that species).

Etymology. Named in honor of the great Chinese taxonomist Zi-Wei Yin. The name was created by adding the singular Latin genitive case suffix -i to the first name of a male person. The orthography of an eponym is unchangeable and does not depend on the generic name for which the epithet is used.

†***Megabythinus*** Yin, Zhao and Cai, 2021

Type species. †*Megabythinus spinitibialis* Yin, Zhao and Cai, 2021.

Diagnosis. Body large-sized, length over 2.5 mm. Antennae with scape relatively elongate, longer than pedicel and antennomere 3 combined; apical three segments forming a conspicuous club, antennomeres of the club elongate but not particularly thick. Interantennal ridge absent or poorly developed, not elevated. Antennal tubercles low and widely separated. Frons without deep excavation. Maxillary palp slightly shorter than half antennal length; palpomere 2 elongate, gradually thickening toward the apex (as opposed to abruptly thickening posterad midlength); palpomere 3 short, subtrapezoid; palpomere 4 enlarged, oval, with a relatively thick and large

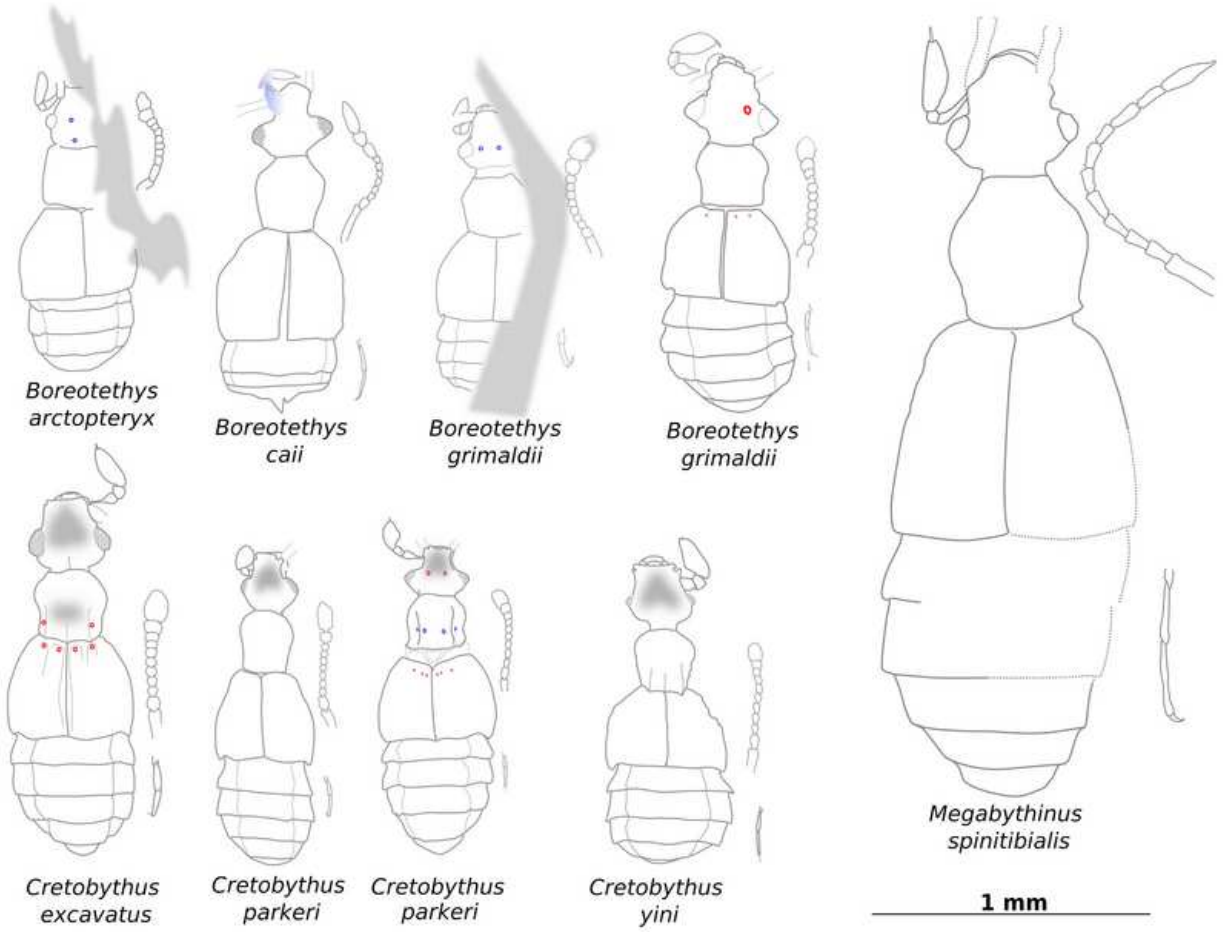

Fig. 14. Habitus of the Cretaceous Pselaphinae with detail of antenna and tarsus next (right side) to each species. Figure in the same scale as Fig.13.

apical sensilla (clearly visible in the habitus dorsal view). Compound eyes large, anterolaterally directed. Pronotum about as long as wide, with an even surface and lacking conspicuous cavities and carinae. Metacoxae contiguous. Tarsomere 2 about twice as long as tarsomere 1, and about half as long as tarsomere 3; pretarsal claws slightly asymmetrical.

Notes. The lack of excavations on the head and even pronotal surface, as well as the poorly developed to absent interantennal ridge, makes †*Megabythinus* morphologically closer to †*Boreotethys*. The single species in †*Megabythinus* is very large, similar in size to †*Burmagluta rougemonti*, but aside from

that, both have few, if any, diagnostic traits in common.

†***Megabythinus spinitibialis*** Yin, Zhao and Cai, 2021

(Fig. 14)

Type locality. Myanmar: Kachin, Hukawng Valley, early Cenomanian (age 98.79 ± 0.62 Ma).

Diagnosis. As for genus.

3.3. Identification

3.3.1. Multi-entry key to the Burmese amber Pselaphinae

The key can be accessed through the link below and is currently restricted to the Burmese fauna:

http://www.xper3.fr/xper3GeneratedFiles/publish/identification/-4517313894653082321/mkey.html

3.3.2. Dichotomous key to the Cretaceous Pselaphinae

1. Spanish amber (Albian) … **2**

- Burmese amber (Cenomanian) … **3**

2. Antennae without club. Elytra width no greater than 1.7x head width (eyes included). Pretarsal claws subequal in size (Figs. 13 and 15A) … †***Cretasonoma corinformibus***

- Antennae with a mildly developed 3-segmented club. Elytra more than twice as wide as head. Pretarsal claws unequally-sized (Figs. 13 and 15B) … †***Penarhytus tenebris***

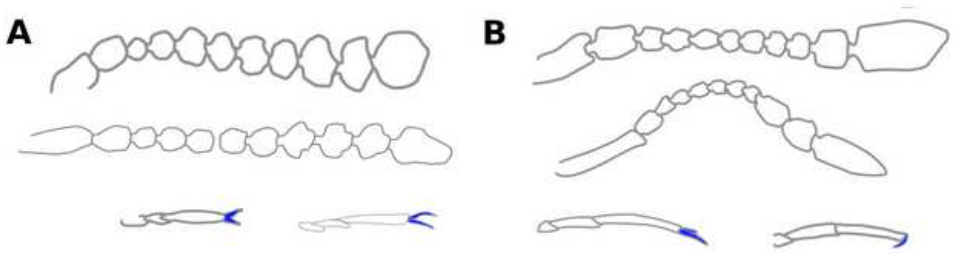

Fig. 15. Types of antennae and pretarsal claws. **A**, antennae without a distinct club and pretarsal claws subequal in size; **B**, antennae with a three-segmented club and pretarsal claws either conspicuously unequal in size or a single one.

3. Body length over 2.5 mm … **4**

- Body length considerably less than 2.5 mm … **5**

4. Antennal tubercle strongly prominent. Pronotum with antebasal and lateral longitudinal sulci, without carinae. Metatibia without an apical cuticular projection/spine (Fig.13) … †***Burmagluta rougemonti***

- Antennal tubercle only slightly raised. Pronotum without sulci or carina. Metatibia with an apical cuticular projection/spine (Fig.14) … †***Megabythinus spinitibialis***

5. Antennae without club; antennomeres gradually increasing in size from third to the apical (Figs. 1, 2, 13, 15A). Tarsomere 2 not much longer than tarsomere 1; pretarsal claws equally sized ... †***Burmalogasa perisi*** **gen. et sp. nov.**

- Apical three antennomeres forming a club, sometimes distinct, sometimes loosely-formed (Fig. 15B). Tarsomere 2 at least twice as long as tarsomere 1; pretarsal claws unequally developed, sometimes one claw is extremely reduced or lost … **6**

6. Frontovertexal area without excavation, at most shallowly depressed … **7**

- Frontovertexal area deeply excavated … **10**

7. Medium to large-sized species (length almost 2 mm) (Fig. 13). Maxillary palpomere 4 less than twice as long as palpomere 3 (Fig. 16A). Gular ridge present … †***Cretobrachygluta laurasiensis***

- Smaller species (length less than 1.5 mm). Maxillary palpomere 4 twice as long as palpomere 3, or longer (Fig. 16B). Gular ridge absent … **8**

Fig. 16. Maxillary palpomere 4 relative size. **A**, not twice as large as palpomere 3; **B**, easily larger than twice palpomere 3.

8. Scape very elongate, about as long as antennomeres 2–5 combined; antennal club sharply defined (Figs. 5, 6, and 14) … †***Boreotethys caii*** **sp. nov.**

- Scape not as elongate, at most as long as antennomeres 2–4 combined; antennal club present, but loosely-formed … **9**

9. Scape about as long as antennomere 2. Body densely setose (Fig. 14) … †***Boreotethys arctopteryx***

- Scape clearly longer than antennomere 2. Body only sparsely setose (Fig. 14) … †***Boreotethys grimaldii***

10. Maxillary palps reduced. Pronotal lateral longitudinal carinae runs across entire pronotum length; anterolateral corners of pronotum strongly marked … **11**

- Maxillary palps usually greatly enlarged. Pronotal lateral longitudinal carinae, if present, restricted to the posterior half; anterolateral corners of pronotum softly diverging … **12**

11. Pronotum clearly broader than long. Elytra with strongly marked discal carinae … **†*Priscaplectus carinatus*** (Fig. 13)

- Pronotum about as broad as long. Elytra without strongly marked Sdiscal carinae … **†*Priscaplectus grandiceps*** (Fig. 13)

12. Thick, transverse ridge posterior to frontovertexal cavity present. In dorsal view, pronotum broadest posteriorly (Fig. 17A) … **†*Protrichonyx rafifrons*** (Fig. 13)

- Thick, transverse ridge posterior to frontovertexal cavity absent. In dorsal view, pronotum broadest at about the anterior third or mid-length, with lateral margins converging posteriorlly or, at most, subparallel (Fig. 17B) … **13**

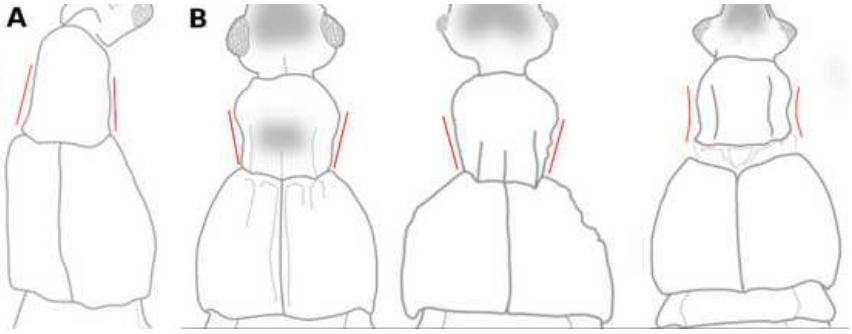

Fig. 17. Pronotal shape differences. **A**, lateral margins converging posteriorly; **B**, lateral margins either concave or diverging posteriorly.

13. Compound eyes small, smaller or about as large as palpomere 3 (Fig. 18A). In profile view, head strongly compressed dorsoventrally at the eye level (Fig.12D) … **†*Cretobythus yini* sp. nov.** (Figs. 11, 12, and 14)

- Compound eyes large, easily larger than palpomere 3 (Fig. 18 B). In profile view, head not compressed at the eye level (Fig.10H) … **14**

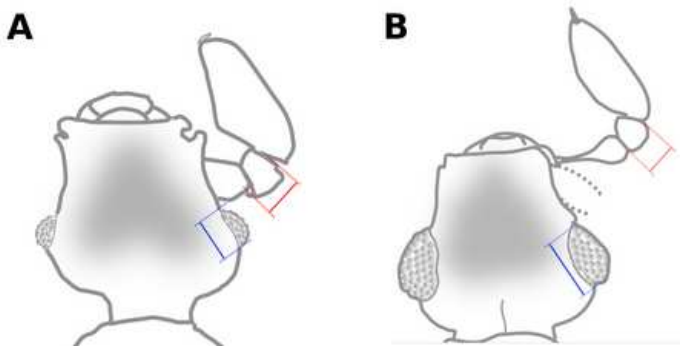

Fig. 18. Compound eyes size differences. **A**, eyes roughly the same size of palpomere 3; **B**, eyes much longer than palpomere 3.

14. Antennomere 11 oval; antennomere 10 much broader than long (Fig. 19 A). Tibial outer surfaces not crenulate … **†*Cretobythus excavatus*** (Fig. 14)

- Antennomere 11 fusiform and apically notched; antennomere 10 about as broad as long (Fig. 19 B). Tibial outer surfaces crenulate ... **†*Cretobythus parkeri* sp. nov.** (Figs. 9, 10 and 14)

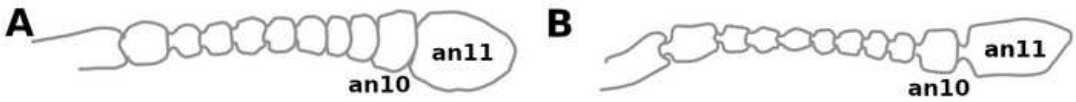

Fig. 19. Antennomeres shape differences in *Cretobythus*. **A**, antennomere 10 wider than long and antennomere 11 globose; **B**, antennomere 10 about as long as wide and antennomere 11 fusiform.

3.4. Phylogenetic results

We recovered †*Burmalogasa perisi* as a member of the Faronitae clade, with all relations between the species of this clade unresolved. The remaining described species (†*Boreotethys caii*, †*Cretobythus*

parkeri, and †*C. yini*) appeared all grouped together in a large polytomy with modern Bythinini and previously described species of †*Boreotethys* (†*Boreotethys grimaldii* and †*Boreotethys arctopteryx*) and †*Cretobythus* (†*C. excavatus*). The species †*Protopselaphus thayerae*, included in the phylogeny for the first time, formed a polytomy with Dasycerinae and Pselaphinae (Fig. 20).

4. DISCUSSION

The newly described taxa considerably sum to the diversity of Cretaceous Pselaphinae, raising the total number of species from 11 to 15 and from 9 to 10 the number of genera. †*Cretobythus* and †*Boreotethys* are the most speciose Cretaceous pselaphine genera, each with three species, followed by †*Priscaplectus* with two. The remaining genera, †*Cretasonoma*, †*Burmalogasa*, †*Penarhytus*, †*Protrichonyx*, †*Megabythinus*, †*Cretobrachygluta*, and †*Burmagluta*, are all monotypic. Among the species described here, †*Boreotethys caii* is odd enough to raise suspicion of whether it should remain in its genus or deserve a separate genus to fit in. Nevertheless, preservation issues prevented a deeper examination of the specimen (see the Comment section for that species); future discoveries might shed light on the generic assignment of †*B. caii*.

Foveation pattern is a key character in the taxonomy of Pselaphinae (Chandler, 2001). Despite the excellent amber preservation compared to other types of fossils, there are still taphonomic issues that make the visualization of certain characters, such as the foveae on the body, very difficult. Debris, bubbles, dehydrated/wrinkled cuticle, portions of darkened cuticle, and stretching or compression of sclerites are some examples of artifacts that can prevent a full assessment of the specimens. Therefore, establishing the foveation pattern is a difficult task, especially undoubtly confirm the absence of foveae in "hidden" regions of the body (e.g. median mesoventrital foveae). Still, a precise scoring of the foveation pattern for the fossil species could greatly enhance phylogenetic resolution of stem pse-

laphines. A complete and precise foveation scoring of the fossil species is lacking, except perhaps for †*Cretobrachygluta laurasiensis*, a species based on an excellent specimen which has clear view for all surfaces of the body, a rare situation. We attempted to score all of our specimens as best as possible for all foveal types (Table 1, acronyms of each fovea type as defined by Chandler, 2001). We also coded the other Cretaceous species based on their descriptions (Supplementary Material 1, Foveation tab).
We believe that maintaining this practice in future publications is ideal for building a complete foveation pattern database for the fossils. The use of confocal microscopy, which was not available to us, enhances the definition of the cuticle surfaces, allowing a more reliable scoring of the foveae, as seen for both †*Priscaplectus* species (Yin et al., 2019).

In both morphological phylogenetic analyses (with and without molecular constraints), †*Protopselaphus thayeri* was recovered as a sister group of all Pselaphinae (Supplementary Material 2). However, in the combined morphological and molecular data reconstruction, it formed a polytomy with all Pselaphinae and the Dasycerinae clade (non-Pselaphinae) (Fig. 20). In all phylogenetic analyses, †*Burmalogasa perisi* was recovered as part of the Faronitae clade (Fig. 20 and Supplementary Material 2); this clade was the sister group of higher Pselaphinae with good support in the combined data (Fig. 20). Parker (2016) discussed the difficulty of placing fossiltaxa in Faronitae, as the autapomorphy of this group is an internal character that requires dissection to assess and, therefore, is not available for fossils (at least with the techniques used here). One of the characters that placed †*Burmalogasa* within the Faronitae is the [21; Vertex, sulcus] (Supplementary Material 1, Characters tab, and Supplementary material 2); however, its presence is also shared with many higher Pselaphinae. The other character is the presence of elytral discal fovea, a trait unique to the Faronitae among Pselaphinae. Despite being an external feature, it is very difficult to be scored undoubtedly in the fossils. In addition, †*Burmalogasa* was excluded from the higher Pselaphinae due to the lack of two characters shared between the latter,

Table 1. Foveation pattern scoring for the described species. Difficulty in scoring foveae in fossils led to this proposal for using codes representing the likeliness of presence, which vary from 0 to 3, where "0" means *absent*, "1" means *likely absent*, "2" means *likely present*, "3" means *present*, and "-" was coded when spot was obscured preventing examination. For ease of visualization, 0 and 1 are in red, and 2 and 3, in blue. Foveae terminology is according to Chandler (2001, except for a few exceptions, see Material and Methods). The names and abbreviations adopted are as follows (whenever tha name of the fovea does not explicitly link it to the sclerite it is on, we named the sclerite in brackets): **ff**, frontal fovea; **vf**, vertexal foveae; **aldf**, anterolateral discal foveae (pronotum); **ldf**, lateral discal foveae (pronotum); **maf**, medial antebasal fovea (pronotum); **laf**, lateral antebasal foveae (pronotum); **iblf**, inner basolateral foveae (pronotum); **oblf**, outer basolateral foveae (pronotum); **apsf**, antero prosternal foveae; **lpcf**, lateral procoxal foveae (prosternum); **mpcf**, medial procoxal fovea (prosternum); **pef**, proepimeral foveae; **sef**, subbasal elytral foveae; **bef**, basal elytral foveae; **shef**, subhumeral elytral foveae; **def**, discal elytral foveae; **ppf**, preppectal foveae; **mmsvf**, median mesoventrital fovea; **almsvf**, anterolateral mesoventrital foveae; **lmsvf**, lateral mesoventrital foveae; **pmcf**, promesocoxal foveae (mesoventrite); **lmcf**, lateral mesocoxal foveae (metaventrite); **mmtvf**, median metaventrital fovea; **lmtvf**, lateral metaventrital foveae; **ptf**, paratergal foveae (tergite); **mbf**, mediobasal foveae (tergite and sternite); **blf**, basolateral foveae (sternite).

	ff	vf	gf	aldf	ldf	maf	laf	iblf	oblf	apsf	lpcf	mpcf	pef	sef	bef	shef	def	ppf	mmsvf	almsvf	lmsvf	pmcf	lmcf	mmtvf	lmtvf	ptf	mbf	blf
†*Boreotethys grimaldii*	-	2	2	-	-	-	-	-	-	-	-	-	-	-	2	1	0	-	-	-	-	-	-	-	-	-	-	-
†*Boreotethys caii*	-	2	2	-	-	-	-	-	-	-	2	-	-	-	2	-	0	-	-	-	-	-	-	-	-	-	-	-
†*Burmalogasa perisi*	1	2	-	0	0	2	2	1	1	1	2	1	-	1	2	1	3	-	-	-	-	-	-	-	2	2	-	2
†*Cretobythus parkeri*	1	2	2	0	0	1	2	0	0	0	-	-	1	-	2	0	0	-	-	-	-	2	-	1	2		-	-
†*Cretobythus parkeri* (par)	1	3	-	1	1	0	3	1	1	-	-	-	-	1	2	-	1	-	-	-	-	-	-	-	2	-	-	-
†*Cretobythus yini*	-	2	2	0	0	0	2	0	0	-	2	-	-	-	3	2	0	-	-	2	-	-	2	-	2	2	-	-

the elytral sutural stria [character 35] and the unequally sized pretarsal claws [character 56]. Within Faronitae, †*Burmalogasa* was recovered in the morphological analysis as sister to the extant species due to the presence of the frontal rostrum in the head [character 21], whereas the whole group was a poly

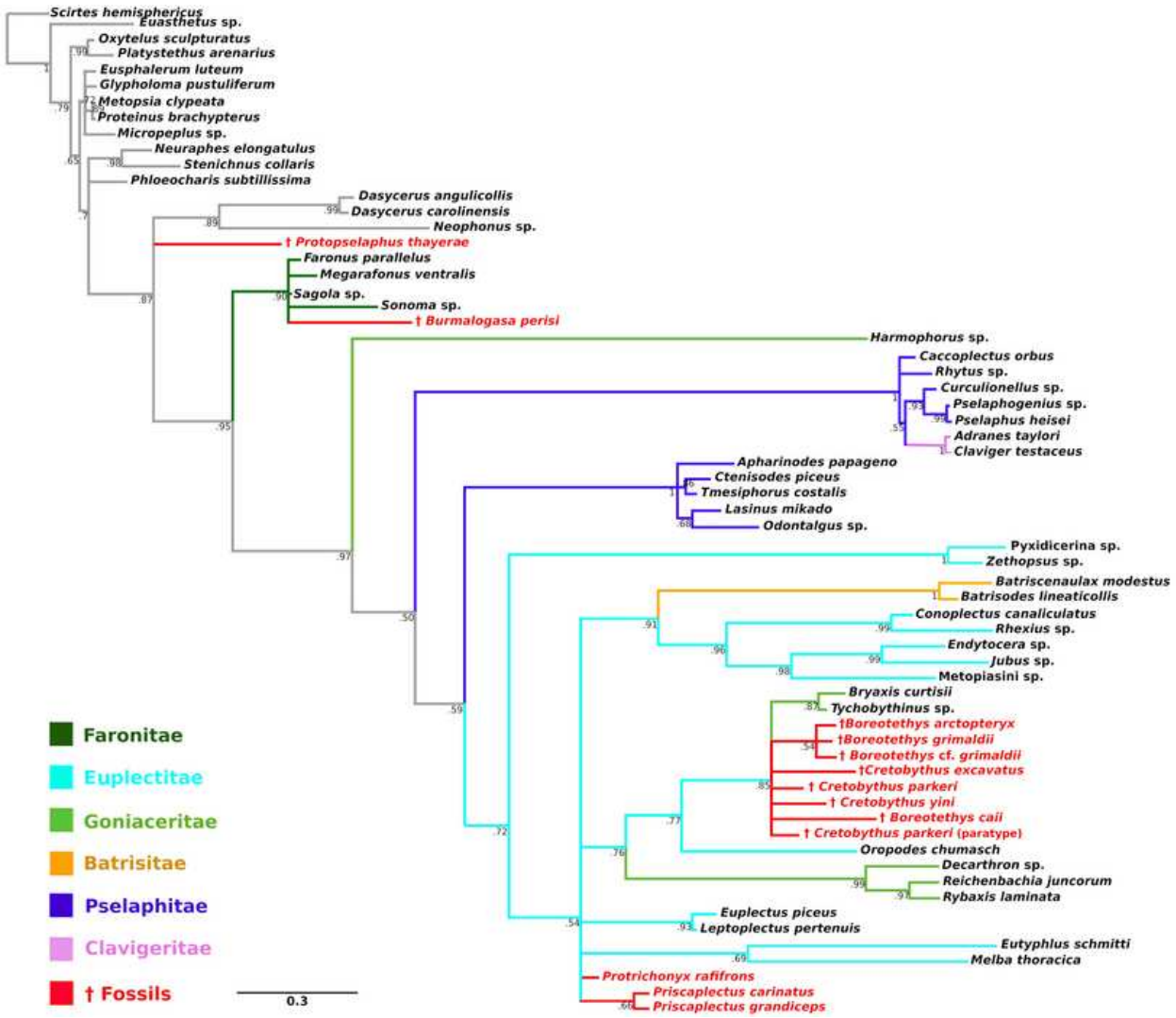

Fig.20. Bayesian phylogenetic reconstruction of the Pselaphinae based on molecular and morphological data. Original morphological matrix by Parker (2016).

tomy in the combined molecular and morphological analysis (Fig. 20). These results led us to suspect that †*Burmalogasa* is a stem Faronitae. Recent advances in micro-CT scanning techniques applied to amber fossils have proven that internal features can be assessed (Boudinot et al., 2022; Zhuang et al., 2022). Such techniques as well as the addition of more characters in the morphological matrix, will

help to better understand the relationships between the extinct Cretaceous and extant Faronitae. †*Boreotethys caii*, †*Cretobythus yini*, †*Cretobythus parkeri*, and †*Boreotethys grimaldii* were all recovered among the members of Goniaceritae, a group that includes previously described fossils, and Euplectitae, with better support only for the combined data (Fig. 20). †*Boreotethys grimaldii* was the only species with a consistent phylogenetic placement, as it was grouped with other †*Boreotethys* with relatively good support in all analyses. These new *taxa* fall within the higher pselaphine clade together with the modern Bythinini, as was also recovered previously (Parker, 2016, Yin et al., 2017; Yin et al. 2019) (Fig. 14). The new taxa were recovered as distantly related to the fossil genera †*Priscaplectus* and †*Protrichonyx*, both arising from a polytomy at the base of the higher Pselaphinae clade.

Although only known by a few representative species, the morphological diversity of the Cretaceous pselaphines is already considerably high, with a great number of characters being strongly different among the species. The most important of these are variation in size and shape of the maxillary palps, strong differences in the cephalic capsule shape, the development, shape, and positioning of the compound eyes, development of the antennal tubercles (a character linked to the shape/width of the interantennal ridge), shape of the pronotum and elytra, depth of the body, setation (mostly setae abundance), the relative size of the tarsomeres, and the shape and number of the pretarsal claws (Table 2). This large morphological variation suggests that by mid-Cretaceous, Pselaphinae were already considerably old and established in the environment.

Despite the great morphological diversity between the Cretaceous genera, a few characters are shared between some genera (Table 2). One such is the frontovertexal excavation or cavity, bordered anteriorly by the interantennal ridge and laterally by the ocular-antennal ridges (and also posteriorly by a vertexal transversal ridge in †*Protrichonyx*). The excavation is absent in †*Boreotethys* and †*Megabythinus*, but strong in †*Protrichonyx*, †*Cretobythus*, and †*Priscaplectus.*

Table 2. Main characters separating the Cretaceous Pselaphinae genera. Coding: **0**, "absent" or "no"; **1**, "present" or "yes", except in character 1 where the coding is according to Table 1. Characters: **ch01**, discal elytral foveae; **ch02**, Tarsomere 2 not greater than twice tarsomere 1; **ch03**, pretarsal claws subequal; **ch04,** antennal tubercles raised; **ch05**, antennal tubercles notched; **ch06**, interantennal sulcus; **ch07**, interantennal ridge developed; **ch08**, frontovertexal deep cavity; **ch09**, maxillary palpomere 2 much longer than twice the length of palpomere 1; **ch10**, maxillary palpomere 4 thicker than scape; **ch11**, pronotal antebasal sulcus; **ch12**, pronotal lateral longitudinal carinae; **ch13**, pronotal posteromedial cavity; **ch14**, body conspicuously broadened at the elytra level.

	ch01	**ch02**	**ch03**	**ch04**	**ch05**	**ch06**	**ch07**	**ch08**	**ch09**	**ch10**	**ch11**	**ch12**	**ch13**	**ch14**
†*Cretasonoma*	2	1	1	1	?	1	0	0	0	0	?	?	?	0
†*Burmalogasa*	3	1	1	1	0	1	0	0	0	0	0	0	1	0
†*Penarhythus*	1	1	0	?	?	0	?	0	?	0	?	?	?	1
†*Boreotethys*	0	0	0	0	0	0	0	0	1	1	0	0	0	1
†*Protrichonyx*	0	0	0	1	1	0	1	1	1	1	0	1	1	?
†*Cretobythus*	0	0	0	1	1	0	1	1	1	1	0	1	1	1
†*Priscaplectus*	0	0	0	1	1	0	1	1	1	0	0	1	0	1
†*Cretobrachygluta*	0	0	0	0	0	0	0	0	1	0	1	0	0	1
†*Burmagluta*	0	0	0	1	0	0*	0	0	1	1	1	0	0	1
†*Megabythinus*	1	0	0	0	0	0	0	0	1	1	0	0	0	1

* The frons is broad in between the antennal tubercles in †*Burmagluta*, therefore it is coded here as not having the sulcus

Although various types of excavations on the dorsum of the cephalic capsule have been observed in extant pselaphines, the shape and position of the excavations are very similar among these three genera. Moreover, the antennal tubercles (the anterolateral borders of the excavation) in these three genera are notched in a peculiar way that is not found in extant taxa. Another interesting character is the unusual notched ocular-mandibular carina, which is only known to be shared between †*Priscaplectus grandiceps* and †*Boreotethys grimaldii*. This could be present in more species, but it is difficult to be

seen because of its position on the cephalic capsule, discussed in more detail under the Comments sections of those species. The pronotum lacking antebasal and lateral longitudinal sulci is shared among †*Boreotethys*, †*Protrichonyx*, †*Cretobythus*, †*Priscaplectus*, *and* †*Megabythinus*, and in the case of †*Priscaplectus*, †*Cretobythus* and possibly †*Protrichonyx* (Fig. 2, C in Parker, 2016, although not mentioned in the original description), lateral longitudinal carinae and a posteromedial cavity are present. Finally, a few species have bifurcated pretarsal claws in the anterior leg, and simple pretarsal claw in the middle and posterior legs. A careful and conclusive investigation of the pretarsal claws of the Cretaceous species remains to be conducted, as this character is difficult to precisely determine because of to the minute size of the secondary ("acessory") pretarsal claw in some species (the scoring of that character is highly dependent on the preservation of the fossil) (Fig. 10, F, Fig. 12, H). Including these characters in future phylogenetic studies might help bring finer resolution to portions of the tree that are currently polytomies.

Regarding identification, the multi-entry key will hopefully be a useful tool for poorly preserved specimens that have only a few recognizable characters left to be examined, often the case of fossils where characters are commonly obscured or missing. These specimens easily get "stuck" in couplets of regular dichotomous keys, and identification cannot be concluded. In the multi-entry key, the user can choose any character at any time, without a specific order. The key also has the advantage of being editable (by the authors or by invited collaborators), with the possibility of being constantly updated to include new species, morphospecies, sexual dimorphism, or intraspecific variation when/if they are reported. Another advantage is the potential of stimulating identification among non-specialists due to its user-friendly layout, which is more pictorial than the dichotomous key (the user is less dependent on the field jargon). It is widely known that the Burmite trade on the Internet is abundant and that amateurs have valuable specimens housed in their private collections. Each fossil specimen is highly valuable in the challenge of reconstructing animal phylogeny. Providing user-friendly identification tools,

quickly accessible through web browsers, can stimulate amateurs to identify their specimens to the species level, which can eventually lead to an approach between them and professional taxonomists. This could finally lead to the availability of the specimens of their private collections, either remotely, through images and catalogues, or physically, through donation of specimens to public institutions. In a recent review of the ant genus †*Zigrasimecia*, for example, two amateurs contributed to almost 20% of the examined material of that revision (Chaul, 2023).

This contribution augmented the diversity of Cretaceous Pselaphinae, provided tools for their identification (identification keys and complementary diagnosis for each species), and attempted to further explore the relationship between extinct and extant lineages by adding the newly described species to the previously available phylogenetic tree. We discussed important characters that we believe, if included in future phylogenetic inferences, could enhance phylogenetic resolution and help understand these elusive stem lineages within the higher Pselaphinae.

ACKNOWLEDGMENTS

Financial support was provided by Fundação de Amparo à Pesquisa do Estado de Minas Gerais (FAPE-MIG) and Conselho Nacional de Desenvolvimento Científico e Tecnológico (CNPq; research grant number 304339/2022-9 to CLA). Coordenação de Aperfeiçoamento de Pessoal de Nível Superior—Brasil—funded the scholarship of two of us (JCMC and IG, CAPES; Finance Code 001).

REFERENCES

Boudinot, B., Perrichot, V., Chaul, J., 2020. †*Camelosphecia* gen. nov., lost ant-wasp intermediates

from the mid-Cretaceous (Hymenoptera, Formicoidea). ZooKeys 1005, 21e55. https://doi.org/10.3897/zookeys.1005.57629

Beutel, R., Luo. X-Z., Yavorskaya, M., Jałoszyński, P., 2021. Structural megadiversity in leaf litter predators – the head anatomy of *Pselaphus heisei* (Pselaphinae, Staphylinidae, Coleoptera). Arthropod Systematics and Phylogeny 79, 443–463. https://doi.org/10.3897/asp.79.e68352

Chandler, D., 2001. Biology, morphology, and systematics of the ant-like litter beetles of Australia (Coleoptera: Staphylinidae: Pselaphinae). Memoirs of Entomology International 15 i–viii + 1–560.

Chaul, J., Lopes-Andrade, C., 2022. First record of Mayetiini (Coleoptera: Staphylinidae: Pselaphinae) from Brazil, with the description of a new macropterous and macrophthalmic species of *Mayetia* Mulsant & Rey, 1875. Zootaxa, 5175 (1), 126–136. https://doi.org/10.11646/zootaxa.5175.1.6

Chaul, J., 2023. A revision of the Cretaceous ant genus *Zigrasimecia* Barden & Grimaldi, 2013 (Hymenoptera: Formicidae: †Zigrasimeciinae). Zootaxa 5325, 301–341. https://doi.org/10.11646/zootaxa.5325.3.1

Delclòs, X., Peñalver, E., Barrón, E., Peris, D., Grimaldi, D., Holz, M., Labandeira, C., Saupe, E., Scotese, C., SolórzanoKraemer, M., Álvarez-Parra, S., Arillo, A., Azar, D., Cadena, E., Dal Corso, J., Kvaček, J., Monleón-Getino, A., Nel, A., Peyrot, D., Bueno-Cebollada, C., Gallardo, A., GonzálezFernández, B., Goula, M., Jaramillo, C., Kania-Kłosok, I., LópezDel Valle, R., Lozano, R., Meléndez, N., Menor-Salván, C., Peña-Kairath, C., Perrichot, V., Rodrigo, A., Sánchez-García, A., Santer, M., Sarto i Monteys, V., Uhl, D., Viejo, J. and Pérez-de la Fuente, R., 2023. Amber and the Cretaceous resinous

interval. Earth-Science Reviews, 243, 104486. https://doi.org/10.1016/j.earscirev.2023.104486

Engel, M., Barden, P., Riccio, M., Grimaldi, D., 2016. Morphologically specialized termite castes and advanced sociality in the Early Cretaceous. Current Biology, 26, 515–521. https://doi.org/10.1016/j.cub.2015.12.061

Evenhuis, N., 2021. The insect and spider collections of the world website. Available at: http://hbs.bishopmuseum.org/codens/ (accessed 03 January 2024).

Fu, Y.-Z., Li, Y.-D., Su, Y.-T., Cai, C.-Y., Huang, D.-Y., 2021. Application of confocal laser scanning microscopy to the study of amber bioinclusions. Palaeoentomology, 4 (3), 266–278. https://doi.org/10.11646/palaeoentomology.4.3.14

Goloboff, P., Farris, J., and Nixon, K., 2008. TNT, a free program for phylogenetic analysis. Cladistics, 24(5), 774–786. https://doi.org/10.1111/j.1096-0031.2008.00217.x

Grimaldi, D., Engel, M., Nascimbene, P., 2002. Fossiliferous Cretaceous amber from Myanmar (Burma): its rediscovery, biotic diversity, and paleontological significance. American Museum Novitates 3361, 1–72. https://doi.org/10.1206/0003-0082(2002)361<0001:FCAFMB>2.0.CO;2

Guo, M., Xing, L., Wang, B., Zhang, W., Wang, S., Shi, A., Bai, M., 2017. A catalogue of Burmite inclusions. Zoological Systematics, 42 (3), 249–379. https://doi.org/10.11865/zs.201715

Jałoszyński, P., Luo, X.-Z, Beutel, R., 2020. Profound head modifications in *Claviger testaceus* (Pse-

laphinae, Staphylinidae, Coleoptera) facilitate integration into communities of ants. Journal of Morphology, 281 (9), 1072–1085. https://doi.org/10.1002/jmor.21232

Jałoszyński, P., Luo, X.-Z., Beutel, R., 2022. Evolution of cephalicstructures in extreme myrmecophiles: A lesson from Clavigeritae (Coleoptera: Staphylinidae: Pselaphinae). Cladistics, 38, 335–358. https://doi.org/10.1111/cla.12498

Kang, J., Chandler, D., Park, J., 2019. Revision of the Australian genus *Logasa* Chandler (Staphylinidae, Pselaphinae, Faronitae) with description of three new species. ZooKeys, 886, 145–154. https://doi.org/10.3897/zookeys.886.39446.

Kerner, A., Bouquin, S., Portier, R., Vignes-Lebbe, R., 2021. The 8 Years of Existence of Xper3: State of the art and future developments of the platform. Biodiversity Information Science and Standards, 5, e74250. https://doi.org/10.3897/biss.5.74250

Kimball, S., Mattis, P., 1996. GIMP – The GNU Image Manipulation Program. Available from: https://www.gimp.org (accessed 15 May 2023).

Lawrence, J., Slipinski, A., Seago, A., Thayer, M., Newton, A., 2011. Phylogeny of the Coleoptera based on morphological characters of adults and larvae. Annales zoologici (Warsowa), 61 (1), 1–217. https://doi.org/10.3161/000345411X576725

Li, Y-D., Yamamoto, S., Newton, A., Cai, C.-Y., 2023. *Kekveus brevisulcatus* sp. nov., a new featherwing beetle from mid-Cretaceous amber of northern Myanmar (Coleoptera: Ptiliidae). PeerJ, 11,

e15306. http://doi.org/10.7717/peerj.15306

Liu, Y., Tihelka, E., Yamamoto, S., Yin, Z.-W., Huang D.-Y., Tian, L., Cai, C.-Y., 2020a. The first fossil record of the rove beetle subfamily Protopselaphinae (Coleoptera: Staphylinidae) from mid-Cretaceous Burmese amber. Cretaceous Research 110, 104416. http://doi.org/10.1016/j.cretres.2020.104416

Liu, Y., Tihelka, E., Huang, D., Tian, L., Cai, C.-Y., 2020b. A new fossil species of the rove beetle subfamily Protopselaphinae (Coleoptera: Staphylinidae) from mid-Cretaceous Burmese amber. Historical Biology, 33 (10), 1–6. https://doi.org/10.1080/08912963.2020.1762594

Luo, X.-Z., Hlaváč, P., Jałoszyński, P., Beutel, R., 2021a. In the twilight zone – the head morphology of *Bergrothia saulcyi* (Pselaphinae, Staphylinidae, Coleoptera), a beetle with adaptations to endogean life but living in leaf litter. Journal of Morphology, 282, 1170–1187. https://doi.org/10.1002/jmorp21361.

Luo, X.-Z., Jałoszyński, P., Stoessel, A., Beutel, R., 2021b. The specialized thoracic skeletomuscular system of the myrmecophile *Claviger testaceus* (Pselaphinae, Staphylinidae, Coleoptera). Organism Diversity and Evolution, 21, 317–335. https://doi.org/10.1007/s13127-021-00484-1

Luo, X.-Z., Jałoszyński, P., Beutel, R., 2022. The thoracic anatomy of *Pselaphus heisei* (Pselaphinae, Staphylinidae, Coleoptera). Journal of Morphology, 284, e21527. https://doi.org/10.1002/jmor.21527

Mey, W., Wichard, W., Müller, P., Wang, B., 2017. The blueprint of the Amphiesmenoptera – Tara-

choptera, a new order of insects from Burmese amber (Insecta, Amphiesmenoptera). Fossil Record, 20, 129–145. https://doi.org/10.5194/fr-20-129-2017

Miller, M., Pfeiffer, W., Schwartz, T., 2010. Creating the CIPRES Science Gateway for inference of large phylogenetic trees. Pp. 1–8 in M. Miller, W. Pfeiffer and T. Schwartz (eds) Proceedings of the Gateway Computing Environments Workshop (GCE). New Orleans, Louisiana.

Newton, A., Chandler, D., 1989. World catalog of the genera of Pselaphidae (Coleoptera). Fieldiana Zoology, 53, 1–93. https://doi.org/10.5962/bhl.title.3209

Newton, A., Thayer, M., 1995. Protopselaphinae new subfamily for *Protopselaphus* new genus from Malaysia, with a phylogenetic analysis and review of the Omaliine Group of Staphylinidae including Pselaphidae (Coleoptera). Biology, Phylogeny, and Classification of Coleoptera: Papers Celebrating the 80th Birthday of Roy A. Crowson (ed. by J. Pakaluk and A. Ślipiński), 221–320. Muzeum i Instytut Zoologii PAN, Warszawa.

Parker, J., 2016. Emergence of a superradiation: pselaphine rove beetles in midCretaceous amber from Myanmar and their evolutionary implications. Systematic Entomology 41, 541–566. https://doi.org/10.1111/syen.12173

Parker, J., Owens, B., 2018. *Batriscydmaenus* Parker and Owens, new genus , and convergent evolution of a “reductive ” ecomorph in socially symbiotic Pselaphinae (Coleoptera : Staphylinidae). The Coleopterists Bulletin, 72 , 219–229. https://doi.org/10.1649/0010-065X-72.2.219

Pérez-de la Fuente , R., Delclòs, X., Peñalver, E., Arillo, A., 2011. Biting midges (Diptera: Ceratopogonidae) from the Early Cretaceous El Soplao amber (N Spain). Cretaceous Research, 32 (6), 750–761. https://doi.org/10.1016/j.cretres.2011.05.003

Pérez-de la Fuente , R., Engel, M., Azar, D., Peñavelver, E., 2019. The hatching mechanism of 130-million-year-old insects: an association of neonates, egg shells and egg bursters in lebanese amber. Palaeontology, 62 (4), 547–559. https://doi.org/10.1111/pala.12414

Peris, D., Chatzimanolis, S., Delclòs, X., 2014. Diversity of rove beetles (Coleoptera: Staphylinidae) in Early Cretaceous Spanish amber. Cretaceous Research, 48, 85–95. https://doi.org/10.1016/j.cretres.2013.11.008

Peris, D., Rust, J., 2019. Cretaceous beetles (Insecta: Coleoptera) in amber: the palaeoecology of this most diverse group of insects. Zoological Journal of the Linnean Society, 189 (4), 1085–1104. https://doi.org/10.1093/zoolinnean/zlz118

Peris, D., 2020. Coleoptera in amber from Cretaceous resiniferous forests. Cretaceous Research, 113, 104484. https://doi.org/10.1016/j.cretres.2020.104484

Schaufuss, L., 1890. System-schema der Pselaphiden, ein Blick in die Vorzeit, in die Gegenwart und in die Zukunft. Tijdschrift Voor Entomologie 33, 101–162.

Shi, G., Grimaldi, D., Harlow, G., Wang, J., Wang, J., Yang, M., Lei, W., Li, Q., Li, X., 2012. Age constraint on Burmese amber based on U–Pb dating of zircons. Cretaceous Research 37, 155–163.

https://doi.org/10.1016/j.cretres.2012.03.014

Schneider, C., Rasband, W., Eliceiri, K., 2012. NIH Image to ImageJ: 25 years of image analysis. Nature Methods, 9, 671–675. https://doi.org/10.1038/nmeth.2089

Ung, V., Dubus, G., Zaragüeta-Bagils, R., Vignes-Lebbe, R., 2010. Xper2: introducing e-taxonomy. Bioinformatics, 26 (5), 703–704. https://doi.org/10.1093/bioinformatics/btp715

Vignes-Lebbe, R., Bouquin, S., Kerner, A., Bourdon, E., 2017. Desktop or remote knowledge base management systems for taxonomic data and identification keys: Xper2 and Xper3. Proceedings of TDWG, 1, e19911. https://doi.org/10.3897/tdwgproceedings.1.19911

Yin, Z.-W., Parker, J., Cai, C.-Y., Huang, D.-Y., Li, L.-Z., 2017. A new stem bythinine in Cretaceous Burmese amber and early evolution of specialized predatory behaviour in pselaphine rove beetles (Coleoptera: Staphylinidae). Journal of Systematic Palaeontology, https://doi.org/10.1080/14772019.2017.1313790. [volume and issue information and pagination were assigned in 2018 as follows: 16 (7), 531–541]

Yin, Z.-W., Cai, C.-Y., Huang, D., 2018. Last major gap in scydmaenine evolution filled (Coleoptera: Staphylinidae). Cretaceous Research, 84, 62–68. https://doi.org/10.1016/j.cretres.2017.10.02

Yin, Z.-W., Chandler, D., Cai, C.-Y., 2019a. *Priscaplectus* gen. nov. and two new species in mid-Cretaceous amber from Myanmar (Coleoptera: Staphylinidae: Pselaphinae). Cretaceous Research 103, 104174. https://doi.org/10.1016/j.cretres.2019.07.004

Yin, Z.-W., Kurbatov, S., Cuccodoro, G., Cai, C.-Y., 2019b. *Cretobrachygluta* gen. nov., the first and oldest Brachyglutini in mid-Cretaceous amber from Myanmar (Coleoptera: Staphylinidae: Pselaphinae). Acta Entomologica Musei Nationalis Pragae, 59, 101–106. https://doi.org/10.2478/aemnp-2019-0008

Yin, Z.-W., Cai, C.-Y., 2019. A new species of minute Scydmaenini (Coleoptera: Staphylinidae: Scydmaeninae) in mid-Cretaceous amber from Myanmar. Cretaceous Research, 101, 70–75. https://doi.org/10.1016/j.cretres.2019.05.001

Yin, Z.-W., Zhou, D., 2020. *Scydmaenus linqibini* sp. nov., a new fossil Scydmaenini in mid-Cretaceous amber from northern Myanmar (Coleoptera: Staphylinidae: Scydmaeninae). Palaeoentomology, 003 (1), 036–040. https://doi.org/10.11646/palaeoentomology.3.1.4

Yin, Z.-W., Cai, C.-Y., 2021. A new Brachyglutini from mid-Cretaceous amber of northern Myanmar (Coleoptera: Staphylinidae: Pselaphinae). Cretaceous Research, 124, 104807. https://doi.org/10.1016/j.cretres.2021.104807

Yin, Z.-W., Lu, L., Yamamoto, S., Thayer, K., Newton, A., Cai, C.-Y., 2021a. Dasycerine rove beetles: Cretaceous diversification, phylogeny and historical biogeography (Coleoptera: Staphylinidae: Dasycerinae). Cladistics, 37, 185–210. https://doi.org/10.1111/cla.12430

Yin, Z.-W., Zhao, Q.-H., Cai, C.-Y., 2021b. *Megabythinus* gen. nov., a new stem-group Pselaphinae from mid-Cretaceous Myanmar amber (Coleoptera, Staphylinidae). Cretaceous Research, 125, 104879.

https://doi.org/10.1016/j.cretres.2021.104879

Zhuang, Y., Xu, W., Zhang, G., Mai, H., Li, X., He, H., Ran, H., Liu, Y., 2022. Unparalleled details of soft tissues in a Cretaceous ant. *BMC Ecology and Evolution*, 22, 146, 1–10. https://doi.org/10.1186/s12862-022-02099-2

III. CAPÍTULO 2

FIRST RECORD OF MAYETIINI (COLEOPTERA: STAPHYLINIDAE: PSELAPHINAE) FROM BRAZIL, WITH THE DESCRIPTION OF A NEW MACROPTEROUS AND MACROPHTHALMIC SPECIES OF *MAYETIA* MULSANT & REY, 1875

Published as Chaul, J.C.M.; and Lopes-Andrade, C., 2022,
in Zootaxa, 5175 (1): 126–136.
doi: https://doi.org/10.11646/zootaxa.5175.1.6

Zootaxa 5175 (1): 126–136
https://www.mapress.com/zt/

Article

ISSN 1175-5326 (print edition)
ZOOTAXA
ISSN 1175-5334 (online edition)

https://doi.org/10.11646/zootaxa.5175.1.6
http://zoobank.org/urn:lsid:zoobank.org:pub:01C1CF8D-F8BE-44DB-B2B4-B2856B4FA259

First record of Mayetiini (Coleoptera: Staphylinidae: Pselaphinae) from Brazil, with the description of a new macropterous and macrophthalmic species of *Mayetia* Mulsant & Rey, 1875

JÚLIO CEZAR MÁRIO CHAUL[1,2] & CRISTIANO LOPES-ANDRADE[1,3]
[1]*Pós-Graduação em Ecologia, Departamento de Biologia Geral, Universidade Federal de Viçosa, 36570-900, Viçosa, Minas Gerais, Brazil.*
[2]*Departamento de Biologia Animal, Universidade Federal de Viçosa, 36570-900, Viçosa, Minas Gerais, Brazil.*
https://orcid.org/0000-0002-6285-1017
[3] *https://orcid.org/0000-0001-9652-1369*

Abstract

Mayetia atlantica **sp. nov.**, the third Neotropical and first Brazilian species of Mayetiini Scheerpeltz, 1925, is described. It is the third macropterous and macrophthalmic species of the genus, alongside *M. peruana* Orousset, 1995 (Neotropical) and *M. nepalensis* Orousset, 1995 (Oriental). The new species is known from three forest remnants of the Brazilian Atlantic Forest, in the states of Espírito Santo, Minas Gerais (both in Southeast Brazil) and Bahia (Northeast Brazil), being the southernmost record of *Mayetia* in the New World. The description of *M. atlantica* is based mostly on females, but includes the first known male macropterous and macrophthalmic *Mayetia*. In this work, the tropical diversity of the genus is increased and its Neotropical distribution is greatly enlarged.

Key words: Taxonomy, rove beetles, Pselaphinae, miniaturization

Resumo

Mayetia atlantica **sp. nov.**, a terceira espécie Neotropical e primeira brasileira de Mayetiini Scheerpeltz, 1925, é descrita. A espécie é a terceira macróptera e macroftálmica do gênero, junto a *M. peruana* Orousset, 1995 (Neotropical) e *M. nepalensis* Orousset, 1995 (Oriental). *Mayetia atlantica* é conhecida de três fragmentos florestais da Mata Atlântica brasileira, nos estados do Espírito Santo, Minas Gerais (ambos no Sureste do Brasil) e Bahia (Noreste do Brasil), representando o registro mais ao sul de *Mayetia* no Novo Mundo. A descrição de *M. atlantica* é baseada majoritariamente em fêmeas, mas também inclui o primeiro macho macróptero e macroftálmico já descrito em *Mayetia*. Neste trabalho, incrementamos a diversidade tropical do gênero e sua distribuição nos Neotrópicos é muito ampliada.

Palavras-chave: Taxonomia, besouros estafilinídeos, Pselaphinae, miniaturização

Resumen

Describimos por primera vez *Mayetia atlantica* **sp. nov.**, la tercera especie Neotropical y primera especie Brasilera de Mayetiini Scheerpeltz, 1925. Junto con *M. peruana* Orousset, 1995 (Neotropical) y *M. nepalensis* Orousset, 1995 (Oriental); *M. atlantica* es la tercera especie macroptera y macroftalmica del género. La nueva especie fué encontrada en tres fragmentos del bosque Atlántico Brasilero, en el Sureste en los estados de Espírito Santo y Minas Gerais, y en el Noreste en el estado de Bahía. Este registro corresponde a la observación más meridional realizada para el Nuevo Mundo. La descripción de *M. atlantica* presentada aqui, está baseada principalmente en la observación de hembras, sin embargo incluimos también el registro del primer macho macroptero y macroftalmico de *Mayetia*. Con este trabajo incrementamos el número de especies Tropicales conocidas y su distribución en el Neotropico.

Palabras clave: Taxonomía, escarabajos estafilinidos, Pselaphinae, miniaturización

 Accepted by Z.-W. Yin: 12 Jul. 2022; published: 15 Aug. 2022

Introduction

Mayetia Mulsant & Rey, 1875 (Coleoptera: Staphylinidae: Pselaphinae) figures among the smallest beetles with a body length of 0.7–1.3 mm (Orousset, 2022). The genus shares the tribe Mayetiini Scheerpeltz, 1925 with *Typhloleptus* Jeannel, 1951 and *Typhloleptodes* Jeannel, 1953, both ocurring in the Ethiopian region (Newton & Chandler, 1989; biogeographical regionalisation *sensu* Morrone, 2015). Mayetiini is included in the supertribe Euplectitae (Chandler, 2001), an aggregation of tribes which, according to morphological and combined morphological and molecular data, is unlikely monophyletic (Parker, 2016). Recently, a catalog of *Mayetia* was published, covering all publications on species of the genus up to date (Orousset, 2022).

Among pselaphines, species of *Mayetia* can be recognized by the following combination of traits: medially notched anterior edge of the labrum; 11-segmented antennae, with 2-segmented globose club; apical antennomere bearing six large spatulate sensilla; maxillary palp 4-segmented, the palpomere 4 with a palpal cone (sometimes reduced) as well as 2 sensilla (but see description below); tarsus 3-segmented, the first extremely reduced (see description and comments below); V- or U-shaped posterior margin of male's sternite VIII; male urite IX with the sternite divided into two hemisternites; aedeagus simple, without tegmen or parameres; inner sac without copulatory parts; spermatheca absent (Orousset, 2022). Moreover, almost all species are anophthalmic (a few species sometimes with one to three minute, depigmented ommatidia) and apterous (except for two macropterous and macrophthalmic species: *M. peruana* Orousset, 1995 and *M. nepalensis* Orousset, 1995 and the new species here described).

Mayetia encompasses 173 described species (not counting the one described below), and peaks in diversity in the Palearctic region, with 151 species (~87% of all described species), of which the majority are found in the Mediterranean. It is followed in diversity by the Nearctic region, with 18 species. Other biogeographic regions have very low diversity, as follows: the Ethiopian region with one species (*Mayetia gabonica* Coiffait, 1967); the Oriental with one (*M. nepalensis*); and the Neotropical region with two (*M. peruana* and *M. venezuelica* Decu, 1991). Note that the Japanese *M. ishiiana* Nomura & Naomi, 1997 is treated here as a Palearctic species. The genus has not been found in the Andean, Antarctic, Australian and Cape regions up to date.

Mayetia was found in the neotropics only in the 1990's, with the description of *M. venezuelica* based on a single female, anophthalmic and apterous as all other *Mayetia* known at that time (Decu, 1991). Four years later, the first two macropterous and macrophthalmic species of *Mayetia* were described, one Neotropical (*M. peruana*) and one Oriental (*M. nepalensis*), each based on a single female (Orousset, 1995). Here we describe a third Neotropical species from Southeast and Northeast Brazil, the first record of the tribe from the country, based mostly on female specimens, but including the first description of a male macropterous and macrophthalmic in the genus.

Material and methods

Sampling technique and preparation of specimens. All examined specimens were collected through winkler extractors (Besuchet *et al.*, 1987) from samples of mixed litter and soil. The material was left drying in the extractors no less than 4 days, sometimes up to 10 days. Each specimen was given an unique specimen identifier. Specimens were either regularly pinned dry or mounted in polyvinyl alcohol-lactic acid-glycerol (PVLG) medium (Omar *et al.*, 1979), between a pair of round cover glasses, where they were either mounted complete or disarticulated. Dissected specimens were not treated with KOH or any other chemicals. Then each dissected specimen was mounted between cover glasses within the PVLG layer, a card was glued at the edge of the cover glasses and pinned, so it could be stored in the dry collection.

Measurements. We selected measurements which could be accurately taken from dry, pinned specimens. Measurements of length of the abdomen, either the entire abdomen or its segments, were not taken as those seemed prone to much error due to the telescoping arrangement of the segments. The total length was also not taken, because the degree of body curvature was visually different between preserved specimens, making it an unreliable measurement. Measurements are presented in millimeters. The following measurements were taken:

- Head width (HW), maximum width of head posterior to the eyes;
- Head length (HL), measured from midpoint of ocular-clypeal carina to midpoint of an imaginary line which touches both vertexal protuberances;

- Pronotal length (PrnL), maximum length of pronotum, measured with the anterior and posterior margins at the same focus plane;
- Pronotal anterior width (PrnaW), the width at the pronotal-occipital articulation level, measured in the same view as PrnL;
- Pronotal maximum width (PrnW), the maximum width of pronotum, measured in the same view as PrnL;
- Pronotal posterior width (PrnptW), the width at the pronotal-mesothorax articulation level, measured in the same view as PrnL;
- Elytra length (EL), the maximum length of elytra, measured with the anterior and posterior margins at the same focus plane;
- Elytra width (EW), maximum width of elytra, measured in tha same view as EL;
- Abdominal segment 7 (5th visible) width (Abd7W), the maximum width of the segment, measured in dorsal view (tergite and paratergites included).

The range of all measured specimens is presented, with measurement of the holotype in parentheses.

Terminology. We used the terminology of Chandler (2001) with some modifications based on Orousset (2022). In the latter case, the terms were freely translated from French to English.

Repository institutions. The holotype, two paratypes and six non-type specimens are deposited at Coleção Entomológica do Laboratório de Sistemática e Biologia de Coleoptera (CELC, collection abbreviation follows Evenhuis, 2022), of the Universidade Federal de Viçosa, in Viçosa, Minas Gerais, Brazil; one paratype is deposited at Coleção Ayr de Moura Bello (CAMB) in Rio de Janeiro, state of Rio de Janeiro, Brazil; and one paratype is deposited at Museu de Zoologia da Universidade de São Paulo (MZSP) in São Paulo, state of São Paulo, Brazil. The repository institution where each specimen is deposited is given under the description section.

Imaging. Images of dry specimens were taken under a Zeiss Stereo DiscoveryV20 stereomicroscope. Mounted specimens were imaged either under an Olympus CX40 light microscope with a mounted Canon 1100d DSLR camera or in an epifluorescent microscope Olympus BX60 attached to an image system QColor Olympus®. The series of images were stacked in Zerene software and final images were edited in GIMP (Kimball & Mattis, 1996) for enhancing, rotation and cropping. Plates were put together on GIMP. For illumination of the dried specimens, a modified version of the dome illumination system presented in Kawada and Buffington (2016) was made.

Due to the difficulties to assess the morphology of such tiny beetles, the description is not based solely in the holotype, but in the entire type series, which has both dry-pinned and slide-mounted specimens. The study of specimens preserved in both ways is necessary in order to adequately prospect all morphological features which may satisfactorily characterize a species in this genus.

Results

Taxonomy

Order Coleoptera Linnaeus, 1758

Family Staphylinidae Latreille, 1802

Subfamily Pselaphinae Latreille, 1802

Supertribe Euplectitae Streubel, 1839

Tribe Mayetiini Scheerpeltz, 1925

Genus *Mayetia* Mulsant & Rey, 1875

***Mayetia atlantica* Chaul & Lopes-Andrade sp. nov.**
(Figs. 1–4)

Type material. *Holotype*. Male, dry-pinned: Brazil, Espírito Santo, Santa Teresa, -19.9460715 -40.6797418, 829 m, 21.xi.2018, winkler JCMC00438, Leg. Chaul, J.; Prado, L.; Silva, O. [unique specimen identifier CELC003054, previously slide-mounted for imaging and then dry-pinned, housed at CELC].

Paratypes. Four specimens with the same collection data as the holotype: one dry-pinned female [CELC000072, housed at CAMB]; one dry-pinned female [CELC000087, housed at MZSP]; one female slide-mounted [CELC003038, housed at CELC]; one dry-pinned female [CELC000148, housed at CELC].

Non-type material. Three slide-mounted specimens with the same data as the holotype: one with several body parts missing, impossible to determine sex [CELC003063, housed at CELC], one female [CELC003058, housed at CELC and pinned together with paratype CELC003038]; one female [CELC001034, housed at CELC]. One female, dry-pinned: Brazil, Bahia, Parna do Pau-Brasil, regeneration area (17 years), -16.522167 -39.310778, 87 m, 14.ii.2020, 30x30cm winkler of litter plus 2 cm of soil, JCMC00773, Leg. Safar, N.; Deambrozi, S.; Moreira, T.; Jacintho, G.; Martins, G. [CELC001048; housed at CELC]. One female, slide-mounted: Brazil, Bahia, RPPN Estação Veracel, regeneration area (26 years), -16.459152 -39.200219, 5.ii.2020, 76 m, 30x30cm winkler of litter plus 2 cm of soil, JCMC00731, Leg. Safar, N.; Deambrozi, S.; Moreira, T.; Jacintho, G.; Martins, G.[CELC001049, housed at CELC]. One dry-pinned female: Brazil, Minas Gerais, Cataguases, Sinimbú, 10.xii.2021, Vieira, V.; Assis. C. [CELC000969, housed at CELC previously slide-mounted for imaging and then dry-pinned].

Measurements. HW 0.107–0.111 (0.107), HL 0.107 (-), PrnL 0.119–0.131 (0.119), PrnatW 0.066–0.074 (0.074), PrnW 0.107–0.115 (0.107), PrnptW 0.066–0.074 (0.070), EL 0.156–0.164 (0.156), EW 0.123–0.152 (0.152), Abd7W 0.123–0.131 (0.131).

Distribution. Known from forest remnants of the Brazilian Atlantic Forest biome in the states of Minas Gerais and Espírito Santo (Southeast Region) and Bahia (Northeast Region).

Diagnosis. Having all the diagnostic characters of the genus (Orousset, 2022, and see above) plus the following: macrophtalmic; macropterous; vertexal foveae small and at the eye level; sulci anterior to vertexal foveae very shallow, fainting; sensorial tubercles present dorsally on maxillary palpomeres 3 and 4.

Description. *Female and male.* Head, including mouthparts, roughly piramidal in dorsal view. Relative dimensions: about as long as wide; head depth about 0.85x head width; in lateral view, maximum diameter of eye about 0.4x head depth; occiput as wide as anterior head width, about 0.7x maximum head width. In dorsal view, vertexal corners curved, slightly protuberant; median section of posterior vertexal margin slightly concave. In lateral view, dorsal margin almost straight, except for section of antennal tubercle, which bumps dorsally; ventral margin convex. Antennal insertions close to each other; distance between lateralmost points of the margins of antennal tubercles a third of head width; interantennal bridge almost straight; antennal tubercles not separated from each other by cleft. Anterior margin of cephalic capsule delimited by an arched carina, which originates next to anteriormost point of compound eye and arches all through clypeus to the other compound eye (here called the ocular-clypeal carina, occlc). Submentum with a pair of relatively long setae (compared to the setae on gular region) positioned imediately posterad mentum basolateral corners; mid way between each seta of the pair is positioned a pit which is larger than the sockets of these setae but smaller than gular fovea. Compound eyes with 10 to 13 ommatidia; each ommatidium coarse and slightly bumping. Labrum with three pairs of spiny protuberances, the outermost pair more developed and more separated from the two medial pairs; medial notch very reduced; three pairs of long setae, the longest (macrochatae) as long as or longer than labrum width. Left mandible with a single retinacle, right with bifid retinacle; terebra very long, falciform. Maxilla with first palpomere L-shaped, very small; second palpomere the largest, its outer surface curving broadly, separated from the inner surface by carinae both ventrally and dorsally, longitudinal imaginary axis crossing its basal foramen through the middle forming an angle of 45 to 60 degrees with the axis of the apical foramen; third palpomere disc-shaped, about twice as wide as long, partially buried on the apical surface of the previous, with a basal, dorsolateral conical tubercle which bears tiny setae on its truncate apex; fourth palpomere ovoid to round, also with a similar basal tubercle in the same position as in the previous palpomere, with palpal cone about the size of the basal tubercle, positioned slightly ventromesad from the apex, and with one tiny sensilla smaller than the palpal cone and positioned close to it, slightly laterad to the apex. Maxillary cardo wider than long, with a curved basal margin; palpifer longer than wide, with curved outer margin; basistipe triangular; mediostipe roughly square, but with irregular apical margin; galea bearing a tuft of setae about as long as the fourth palpomere; lascinia with a set of very tiny thickened setae about the length of the second labial palpomere. First and second labial palpomeres cylindrical, second slightly larger, their combined length less than

the width of the third maxillary palpomere; third labial palpomere subulate. Ligula width less than the combined length of first and second palpomeres. Tentorium internally Y-shaped, perpendicular to the longitudinal axis of the head, giving rise to gular fovea ventrally and to vertexal foveae dorsally. Gular region simple, mildly convex, except for middle section where the gular fovea is located. Each vertexal fovea slightly smaller than gular fovea. Frons and vertex forming a simple, mildly convex surface, without marked ridges or cavities, except for a pair of inconspicuous sulci and by anterolateral ridges formed by the elevated antennal tubercles. Sulci barely visible, anteromedially turned, originating just anterad of the vertexal foveae and fading well before meeting. Antenna 11-segmented; 10th and 11th antennomeres forming a globular apical club; scape only slightly longer and wider than pedicel; antennomeres from 3rd to 9th disc-like, gradually enlarging towards apex, except for the 7th larger than the 8th; apical antenomere with long, basally originated, flatenned sensilla.

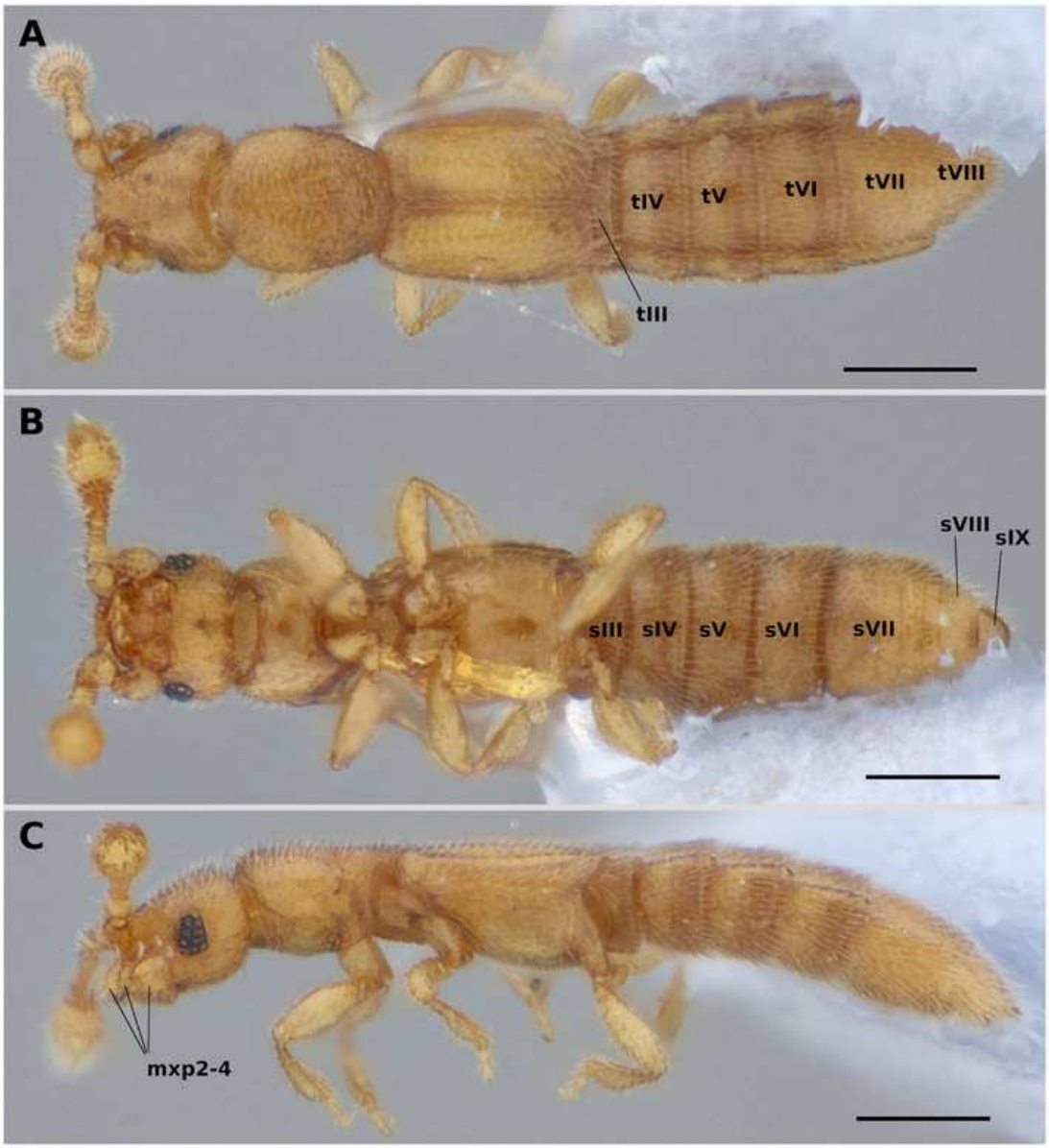

FIGURE 1. Dorsal (A), ventral (B) and profile (C) views of female paratype (CELC000148) of *Mayetia atlantica* from Espírito Santo. Abbreviations: **sIII-IX**, sternites III to IX; **tIII-VIII**, tergites III to VIII; **mxp2-4**, maxillary palpomeres 2 to 4. Scale bars: 0.1 mm.

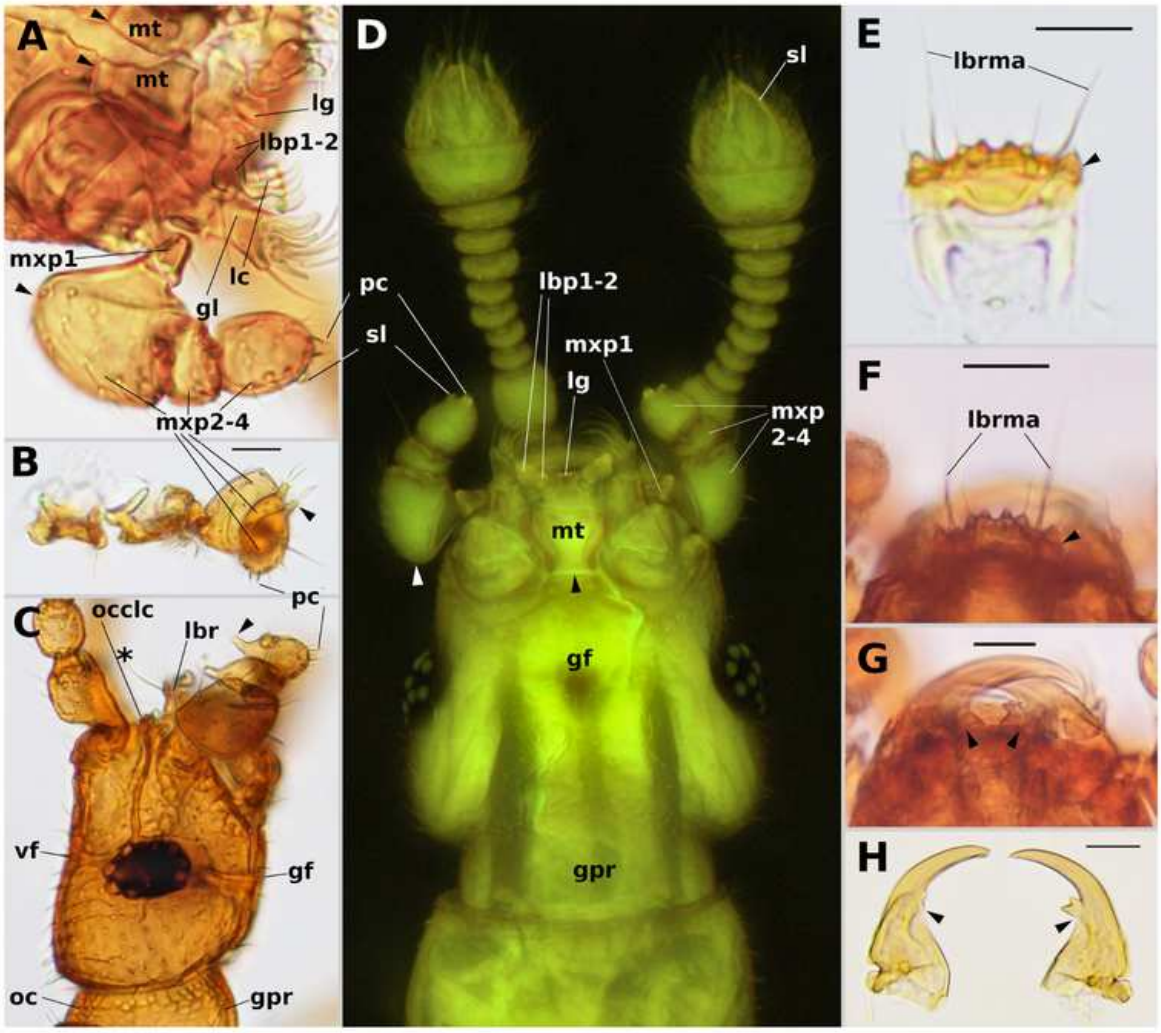

FIGURE 2. Various features of the head of *Mayetia atlantica*. A, ventral view of right maxilla and labium (CELC003058); B, anterior view of maxilla and labium (CELC003063); C and D, lateral and ventral views of head, respectively (CELC003038), asterisk indicates labral macrocheta; E and F, labrum dissected and *in situ*, respectively (female CELC003063 and holotype male CELC003054, respectively); G and H, mandibles *in situ* and dissected, respectively (male CELC003054 and female CELC003063). Triangles in A and D point to the base of mentum (mentum torn in A) and the curvature of maxillary palpomere 2; triangles in B and C point to the tip of tubercle of palpomere 4; triangles in E and F point to the right corner of labrum; and triangles in G and H point to the base of retinacle (left retinacle lost in specimen in H during preparation). Abbreviations: **gf**, gular fovea; **gl**, galea; **gpr**, posterior gular region; **lbr**, labrum; **lbrma**, labrum macrocheta; **lbp1-2**, labial palpomeres 1 and 2; **lc**, lascinia; **lg**, ligula; **mt**, mentum; **mxp**, maxillary palpomeres; **oc**, occipital region; **occlc**, ocular-clypeal carina; **pc**, palpal cone; **sl**, sensillum; **vf**, vertexal fovea. Scale bars are 0.02 mm.

Thorax. Pronotum disc mildly convex, slightly longer than wide; anterior corners round, posterior corners slightly more angled, but still round. Pronotal maximum width anterior to midlength and about as much as head width; lateral margins curved, with inconspicuous notches just posterad midlength. Pronotal antebasal sulcus absent, but a faint line can be seen in some mounted specimens; foveae or cavities absent from pronotal disc, except for longitudinal medial sulcus almost entirely confined to the pronotum posterior half. Elytra longer than wide, widest posterior to its midlength; without carinae or striae, except for sutural striae; basal elytral foveae present; some specimens with one pit, some with two. Hind wing developed, membranous, about four times as long as elytron; venation absent, its margin fringed with setae twice as long as hind wing's width. Propleura trapezoidal, posterolaterally with a pair of lateral procoxal foveae. Scutellar shield roughly triangular; margins sinuous. Metendosternite stalk

and furcal arms cylindrical, about the same caliber, except for tips of furcal arms which get thinner; stalk straight and furcal arms U-shaped; entire structure anterodorsally inclined. Intermetacoxal space reduced to the width of bispinose intermetacoxal process. Legs subequal in length, each smaller than the combined length of pronotum and elytra. Coxae adjuct, pro- and mesocoxae pyramidal, dorsoventrally tall; metacoxae dorsoventrally short, broad mediolaterally, triangular. Trochanters small, with mildly convex ventral margins. Femora thicker at midlength; tibiae thickiest point past midlength. Inner and outer margins of coxae convex; inner margin of tibiae flat, outer margins convex. Apex of each tibia with a single short and thick spiny spur; distally, tibiae with dense suberect, simple setae. Tarsomeres appearing to be only two (see discussion), the basal (tarsomere 2) only slightly longer than half the length of the apical (tarsomere 3). Pretarsal claw single.

Abdomen elongate, about as long as head and thorax, slightly dorsoventrally flattened, curving ventrally. In dorsal view, widest at about sixth or seventh abdominal segment (4th or 5th visible); segments 3–6 subequal in shape, but gradually elongating and widening posteriorly; paratergites conspicuous from third to sixth, thinner on seventh. Seventh tergite (fifth visible) square, the longest in abdomen. Tergite spiracles on tergites II (internal), III, VII and VIII. Conspicuous, brick-like; intersegmental membrane between segments 3 and 4, 4 and 5, 5 and 6, and 6 and 7. Sternite III anteromedially keeled; sternite VIII posterior margin with two concavities; sternite IX of females small, triangular.

Male. No pronounced sexual dimorphism, except for a tiny pair of spines on the metatrochanters, tergite VIII apparently longer than in females, posterior margin of sternite VIII V-shaped and presence of hemisternites. Aedeagus sinuose both in lateral and in ventral (or dorsal) views, more so in ventral view, as the apex of distal apophysis is inclined to left; a few calluses or swellings laterad the basal foramen; ventral sulcus or constriction separates basal portion from basal capsule, the latter is not swollen and is continuous to the flattened and apically truncate distal apophysis.

Etymology. The name is in reference to the Brazilian Atlantic Forest biome, from where the species is known.

Biology. Nothing is known about the biology of the species, except that all Winkler/Berlese extractors samples in which specimens were found were composed of a mixture of litter and a few centimeters of the soil below the litter (and not the litter only, as is usual, at least when the process is made through Winkler extractors). All eight specimens from the type locality (types and non-types) were sampled in the same extractor, that is, within less than one meter square.

Discussion

Mayetia atlantica can be easily differentiated from *M. venezuelica* for being macrophtalmic and macropterous, while *M. venezuelica* is anophtalmic and apterous. *Mayetia peruana*, on the other hand, is similar to *M. atlantica* in being macrophtalmic and macropterous, but both can be told apart by the following features: (**i**) *M. atlantica* has a pair of vertexal foveae which are more anteriorly positioned on the head, at about the eye level, while *M. peruana* have them posterior to the eye level, and the foveae appear to be smaller and/or shallower in *M. atlantica* (Fig. 3, C and Fig. 4, B); (**ii**) sulci anterior to the vertexal foveae are inconspicuous in *M. atlantica* (very shallow and small in length, Fig. 3, C and Fig. 4, B); (**iii**) the eyes in *M. atlantica* appear to have less ommatidia, up to 13 (Fig. 1, C and Fig. 2, C) while there are about 15 in *M. peruana* (observation in more specimens, especially of *M. peruana*, is needed to confirm that); (**iv**) medial labral notch in *M. atlantica* (Fig. 2, E and F) appears to be even shallower than in *M. peruana*; (**v**) palpomeres 3 and 4 of *M. atlantica* have dorsal tubercles (Fig. 2, B and C and Fig. 4, A) which are absent in *M. peruana*; (**vi**) there are no shallow pair of pits posterolaterally on the pronotum of *M. atlantica* (Fig. 3, C and Fig. 4, D) as in *M. peruana*; (**vii**) the medial longitudinal pronotal sulcus in *M. atlantica* is entirely confined to the posterior half of the pronotum (Fig. 3, C and Fig. 4, D), while it spans the two halves in *M. peruana* and appears to be slightly longer; (**viii**) basal elytral foveae are present in *M. atlantica* and absent in *M. peruana* (Fig. 4, D–F). Basal elytral foveae were observed to vary between specimens of *M. atlantica* (Fig. 4, D–F) from one tiny pit located within a depression to two pits; that variation was observed within the series of Espírito Santo (male with two pits, females having one or two pits, Fig. 4, E and F) and between specimens from different localities (one pit in the female from Minas Gerais, Fig. 4, D). No other morphological variation was observed between the larger series from Espírito Santo and the two females from Bahia. The shape of the palpomeres 2–4 of the specimen from Minas Gerais (Fig.4, A) can be considered slightly different from the others (Fig. 2, A, C and D), but that might also be a result of the angle of observation.

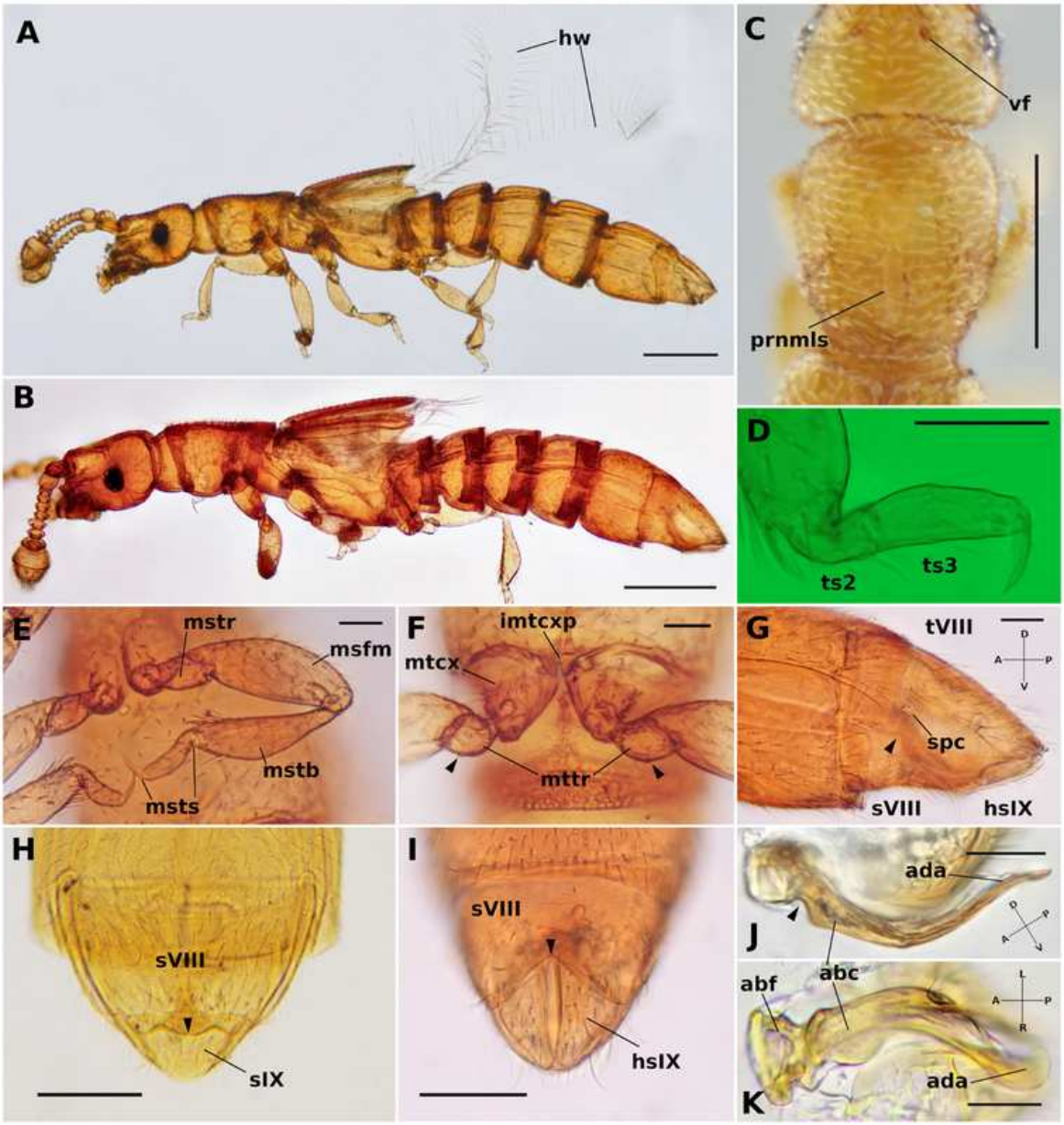

FIGURE 3. Various features of *Mayetia atlantica.* A and B, female (CELC003038) and holotype male (CELC003054), respectively, in profile view; C, zoomed dorsal view of the pronotum and vertex (CELC001048); D, protarsus (CELC003063); E and F, middle and zoomed hind legs, respectively (CELC003054, triangles in F point to metatrochanter spines); G, apex of abdomen of male (CELC003054) in lateral view with aedeagus, prior to dissection, visible by transparency (triangle in G and J point to the same spot, the constriction basal to aedeagus basal capsule); H and I, apex of abdomen in ventral view of female (CELC003038) and male (CELC003054), respectively (triangles indicate posterior margin of sternite VIII; J and K, aedeagus in ventral and lateral views, respectively (CELC003054, triangle points to constriction). Abbreviations: **abc**, aedeagus basal capsule; **abf**, aedeagus basal foramen; **ada**, aedeagus distal apophysis; **hsIX**, hemi-sternite; **hw**, hind wing; **imtcxp**, intermetacoxal process; **msfm**, mesofemur; **mstb**, mesotibia; **mstr**, mesotrochanter; **msts**, mesotarsus; **mtcx**, metacoxa; **mttr**, metatrochanter; **prnmls**, pronotal medial longitudinal sulcus; **sVIII** and **sIX**, sternites VIII and IX; **spc**, spiracle; **tVIII**, tergite VIII; **ts**, tarsomere; **vf**, vertexal fovea. Scale bars in A, B, and C are 0.1 mm; in H and I are 0.05 mm; in D, E, F, G, J and K are 0.02 mm. Cross in J indicates anterior, posterior, dorsal and ventral positions and in K, anterior, posterior, left and right.

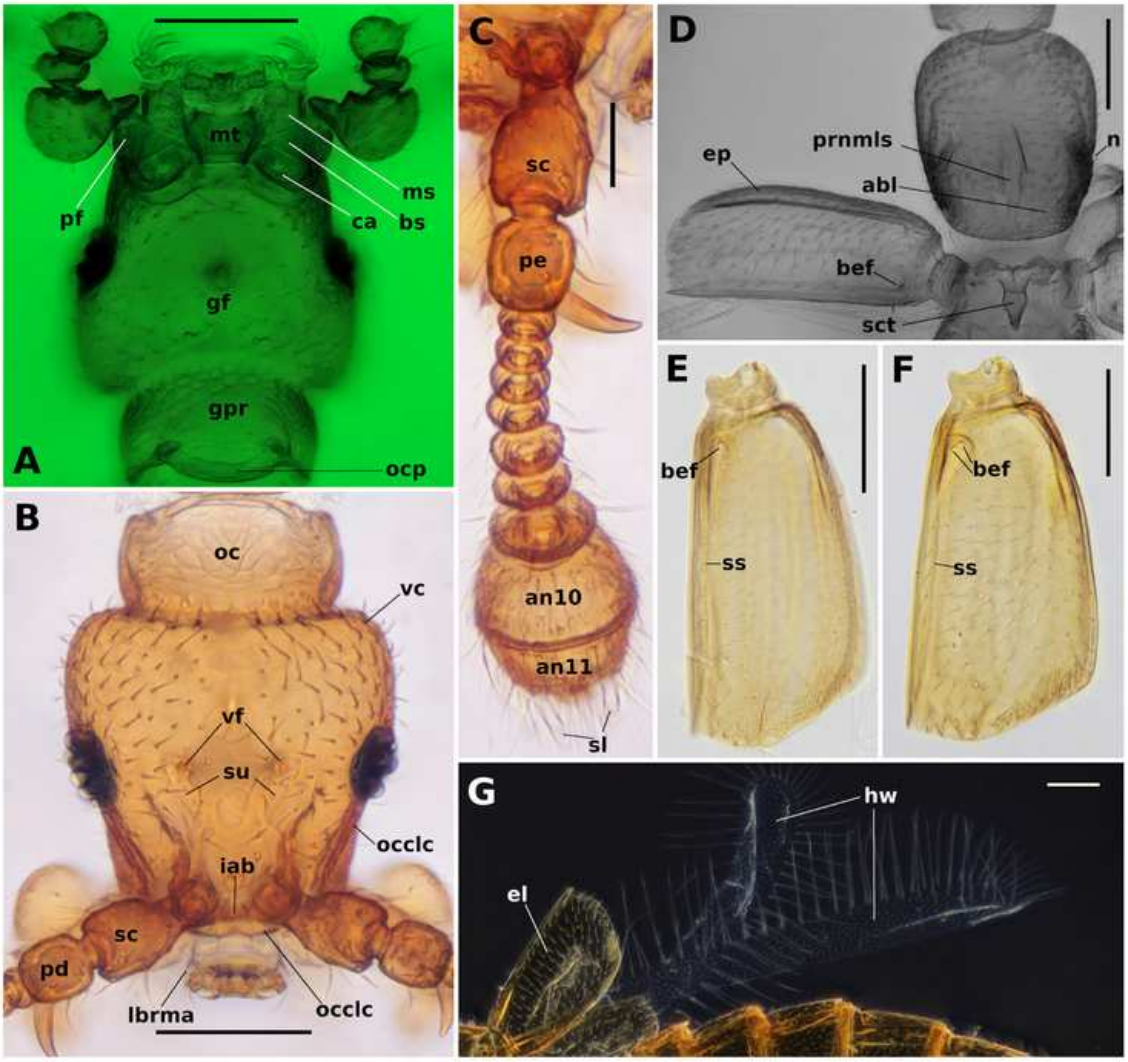

FIGURE 4. Various features of *Mayetia atlantica*. A, ventral view of the head (CELC000969); B, dorsal view of the head (CELC000969); C, dorsal view of right antenna (CELC000969); D, pronotum and left elytron (CELC000969); E, right elytron of female (CELC003058); F, right elytron of holotype male (CELC003054, two basal elytral foveae is not a male-only characteristic, see text); G, hind wings (CELC000358). Abbreviations: **abl**, antebasal line; **an**, antennomere; **bef**, basal elytral fovea; **bs**, basistipe; **ca**, cardo; **ep**, epipleuron; **el**, elytron; **gf**, gular fovea; **gpr**, posterior gular region; **hw**, hind wing; **iab**, interantennal bridge; **lbrma**, labrum macrocheta; **ms**, mediostipe; **mt**, mentum; **n**, notch; **oc**, occiput; **occlc**, ocular-clypeal carina; **ocp**, postocciput; **pe**, pedicel; **pf**, palpifer; **prnmls**, pronotal medial longitudinal sulcus; **sc**, scape; **sct**, scutellar shield; **sl**, sensilla; **ss**, sutural stria; **su**, sulcus; **vc**, vertexal corners; **vf**, vertexal fovea. Scale bars 0.05 mm, except for C where it is 0.02.

We examined as best as we could the tarsomeres of mounted specimens and we could not confirm the existence of a very reduced tarsomere 1 (out of 3 tarsomeres, as depicted in Orousset, 2022, Fig. 19). Instead, all specimens appear to have only two tarsomeres (Fig. 3, D). Despite that, because the shape of the observed tarsomeres of *M. atlantica* match the shape of tarsomeres 2 and 3 of Orousset's drawing, we maintain the terminology and called the observed tarsomeres as ts2 and ts3, assuming the first has been lost.

Mayetia atlantica has the largest known series among the three macropterous and macrophthalmic species of the genus and is the only one which has the male described. There is a register of a morphospecies from Colombia, represented by the male and the female, which has not been described (Orousset, 2022). The aedeagus of *M. atlantica*

described here will be an important diagnostic feature when the males of the other two Neotropical species or males of new species are discovered. The two extremes of the known distributional range of *M. atlantica* (Porto Seguro, state of Bahia, to Cataguases, state of Minas Gerais) are about 660 Km apart. The distributional range covers a wide and very heterogeneous area of the Brazilian Atlantic Forest. However, it is important to note that habitus similarity is common in *Mayetia* and the aedeagus is the main identification character (Struyve, 2018). Since only one of *M. atlantica* populations has the male known, it is still a possibility that the discovering of the males in the other localities could reveal that *M. atlantica* is, in fact, a complex of species. For that reason, we made the type series to be composed only of specimens of the Espírito Santo state population.

Mayetia atlantica expands the genus distribution in the Neotropics by about 3.500 km to the southeast, reaching the opposite side of the continent from the places where it was previously found, Peru and Venezuela (Fig. 5). The Venezuelan species, for instance, is geographically closer to some Nearctic species from southern USA than it is to *M. atlantica*. The new occurrence in the Brazilian Atlantic Forest, in practical terms, makes the genus expected to be found in most other countries of South America.

FIGURE 5. Occurrence of the genus *Mayetia* in South America. *Mayetia peruana* is represented by the squares; *M. venezuelica* by the triangle and *M. atlantica* by the circles.

Acknowledgements

We thank Tim Struyve (Mechelen, Belgium) and Jean Orousset (Muséum national d'Histoire naturelle, Paris, France) for reviewing the paper and Julieth Castiblanco for reviewing the Spanish version of the abstract. We also thank the researchers Nathália Safar, Glauco Martins, Gabriela Jacintho, Clodoaldo Assis and Eduarda Vieira from the Universidade Federal de Viçosa, Minas Gerais, Brazil, which made available for our study dozens of litter and soil samples collected by them in the states of Bahia and Minas Gerais, and in which were found some of the specimens studied here. Financial support was provided by Conselho Nacional de Desenvolvimento Científico e Tecnológico (CNPq; research grant number 308432/2018-5 to the junior author), Fundação de Amparo à Pesquisa do Estado de Minas Gerais (FAPEMIG; Edital 02/2018—Programa Pesquisador Mineiro XII—PPM-00314-18) and Coordenação de Aperfeiçoamento de Pessoal de Nível Superior—Brasil (CAPES; Finance Code 001; doctorate degree grant to the senior author).

References

Besuchet, C., Burckhardt, D.H. & Löbl, I. (1987) The "Winkler/Moczarski" Eclector as an Efficient Extractor for Fungus and Litter Coleoptera. *The Coleopterists Bulletin,* 41 (4), 392–394.

Chandler, D.S. (2001) *Biology, morphology, and systematics of the ant-like litter beetle genera of Australia (Coleoptera: Staphylinidae: Pselaphinae).* Memoirs on Entomology International, Associated Publishers, Florida, VIII + 560 pp.

Decu, V. (1991) Coléoptères édaphobiontes du Venezuela. II. *Mayetia venezuelica* n. sp. (Pselaphidae – Mayetiini). *Travaux de l'Institut de Spéologie "Emile Racovitza"*, XXX, 47–49.

Evenhuis, N.L. (2022) *The insect and spider collections of the world website.* Available from: http://hbs.bishopmuseum.org/codens/ (accessed 28 March 2022)

Kawada, R. & Buffington, M.L. (2016) A Scalable and Modular Dome Illumination System for Scientific Microphotography on a Budget. *PLoS ONE,* 11 (5), 1–20. https://doi.org/10.1371/journal.pone.0153426.

Kimball, S. & Mattis, P. (1996) *GIMP – The GNU Image Manipulation Program.* Available from: https://www.gimp.org (accessed 30 May 2022)

Morrone, J.J. (2015) Biogeographical regionalisation of the world: a reappraisal. *Australian Systematic Botany*, 28, 81–90. https://doi.org/10.1071/SB14042

Newton, A.F. & Chandler, D.S. (1989) World catalog of the genera of Pselaphidae (Coleoptera). *Fieldiana Zoology,* 53, 1–93. https://doi.org/10.5962/bhl.title.3209

Omar, M.B., Bolland, L. & Heather, W.A. (1979) A permanent mounting medium for fungi. *Bulletin of the British Mycological Society*, 13 (1), 13–32. https://doi.org/10.1016/s0007-1528(79)80038-3

Orousset, J. (1995) Découverte de *Mayetia* macrophthalmes et macroptères en régions néotropicale et asiatique (Coleoptera, Pselaphidae). *Annales de la Société entomologique de France*, New Series, 31 (1), 57–61.

Orousset, J. (2022) Le genre *Mayetia* Mulsant & Rey, 1875: catalogue commenté (Coleoptera, Staphylinidae, Pselaphinae). *Revue Française d'Entomologie Générale*, 4 (1–2), 1–152.

Parker, J. (2016) Emergence of a superradiation: pselaphine rove beetles in midCretaceous amber from Myanmar and their evolutionary implications. *Systematic Entomology,* 41, 541–566. https://doi.org/10.1111/syen.12173

Struyve, T. (2018) On the soil dwelling Staphylinidae of Northwest Spain (Coleoptera). *Belgian Journal of Entomology,* 72, 1–59.

IV. CAPÍTULO 3

A NEW SPECIES OF *METOPIELLUS* RAFFRAY (COLEOPTERA: STAPHYLINIDAE: PSELAPHINAE) FROM THE ATLANTIC FOREST OF BRAZIL, WITH KEYS TO SPECIES OF THE GENUS AND TO THE GENERA OF METOPIASINI

Artigo aceito para publicação na revista
Studies on Neotropical Fauna and Environment.
DOI: 10.1080/01650521.2024.2333103

A new species of *Metopiellus* Raffray (Coleoptera: Staphylinidae: Pselaphinae) from the Atlantic Forest of Brazil, with keys to species of the genus and to the genera of Metopiasini

Júlio Cezar Mário Chaul[1, 2] & Cristiano Lopes-Andrade[2]

1. Programa de Pós-Graduação em Ecologia, Departamento de Biologia Geral, Universidade Federal de Viçosa, 36570-900, Viçosa, Minas Gerais, Brazil.

2. Laboratório de Sistemática e Biologia de Coleoptera, Departamento de Biologia Animal, Universidade Federal de Viçosa, Viçosa, Minas Gerais, Brazil.

Correspondence: Laboratório de Sistemática e Biologia de Coleoptera, Departamento de Biologia Animal, Universidade Federal de Viçosa, Av. P.H. Rolfs, s/n, CEP 36570-900, Viçosa, MG, Brasil. Email: juliocchaul@gmail.com

A new species of *Metopiellus* Raffray (Coleoptera: Staphylinidae: Pselaphinae) from the Atlantic Forest of Brazil, with keys to species of the genus and to the genera of Metopiasini

A new Brazilian species of *Metopiellus* Raffray from the Atlantic Forest biome is described. The species, *Metopiellus emavieirae* sp. nov., the seventh described for the genus so far, belongs to Metopiasini, a tribe suspected to be composed mainly of myrmecophiles. Nothing is known about the biology of the new species, which is morphologically similar to the recently described *Metopiellus guanano* Fiorentino, Tocora & Ramirez from Colombia. A key to the species of *Metopiellus* is provided, as well as two keys to genera of Metopiasini, one dichotomous and one multi-entry, online-based.

Keywords: Biodiversity; Neotropical; Interactive key

Introduction

Metopiasini (formerly treated as Metopiini, see Thayer and Newton 1992) is a morphologically remarkable tribe of the supertribe Euplectitae of Pselaphinae rove beetles. They are divided into two subtribes, Metopiasina and Rhinoscepsina, totaling nine genera and 68 species (Chandler 2002; Asenjo et al. 2019). The monogeneric Rhinoscepsina is composed of *Rhinoscepsis* LeConte, 1878, with 11 Nearctic and Neotropical species (from now on in the text, biogeographical regionalisation sensu Morrone and Ebach 2022), but used to include the genus *Morius* Casey, 1894 (now in Trichonichyni) (Newton and Chandler 1989; Newton et al. 2000; Chandler 2002). Metopiasina is composed of eight genera restricted to the Neotropical region: *Barrometopia* Park, 1942 (1 sp.); *Bibrax* Fletcher, 1927 (1 sp.); *Macrommatias* Gaudin and Coache, 2022 (5 spp.; Comellini 1998); *Metopias* Gory, 1832 (4 spp.; Comellini 1993); *Metopiasoides* Comellini, 2000 (10 spp.); *Metopiellus* Raffray, 1908 (7 spp., including the one

described here); *Metopiosoma* Raffray, 1908 (9 spp.); and *Metopioxys* Reitter, 1885 (20 spp.; Comellini 1983).

A recent phylogenetic study (Parker 2016a), of combined morphology and molecular datasets, recovered one Metopiasini species ("Metopiasini sp.") as sister to a clade of two Jubini species (*Jubus* sp. + *Endytocera* sp.). The clade formed by these three species was recovered as sister to the clade *Conoplectus* sp. + *Rhexius* sp., and these five terminals, for their turn, formed a clade within the polyphyletic Euplectitae, mixed with terminals of other supertribes and fossil species.

The Metopiasini are one of the tribes of Pselaphinae suspected to be composed primarily (maybe exclusively) of myrmecophiles (Parker 2016b), although many times they are collected by litter/soil extracting techniques (soil sample by flotation, Berlese extractors, or Winkler extractors), a situation in which their association with ant colonies cannot be inferred. Even so, some species have been collected with ants, as *Metopiellus aglenus* Schaufuss, 1890 with "*Tetramorium reitteri* Mayr, 1887" (Asenjo et al. 2017), an ant species currently belonging to the genus *Hylomyrma* Forel, 1912 (Bolton 2024). Curiously, as pselaphines are not usually found in association with termites, one metopiasine species, *Barrometopia quasimoda* Park, 1942 had part of its type series sampled within the nest of the termite *Termes panamaensis* (Snyder, 1923) (Park 1942).

The tribe is morphologically defined mainly by the juxtaposed and protruded antennal insertions forming a conspicuous projection on the frons (Fig. 1, A and B, black triangles), which projects the antennal tubercles anterodorsally (Fig. 1, A, white triangles). They usually have very long scapes (Metopiasina only) (Fig. 1, C and D) and a thickened protibia, with a carina-delimited, concave medial surface (Fig. 4, D and E); and males have a divided tergite IX (sixth visible; treated as sternite IX, or "hemisternites", in previous publications; e.g. Park 1942; Chandler 2002) (Park 1942). Within the tribe, the genus *Metopiellus* is distinguished by the combination of the following traits: second antennomere much longer than the third, protibia

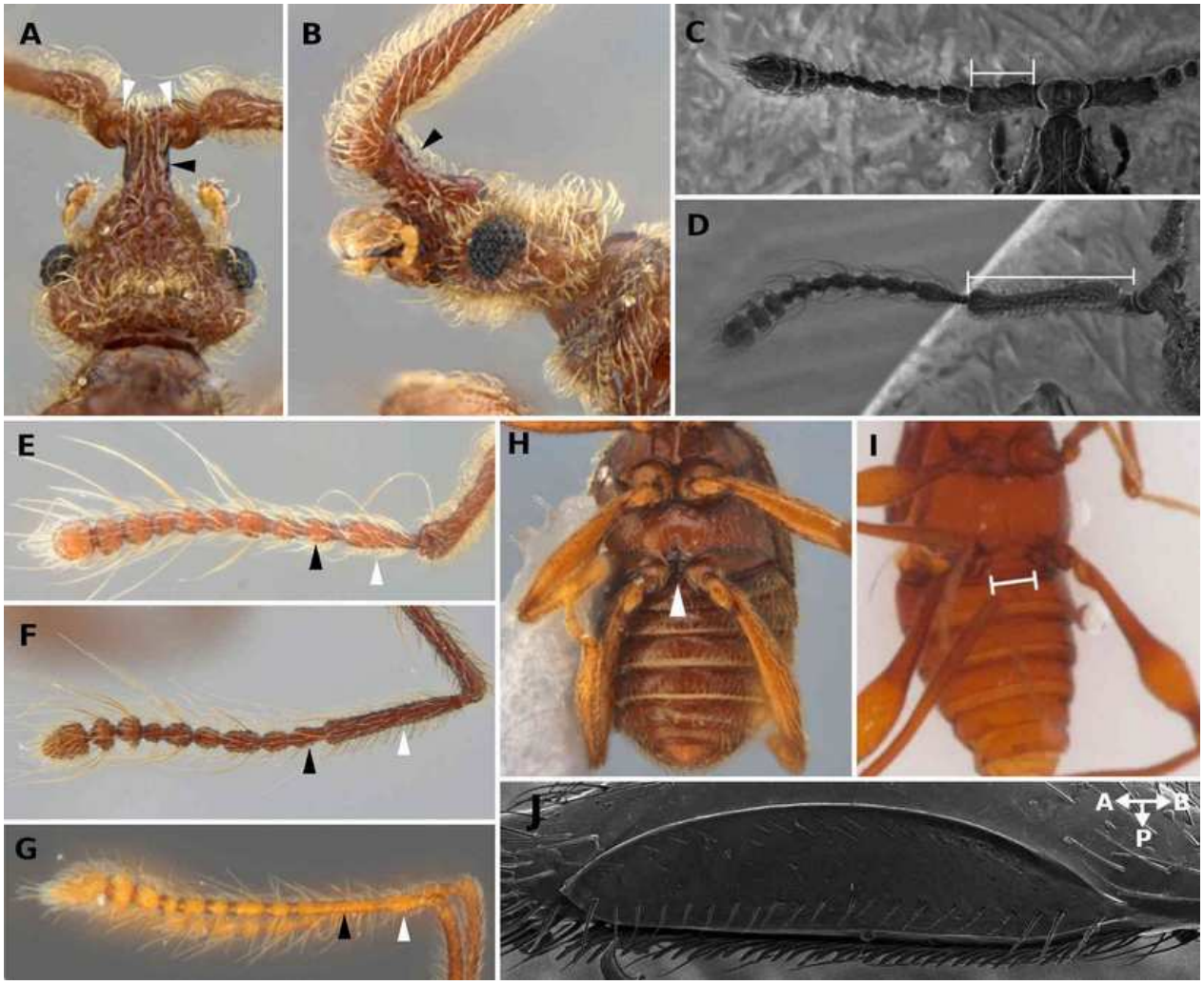

Figure 1. Key features of the Metopiasini. Head in dorsal (**A**) and lateral (**B**) views, showing frontal projection (black triangle) with antennal tubercles (white triangles). Antennae with short scape of Rhinoscepisina (**C**) and a long scape of Metopiasina (**D**). Antennomeres 2–11 showing relative length of second (white triangle) in relation to third (black triangle) of *Metopias* sp. (**E**), *Metopiellus emavieirae* **sp. nov.**, and *Metopioxys seeversi* (**G**, image by Andrea Gruver, courtesy of the Field Museum of Natural History). Ventral view of *Rhinoscepsis* sp. (**H**) and of *Metopioxys* sp. (**I**, image by Daniel Llavaneras), comparing different shapes of metacoxae, adjunct in H and widely separated in I. Inner surface of the protibia of *Metopias* sp., A, B, and P being apical, basal and posterior, respectively.

carinated anteromedially (carina open at base and posteromedially absent or weak), metacoxae contiguous or nearly so and pronotum without sharp spines on the lateral edge, at most having thickened spinose protuberances mediolaterally on the pronotal disc. Recently, three new species

were added to the genus: *Metopiellus painensis* Asenjo, Ferreira & Zampaulo, 2017, from the Southeast Region of Brazil; *Metopiellus guanano* Fiorentino, Tocora & Ramirez, 2022, from Colombia; and *Metopiellus crypticus* Asenjo, 2023, from the North Region of Brazil. *Metopiellus guanano* stands out in the genus for being the only one so far having the pronotal spinose protuberances mentioned above. Here we describe *Metopiellus emavieirae* sp. nov. from the Brazilian Atlantic Forest, a species strikingly similar to *M. guanano*. The type locality of the new species is 3,800 km distant from that of *M. guanano*, and they differ significantly in male secondary sexual characteristics and in the shape of the aedeagus.

Material and Methods

The repository institution is Coleção Entomológica do Laboratório de Sistemática e Biologia de Coleoptera (CELC; Federal University of Viçosa, Minas Gerais, Brazil) (Evenhuis 2024).

Images of the type series, both submerged in ethanol gel and dry-mounted, were taken through a Leica M205A stereomicroscope with a Leica MC170 HD camera attached. Acquired images were stacked in Zerene Stacker (Zerene Systems LLC, 2023) and then enhanced in the freeware GIMP (Kimball and Mattis 1996). Dissected sclerites, including aedeagus, were mounted between two pairs of round cover glasses (10 mm diameter) pinned below the specimen, using polyvinyl alcohol-lactic acid-glycerol (PVLG) as mounting medium (Omar et al. 1979).

The terminology is based on Chandler (2001) and on free translations from the terms used by Comellini (1983, 1993, 1994, 1998, 2000). Measurements given in the description are in millimeters, and their abbreviations and explanations are as follows:

- Head width (HW), the maximum width of head at the level just posterior to the eyes;
- Head length (HL), measured from the anteriormost point of antennal platform to midpoint of the vertexal margin (at the vertex-occiput constriction);
- Scape length (SL), the maximum length of scape, position adjusted accordingly;

- Antennomeres 1–11 length (AntL), the maximum length of each antennomere, in order from antennomere 1 to antennomere 11 (eleven numbers separated by commas);
- Antennomeres 1–11 width (AntW), the maximum width of each antennomere, in order from antennomere 1 to antennomere 11 (eleven numbers separated by commas);
- Pronotal length (PrnL), maximum length of pronotum, measured with the anterior and posterior margins at the same plane of focus;
- Pronotal anterior width (PrnaW), the width at the pronotal-occipital articulation level, measured in the same view as PrnL;
- Pronotal maximum width (PrnW), the maximum width of pronotum, measured in the same view as PrnL;
- Pronotal posterior width (PrnpW), the width at the pronotal-mesothorax articulation level, measured in the same view as PrnL;
- Elytra length (EL), the maximum length of elytra, measured with the anterior and posterior margins at the same focus plane;
- Elytra width (EW), maximum width of elytra, measured in the same view as EL;
- Abdomen length (AbdL), the maximum length of the abdomen in dorsal view measured in the same position of EL;
- Metafemur length (MtfmL), the maximum length of the metafemur, position adjusted accordingly;
- Metatibia length (MttbL), the maximum length of the metatibia, position adjusted accordingly;
- Metatarsus length (MttsL), the maximum length of the metatarsus, position adjusted accordingly;
- Metatarsomere 2 length (Ts2L), maximum length of metatarsomere 2, measured in the same view as MttsL;

- Metatarsomere 3 length (Ts3L), maximum length of metatarsomere 3, measured in the same view as MttsL.

Apart from the dichotomous key for the genera of Metopiasini, an interactive multi-entry key was also constructed and is hosted in the Xper^3 platform (Ung et al. 2010; Vignes-Lebbe et al. 2017; Kerner et al. 2021). This key can be used online in any web browser. It works by the user choosing any character and one of its states that suits better the specimen being identified. The characters can be chosen in any order. The list of possibilities will gradually reduce as the user repeats this process, up to the point when only one possibility, ideally, is left. Xper3 is a freeware for both users and key developers.

Results

Taxonomy

Keys to the extant genera of Metopiasini

Note 1: See above the diagnosis of Metopiasini to find out which Pselaphinae specimens are suitable to run in the keys below (for a more complete discussion on the tribe's definitions, see Park, 1942).

Note 2: The extinct monospecific *Hagnometopias* Schaufuss, 1890 from Baltic amber was not included in the key below, but it was included in the multy-entry key (see Discussion for more information).

The multi-entry, interactive key can be accessed in the following link:

https://app.xper3.fr/xper3GeneratedFiles/publish/identification/8355317217902741225/mkey.html

1. Scape (antennomere 1) moderately long, less than half the length of the remaining antennomeres together (Fig. 1, C) ... **Rhinoscepsina** ... ***Rhinoscepsis* LeConte in Schwarz, 1878**

- Scape very elongate, much longer than half the length of the remaining antennomeres together (usually about as long as them) (Fig. 1, D) ... **Metopiasina** ... 2

2. Second antennomere subequal or longer than the third (Fig. 1, E and F) ... 3

- Third antennomere longer than the second (Fig. 1, G) ... 7

3. Second antennomere only slightly longer than the third (Fig. 1, E) ... ***Metopias*** **Gory, 1832**

- Second antennomere much longer than the third (Fig. 1, F) ... 4

4. Metacoxae contiguous or nearly so (Fig. 1, H) ... 5

- Metacoxae separated (Fig. 1, I) ... 6

5. Abdominal sternite III (first visible) longer than metacoxa. Gula with a longitudinal, medial groove and a single fovea ... ***Bibrax*** **Fletcher, 1927**

- Abdominal sternite III (first visible) shorter than metacoxa. Gula with or without a longitudinal groove and with a pair of foveae (Fig. 1, I) ... ***Metopiellus*** **Raffray, 1908**

6. Compound eye in the male reduced or vestigial. Setation on the body, dense. Elytra each with a well-defined sutural stria ... ***Barrometopia*** **Park, 1942**

- Compound eyes in the male well-developed. Setation on the body, sparse. Usually having a darkened, medial vertexal tooth. Elytra with no sutural striae ... ***Metopiosoma*** **Raffray, 1908**

7. Pronotum with a pair of acute spines at about the middle of the lateral margins ... ***Metopioxys*** **Reitter, 1885**

- Pronotum without spines ... 8

8. Antennomere 3 somewhat thickened in relation to antennomere 2 ... ***Macrommatias*** **Gaudin and Coache, 2022**

- Antennomere 3 not thickened in relation to antennomere 2 ... ***Metopiasoides*** **Comellini, 2000**

Key to the species of Metopiellus

Note: Adapted from Asenjo et al. (2017) and Fiorentino et al. (2022), see those references for images and illustrations for part of the couplets of the key.

1. Vertex with a pair of horn-like projections (Fig. 3 B); pronotum with two pairs of mediolateral, thick, spinose projections (Fig. 3 B and D) ... 2

- Vertex without horn-like projections; pronotum without two pairs of mediolateral, thick, spinose projections, either simply convex, or with a series of well-defined ... 3

2. Basal elytral fovea absent. Sternite VI and tergite VIII surfaces without processes in the male ... ***M. guanano*** **Fiorentino et al., 2022**

- Basal elytral foveae present, two pairs (Fig. 3, A). Sternite VI with a pair of mediolateral setose processes (Fig. 3, F) and tergite VIII with a medial subquadrate thick process in the male (Fig. 3, G) ... ***M. emavieirae*** **nov. sp.**

3. Head similar in width to pronotum; eyes absent ... ***M. aglenus*** **(Reitter, 1885)**

- Head narrower than pronotum; eyes small, but conspicuous, or very reduced, inconspicuous ... 4

4. Antennomere 2 about half as long as scape; antennomere 5 longer than antennomere 3 and 4 together ... 5

- Antennomere 2 less than half as long as scape; antennomere 5 shorter than length of antennomere 3 and 4 together... 6

5. Antennomere 7 rounded. In dorsal view of the head, lateral margins strongly constricted anterad the eyes. Paramere with apex bifurcated; median lobe curved and edge with long line of small teeth ... ***M. crypticus*** **Asenjo, 2023**

- Antennomere 7 rectangular. In dorsal view of the head, lateral margins gradually converging anterad the eyes. Paramere not bifurcated apically; median lobe almost straight, with the apex curved, without small teeth along its length ... ***M. painensis*** **Asenjo et al., 2017**

6. Antennomere 8 transverse; eyes small, but conspicuous ... ***M. hirtus*** **(Reitter, 1885)**

- Antennomere 8 obconical; eyes very reduced, inconspicuous ... ***M. silvaticus*** **Bruch, 1933**

Figure 2. *Metopiellus emavieirae* **sp. nov.** male holotype in profile (**A**), dorsal (**B**), and ventral (**C**) views. Scale bars are 1 mm.

Species accounts

Metopiellus emavieirae Chaul and Lopes-Andrade **sp. nov.**

(Figs. 2–6)

Type material. Holotype, male. Measurements: HW 0.60; HL 0.75; AntL (1st–11th) 1.35, 0.60, 0.12, 0.10, 0.15, 0.10, 0.11, 0.07, 0.10, 0.12, 0.18; AntW (1st–11th) 0.13, 0.10, 0.08, 0.08, 0.08, 0.08, 0.09, 0.07, 0.12, 0.13, 0.15; CEL 0.08; PrnL 0.63; PrnaW 0.33; PrnW 0.72; PrnpW 0.42; EL 1; EW 1.05; AbdL 1.22; MtfmL 1.35; MttbL 1.20; MttsL 0.60; Ts2L 0.38; Ts3L 0.22. Brazil: Minas Gerais, Araponga, Serra do Brigadeiro, Sítio Encontro dos Muriquis, 08.x.2022, winkler of soil, Vieira, E.M.A. (CELC002173) [CELC-UFV].

Paratype, female. Measurements: HW 0.59; HL 0.70; AntL (1st–11th) 1.35, 0.60, 0.12, 0.10, 0.15, 0.10, 0.10, 0.08, 0.08, 0.08, 0.18; AntW (1st–11th) 0.13, 0.10, 0.08, 0.08, 0.08, 0.08, 0.10, 0.09, 0.11, 0.12, 0.14; CEL 0.08; PrnL 0.63; PrnaW 0.35; PrnW 0.70; PrnpW 0.38; EL 1.03; EW 1.10; AbdL 1.15; MtfmL 1.35; MttbL 1.22; MttsL 0.62; Ts2L 0.35; Ts3L 0.19. Brazil: Minas Gerais, Araponga, Serra do Brigadeiro, -20.648460, -42,499991, 1280m, iv.2022, Native vegetation, manual sampling in soil blocks (TSBF), França. E. (CELC000246) [CELC-UFV].

Diagnosis. Antennomere 2 at least 3x longer than antennomere 3 (Fig. 4C). Protibiae anteromedially carinated (Fig. 4, D and E). Metacoxae contiguous (Fig. 2C, Fig. 3C and Fig. 6B). Vertex with a pair of blunt spines posterad the vertexal foveae (Fig. 3B, D and 6C). Pronotum without acute spines near the middle height of the lateral margins, but with two pairs of large-based, spinose protuberances more medially positioned, one pair anterior to the antebasal sulcus and the other posterior to it (Fig. 3B, D and 6C). Abdominal sternite VI with a pair of thick and blunt tubercles (male, Fig. 3C, E, F, and G). Abdominal tergite VIII with one medial subquadrate tubercle (male, Fig. 3A, C, E, F, H).

Geographic distribution. Serra do Brigadeiro, Minas Gerais, Southeast Region of Brazil.

Description. *General habitus*. Very large species, from anteriormost point of head to posteriormost point of abdomen, 3.75 mm. Entirely covered by very dense, relatively long dark setae; vertexal and pronotal protuberances almost hidden by the pilosity in the dry specimen; processes on abdominal sternite VI and tergite VIII of male more evident. Antennae strongly

geniculate, inserted in a conspicuous tubular projection of the frons. Legs not greatly elongate in relation to the body. Pronotum two thirds as wide as the elytra and slightly wider than the head in dorsal view. Elytra about as wide and as long as abdomen in dorsal view.

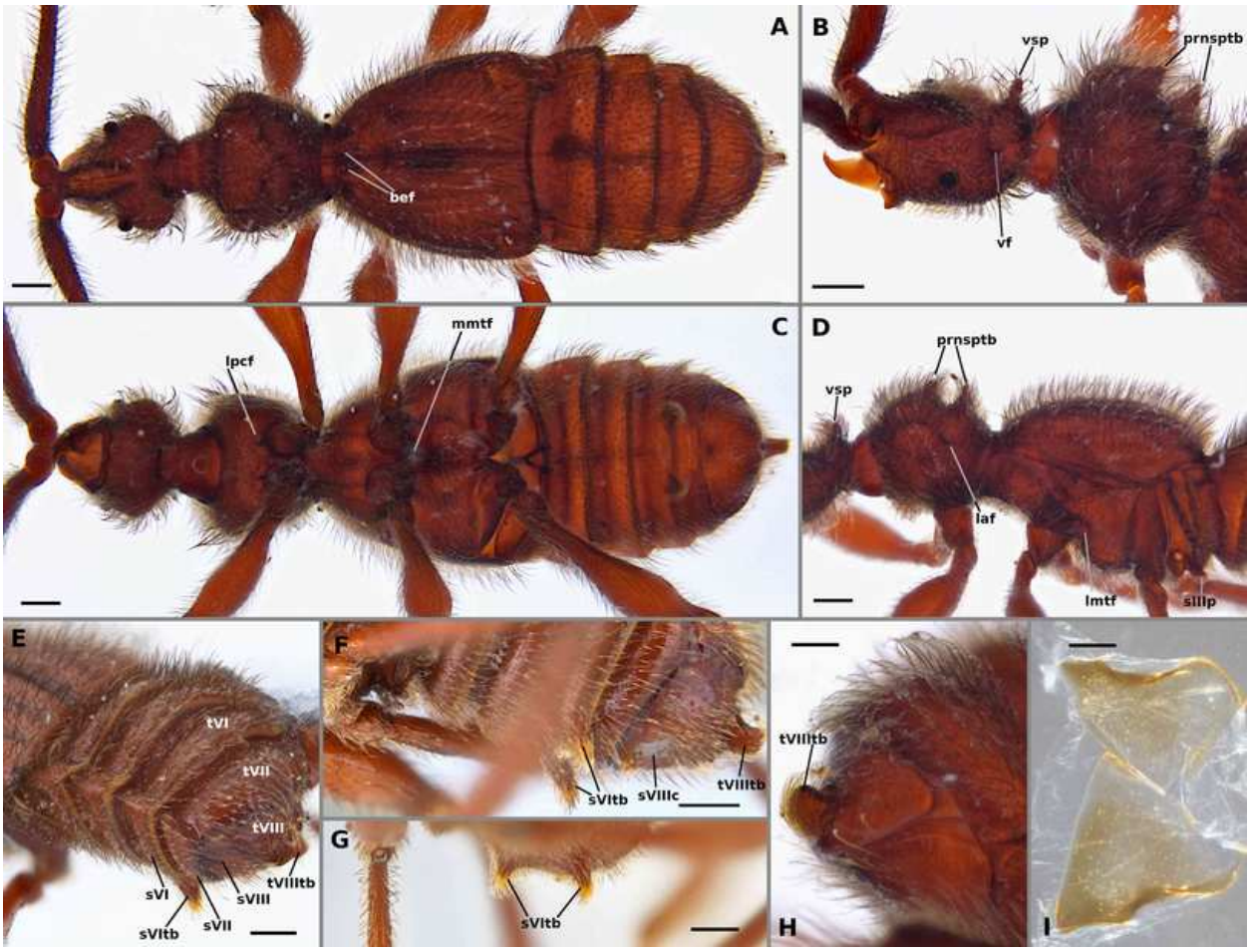

Figure 3. *Metopiellus emavieirae* **sp. nov.** male holotype: ethanol submerged (**A–D** and **H**), dry-mounted (**E–G**), and slide-mounted (I). Dorsal view of body (**A**); head and pronotum in anterodorsolateral view (**B**); ventral view of body (**C**); lateral view of thorax (**D**); abdomen in a posterodorsolateral view (**E**); abdomen in an anteroventrolateral view (**F**); pair of processes on abdominal sternite VI in anteroventral view (**G**); process on tergite VIII in posterodorsolateral view (**H**); divided tergite IX (**I**) . Scale bars: 0.2 mm (A–G), 0.1 mm (H and I). Acronyms (foveation pattern according to Chandler, 2001): **bef**, basal elytral foveae; **laf**, lateral antebasal foveae; **lmtf**, lateral metasternal foveae; **lpcf**, lateral procoxal foveae; **mmtf**, median metasternal fovea; **prnsptb**, pronotal spinose tubercle; **s** (III–VIII), sternites; **sVItb**,

sternite VI tubercles; **sVIIc**, sternite VIII concavity; **t** (IV–VIII), tergites; **tVIIItb**, tergite VIII tubercle; **vf**, vertexal foveae; **vsp**, vertexal spines.

Head. Positioned as to make the anterior margin of the antennal tubercles in plane with the vertexal margin, drop-shaped, discounting the antennal platform itself. Antennal platform roughly scissors-like, considering the antennal tubercles and the central tubular projection that connect them to the frons and vertex; a medial sulcus runs across the entire projection up to the anterior edge between the antennal tubercles. A pair of blunt, spinose tubercles originate posteromedially on the vertex, each subtended anteriorly by a vertexal fovea. Compound eyes very small, protruded. Head devoid of carinae, except for entire anterior clypeal margin, for a small medial and longitudinal carina on middle clypeus and anterior to the antennal platform, and for a pair of minute, oblique carinae posterior to the antennal insertions, which descends anterolaterally on clypeus (difficult to see, hidden by scapes). In lateral view, the posterior section of the antennal platform appears as a thick ridge that raises from the cephalic capsule. Cuticle on the head verrucose, each tiny bump is the origin of a seta. Anterior clypeal margin with a pair of macrochaetae (right one is abraded in the holotype). Antennae covered on dense pilosity recurved to the apex; among this pilosity, some thicker macrochaetae originate from each antennomere. Scape (antennomere 1) very long, thickened at its basal third, about 80% the length of the remaining antennomeres together; having two macrochaetae, one at about its mid-length and the other in between the first and the apex. Pedicel (antennomere 2) very long, about half as long as scape and about 4x as long as antennomere 3; four macrochaetae originate apically on the pedicel. Antennomeres 3–11 all fringed laterally with four or more macrochaetae. Antennomeres 3 and 4 small, subequal; antennomere 5 slightly larger than previous antennomeres 3 and 4; antennomere 6 about as long as 3 and 4; antennommere 7 as long as and just slightly thicker than 6; antennomere 8 the smallest; antennomeres 9–11 forming a club; antennomeres 9 and 10 of similar form and size; apical antennomere longer and as wide as the previous two together, basally flattened, apically oval, without concave faces. Mandible roughly triangular, forming clear dorsal and ventral surfaces; 11–12 teeth; discounting the apical tooth, teeth gradually increasing in size towards the apex, the apical one considerably longer than the previous; basally having a round (convex) lobe on the inner margin. Maxillary palps medium-sized; first palpomere minute, bent almost 90 degrees laterally; second palpomere much longer than wide

and gradually thickening towards apex, with a slight bent at about its mid-length; third palpomere only a little longer than wide, also gradually thickening towards the apex; fourth

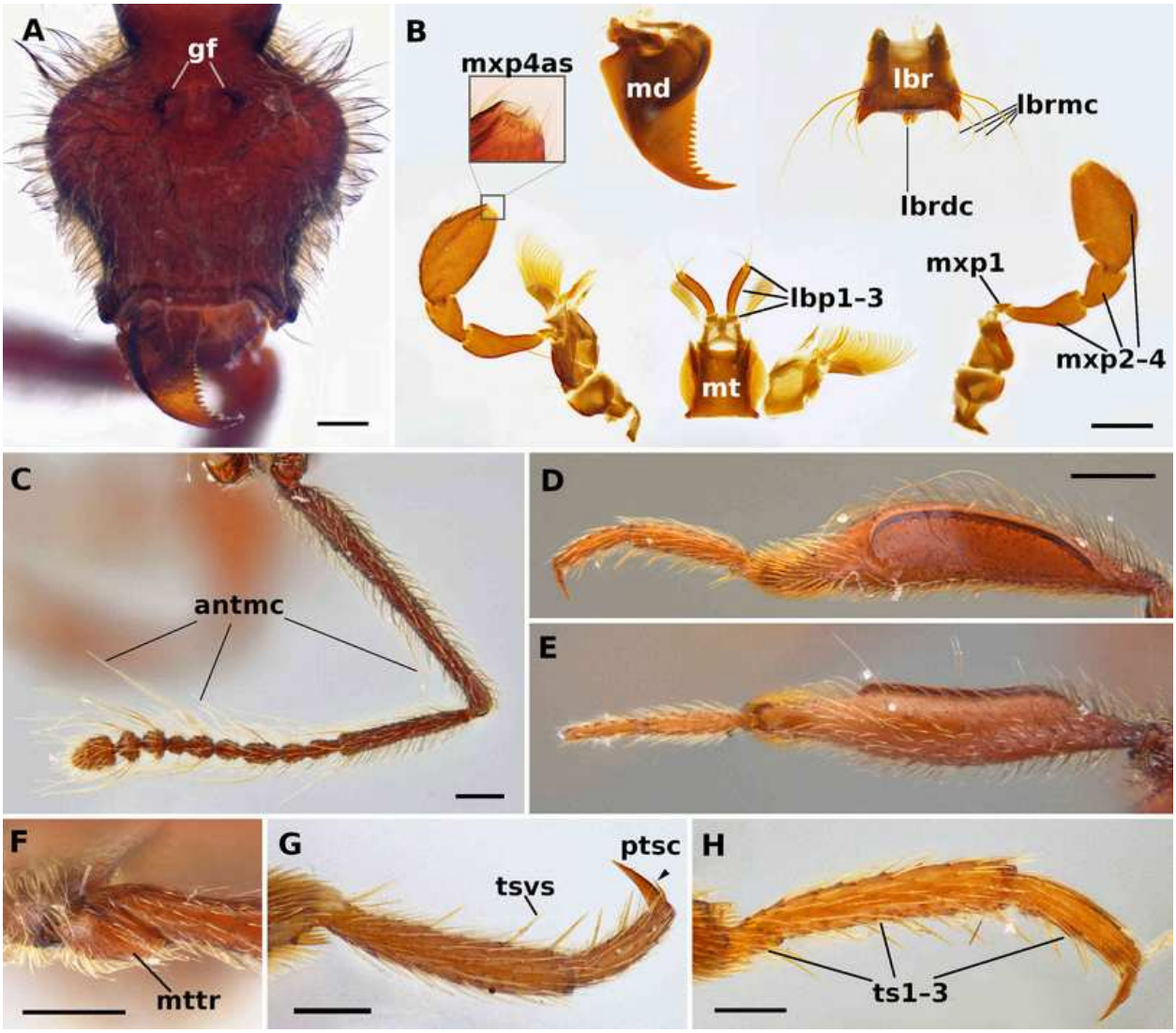

Figure 4. *Metopiellus emavieirae* **sp. nov.** male holotype, body details: head in ventral view (**A**, submerged in ethanol); mouthparts: mandible and labrum on top layer and labiomaxillary complex on bottom layer (**B**, parts dissected and mounted on slide); left antenna (**C**); right protibia and tarsus inner view (**D**); left protibia and tarsus in anterior view (**E**); left metatrochanter in anteroventral view (**F**); tarsi (**G** and **H**, seta-like claw indicated in G). Scale bars: 0.1 mm (A, B, G, H), 0.2 mm (C, D, F. Scale of E same of D). Acronyms: **antmc**, antennomeres macrochaetae; **gf**, gular foveae; **lbp** (1–3), labial palpomeres; **lbr**, labrum; **lbrdc**, labral dentiform chaetae; **lbrmc**, labral macrochaetae; **md**, mandible; **mt**,

mentum; **mttr**, metatrochanter; **mxp** (1–4), maxillary palpomeres; **mxp4as**, maxillary palpomere 4 apical sensilla; **ptsc**, pretarsal claws; **ts** (1–3), tarsomeres; **tsvs**, tarsomere row of ventral erect setae.

palpomere the largest, suboval, with a flat apex in profile and in anterior view with a small cavity where a minute apical sensilla sits. Labrum trapezoidal, indented apicolaterally and with at least four filiform, curved, macrochaetae close to each indentation and pair of tiny, dentiform chaetae medially on the distal margin. First and second labial palpomeres cylindrical, the first minute and wider than long, the second much longer than wide and much longer than the first, the combined lengths of labial palpomeres slightly less than the second maxillary palpomere; third labial palpomere subulate. Ligula about as wide as first labial palpomere. Mentum subquadrate, with indented (outwards) basal corners, lateral margins convex and with somewhat complex distal corners. A pair of gular fovea is located posteriorly on gular surface and have a small medial cavity in between them. Gular foveae are close to each other about as much as half the distance the vertexal foveae are close to each other. *Thorax*. Pronotum in dorsal view roughly trapezoidal, with round corners, posteriorly narrower than anteriorly. Most of the surface on each side of the anterior two thirds of the pronotum raising to form a more or less medially positioned pair of spinose, large-based tubercles; surface of posterior third with similar pair of slightly less robust spines. Pronotal transversal sulcus (antebasal sulcus) absent, a shallow transversal "corridor" or "valley" forms in between the pronotal anterior and posterior pairs of projections (resulting mostly from the projections themselves than a proper sulcus); this transversal corridor has a medial fovea and terminates laterally with a pair of lateral pronotal foveae. Cuticle on pronotal dorsum overall just verrucose as on head, but bumps are slightly more spaced; the transversal corridor is smooth. Elytra gradually widens posteriorly; humeral corners poorly-marked. Two pairs of basal elytral foveae; from the medial pair of foveae a pair of sulci follow posteriorly attaching to the sutural striae; and from the lateral pair, the discal striae follow posteriorly almost reaching the posterior elytral margins, fading only at the posterior fifth of the elytra. Another pair of discal striae, the lateralmost, do not originate from elytral foveae, but forms at the anterior two fifths and terminates at the posterior fifth level, failing to reach the posterior elytral margin. Membranous hind wings not verified for neither sexes. Lateral procoxal foveae present. Prosternal surface anterior to procoxae as long as or longer than procoxae. Metaventrite with a pair of low protuberances and a shallow medial, broad, longitudinal sulcus. Mesometasternal

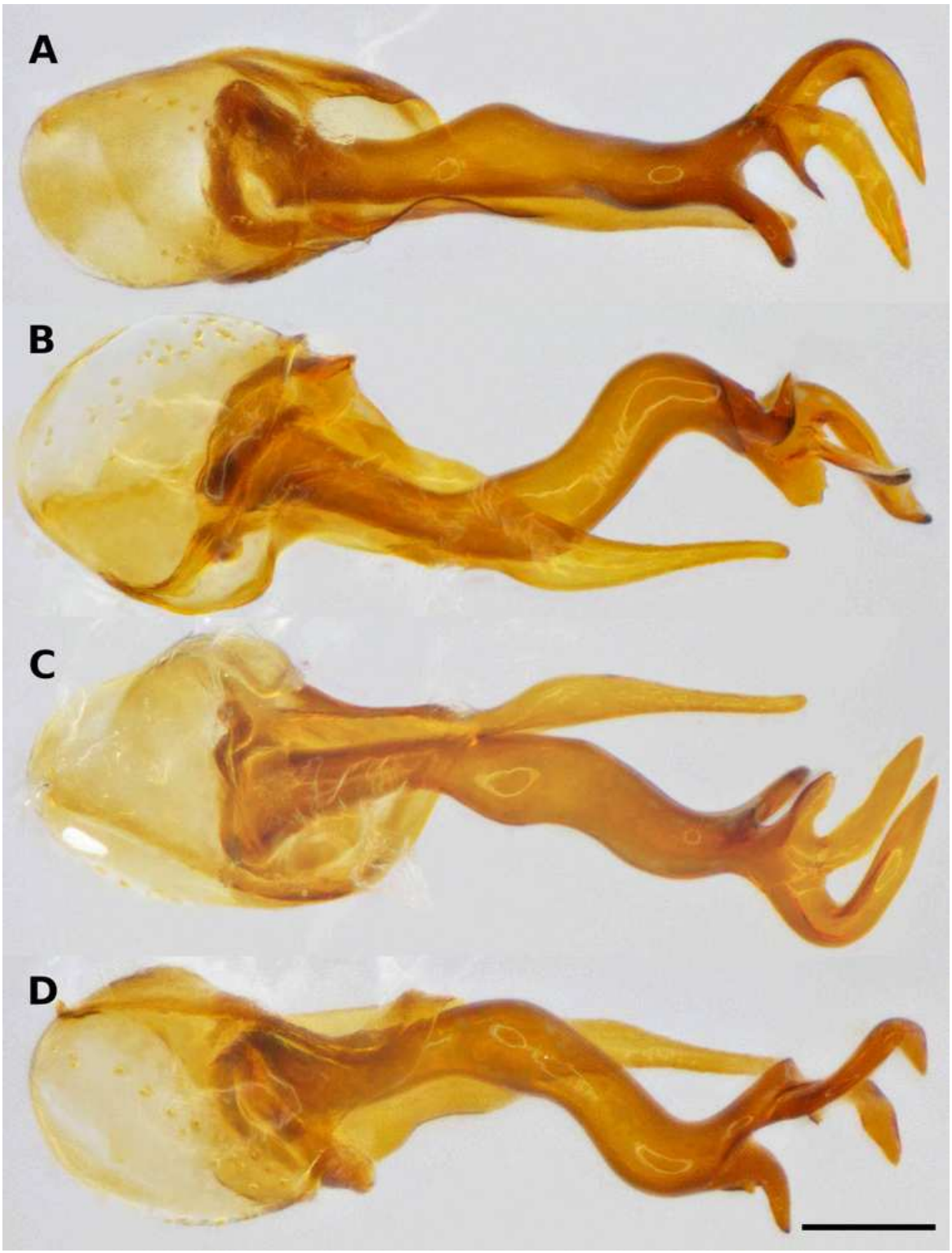

Figure 5. *Metopiellus emavieirae* **sp. nov.** male holotype aedeagus (dissected and mounted on slide) in ventral view (**A**), right side view (**B**), dorsal view (**C**), and left side view (**D**). Scale bar: 0.1 mm (A–D).

fovea and lateral metasternal foveae present. The three pairs of coxae are contiguous, all trochanters are simple. Femora are only mildly clavate, their apexes are about twice as broad as their bases. Tibiae arched; meso- and metatibiae somewhat thin; protibia thicker, specialized. Protibia seen in the profile view have an inflated appearance; in the inner view, with an elliptical, carina-delimited, mildly concave smooth area; the carina is much stronger anteriorly than posteriorly. A dense brush of golden, short setae is a bit ahead of the smooth patch, on the apical portion of the inner surface of the protibia. Meso- and metatibiae also with the apical brush of golden setae, in the former positioned on the edge of the anterior surface and in the latter on the edge of the posterior surface. Ventral (inner) margin of tarsi with two rows of short, erect setae; tarsomere 2 about twice as long as tarsomere 3; ventral surface of tarsomeres fringed with a row of erect setae that differ from the ground pilosity that is composed of denser, decumbent and thinner hairs. Pretarsal claws on all legs composed of a well-developed claw and a seta-like claw, the latter is, in relation to the first, in the outer position in the foreleg, and in the posterior position in the mid and hind legs. *Abdomen*. In dorsal view of the body, tergites IV to VII subequal in length and paratergites conspicuous from abdominal segments IV to VI, small in VII. Tergite VIII in full view, roughly triangular, with a posteromedial thick, blunt, block-like, subquadrate process that has a patch of anteriorly inclined golden setae. Anteromedial margin of sternite III (first exposed abdominal sternite = first abdominal ventrite), in between the metacoxae, with three small processes, triangularly disposed. Sternite VI slightly longer than IV, V and VII; in the male with a pair of robust, posteroventrally oriented processes each covered on a dense patch of golden setae; in the female sternite VI a simple convex tranverse surface. Sternite VIII in the male with a denser brush of setae anteromedially, just next to the posterior margin of sternite VII, its medial surface concave, its apical margin medially concave; in the female sternite VIII convex, without such modifications. Tergite IX in the male a pair of roughly triangular, membranous plates, probably entirely internalized (see Discussion); likely absent in the female (not verified in the paratype through dissection). Aedeagus basally ovoid; paramere thick, cylindrical, and sinuous in ventral and dorsal views, apically split into four spatulate curved tips; median lobe broad basally and gradually getting thinner apically, thinly spatulate, without teeth along its length. Female genital complex not studied.

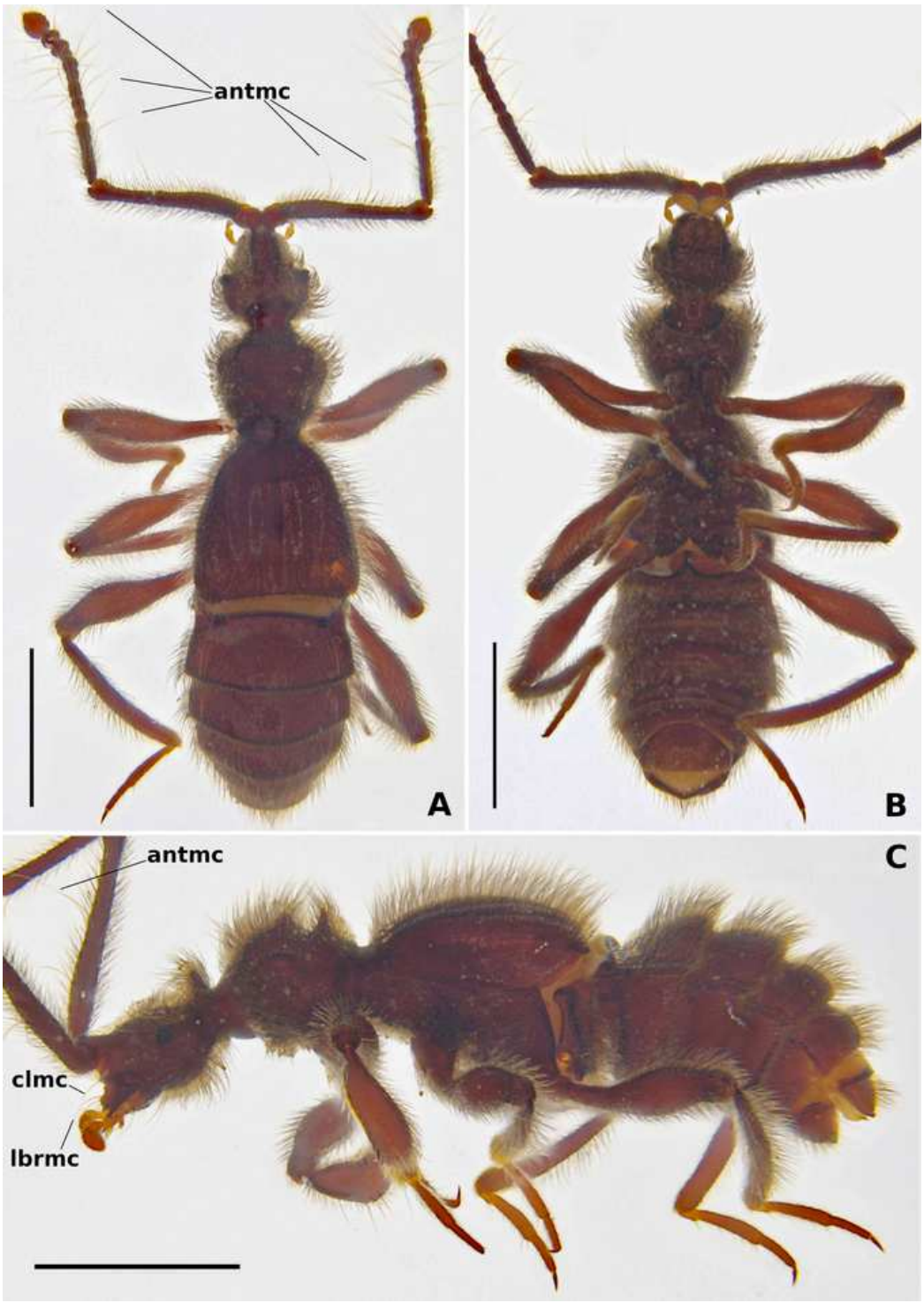

Figure 6. *Metopiellus emavieirae* **sp. nov.** female paratype in dorsal view (A), ventral view (B), and in profile view. Photographed submerged in ethanol prior to dry-pinning mounting. Scale bars: 1 mm. Acronyms: **antmc**, antennal macrochaetae; **clmc**, clypeal macrochaetae; **lbrmc**, labral macrochaetae.

Etymology. The name is in honor of the biologist Eduarda Melo de Abreu Vieira, who has consistently enriched the beetle and ant collections of CELC with precious specimens, including the holotype of this species. The name was created by adding the singular Latin genitive case suffix -ae to a word formed by the combination of the initial letters of her first and middle names (E, M and A) and her last name (Vieira). The orthography of an eponym is unchangeable and does not depend on the generic name in which the epithet is used.

Discussion

The new species is very similar to the recently described *M. guanano* from Colombia. The differences between the two species are mainly based on the male secondary sexual characters (see couplet 2 in the key above), as well as the strong differences in the aedeagus. Indeed, the female of *M. emavieirae* is morphologically very close to that of *M. guanano*. Nevertheless, a few traits that are not male secondary sexual characters (shared between the sexes of each species and differing between the species) can be pointed out: (i) a relatively smaller posterior pronotal spinose tubercle (when compared to the anterior) in *M. guanano* (male and female depicted in Fig.4 of Fiorentino et al., 2022), the anterior and posterior spinose tubercles in *M. emavieirae* reaching almost the same height in profile view; (ii) somewhat more compressed antennomeres in *M. guanano*, this being more evident when comparing antennomeres 3, 4, and 8 of that species to *M. emavieirae*, which have them slightly longer; and (iii) overall body length, with *M. guanano* being slightly smaller than *M. emavieirae*. These non-sexual-linked specific differences are important and must be better understood in the genus and tribe to clarify if new species should be or not described based on males only. The fact that non-sexual differences are subtle but exist between *M. guanano* and *M. emavieirae* indicates that if new species are described based on females, then descriptions must be very detailed and many measurements must be taken to allow future pairing to the males. These two species can be treated as a species-group within *Metopiellus* for sharing the dense and dark overall pilosity, and the odd vertexal and pronotal spinose projections. Considering how much the two species occur far away from each other in the continent, other undescribed species of this species-group may be found in South America's forests.

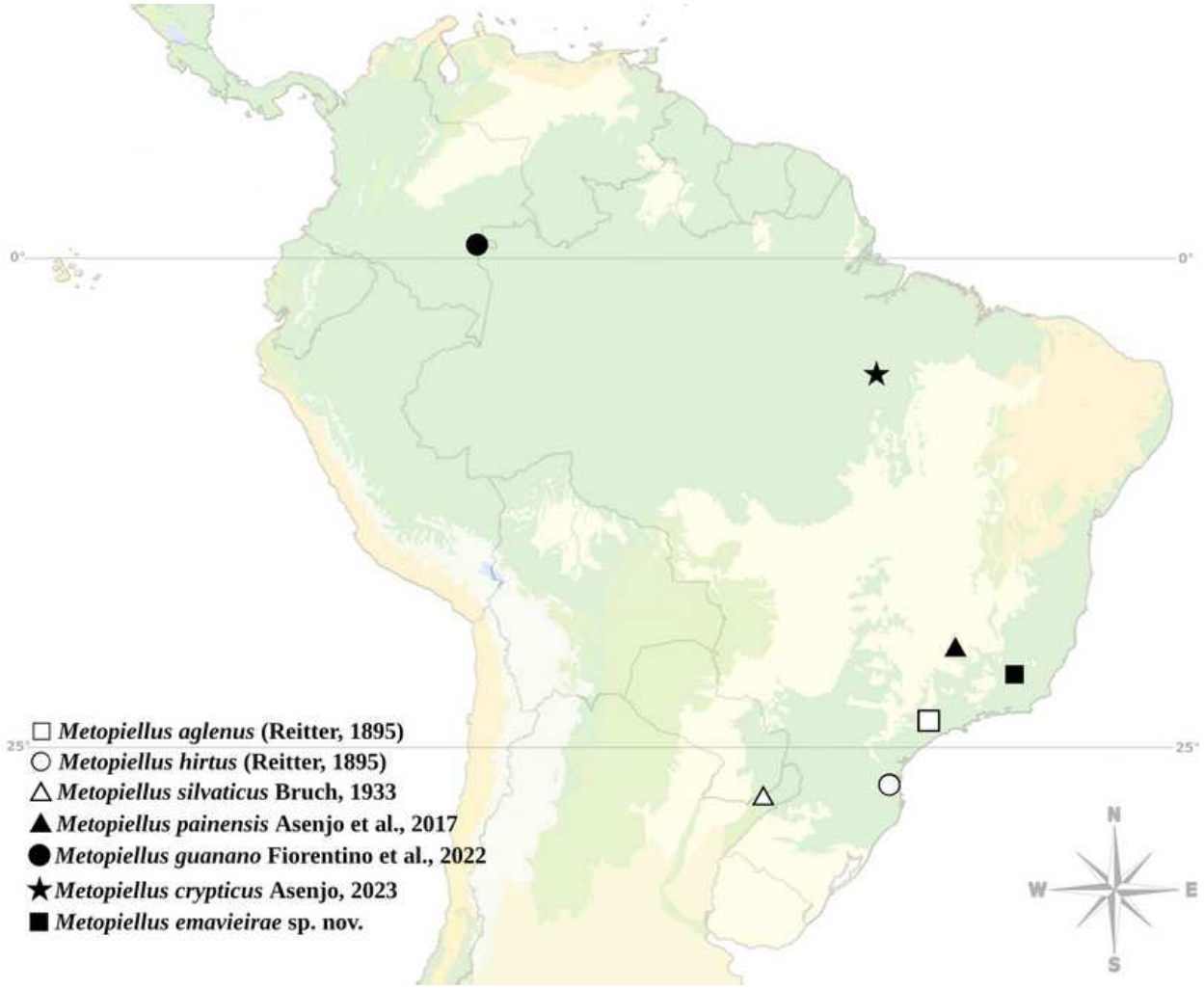

Figure 7. Distribution of *Metopiellus* species.

Metopiellus emavieirae and *M. painensis* are from relatively close localities within the Atlantic Forest biome. Therefore, there are chances of both being found in sympatry. These two species are easily distinguished, as *M. painensis* (i) has a vestigial eye with a single ommatidium, rather than a small eye with multiple ommatidia; (ii) does not have spinose vertexal and pronotal projections; (iii) the distal margin of its sternite VIII is deeply notched medially, as opposed to only mild notched; and (iv) its aedeagus is greatly different in shape (compare Figs. 10–12 of Asenjo et al. 2017 to Fig. 5 of this paper). The recently described species *M. crypticus* is morphologically close to *M. painensis* and can be differentiated from *M. emavieirae* by the same characters *M. painensis* differs from *M. emavieirae*.

The divided, membranous, apparently internalized tergite IX is an unusual condition of *M. emavieirae* as it deviates from the tribe pattern of sclerotized and exposed plates. The holotype of *M. emavieirae* has the sternite VIII perfectly locking into the tergite VIII (Fig. 3G), lacking the broad notch medially on the distal margin of sternite VIII, as seen in males of the other species of the tribe that have the tergite IX plates sitting within this notch (see Fig. 7 of Asenjo et al. 2017, Fig. 1D of Fiorentino et al., 2022, and Fig. 2F of Asenjo et al. 2023). The absence of the notch indicates the internalization of the tergite IX pieces, although that was not verified with the intact specimen at the moment of its dissection.

Here a dichotomous and a multi-entry keys were made to provide an updated key allowing identification of the tribe's genera. However, the amount and strength of the characters used are very limited, mostly due to the lack of images of representatives of these genera. Even though most of the tribe's genera were revised by Comellini's series of works, habitus depiction and a detailed description of each species are lacking. With rare exceptions, few museums and collections had put out high-resolution photos of their specimens. Some genera have few or no images of any of their species (e.g. *Metopias* and *Metopiosoma*). When comparing the information paucity of the species described in the past to the recently described species, which were carefully scrutinized, various morphological gaps arise; that make fragile any attempt to build identification tools not based on physical examination of specimens. With more material becoming available in the future, it will be possible to revise the generic key (both dichotomous and multi-entry) and they will certainly be stronger than the present version.

Five out of seven species in the genus are concentrated in southern South America. Among these five species, four (*M. aglenus*, *M. hirtus*, *M. silvaticus*, and *M. emavieirae*) are within the Atlantic Forest biome; and one, *M. painensis*, is known from a locality in the transition between the Atlantic Forest and the Cerrado (Brazilian savanna) biomes. Two species in the genus occur in the Amazon biome, *M. crypticus* and *M. guanano*, the first occurs in the state of Pará (eastern Amazon) and the latter occurs in Colombia (western Amazon) and has the northernmost record for the genus (Fig. 7).

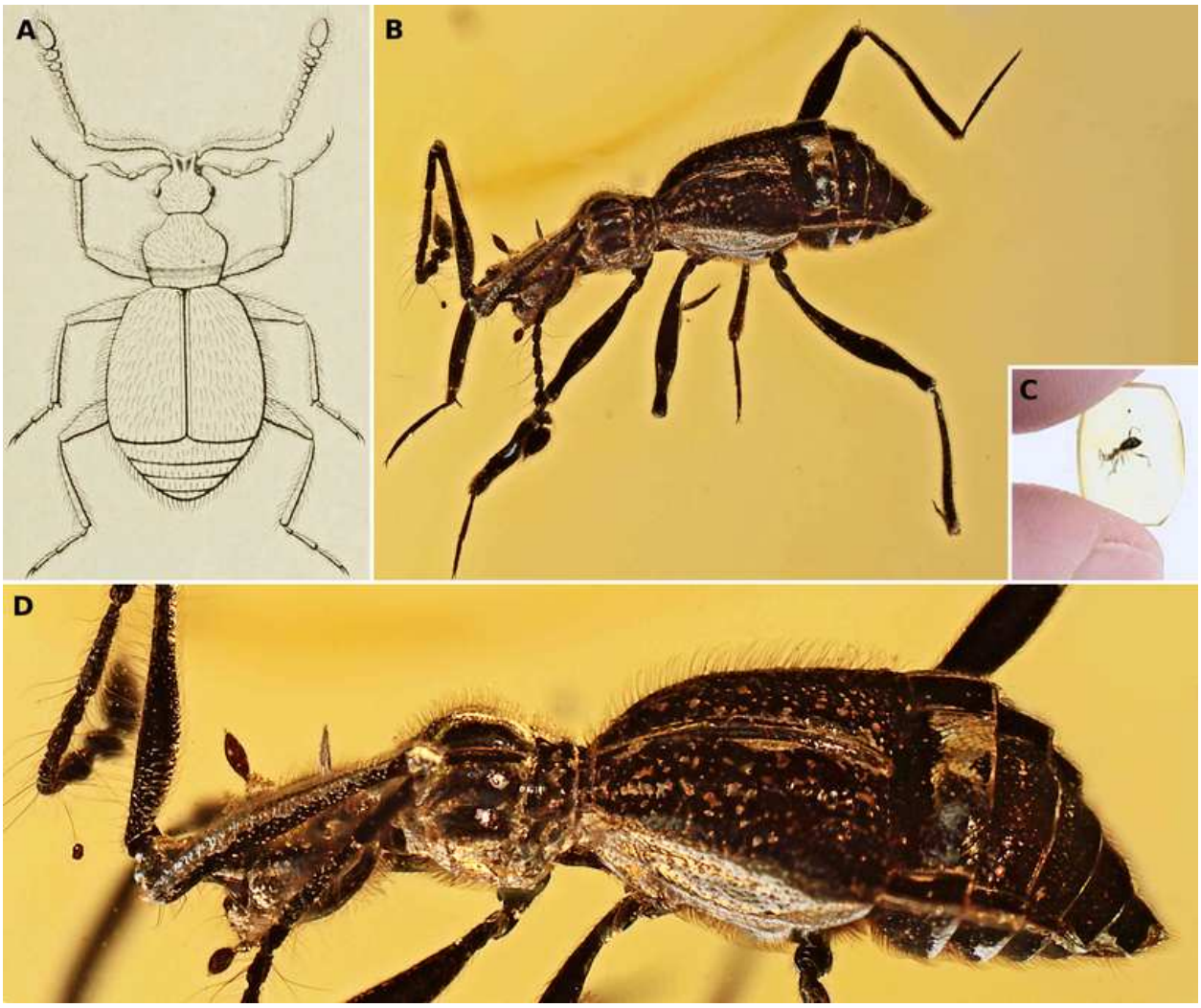

Figure 8. Baltic amber Metopiasini representatives. Original drawing of *Hagnometopias pater* Schaufuss, 1890 (**A**) . Photographs of an undescribed species from Yantarny mine, Kaliningrad (**B–D**), that has been traded (images by Baltic amber seller and professional photographer Marius Veta, ambertreasure4.com, reproduced with permission).

The fossil species *Hagnometopias pater* Schaufuss, 1890 was not included in the dichotomous key to the genera of the tribe (included in the multi-entry key). This Eocene fossil is a biogeographic and temporal conundrum, as the tribe is nowadays exclusively Neotropical. The original description by Schaufuss is based on a drawing received from "Herrn von Schlereth", who, in turn, was based on the specimen itself (Fig.8, A). The drawing certainly shows a specimen similar to a Metopiasini, however with simple protibiae and the antennal tubercles not excessively raised from the frons as usual for the tribe. Indeed, Schaufuss (1890), in the original

description, raised some doubts on the association of the specimen with the Metopiasini, but trusted Motschulsky in that association, as the latter had probably examined the specimen physically. No other similar Baltic specimen is known, except for one recently traded that was mined in the Kaliningrad mine of Yantarny (Fig. 8, B–D, courtesy images by the Baltic amber dealer and professional photographer Marius Veta). This incredibly preserved specimen represents a morphospecies extremely metopiasine-like, more so than *H. pater* itself, to which it does not seem to be conspecific to. Taking this morphospecies and *H. pater* into account makes more plausible the idea that the tribe really occured in the Eocene Baltic fauna, rather than interpreting *H. pater* as a convergent lineage to the Metopiasini. These two Baltic species differ by the general habitus, with *H. pater* having the abdomen length relatively small in dorsal view (when compared to elytral length) than the morphospecies; by the much less projected antennal tubercles in *H. pater* than in the morphospecies, the latter having the antennal tubercles projected very likely as the way observed in modern Metopiasini; by the pronotum, whichhas deep longitudinal sulci in the morphospecies which are not depicted for *H. pater*. The occurrence of the lineage in the European Eocene is intriguing and could indicate a Palearctic or even a Laurasian origin with later dispersion to the Neotropics and extinction in the region of origin. Alternatively, as in the case of the Bythiniplectini (Parker, 2022) found in Ypressian amber of Cambay, India, the lineage could have southern Gondwanan origins and its presence in Europe being explained by a northern drift with the Indian subcontinent and subsequent spread across Asia and Europe, so to allow its recording by mid to late Eocene in the Baltic amber. In that scenario, extinction in the Afrotropics (due to the Gondwanan vicinity of India and Africa) and Asia must have happened at some point. Future studies of Ypressian Cambay amber, more discoveries of Baltic amber, and a more thorough phylogenetic hypothesis which includes these important fossils will be needed to better explain this odd biogeographic issue of the subfamily.

Acknowledgements. We thank Jacki Whisenant for the images of the types of *Bibrax bradleyi* deposited in the Cornell University Insect Collection (CUIC). We also thank Emmeline França who has sampled the female paratype while this paper was being revised and kindly donated the specimen to us on time to be studied and included in the final version. Anonymous reviewers pointed out important missing issues and significantly enhanced the quality of the manuscript. Financial support was provided by the Brazilian funding agencies Conselho Nacional de Desenvolvimento Científico e Tecnológico (CNPq; research grant

number 304339/2022-9 to the junior author), Fundação de Amparo à Pesquisa do Estado de Minas Gerais (FAPEMIG) and Coordenação de Aperfeiçoamento de Pessoal de Nível Superior—Brasil (CAPES; Finance Code 001; doctorate grant to the senior author).

References

Asenjo A, Ferreira RL, Zampaulo RDA. 2017. Description of *Metopiellus painensis* sp. nov. (Coleoptera, Staphylinidae), first troglobitic Pselaphinae from Brazil. Zootaxa 4269(1):115–123. doi: 10.11646/zootaxa.4269.1.5

Asenjo A, Irmler U, Klimaszewski J, Chandler DS, Fierros-López HE, Vieira JS. 2019. Staphylinidae (Insecta: Coleoptera) in Latin America: synopsis, annotated catalog, diversity and distribution. Zootaxa. 4621(1):001–406. doi: 10.11646/zootaxa.4621.1.1

Asenjo A, de Oliveira MPA, Oliveira RRM, Pires ES, Valois M, Oliveira G, Vasconcelos S. 2023. The complete mitochondrial genome and description of a new cryptic Brazilian species of *Metopiellus* Raffray (Coleoptera: Staphylinidae: Pselaphinae). PeerJ. 11:e15697. doi: 10.7717/peerj.15697

Bolton B. 2024. An online catalog of the ants of the world. Available from https://www.antcat.org/catalog/438235 (accessed 12 March 2024).

Chandler DS. 2001. Biology, morphology and systematics of the ant-like litter beetles of Australia (Coleoptera: Staphylinidae: Pselaphinae). Associated Publishers, Gainsville, Florida: Mem. Entomol. Int., Vol. 15.

Chandler DS. 2002. Subfamilia Pselaphinae Latreille, 1802. In Navarrete Heredia JL, Newton AF, Thayer MK, Ashe JS, Chandler DS. Guía ilustrada para los géneros de Staphylinidae (Coleoptera) de México. Illustrated guide to the genera of Staphylinidae (Coleoptera) of Mexico. Universidad de Guadalajara & CONABIO, México. p. 49–102.

Comellini A. 1983. Notes sur les Psélaphides néotropicaux (Coleoptera) 9 - Le genre *Metopioxys* de la tribu des Metopiini. Rev. Suisse Zool. 90(2):437–456.

Comellini A. 1993. Notes sur les Psélaphides néotropicaux (Coleoptera). 8–Le genre *Metopias* Gory de la tribu des Metopiasini. Rev. Suisse Zool. 100(4):921–927. doi: 10.5962/bhl.part.79892

Comellini A. 1994. Notes sur les Psélaphides néotropicaux (Coleoptera). 9–Le genre *Metopiosoma* de la tribu des Metopiasini. Rev. Suisse Zool. 101(1):107–115. doi: 10.5962/bhl.part.79902

Comellini A. 1998. Notes sur les Psélaphides néotropicaux (Coleoptera, Staphylinidae, Pselaphinae). 10–un nouveau genre et quatre nouvelles espèces de la tribu des Metopiasini. Rev. Suisse Zool. 105(2):345–350.

Comellini A. 2000. Notes sur les Psélaphides néotropicaux (Coleoptera, Staphylinidae, Pselaphinae). 11–un nouveau genre et sept espèces nouvelles de la tribu des Metopiasini. Rev. Suisse Zool. 107(4):765–776. doi: 10.5962/bhl.part.80147

Evenhuis NL. 2024. The insect and spider collections of the world website. Available from: http://hbs.bishopmuseum.org/codens/ (accessed 12 March 2024)

Fiorentino G, Tocora MC, Ramirez S. 2022. A new species of *Metopiellus* (Coleoptera, Staphylinidae, Pselaphinae) from the northern Colombian Amazon. ZooKeys. 1108:1–9. doi: 10.3897/zookeys.1108.76077

Fletcher FC. 1927. Undescribed Pselaphidae collected by Dr. J. C. Bradley in Panama (Coleoptera). Entomol. News. 38:149–153.

Gaudin J, Coache A. 2022. *Macrommatias* nom. nov., un nouveau nom de remplacement pour *Chandleria* Comellini, 1998 (Coleoptera, Staphylinidae), homonyme récent de *Chandleria* Yamaguti, 1959 (Cestoda, Anoplocephalidae). Faunitaxys. 10(9):1–2.

Gory HL. 1832. Description du genre *Metopias*. Mag. Zool. 2:2 (unnumbered pages, pl. 42).

Kerner A, Bouquin S, Portier R, Vignes-Lebbe R. 2021. The 8 Years of Existence of Xper3: State of the art and future developments of the platform. Biodiversity Inf. Sci. Standards. 5:e74250. doi: 10.3897/biss.5.74250

Kimball S, Mattis P. 1996. GIMP – The GNU Image Manipulation Program. Available from: https://www.gimp.org (accessed 30 May 2022).

LeConte JL. 1878. Additional descriptions of new species. In Schwarz EA. The Coleoptera of Florida. Proc. Am. Phil. Soc. 17:373–434.

Morrone JJ, Ebach MC. 2022. Toward a terrestrial biogeographical regionalisation of the world: historical notes, characterisation and area nomenclature. Aust. Syst. Bot. 35(3):89–126. doi: 10.1071/SB22002

Newton AF, Chandler DS. 1989. World catalog of the genera of Pselaphidae (Coleoptera). Fieldiana Zool. (New Series). 53:1–93.

Newton AF, Thayer MK, Ashe JS, Chandler DS. 2000. Staphylinidae Latreille, 1802. In: Arnett Jr. RH, Thomas MC, editors. American Beetles, Vol. 1. Archostemata, Myxophaga, Adephaga, Polyphaga: Staphyliniformia. CRC Press, Boca Raton, Florida. p. 272–418

Omar MB, Bolland L, Heather WA. 1979. A permanent mounting medium for fungi. Bull. Br. Mycol. Soc. 13(1):13–32. doi: 10.1016/s0007-1528(79)80038-3

Park O. 1942. A study in Neotropical Pselaphidae. Northwestern University Studies in the Biological Sciences and Medicine. Northwestern University, Evanston and Chicago. 1, 1: x + 403 pp, 21 pls.

Parker J. 2016a. Emergence of a superradiation: pselaphine rove beetles in midCretaceous amber from Myanmar and their evolutionary implications. Syst. Entomol. 41:541e566. doi: 10.1111/syen.12173

Parker J. 2016b. Myrmecophily in beetles (Coleoptera): Evolutionary patterns and biological mechanisms. Myrmecol. News. 22:65–108. doi: 10.25849/myrmecol.news_022:065

Parker J. 2022. Transitional morphology and Afrotropical affinity of a bythinoplectine rove beetle from the early Eocene of India (Coleoptera: Staphylinidae: Pselaphinae). Palaeoentomology 005 (5): 452–460 doi: 10.11646/palaeoentomology.5.5.6

Raffray A. 1908. Coleoptera. Fam. Pselaphidae. In Wytsmann P., editor. Genera Insectorum, 64th fascicule. Rome. 487 pp., 9 pls.

Reitter E. 1885. Abbildungen und Bemerkungen zu wenig gekannten selaphiden-Gattungen mit Beschreibungen neuer Arten. Dtsch. Entomol. Zeitschrift. 29: 333–339, pls.2–3.

Schaufuss LW. 1890. System-Schema Der Pselaphiden, ein Blick in die Vorzeit, in die Gegenwart und in die Zukunft. Tijdschrift voor Entomologie. 33, 101–162.

Thayer MK, Newton AF, Pape T. 1992. METOPIINAE Foerster, 1868 (Insecta, Hymenoptera), METOPIINI Raffray, 1904 (Insecta, Coleoptera), and METOPIINI Townsend, 1908 (Insecta, Diptera): proposed removal of homonymy. Bull. Zool. Nomencl. 49(3):200–204.

Ung V, Dubus G, Zaragüeta-Bagils R, Vignes-Lebbe R. 2010. Xper2: introducing e-taxonomy. Bioinformatics. 26, 5, 703–704. doi: 10.1093/bioinformatics/btp715

Vignes-Lebbe R, Bouquin S, Kerner A, Bourdon E. 2017. Desktop or remote knowledge base management systems for taxonomic data and identification keys: Xper2 and Xper3. Proc. of TDWG. 1:e19911. doi: 10.3897/tdwgproceedings.1.19911

V. CAPÍTULO 4

PHYLOGENETIC PLACEMENT OF CRETACEOUS PSELAPHINAE (COLEOPTERA: STAPHYLINIDAE)

INTRODUCTION

Pselaphinae form a large subfamily of the Staphylinidae, with around 10000 described species and many awaiting formal description (Parker, 2016a; Yin et al., 2017). They are distinguishable from other staphylinids by the three-segmented tarsomeres, strongly developed body foveation, fourth maxillary palpomere with an apical sensilla (the "palpal cone" or "apical pseudosegment"), antennal sockets ventrally turned and covered by frons shelf-like projections (usually developed in antennal tubercles), procoxal fissure closed, trochantin concealed, among other traits that are widespread, but with many exceptions in the subfamily (Chandler, 2001). The subfamily is traditionally divided into six supertribes: Batrisitae, Clavigeritae, Euplectitae, Faronitae, Goniaceritae and Pselaphitae (Newton and Thayer, 1995). It is currently known certainty that not all of these supertribes are natural groups (Parker, 2016a). One relation that is supported by both morphological and molecular analysis is the basalmost split of the subfamily into two major clades, the Faronitae as a sister group to all remaining pselaphines, and the so-called "higher Pselaphinae". The Faronitae share the following traits: presence of discal elytral foveae (along with basal elytral foveae); second tarsomere short (not conspicuously greater than first); pretarsal claws paired and subequally-sized; parallel-sided body; antennae without a club. The higher Pselaphinae, the vast majority of the subfamily in number of species, are much less uniform than the Faronitae. However, they all share an elongate second tarsomere (much longer than the reduced first tarsomere), and discal elytral foveae are absent in all species (only basal elytral foveae are present). Other common traits of the higher Pselaphinae, but not universal, are the clubbed antennae (which can be very loosely defined or absent in some myrmecophilous lineages); pretarsal claws unequally-sized or single (subequally-sized do occur); and body not parallel-sided (some species have slender body outlines) (Chandler, 2001).

Until recently, fossils of Pselaphinae have only been found in Cenozoic sites, most notably from the Eocene Baltic amber, where several species were described in the late 19th century (Schaufuss, 1890). Those species, although without certainty, were assigned to modern tribes (Newton and Chandler, 1989). The descriptions of Cretaceous Pselaphinae, on the other hand, are all very recent, with all descriptions published in the past decade. In 2014, two species from

the Spanish amber, early Albian in age, were the first ones to be described (Peris et al., 2014). One of these was a member of the Faronitae, †*Cretasonoma corinformibus* Peris, Chatzimanolis and Delclòs, 2014, and the other, †*Penarhytus tenebris* Peris, Chatzimanolis and Delclòs, 2014, an enigmatic lineage originally tentatively placed in the higher pselaphine tribe Arhytodini, but then considered as incertae sedis in the subfamily by Parker (2016a). From that year onwards, all subsequent works on Cretaceous pselaphines were based on species found in Burmese amber, early Cenomanian in age, all of them unequivocal members of the higher Pselaphinae. In 2016, three additional species were described and placed in a phylogenetic proposition of the subfamily, the first one to combine molecular and morphological data (Parker, 2016a). These three species were described in two genera: †*Boreotethys arctopteryx* Parker, 2016, †*Boreotethys grimaldii* Parker, 2016, and †*Protrichonyx rafifrons* Parker, 2016. A new species in a new genus was described in the next year, †*Cretobythus excavatus* Yin, Parker, Cai, Huang and Li, 2017, and was inserted in the phylogeny. The authors did that simply by coding †*C. excavatus* to all characters of the matrix and then running the same analysis to generate a tree in which the new species appears. The authors also added one character in the matrix, which grew from 57 morphological characters to 58, meaning that all taxa treated in Parker (2016a) and †*C. excavatus* had to be coded for this additional character. In 2019, three species in two genera were described. First, †*Cretobrachygluta laurasiensis* Yin, Kurbatov, Cuccodoro and Cai, 2019 was described, based on a superbly preserved specimen, but was not included in the existing phylogeny. Then, in the same year, †*Priscaplectus carinatus* Yin, Chandler and Cai, 2019 and †*Priscaplectus grandiceps* Yin, Chandler and Cai, 2019 were the last species inserted in the phylogeny, in the same way †*C. excavatus* was. The last two species described before chapter one of this thesis, †*Burmagluta rougemonti* Yin and Cai, 2021 and †*Megabythinus spinitibialis* Yin, Zhao and Cai, 2021, were not studied phylogenetically. Therefore, before this thesis, among the described Cretaceous genera of Pselaphinae, †*Cretasonoma*, †*Penarhytus*, †*Cretobrachygluta*, †*Burmagluta*, and †*Megabythinus* were never phylogenetic analysed, while †*Boreotethys*, †*Protrichonyx*, †*Cretobythus*, and †*Priscaplectus* were.

In Chapter 1 of this thesis, all species above mentioned were reviewed, and four new species were described* and coded to Parker's original matrix (plus the additional characters of Yin et

al., 2017). The new species described in Chapter 1 included one Faronitae, †*Burmalogasa perisi* Chaul and Lopes-Andrade, 2024*, and three of the higher Pselaphinae, †*Boreotethys caii* Chaul and Lopes-Andrade, 2024*, †*Cretobythus parkeri* Chaul and Lopes-Andrade, 2024*, and †*Cretobythus yini* Chaul and Lopes-Andrade, 2024*. The resulting phylogeny presented in that chapter showed a similar topology to those of Parker (2016a) and Yin et al. (2017; 2019b), and the necessity of having a new phylogeny, based on more characters, was made. Parker's original matrix had the limiting factors of (**i**) being based on only three fossil species (of two genera) and, therefore, a reduced fossil diversity in comparison to the extant taxa studied and (**ii**) not having its fossils based on excellently preserved specimens, what prevented minute details to be accessed and compared to the extant taxa. Subsequently described fossils, such as †*Cretobrachygluta laurasiensis* or †*Priscaplectus grandiceps*, had such high standards of preservation (see Chapter 1 of this thesis for information on the preservation conditions of these fossils). As pointed out above, since Parker's matrix was presented, six very different genera were described, significantly raising the number of possible characters to be used in morphology-based phylogenetic analyses.

Moreover, recent works, either taxonomic, phylogenetic, or purely morphological investigations, have explored a vast number of characters among extant species (Parker and Owens, 2018; Owens and Carlton, 2016; Beutel et al., 2021; Jałoszyński et al., 2020; Jałoszyński et al., 2022; Luo et al., 2021a; Luo et al., 2021b; Luo et al., 2022), making easier the task to adapt these characters to be applied in a phylogenetic context.

One solution to the challenge of building a phylogeny of the Pselaphinae that satisfactorily covered the Cretaceous diversity would be to use Parker's matrix as a starting point and then simply increase it with new characters (as in Yin et al., 2017, that added one character to it). However, this would require access to the taxa used in Parker (2016a) so that these taxa could also be coded for each new character added to the matrix. Since we did not have these species

*** Paper submitted to Palaeoentomology in July, 2024, species names are not valid yet. See Chapter 1 disclaimer.**

available to us, we built an entirely new morphological matrix. By doing so, most species of the phylogeny would be available to us for direct examination, and coding for any new character would be possible. We retained most characters of Parker (2016a) and Yin et al. (2017; 2019b) and added many others, almost tripling the number of characters from those first studies. Despite not having access to the physical study of part of the described fossils, for most of these the images and original descriptions were enough to allow for their proper coding in the new morphological matrix. In this final chapter, we present this new phylogenetic scenario that covers more broadly than ever the Cretaceous Pselaphinae.

MATERIAL AND METHODS

Specimens studied and image databank

The entire Pselaphinae collection of the Entomological Collection of the Coleoptera Laboratory (CELC), at the Universidade Federal de Viçosa, Minas Gerais, Brazil (Evenhuis, 2024), was studied and a set of species were selected to be included in the phylogenetic analyses. In the case of fossils, species represented by better preserved specimens, those that allowed the scoring of the majority of the selected characters, were chosen. As for the extant species, a set of species that homogeneously represented the known phylogenetic diversity of the subfamily was chosen. In total, 39 species were chosen, 15 fossils and 24 extant (Table 1), and all were coded for the 154 characters studied here.

Among the 15 fossil species, eight were coded based on the literature (Parker and Grimaldi, 2014; Yin et al., 2017; Yin et al., 2019a; Yin et al., 2019b; Liu et al., 2020; Yin et al., 2021; Yin and Cai, 2021), and seven were coded from physically studied specimens (deposited in CELC, some of them described in Chapter 1). Preparation of the fossils for study were made as described in Chapter 1. A few described Cretaceous pselaphines were not not included in this phylogenetic analysis because their preservation conditions did not allow to code for more than 50% of the total number of characters, they are: †*Cretasonoma corinformibus,* †*Penarhytus tenebris,* †*Boreotethys arctopteryx,* and †*Protrichonyx rafifrons*.

Among the extant species included, one was coded based on the literature (Yin and Hlaváč,

Table 1. Species included in the phylogenetic analysis.

Genus and species/morphospecies	Tribe	Supertribe	Subfamily	Locality
Anotylus CELC000244			Oxytelinae	Brazil
Arthmius ufv-16	Batrisini	Batrisitae	Pselaphinae	Brazil
Barrojuba ufv-03	Jubini	Euplectitae	Pselaphinae	Brazil
†*Boreotethys caii*	Bythinini	Goniaceritae	Pselaphinae	Burmese amber, Myanmar
†*Boreotethys* cf. *grimaldii*	Bythinini	Goniaceritae	Pselaphinae	Burmese amber, Myanmar
†*Burmagluta rougemonti*	Brachyglutini	Goniaceritae	Pselaphinae	Burmese amber, Myanmar
†*Burmalogasa* CELC002162		Faronitae	Pselaphinae	Burmese amber, Myanmar
†*Burmalogasa perisi*		Faronitae	Pselaphinae	Burmese amber, Myanmar
†*Cretobrachygluta laurasiensis*	Brachyglutini	Goniaceritae	Pselaphinae	Burmese amber, Myanmar
†*Cretobythus yini*	Bythinini	Goniaceritae	Pselaphinae	Burmese amber, Myanmar
†*Cretobythus excavatus*	Bythinini	Goniaceritae	Pselaphinae	Burmese amber, Myanmar
†*Cretobythus parkeri*	Bythinini	Goniaceritae	Pselaphinae	Burmese amber, Myanmar
Curculionellus ufv-57	Pselaphini	Pselaphitae	Pselaphinae	Australia
Durbos ufv-117	Tyrini	Pselaphitae	Pselaphinae	Australia
Euphalepsus ufv-107	Brachyglutini	Goniaceritae	Pselaphinae	Brazil
Eurhexius ufv-11	Trogastrini	Euplectitae	Pselaphinae	Brazil
Fustiger ufv-27	Clavigerini	Clavigeritae	Pselaphinae	Brazil
Fustiger ufv-41	Clavigerini	Clavigeritae	Pselaphinae	Brazil
†Gen-nov-1 CELC003040		Insertae sedis	Pselaphinae	Burmese amber, Myanmar
Hamotus ufv-05	Tyrini	Pselaphitae	Pselaphinae	Brazil
Listriophorus ufv-29	Goniacerini	Goniaceritae	Pselaphinae	Brazil
Mareeba storeyi	Pselaphini	Pselaphitae	Pselaphinae	Australia
Mayetia atlantica	Mayetiini	Euplectitae	Pselaphinae	Brazil
†*Megabythinus spinitibialis*	Bythinini	Goniaceritae	Pselaphinae	Burmese amber, Myanmar
Megarafonus sp.		Faronitae	Pselaphinae	United States of America
Metopiellus emavieirae	Metopiasini	Euplectitae	Pselaphinae	Brazil
Peckiella ufv-60	Pselaphini	Pselaphitae	Pselaphinae	Australia
Phalepsus ufv-103	Phalepsini	Pselaphitae	Pselaphinae	Brazil
Praeruptifrons arnhemensis	Trichonychini	Euplectitae	Pselaphinae	Australia
†*Priscaplectus carinatus*		Insertae sedis	Pselaphinae	Burmese amber
†*Priscaplectus grandiceps*		Insertae sedis	Pselaphinae	Burmese amber
†*Protoclaviger trichodens*	Protoclavigerini	Clavigeritae	Pselaphinae	Cambay Amber, India
†*Protopselaphus thayerae*			Protopselaphinae	Burmese amber, Myanmar
Pyxidion ufv-07	Bythinoplectini	Euplectitae	Pselaphinae	Brazil
Rhinoscepsis ufv-30	Metopiasini	Euplectitae	Pselaphinae	Brazil
Sagola poortmani		Faronitae	Pselaphinae	New Zealand
Syrraphesina agostii	Clavigerini	Clavigeritae	Pselaphinae	Indonesia
Tmesiphorus ufv-116	Tmesiphorini	Pselaphitae	Pselaphinae	Australia
Tuberoplectus ufv-06	Dimerini	Euplectitae	Pselaphinae	Brazil

2020), two from available images in the internet (*Megarafonus* sp. and *Sagola poortmani*), and 21 were coded from physically studied specimens (deposited in CELC). Preparation of the specimens was as described in the Chapters 2 and 3, with ideally at least one specimen per species available for dissection, so to allow visualization of very small characters under the

compoundmicroscope (mostly mouthparts characters). The selected extant species belong to different tribes, representing all six recognized supertribes of Pselaphinae. All species included are identified to genus level, but most are not identified to species level, mostly due to the lack of taxonomical studies and, therefore, unavailability of identification tools (updated keys and diagnosis). Nonetheless, they are properly characterized as morphospecies and in the collection received morphospecies codes — "ufv-XX" — that, for practical purposes, serve for specific recognition in the Pselaphinae CELC collection. An extant species of *Anotylus* sp. (CELC000244) of Oxytelinae and the Burmese amber fossil †*Protopselaphus thayeri* Liu, Tihelka and Cai, 2020 was chosen as outgroups. The fossil Clavigeritae †*Protoclaviger trichodens* Parker and Grimaldi, 2014, from the Cenozoic Cambay amber, was also added to the phylogenetic analysis. Table 1 provides a list of the studied species and their current supertribes and tribes.

All physically studied species were imaged and high-resolution images can be accessed through the following link in an online databank hosted in the Xper3 platform (Ung et al. 2010; Vignes-Lebbe et al. 2017; Kerner et al. 2021):
https://app.xper3.fr/xper3GeneratedFiles/publish/identification/442879887097154347/mkey.html

The databank consists of 509 images of 31 species (out of the 39 species of the phylogenetic analysis). The eight species that are not in the databank are the fossils that were not physically examined. Their characters, through their descriptions and images, can be checked in their respective publications (Parker and Grimaldi, 2014; Parker, 2016a; Yin et al., 2017; Yin et al., 2019a; Yin et al., 2019b; Yin et al., 2021; Yin and Cai, 2021).

Morphological characters, matrix and phylogenetic analysis

The characters used here were either compiled from previously published phylogenetic proposals on Staphylinidae or Pselaphinae (Newton and Thayer, 1995; Lawrence et al., 2011; Hlaváč et al., 2013; Hlaváč et al., 2014; Parker, 2016a; Yin et al., 2017; Owens and Carlton, 2016; Jałoszyński et al., 2020; Beutel et al., 2021; Hlaváč et al., 2021; Jałoszyński et al., 2022), from morphological or taxonomical studies on pselaphines (Chandler, 2001; Parker and Maruyama,

2013; Yin and Hlaváč, 2020; Parker and Owens, 2018; Luo et al., 2021a; Luo et al., 2021b; Luo et al., 2022; Parker, 2022), or were newly established during the examination of the specimens.

To test the phylogenetic placement of the new species, the dataset was analyzed under parsimony using TNT v.1.1. (Goloboff et al., 2008a). All default parameters of TNT were maintained, random seed 1 was adopted, memory was adjusted to 10000 trees, 499 megabytes, and Display Buffer 10000 was used to obtain the tree. Searches were performed using both equal and implied weights. Implied-weighting procedures involve assigning an a priori constant, the k value; therefore the script setk.run, developed by Salvador Arias (Instituto Miguel Lillo, San Miguel de Tucuman, Argentina), was used to calculate the appropriate k value through the formula Goloboff et al. (2008b) suggested. The script obtained a value of 6.093750 for our dataset.
Topology was constrained in some searches to incorporate hypotheses generated from molecular phylogenetics. In these instances, well-supported relationships are enforced. The following command line was used to apply a constraint forcing the recovery of the higher Pselaphinae clade as sisters to the Faronitae clade, a widely supported and accepted relationship within the subfamily (Newton and Thayer, 1995; Chandler, 2001; Parker, 2016):

force = (6 7 8 9 10 11 12 13 14 15 16 17 18 19 20 21 22 23 24 25 26 27 28 29 30 31 32 33 34 35 36 37 38)*; constrain =

Constraint and weighting parameters are used to verify the most parsimonious protocol. Therefore, four combinations were performed: i) without constraint and without weighting analysis, ii) with constraint and without weighting, iii) without constraint and with weighting, and iv) with constraint and weighting. All heuristic searches were done with the command line xmult, using the functionalities “sectorial search,” “drifting,” “fusing” and “ratched” until the tree with the smallest number of steps was found 20 times. To verify the support for the obtained topology, the Bremer support was calculated for the nodes and resampled with bootstrapping (1000 pseudoreplicates). Finally, the WinClada v. 1.61 (Nixon, K. C., 1999-2002) was used to process the obtained topology.

RESULTS

The examination of the specimens, images and pertinent scientific literature resulted in 154 characters, of which 139 are binary and 13 are non-binary. The latter have not exceedeed three character states, except for the Characters 040 and 143, each with four states, and the Character 139, with five states. The list of characters is presented below. And the entire coded matrix for the 39 species is presented in Appendix 1.

List of characters

General body features

Character 001. Pselaphinae pattern of foveation: (0) absent; (1) present, foveae present on body in partial or complete pattern (as depicted in Chandler, 2001, fig. 1).

Character 002. Setation: (0) body with filiform setae, either flexuous or erect, setae at most having a blunt tip; (1) anyhow modified setae, either scale-like, or stiff, tiny, and decumbent, or sugar crystal-like at least in some body regions. Species with patches of hyaline flatenned specialized setae, but otherwise having filiform setae were coded as 0.

Character 003. Body proportions, head width in relation to pronotum (observed in dorsal view): (0) head considerably narrower than pronotum; (1) head wider or about as wide as pronotum.

Character 004. Body proportions, head narrowness (observed in dorsal view of the head): (0) width of head just posterad the compound eyes much greater than that of vertex-occipital constriction, the latter approximatelly 0.6x that of the former; (1) width of head just posterad the compound eyes not much greater than that of vertex-occipital constriction, the latter 0.8x or more that of the former.

Character 005. Body proportions, elytral width in relation to pronotal width (observed in dorsal view): (0) narrow, elytra less than 1.5× as wide as pronotum; (1) wide, elytra 1.5×–1.95x wider than pronotum; (2) very wide, elytra at least twice as wide as pronotum.

Character 006. Body proportions, elytra width in relation to abdomen width (observed in dorsal view): (0) elytra narrower or as wide as abdomen; (1) elytra wider than abdomen.

Character 007. Body proportions, elytra length in relation to body (observed in dorsal view): (0) about a third of body length or more; (1) considerably less than a third of body length.

Character 008. Body proportions, abdomen length (observed in profile view): (0) easily longer than half an elytron length, usually as long as an elytron or more; (1) abdomen about as long as half an elytron length.

Character 009. Elytra-abdomen transition (observed in dorsal view): (0) discontinuous; (1) confluent.

Character 010. Elytra-abdomen transition (observed in profile view): (0) discontinuous; (1) confluent.

Character 011. Body shape, convexity: (0) body dorsoventrally shallow, body appearing flattened in profile; (1) body dorsoventrally deep, body appearing globular.

Character 012. Pronotum widest level (observed in dorsal view): (0) anterior or middle thirds; (1) posterior third.

Character 013. Elytron widest level (observed in dorsal view): (0) at the anterior or middle thirds; (1) at the posterior third.

Character 014. Abdomen widest level (observed in dorsal view of abdomen): (0) anterior or middle thirds; (1) posterior third.

Head, antennae and mouthparts

Character 015. Mandible, position relative to oral cavity: (0) protruding outside oral cavity to at least half mandible length; (1) concealed within oral cavity, at most apical teeth visible in dorsal view.

Character 016. Mandible, shape: (0) dorsoventrally flattened, forming a blade; (1) elongate and curved, horn-like.

Character 017. Mandible, teeth on the inner margin (apart from apical tooth): (0) teeth either absent, or poorly marked, or, at most, having a retinacle; (1) present, teeth well-developed.

Character 018. Labrum, epipharynx, dentiform setae medially on the distal margin: (0) absent; (1) present.

Character 019. Labrum, epipharynx, dentiform setae medially on the distal margin: (0) fewer than four medioapical setae; (1) four medioapical setae.

Character 020. Mentum, lateral margins expanded over maxillae: (0) absent; (1) present.

Character 021. Maxillary cardo shape, strong anterolateral projection: (0) absent; (1) present.

Character 022. Maxillary palp, size: (0) extending well outside oral area and easily visible in dorsal view; (1) scarcely visible, largely recessed inside buccal cavity or at least not visible dorsally.

Character 023. Maxillary palp, size for Pselaphinae standards, excluding lineages with extreme palpal reduction: (0) regular sized; (1) hypertrophied, (2) very small. Applicable only for species coded 0 in the previous character.

Character 024. Maxillary palp, segment number: (0) four, excluding the apical sensilla of the Pselaphinae (see Character 38); (1) fewer than four segments.

Character 025. Maxillary palpomere 2, length: (0) shorter than one-fifth an antenna length; (1) approximately equal to or longer than one-fifth an antenna length. Taxa with fewer than four palpomeres were coded as inapplicable.

Character 026. Maxillary palpomere 2, shape: (0) gradually thickening apically; (1) abruptly thickening apically; (2) complex (apex hyperthropied, block-like, and base inserted to it in a strong angle).

Character 027. Maxillary palpomere 2, lateral thin tubercle: (0) absent; (1) present.

Character 028. Maxillary palpomere 2, longitudinal axis strong change in direction: (0) no; (1) yes, longitudinal axis strongly changes at any point along palpomere so that the basal foramen of the palpomere is at greater than 90º angle in relation to the apical foramen.

Character 029. Maxillary palpomere 3, shape: (0) not or barely pedunculate, various forms; (1) strongly pedunculate.

Character 030. Maxillary palpomere 3, longitudinal axis strongly changing direction: (0) no; (1) longitudinal axis strongly changes at any point along palpomere so that the basal foramen of the palpomere is at greater than 90º angle in relation to the apical foramen.

Character 031. Maxillary palpomere 3, lateral thin/spinose tubercle: (0) absent; (1) present. Taxa with fewer than four palpomeres were coded as inapplicable.

Character 032. Maxillary palpomere 4, length: (0) shorter than one-fifth an antenna length; (1) approximately equal to or longer than one-fifth an antenna length. Taxa with fewer than four palpomeres were coded as inapplicable.

Character 033. Maxillary palpomere 4, lateral thin/spinose tubercle: (0) absent; (1) present. Taxa with fewer than four palpomeres were coded as inapplicable.

Character 034. Maxillary palpomere 4, width: (0) narrower or about as wide as scape; (1) clearly wider than scape. Taxa with fewer than four palpomeres were coded as inapplicable.

Character 035. Maxillary palpomere 4, peduncle: (0) absent; (1) present, palpomere pedunculate with thin stem and broad apex. Taxa with fewer than four palpomeres were coded as inapplicable.

Character 036. Maxillary palpomere 4, inner surface longitudinal sulcus: (0) absent; (1) present.

Character 037. Maxillary palpomere 4, basal margin flat and wide, basal corner (outer) strongly marked: (0) no; (1) yes.

Character 038. Apical sensilla on maxillary palpomere 4 ("apical pseudosegment" of Parker, 2016a, or "palpal cone" of Yin et al., 2019b): (0) absent; (1) present. Taxa with reduced palpomere number that have the sensilla at the apex of their apical palpomere were coded as 1.

Character 039. Maxillary palpomere 4, apex: (0) apical sensilla originates from the apical surface of palpomere 4; (1) apical sensilla originates from a cavity, or flat surface at the apex, of from within a cleft that runs along the inner length of the palpomere. Taxa without apical sensilla were coded as inapplicable.

Character 040. Apical sensilla, shape: (0) apex round; (1) apex truncate or mildly clavate; (2) modified into a group of slender setiform apical sensillae; (3) filiform, seta-like. Taxa without palpal cone were coded as inapplicable.

Character 041. Apical sensilla, size: (0) regular sized or hypertrophied; (1) minute (its presence, or at least its shape, requires a slide preparation to be examined in the compound microscope).

Character 042. Maxillary palpomere 4, a second sensilla next to the apical sensilla: (0) absent; (1) present.

Character 043. Antennal scape, length: (0) scape shorter than antennomeres 3–5 combined; (1) scape as long as or longer than antennomeres 3–5 combined.

Character 044. Antennal scape, length: (0) scape shorter than width of vertexo-occipital constriction; (1) scape as long as or longer than width of vertexo-occipital constriction.

Character 045. Antennal scape, apical notches: (0) absent; (1) present, scapes apically indented both dorsally and ventrally.

Character 046. Scape, width: (0) regular, not obviously wider than or about as wide as antennomere 5; (1) twice as wide as antennomere 5 or wider.

Character 047. Antennomere number: (0) seven or more; (1) six or fewer.

Character 048. Antennal club: (0) absent; (1) present.

Character 049. Antennal club composed of: (0) 3 antennomere; (1) 2 or 1 antennomeres; (2) 4 or more antennomeres.

Character 050. Apical antennomere, apex shape: (0) rounded or acuminate; (1) truncate.

Character 051. Apical antennomere, apex shape: (0) symmetric, without excavation; (1) assymetric, with excavation. Applicable only for species coded as 0 in Character 050.

Head, cephalic capsule

Character 052. Clypeus, visibility in full-face view: (0) exposed; (1) hidden.

Character 053. Clypeus, medial longitudinal carina: (0) absent; (1) present.

Character 054. Head, maximum depth: (0) at the antennal insertion level; (1) at the compound eye/vertexal level.

Character 055. Ocular mandibular carina: (0) absent; (1) present.

Character 056. Head, ocular-clypeal carina: (0) absent; (1) present.

Character 057. Head, ocular-antennal-clypeal carina: (0) absent; (1) present

Character 058. Cuticular projections over antenna: (0) absent, base of antennal scape exposed in full-face view; (1) present, base of antennal scape obscured from above by an expansion of the frons.

Character 059. Cuticular projections over antenna, shape: (0) base of scapes obscured simply by the expanded frons surface, not distinct from adjacent frons surface; (1) a distinct pair of raised, hood-like protrusions of the frons, the "antennal tubercles"; (2) antennal insertion region as a single tumulus.

Character 060. Antennal tubercle, shape: (0) the pair of tubercles (or single tumulus) are restricted to the frons, at the antennal insertion level; (1) the antennal tubercles extend posterad, ending at the vertexal surface, medially to the eyes; (2) the antennal tubercles extend posterad and link to the eyes forming an ocular-antennal ridge/carina (either thicker and truncate or thinner and sharp). Innaplicable for species coded as 0 in Character 059.

Character 061. Ocular-antennal ridge notch: (0) absent; (1) present.

Character 062. Interantennal space: (0) very short, antennal tubercles juxtaposed; (1) short,

antennal tubercles close to each other, separated by a distance greater than half scape width and smaller than 1x scape width; (2) broad, antennal tubercles separated from each other by a distance greater than 1x scape width.

Character 063. Interantennal sulcus: (0) absent; (1) present. Innaplicable for species coded as 2 in Character 062.

Character 064. Antennal tubercles: (0) not raised by basal stalk; (1) dorsally raised by basal stalk. Applicable for species coded as 0 in Character 062.

Character 065. Interantennal transversal ridge: (0) absent; (1) present, antennal tubercles linked by a raised cuticular ridge.

Character 066. Antennal tubercles notch: (0) absent; (1) present, antennal tubercle with a conspicuous notch on its margin.

Character 067. Lateral postantennal pits: (0) absent; (1) present. Species that have the vertexal foveae strongly anteriorolaterally migrated were coded as 0 for this character.

Character 068. Lateral postantennal pits: (0) each a regular pit; (1) each modified into a semicircular sulcus. Coded as innaplicable for species coded as 0 for Character 067.

Character 069. Ocular-antennal carina: (0) absent; (1) present, a low carina (not a raised cuticular ridge) linking the compound eye to the antennal tubercle.

Character 070. Frontal fovea: (0) absent; (1) present.

Character 071. Vertexal foveae: (0) absent; (1) present.

Character 072. Vertexal foveae, relative position: (0) anterior to or at the posteriormost level of the compound eyes; (1) posterior to the posteriormost level of the compound eyes.

Character 073. Malar area, broad excavations: (0) absent; (1) present.

Character 074. Frontovertexal area, broad excavation: (0) absent, sulcus/sulci or shallow cavities might still be present; (1) present, excavation deep and ocupies most of the frontovertexal area, usually laterally and anteriorly limited by ridges.

Character 075. Fontovertexal area, sulcus/sulci or smaller cavities: (0) absent; (1) present. Foveae or sulcus in between raised antennal tubercles not coded as state 1. Species with large excavations coded as innaplicable, even if sulci or smaller excavations occur within the large excavation.

Character 076. Gular, longitudinal carina: (0) absent; (1) longitudinal carina present.

Character 077. Gula, longitudinal carina shape: (0) not forked; (1) forked, V- or Y-shape. Species without longitudinal carina were coded as inapplicable.

Character 078. Gular ridge: (0) absent; (1) present.

Character 079. Gular medial cavity: (0) absent; (1) present.

Character 080. Gular longitudinal sulcus: (0) absent; (1) present.

Character 081. Gular fovea/foveae: (0) absent; (1) present.

Character 082. Gular fovea/foveae: (0) a pair; (1) fused as one. Inapplicable for species coded as 0 in Character 081.

Character 083. Gula, flatenned hyaline setae patch: (0) absent; (1) present.

Character 084. Head lateroventral margins: (0) not delimited by carina; (1) carinated.

Character 085. Head anteroventral lateral digitiform processes: (0) absent; (1) present.

Character 086. Vertex, medial low protuberance: (0) absent; (1) present

Character 087. Vertex, medial longitudinal sulcus originating at the vertexal-occipital constriction and following anterad: (0) absent; (1) present.

Character 088. Vertex, medial longitudinal carina at about the vertexal-occipital constriction, following anterad to vertex and posterad to the occipital surface: (0) absent; (1) present.

Character 089. Compound eye, shape: (0) mostly round; (1) with a posteroventral notch or other shape. Species with eyes composed of a single ommatidium or a few ones were coded as innaplicable.

Character 090. Compound eye, ommatidia size: (0) regular; (1) hypertrophied.

Character 091. Postocular patch of posteroventrally directed setae: (0) absent; (1) present.

Character 092. Postocular spine: (0) absent; (1) present.

Character 093. Ocular-vertexal posterolateral carina/ridge: (0) absent; (1) present.

Character 094. Occiput-vertex junction: (0) no constriction; (1) strong constriction; (2) mild constriction.

Pronotum

Character 095. Pronotal antebasal sulcus or impression: (0) absent; (1) present.

Character 096. Pronotal anterolateral corners strongly marked (observed in dorsal view): (0) absent, usually anterolateral margins are a soft curve leading into the widest section of the

pronotum, which is usually close to the mid-level; (1) present.

Character 097. Pronotal medial longitudinal sulcus: (0) absent; (1) present.

Character 098. Pronotal "wings", lateral portions that are considerably dettached and in a lower level than the medial portion, usually separated from the latter by longitudinal lateral sulcus: (0) absent; (1) present.

Character 099. Pronotal posteromedial large depression or cavity: (0) absent; (1) present. Smaller cavities or pits were coded as 0.

Character 100. Pronotal lateral longitudinal sulci: (0) absent; (1) present.

Character 101. Pronotal lateral longitudinal carinae/ridges: (0) absent; (1) present.

Character 102. Pronotal lateral longitudinal carinae/ridge spanning entire sclerite: (0) no, carinae not reaching the anterior pronotal edge; (1) yes, carinae entire across the pronotum.

Character 103. Pronotal posteromedial longitudinal carina: (0) absent; (1) present.

Character 104. Pronotal medial antebasal fovea (maf): (0) absent; (1) present.

Character 105. Pronotal lateral antebasal foveae (laf): (0) absent; (1) present; (2) two pairs.

Elytra

Character 106. Basal elytral foveae (bef): (0) absent; (1) present.

Character 107. Basal elytral foveae (bef), number: (0) four foveae per elytron; (1) less than four. Inapplicable for species coded as 0 in Character 106.

Character 108. Subhumeral elytral foveae (shef): (0) absent; (1) present.

Character 109. Discal elytral foveae (def): (0) absent; (1) present.

Character 110. Elytral sutural striae: (0) absent; (1) present.

Character 111. Elytral marginal carinae: (0) absent; (1) present, extending from humerus to at least half elytron length.

Character 112. Elytral discal sulci: (0) absent; (1) present.

Character 113. Elytral discal carinae: (0) absent; (1) one; (2) two pairs.

Character 114. Elytral anterior margins: (0) not carinated; (1) carinated.

Character 115. Elytral posterolateral cleft: (0) absent; (1) present.

Pterothorax

Character 116. Prosternum, head rest: (0) absent, prosternum simple, unmodified to accommodate the head when deflexed; (1) present, prosternum and procoxae fashioned into an excavation to receive the head when deflexed.

Character 117. Prosternal anterior margin crenulated or gear-like: (0) no; (1) yes.

Character 118. Prosternal anterior section length: (0) regular-sized or extended; (1) very thin.

Character 119. Prosternal flatenned hyaline setose patch: (0) absent; (1) present.

Character 120. Mesoventrite, medial longitudinal carina: (0) absent; (1) present.

Character 121. Mesoventrite, flatenned hyaline setose patch: (0) absent; (1) present.

Character 122. Metaventrite, length (of medial section) in relation to mesoventrite: (0) less than or about 1.5x mesoventrite length; (1) almost 2x mesoventrite length.

Character 123. Metaventrite, anteromedian fovea: (0) absent; (1) present.

Character 124. Metaventrite, a pair of lateral robust spine/projections: (0) absent; (1) present.

Legs

Character 125. Procoxa, outer surface with a carina-delimited concavity: (0) absent; (1) present.

Character 126. Protrochanter, length of dorsal margin: (0) short, profemur base nearly touching procoxa apex; (1) long, clearly longer than protrochanter width, so profemur base and procoxa apex are widely separated.

Character 127. Protibia inner face, with a concave shiny surface usually carina-delimited in most of its length: (0) no; (1) yes.

Character 128. Mesocoxae: (0) contiguous; (1) separated.

Character 129. Mesotrochanter, length of dorsal margin: (0) short, mesofemur base nearly touching mesocoxa apex; (1) long, clearly longer than mesotrochanter width, so mesofemur base and mesocoxa apex are widely separated.

Character 130. Metacoxae, separation: (0) contiguous or nearly so, with at most a narrow acuminate intercoxal process; (1) widely separated by broad intercoxal process.

Character 131. Metacoxae, shape: (0) projecting posteriorly at articulation with metatrochanter; (1) metacoxae not projecting.

Character 132. Metatrochanter, length of dorsal margin: (0) short, metafemur base nearly touching metacoxa apex; (1) long, clearly longer than metatrochanter width, so metafemur base

and metacoxa apex are widely separated.

Character 133. Metatibia, distal edge cuticular projection (lobate or spiniform): (0) absent; (1) present.

Character 134. Femur, ventral surface with a longitudinal, often carina-delimited sulcus which harbour the retracted tibia: (0) absent, ventral surface of femur either flat or convex; (1) present.

Character 135. Tarsomere, number: (0) four or five; (1) three. Bythinoplectini, Dimerini and Mayetiini show reductions to two tarsomeres, but were also coded as having state 1 of this character. In some of the cases it seems the first tarsomere is present as a diminutive vestige attached to tarsomere 2, in others it appears to be completely lost.

Character 136. Tarsomere 2, relative length: (0) of similar length as tarsomere 1; (1) clearly longer than tarsomere 1.

Character 137. Tarsomeres 2 and 3, relative lengths: (0) tarsomere 2 clearly shorter than tarsomere 3; (1) tarsomere 2 subequal or longer than tarsomere 3.

Character 138. Tarsomere 2 apicoventrally lobate: (0) no; (1) yes.

Character 139. Pretarsal claws/claw: (0) a pair composed of equally or subequally-sized claws; (1) a pair in which one claw is evidently larger than the other, but the smaller is not minute/residual; (2) a pair in which one claw is well-developed and the other is residual, seta-like; (3) a single pretarsal claw; (4) pretarsal claws in one individual combining in different ways in the fore, middle, and hind legs with the conformations described in the previous states 0, 1, 2, or 3.

Character 140. Pretarsal claw: (0) regular; (1) basaly lobate.

Abdomen

Character 141. Abdominal tergite III, dorsal view: (0) covered by elytra; (1) partially or completely exposed.

Character 142. Abdominal trichomes at the edge of tergites and paratergites III and IV: (0) absent; (1) present.

Character 143. Abdominal tergite IV, relative length: (0) subequal in length to tergite V; (1) at least 1.3 times as long as tergite V; (2) twice as long as tergite V or longer; (3) tergite V longer than IV. In taxa with fused tergites (Clavigeritae), the tergite lengths can still be deduced from

the paratergite boundaries.

Character 144. Abdominal tergite IV, medial discal carinae: (0) absent; (1) present.

Character 145. Abdominal tergite IV, flatenned hyaline setae mediobasally: (0) absent; (1) present.

Character 146. Abdominal tergite V and/or VI, flatenned hyaline setae mediobasally: (0) absent; (1) present.

Character 147. Abdominal tergites IV–VI, anteroposterior fusion: (0) absent, tergite boundaries distinct; (1) present, tergites fused into a composite 'tergal plate'.

Character 148. Abdominal tergite VII tergite length in relation to VI: (0) short, tergite VII at most 1.5x as long as tergite VI; (1) long, tergite VII longer than 1.5x tergite VI.

Character 149. Abdominal paratergites: (0) present; (1) absent.

Character 150. Abdominal tergites and sternites IV–VI, dorsoventral fusion: (0) absent, tergites separated from corresponding sternites; (1) present, abdominal margins fully sclerotized via fusion of tergites to corresponding sternites (paratergites absent, or paratergal lines indicated only by carinae).

Character 151. Apex of sternite III/ base of sternite IV shaped into a deep transverse sulcus: (0) no; (1) yes.

Character 152. Abdominal sternites III and IV, basal sulcus setal concentration: (0) basal sulcus setose; (1) sulcus nude. Species without basal sulcus were coded as inapplicable.

Character 153. Sternite VII distal margin middle section covered by sternite VI: (0) no, sternite VII distal margin is complete; (1) at least a small portion of sternite VII distal margin is covered by sternite VI.

Character 154. Abdominal segment IX externally visible: (0) no; (1) yes.

Phylogenetic results

Among the different combinations of parameters attempted, the implied weighting with constraint analyses retrieved the most parsimonious tree with 36.94608 steps (Figure 1). The trees with Bremmer support and bootstrap values for the tree in Figure 1 are presented in Appendix 2.

We recovered a Pselaphinae tree with the following topology: among the two outgroups, the

Oxytelinae is the sister to all remaining species; †*Protopselaphus thayerae* is sister to all species excluding *Anotylus* sp. Then, within the Pselaphinae clade, the first dichotomy separates the Faronitae from the higher Pselaphinae.

The Faronitae was always recovered as a clade, but not necessarily as the sister lineage to the remaining Pselaphinae, as is widely accepted (Newton and Thayer, 1995; Chandler, 2001; Parker, 2016a). Our constraint forced the clade as the sister to the rest of the species, the higher Pselaphinae. Once the Faronitae clade was constrained, the tree's topology looked roughly as previous phylogenies (Parker, 2016a; Yin et al., 2017; Yin et al., 2019). We included the described species of Chapter 1, †*Burmalogasa perisi*, and one congeneric morphospecies, †*Burmalogasa* sp. (specimen CELC002162). They grouped, as expected, and resulted in a clade sister to the clade of the modern species (Fig. 1).

Within the higher Pselphinae, Cretaceous genera included in the analysis were recovered as a clade, except for †*Megabythinus*. Within this larger clade of fossil species, †*Boreotethys*, †*Cretobythus* and †*Priscaplectus* form a subclade; another subclade, sister to the latter, is formed by the genera †*Burmagluta*, †*Cretobrachygluta* and "Gen-nov-1" (an undescribed species, very likely a new genus; specimen's code CELC003040). The species †*Boreotethys caii* is sister to these two subclades, and render its genus paraphyly, as expected and discussed in Chapter 1 of this thesis. †*Megabythinus spinitibialis* was the only that has not gouped to the fossil higher Pselaphinae. It was recovered wthin an Euplectitae lineage together with *Mayetia atlantica* Chaul and Lopes-Andrade, 2022 and *Tuberoplectus* ufv-06.

In our analysis, the Goniaceritae and Euplectitae were not recovered as clades, while the Pselaphitae and Clavigeritae were monophyletic, contrary to previous phylogenetic studies that showed a paraphyletic Pselaphitae, with Clavigeritae arising from within of one of the two lineages of Pselaphitae. The Batrisitae was also poorly represented, only a single OTU, so we could not infer its monophyly.

DISCUSSION

Our analysis included the majority of the Cretaceous genera in a phylogenetic context based on an entirely new morphological matrix that was created to cover most of the morphological diversity known to date. The only genera that were not included in the analysis were the two from Spanish amber, †*Cretasonoma* and †*Penarhytus*, and the Burmese †*Protrichonyx*. The three are key species in the understanding of the Cretaceous fauna, each important in their own way (see Chapter 1 of this thesis), and future attempts to include them in a phylogenetic scenario are indispensable.

Extant Faronitae were not available for our study, and the two species of the topology were coded from images. Currently, there are not enough resolution to test for the hypothesis of the Cretaceous species being stem Faronitae (Parker, 2016a), which would depend on the addition of more extant OTUs, preferably coded from direct examination of specimens, not their images only. Faronitae species are described from Baltic amber (Schaufuss, 1890; Newton and Chandler, 1989), but little is known about their types of those species (short descriptions and no available images). The Faronitae are unknown from Cambay amber, but could possibly be found, as the two described Pselaphinae species from this site that has just started to be studied are very distantly phylogenetically (Parker and Grimaldi, 2014; Parker, 2022), meaning the Cambay pselaphinae is potentialy very diverse. If found, then the Faronitae will be the sole lineage represented in all four amber sites known to contain Pselaphinae, each of these sites being from a geological time considerably distant from the other, so that it would represent a great chance to study Faronitae evolution. For the moment, the re-evaluation of the Spanish amber species, †*Cretasonoma corimformibus*, the inclusion of more extant species, and the inclusion of more Burmese diversity _ undescribed species are known (Parker, 2016a; personal observation) _ are priority and have the potential of greatly improve the resolution of that portion of the tree.

The species †*Boreotethys caii*, as explained in its description in Chapter 1, probably deserves its own genus. In that chapter, the species was *a priori* considered distinct enough from the other two in †*Boreotethys* based on morphology. On the phylogeny presented in that chapter, it did not group with the other †*Boreotethys* species. Instead, it was in a polytomy with many other species. In the present analysis, the topology of the clade of the Burmese fossils was better resolved and †*Boreotethys caii* appeared distant from †*Boreotethys grimaldii*. Once better

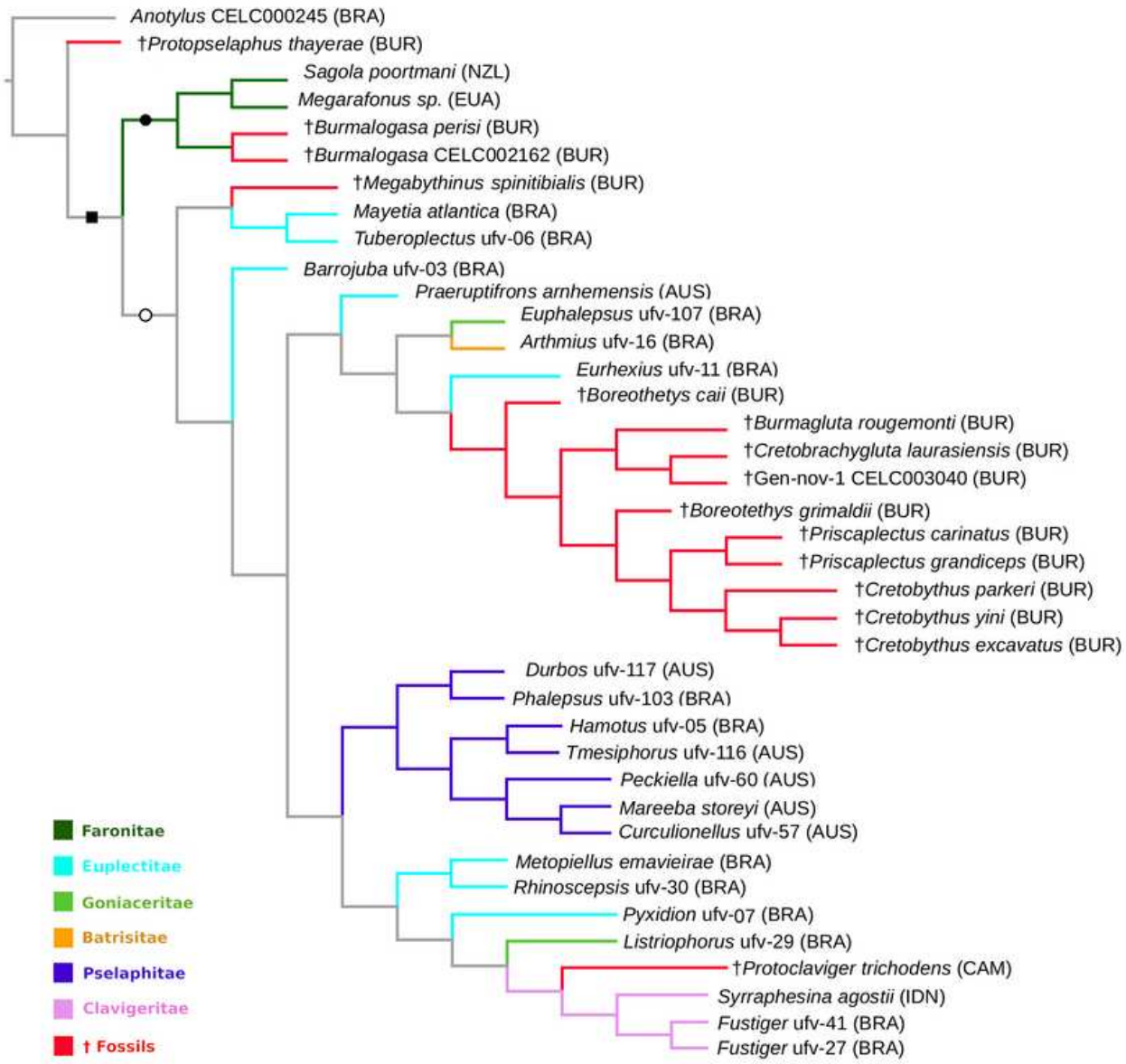

Figure 1. Most parsimonious tree generated with implicit weighting (k=6.093750) and constraint for the higher Pselaphinae (forcing the Faronitae clade as the sister to the remaining Pselaphinae) based on coding of 154 characters for fossils and extant pselaphines. Abbreviations: AUS, Australia; BRA, Brazil; BUR, Burmese amber from Myanmar; CAM, Cambay amber from India; NZL, New Zealand, USA, United States of America. Square indicates the subfamily Pselaphinae, black circle the clade of the supertribe Faronitae and the open circle is the higher Pselaphinae clade.

preserved specimens allow a more precise characterization of the new genus, †*Boreotethys caii* should be moved.

The lack of any Bythinini in the phylogeny represented a shortcoming of the work, as members of this tribe were hypothesized to be related to part of the Cretaceous fauna, namely †*Boreotethys*, †*Cretobythus* and †*Megabythinus* (Parker, 2016a; Yin et al., 2017; Yin et al., 2021). Their absence was simply due to the lack of material to be examined, but it is crucial to test whether any or more of these three genera indeed represents stem Bythinini.

A decade ago when the first Cretaceous pselaphines were starting to be described, the prevailing idea was that the ants were low in diversity and abundance among the Cretaceous arthropod communities, with ant dominance in Earth's biomes only taking place after the Cretaceous-Paleogene boundary (Lapolla et al., 2013). That notion plus the finding of an important transitional fossil of the Clavigeritae myrmecophile lineage from early Eocene (Parker and Grimaldi, 2014) led to the hypothesis that the pselaphine-ant relation arose post to the Cretaceous-Paleogene boundary (Parker and Grimaldi, 2014). Nevertheless, recent myrmecological findings point to a much more diverse ant community than previously thought (Barden et al., 2017; Perrichot et al., 2020; Cao et al, 2020; Boudinot et al., 2020; Lattke and Melo, 2020; Boudinot et al., 2022; Chaul, 2023; Zhuang et al., 2024). The same appears to be true for the pselaphines, although the description rates have not been at the same pace as in the ants. Neither ants nor pselaphines appear to have been inconspicuous by mid-Cretaceous, so that some of the pselaphines of the time could had exploited ant colonies or interacted with ants to some degree. It is tempting to suspect, for example, that body robustness and reduction of mouthparts of †*Priscaplectus* could be adaptations to living among ants, just as they are for many modern lineages (e.g. many Goniacerini, and Arhytodini genera) (Parker, 2016b).

CONCLUSION

The phylogeny presented in this chapter represents the most inclusive so far for the Cretaceous Pselaphinae. We almost tripled the number of characters studied in comparison to previous studies, likely enhancing the resolution of the relations between the Cretaceous lineages. The

new phylogenetic scenario presented show that most of the fossils are closer between themselves and might be only remotely related to extant tribes. Key fossils and extant lineages missing from our data represent a missing piece that must be overcome in future studies, so to reveal a better picture of the Pselaphinae evolution.

ACKNOWLEDGEMENTS

Gabriela de Figueiredo Jacintho helped performing the phylogenetic analysis in TNT. Chloe and Trevor von Loon kindly shared a series of images of *Megarafonus* sp.. Financial support was provided by Fundação de Amparo à Pesquisa do Estado de Minas Gerais (FAPEMIG) and Conselho Nacional de Desenvolvimento Científico e Tecnológico (CNPq; research grant number 304339/2022-9 to CLA). This study was financed in part by Coordenação de Aperfeiçoamento de Pessoal de Nível Superior—Brasil (CAPES; Finance Code 001).

REFERENCES

Beutel, R., Luo. X-Z., Yavorskaya, M., Jałoszyński, P., 2021. Structural megadiversity in leaf litter predators – the head anatomy of *Pselaphus heisei* (Pselaphinae, Staphylinidae, Coleoptera). Arthropod Systematics and Phylogeny 79, 443–463. https://doi.org/10.3897/asp.79.e68352

Boudinot, B., Perrichot, V., Chaul, J., 2020. †*Camelosphecia* gen. nov., lost ant-wasp intermediates from the mid-Cretaceous (Hymenoptera, Formicoidea). ZooKeys, 1005, 21–55. https://doi.org/10.3897/zookeys.1005.57629

Boudinot, B., Richter, A., Katzke, J., Chaul, J., Keller, R., Economo, E., Beutel, R., Yamamoto, S., 2022. Evidence for the evolution of eusociality in stem ants and a systematic revision of †*Gerontoformica* (Hymenoptera: Formicidae). Zoological Journal of the Linnean Society, 195, 1355–1389. https://doi.org/10.1093/zoolinnean/zlab097/6523228

Barden, P., Herhold H., Grimaldi, D., 2017. A new genus of hell ants from the Cretaceous (Hymenoptera: Formicidae: Haidomyrmecini) with a novel head structure. Systematic Entomology, 42, 837–846. https://doi.org/10.1111/syen.12253

Cao, H., Boudinot, B., Wang, Z., Miao, X., Shih, C., Ren, D., Gao, T., 2020. Two new iron maiden ants from Burmese amber (Hymenoptera: Formicidae: †Zigrasimeciini). Myrmecological News, 30, 161–173. https://doi.org/10.25849/myrmecol.news_030:161

Chandler, D., 2001. Biology, morphology, and systematics of the ant-like litter beetles of Australia (Coleoptera: Staphylinidae: Pselaphinae). Memoirs of Entomology International 15 i–viii + 1–560.

Chaul, J., 2023. A revision of the Cretaceous ant genus *Zigrasimecia* Barden & Grimaldi, 2013 (Hymenoptera: Formicidae: †Zigrasimeciinae). Zootaxa, 5325 (3), 301–341. https://doi.org/10.11646/zootaxa.5325.3.1

Chaul, J., Lopes-Andrade, C., 2022. First record of Mayetiini (Coleoptera: Staphylinidae: Pselaphinae) from Brazil, with the description of a new macropterous and macrophthalmic species of *Mayetia* Mulsant & Rey, 1875. Zootaxa, 5175 (1), 126–136. https://doi.org/10.11646/zootaxa.5175.1.6

Evenhuis, N., 2021. The insect and spider collections of the world website. Available at: http://hbs.bishopmuseum.org/codens/ (accessed 03 January 2024).

Goloboff, P., Farris, J., and Nixon, K., 2008a. TNT, a free program for phylogenetic analysis.

Cladistics, 24(5), 774–786. https://doi.org/10.1111/j.1096-0031.2008.00217.x

Goloboff, P. A., Carpenter, J. M., Arias, J. S., and Esquivel, D. R. M., 2008b. Weighting against homoplasy improves phylogenetic analysis of morphological data sets. Cladistics, 24(5), 758-773. https://doi.org/10.1111/j.1096-0031.2008.00209.x

Hlaváč, P., Baňař, P., Parker, J., 2013. The Pselaphinae of Madagascar. II. Redescription of the genus *Semiclaviger* Wasmann, 1893 (Coleoptera: Staphylinidae: Pselaphinae: Clavigeritae) and synonymy of the subtribe Radamina Jeannel, 1954. Zootaxa, 3736 (3), 265 – 276. http://dx.doi.org/10.11646/zootaxa.3736.3.4

Hlaváč, P., Baňař, P., Parker, J., 2014. Endogean and cavernicolous Coleoptera of the Balkans. XIV. Melledobythus bilandzijae, new genus and species of cavernicolous Bythinini (Staphylinidae: Pselaphinae) from the Island Mljet, Croatia. Zootaxa, Zootaxa, 3835 (4), 564 – 572. http://dx.doi.org/10.11646/zootaxa.3835.4.7

Jałoszyński, P., Luo, X.-Z, Beutel, R., 2020. Profound head modifications in *Claviger testaceus* (Pselaphinae, Staphylinidae, Coleoptera) facilitate integration into communities of ants. Journal of Morphology, 281 (9), 1072–1085. https://doi.org/10.1002/jmor.21232

Jałoszyński, P., Luo, X.-Z., Beutel, R., 2022. Evolution of cephalicstructures in extreme myrmecophiles: A lesson from Clavigeritae (Coleoptera: Staphylinidae: Pselaphinae). Cladistics, 38, 335–358. https://doi.org/10.1111/cla.12498

Kerner, A., Bouquin, S., Portier, R., Vignes-Lebbe, R., 2021. The 8 Years of Existence of Xper3: State of the art and future developments of the platform. Biodiversity Information Science and Standards, 5, e74250. https://doi.org/10.3897/biss.5.74250

LaPolla, J., Dlussky, G., Perrichot, V., 2013. Ants and the fossil record. Annual Review of Entomology, 58, 609–630. https://doi.org/10.1146/annurev-ento-120710-100600

Lattke, J., Melo, G., 2020. New haidomyrmecine ants (Hymenoptera: Formicidae) from mid-Cretaceous amber of northern Myanmar. Cretaceous Research, 114, 104502 https://doi.org/10.1016/j.cretres.2020.104502

Lawrence, J., Slipinski, A., Seago, A., Thayer, M., Newton, A., 2011. Phylogeny of the Coleoptera based on morphological characters of adults and larvae. Annales zoologici (Warsowa), 61 (1), 1–217. https://doi.org/10.3161/000345411X576725

Liu, Y., Tihelka, E., Yamamoto, S., Yin, Z.-W., Huang D.-Y., Tian, L., Cai, C.-Y., 2020. The first fossil record of the rove beetle subfamily Protopselaphinae (Coleoptera: Staphylinidae) from mid-Cretaceous Burmese amber. Cretaceous Research 110, 104416. http://doi.org/10.1016/j.cretres.2020.104416

Luo, X.-Z., Hlaváč, P., Jałoszyński, P., Beutel, R., 2021a. In the twilight zone – the head morphology of *Bergrothia saulcyi* (Pselaphinae, Staphylinidae, Coleoptera), a beetle with adaptations to endogean life but living in leaf litter. Journal of Morphology, 282, 1170–1187. https://doi.org/10.1002/jmorp21361.

Luo, X.-Z., Jałoszyński, P., Stoessel, A., Beutel, R., 2021b. The specialized thoracic skeletomuscular system of the myrmecophile *Claviger testaceus* (Pselaphinae, Staphylinidae, Coleoptera). Organism Diversity and Evolution, 21, 317–335. https://doi.org/10.1007/s13127-021-00484-1

Luo, X.-Z., Jałoszyński, P., Beutel, R., 2022. The thoracic anatomy of *Pselaphus heisei* (Pselaphinae, Staphylinidae, Coleoptera). Journal of Morphology, 284, e21527. https://doi.org/10.1002/jmor.21527

Newton, A., Chandler, D., 1989. World catalog of the genera of Pselaphidae (Coleoptera). Fieldiana Zoology, 53, 1–93. https://doi.org/10.5962/bhl.title.3209

Newton, A., Thayer, M., 1995. Protopselaphinae new subfamily for *Protopselaphus* new genus from Malaysia, with a phylogenetic analysis and review of the Omaliine Group of Staphylinidae including Pselaphidae (Coleoptera). Biology, Phylogeny, and Classification of Coleoptera: Papers Celebrating the 80th Birthday of Roy A. Crowson (ed. by J. Pakaluk and A. Ślipiński), 221–320. Muzeum i Instytut Zoologii PAN, Warszawa.

Nixon, K. C. 1999-2002. WinClada ver. 1.0000 Published by the author, Ithaca, NY, USA.

Owens, B., Carlton, C., 2016. Revision of *Eutyphlus* LeConte (Coleoptera: Staphylinidae: Pselaphinae), with Description of a New Species and Phylogenetic Placement within the Tribe Trichonychini. The Coleopterists Bulletin, 70 (1), 1–29. http://dx.doi.org/10.1649/072.070.0102

Parker, J., Grimaldi, D., 2014. Specialized Myrmecophily at the Ecological Dawn of Modern Ants. Current Biology, 24, 2428–2434. http://dx.doi.org/10.1016/j.cub.2014.08.068

Parker, J., 2016a. Emergence of a superradiation: pselaphine rove beetles in midCretaceous amber from Myanmar and their evolutionary implications. Systematic Entomology 41, 541–566. https://doi.org/10.1111/syen.12173

Parker, J., 2016b. Myrmecophily in beetles (Coleoptera): evolutionary patterns and biological mechanisms. Myrmecological News, 22, 65–108. https://doi.org/10.25849/myrmecol.news_022:065

Parker, J., 2022. Transitional morphology and Afrotropical affinity of a bythinoplectine rove beetle from the early Eocene of India (Coleoptera: Staphylinidae: Pselaphinae). Palaeoentomology 005 (5), 452–460. https://doi.org/10.11646/palaeoentomology.5.5.6

Parker, J., Maruyama, M., 2013. *Jubogaster towai*, a new Neotropical genus and species of Trogastrini (Coleoptera: Staphylinidae: Pselaphinae) exhibiting myrmecophily and extreme body enlargement. Zootaxa 3630 (2), 369 – 378. http://dx.doi.org/10.11646/zootaxa.3630.2.11

Parker, J., Owens, B., 2018. *Batriscydmaenus* Parker and Owens, new genus , and convergent evolution of a “reductive ” ecomorph in socially symbiotic Pselaphinae (Coleoptera : Staphylinidae). The Coleopterists Bulletin, 72 , 219–229. https://doi.org/10.1649/0010-065X-72.2.219

Peris, D., Chatzimanolis, S., Delclòs, X., 2014. Diversity of rove beetles (Coleoptera: Staphylinidae) in Early Cretaceous Spanish amber. Cretaceous Research, 48, 85–95. https://doi.org/10.1016/j.cretres.2013.11.008

Perrichot, V., Wang, B., Barden, P., 2020. New remarkable hell ants (Formicidae: Haidomyrmecinae stat. nov.) from mid-Cretaceous amber of northern Myanmar. Cretaceous Research, 109, 104381 (18 pp.) https://doi.org/10.1016/j.cretres.2020.104381

Schaufuss, L., 1890. System-schema der Pselaphiden, ein Blick in die Vorzeit, in die Gegenwart und in die Zukunft. Tijdschrift Voor Entomologie 33, 101–162.

Ung, V., Dubus, G., Zaragüeta-Bagils, R., Vignes-Lebbe, R., 2010. Xper2: introducing e-taxonomy. Bioinformatics, 26 (5), 703–704. https://doi.org/10.1093/bioinformatics/btp715

Vignes-Lebbe, R., Bouquin, S., Kerner, A., Bourdon, E., 2017. Desktop or remote knowledge base management systems for taxonomic data and identification keys: Xper2 and Xper3. Proceedings of TDWG, 1, e19911. https://doi.org/10.3897/tdwgproceedings.1.19911

Yin, Z.-W., Parker, J., Cai, C.-Y., Huang, D.-Y., Li, L.-Z., 2017. A new stem bythinine in Cretaceous Burmese amber and early evolution of specialized predatory behaviour in pselaphine rove beetles (Coleoptera: Staphylinidae). Journal of Systematic Palaeontology, https://doi.org/10.1080/14772019.2017.1313790. [volume and issue information and pagination were assigned in 2018 as follows: 16 (7), 531–541]

Yin, Z.-W., Kurbatov, S., Cuccodoro, G., Cai, C.-Y., 2019a. *Cretobrachygluta* gen. nov., the first and oldest Brachyglutini in mid-Cretaceous amber from Myanmar (Coleoptera: Staphylinidae: Pselaphinae). Acta Entomologica Musei Nationalis Pragae, 59, 101–106. https://doi.org/10.2478/aemnp-2019-0008

Yin, Z.-W., Chandler, D., Cai, C.-Y., 2019b. *Priscaplectus* gen. nov. and two new species in mid-Cretaceous amber from Myanmar (Coleoptera: Staphylinidae: Pselaphinae). Cretaceous Research 103, 104174. https://doi.org/10.1016/j.cretres.2019.07.004

Yin, Z.-W., Hlaváč, P., 2020. A second species of *Syrraphesina* Raffray found adjacent to Wallace's Line (Coleoptera, Staphylinidae, Pselaphinae). Zootaxa, 4852 (2), 203–210. https://doi.org/10.11646/zootaxa.4852.2.5

Yin, Z.-W., Cai, C.-Y., 2021. A new Brachyglutini from mid-Cretaceous amber of northern Myanmar (Coleoptera: Staphylinidae: Pselaphinae). Cretaceous Research, 124, 104807. https://doi.org/10.1016/j.cretres.2021.104807

Yin, Z.-W., Zhao, Q.-H., Cai, C.-Y., 2021. *Megabythinus* gen. nov., a new stem-group Pselaphinae from mid-Cretaceous Myanmar amber (Coleoptera, Staphylinidae). Cretaceous Research, 125, 104879. https://doi.org/10.1016/j.cretres.2021.104879

Zhuang, Y., Liu, Y., Ran, H., Jarzembowski, E., Zhang, Q., 2023 ("2024"). A new species and one new wing type of the iron maiden ants from Kachin amber (Hymenoptera: Formicidae: Zigrasimecia). Cretaceous Research, 154, 105742 (9 pp.) https://doi.org/10.1016/j.cretres.2023.105742

Appendix 1

	001	002	003	004	005	006	007	008	009	010	011	012	013	014	015	016	017	018	019	020	021	022	023	024	025	026	027	028	029	030	031	032	033	034	035	036	037	038	039	040
Anotylus CELC000244	0	0	0	0	0	0	0	0	0	0	0	0	0	0	0	0	1	0	-	0	0	0	0	0	0	0	0	0	0	0	0	0	0	0	0	0	0	0	-	-
Arthmius ufv-16	1	0	1	0	2	1	0	0	0	0	1	0	1	0	0	0	1	?	?	0	0	0	0	0	0	1	0	0	0	1	0	0	0	0	0	1	0	1	1	?
Barrojuba ufv-03	1	0	0	0	0	1	0	0	1	1	0	0	1	0	0	0	1	1	0	1	1	0	0	0	0	0	0	0	0	0	0	0	0	0	0	0	0	1	0	0
†*Boreotethys caii*	1	0	1	0	1	1	0	0	0	0	1	0	0	0	0	0	1	?	?	?	0	0	0	0	0	1	0	?	0	?	0	0	0	1	0	0	?	1	0	?
†*Boreotethys* cf. *grimaldii*	1	0	1	0	1	0	1	0	0	0	0	0	1	0	0	0	1	?	?	?	0	0	1	0	1	1	0	0	0	1	0	1	0	1	0	0	1	1	0	?
†*Burmagluta rougemonti*	1	0	1	0	1	0	0	0	0	0	1	0	1	0	0	?	?	?	?	?	0	0	0	0	0	0	0	0	0	1	0	0	0	0	0	0	0	1	0	0
†*Burmalogasa* CELC002162	1	0	0	0	0	1	1	0	0	0	0	0	1	0	0	0	0	?	?	0	0	0	0	0	0	0	0	0	0	0	0	0	0	0	0	0	0	1	0	1
†*Burmalogasa perisi*	1	0	0	0	0	1	1	0	0	0	0	0	1	0	0	?	0	?	?	0	0	0	0	0	0	0	0	0	0	0	0	0	0	0	0	0	0	?	?	?
†*Cretobrachygluta laurasiensis*	1	0	1	0	1	1	0	0	0	0	1	0	0	0	0	0	?	?	?	0	0	0	0	0	0	1	0	0	0	1	0	0	0	0	0	0	0	1	0	0
†*Cretobythus yini*	1	0	1	0	1	0	1	0	0	0	0	0	1	0	0	?	?	1	0	0	0	0	1	0	1	1	0	0	0	0	0	1	0	1	0	0	1	1	0	0
†*Cretobythus excavatus*	1	0	1	0	1	1	1	0	0	0	0	0	0	0	0	0	?	?	?	?	0	0	1	0	1	1	0	0	0	0	0	1	0	1	0	0	1	1	0	0
†*Cretobythus parkeri*	1	0	1	0	1	1	1	0	0	0	0	0	1	0	0	0	?	?	?	0	0	0	1	0	0	1	0	1	0	0	0	1	0	1	0	0	1	1	0	0
Curculionellus ufv-57	1	0	0	0	2	1	0	0	0	0	1	0	1	0	0	?	?	?	?	0	0	0	0	0	0	0	0	0	0	0	0	0	0	0	0	0	1	1	1	1
Durbos ufv-117	1	0	1	0	2	0	0	0	0	0	1	0	1	0	0	0	1	?	?	0	0	0	1	0	0	1	0	0	1	0	0	0	0	0	1	0	0	1	1	0
Euphalepsus ufv-107	1	0	0	0	2	1	0	0	1	0	1	0	0	0	0	?	?	1	0	0	0	0	2	0	0	1	0	0	0	1	0	0	0	0	0	0	0	1	0	0
Eurhexius ufv-11	1	0	0	0	0	0	0	0	0	0	1	0	1	0	0	0	1	1	1	0	0	0	0	0	0	1	0	0	0	1	0	0	0	0	0	0	0	1	0	1
Fustiger ufv-27	1	0	0	1	1	0	1	0	1	0	0	1	1	0	1	-	-	0	?	-	0	1	-	1	-	-	-	-	-	-	-	-	-	-	-	-	-	1	0	2
Fustiger ufv-41	1	0	0	1	1	0	1	0	1	0	0	1	1	0	1	-	-	0	?	-	0	1	-	1	-	-	-	-	-	-	-	-	-	-	-	-	-	1	0	2
†Gen-nov-1 CELC003040	1	0	0	0	1	0	0	0	0	0	0	0	0	0	0	0	1	?	0	?	0	0	0	0	0	1	0	?	0	1	0	0	0	0	0	0	0	1	0	0
Hamotus ufv-05	1	0	0	0	2	0	0	0	0	0	1	0	1	0	0	0	1	1	0	0	0	0	1	0	0	1	0	0	0	0	0	1	0	1	0	1	1	1	1	1
Listriophorus ufv-29	1	0	0	0	2	1	0	1	1	1	1	1	1	0	0	0	1	0	-	0	0	0	2	0	0	0	0	0	0	0	0	0	0	0	0	0	0	1	0	0
Mareeba storeyi	1	0	0	0	2	1	0	0	0	0	1	0	1	1	0	?	?	?	?	0	0	0	0	0	0	0	0	0	0	0	0	0	0	0	1	0	0	1	0	1
Mayetia atlantica	1	0	1	0	0	0	1	0	0	1	0	0	0	0	0	1	0	0	-	0	0	0	0	0	1	2	0	1	0	0	1	0	1	0	0	0	0	1	0	0
†*Megabythinus spinitibialis*	1	0	0	0	1	0	1	0	0	0	0	0	1	0	0	?	?	?	?	?	0	0	1	0	0	0	0	1	0	0	0	1	0	1	0	0	0	1	0	0
Megarafonus sp.	1	0	0	0	0	0	1	0	1	1	0	0	0	1	0	0	0	?	?	?	0	0	0	0	?	?	0	?	0	0	0	0	0	0	0	0	0	1	0	?
Metopiellus emavieirae	1	0	0	0	1	0	1	0	0	0	1	0	1	0	0	0	1	1	0	0	0	0	0	0	0	0	0	0	0	0	0	0	0	0	0	0	0	1	0	1
Peckiella ufv-60	1	0	0	0	2	1	0	0	0	0	1	0	1	0	0	0	1	?	?	0	0	0	1	0	1	1	0	0	0	0	0	1	0	1	1	0	0	1	1	1
Phalepsus ufv-103	1	0	0	0	1	1	0	0	1	0	1	0	1	0	0	0	1	1	0	0	0	0	1	0	1	1	0	0	1	0	0	0	0	0	1	0	0	1	1	?
Praeruptifrons arnhemensis	1	0	1	0	1	1	0	0	1	1	1	0	0	0	0	?	?	?	?	0	0	0	0	0	0	0	0	0	0	0	0	1	0	1	0	0	0	1	0	0
†*Priscaplectus carinatus*	1	0	1	0	1	1	0	0	0	?	0	1	0	0	0	?	?	?	0	0	0	0	2	0	0	1	0	0	0	1	0	0	0	0	0	0	1	1	0	0
†*Priscaplectus grandiceps*	1	0	0	0	1	1	0	0	0	?	0	0	0	0	0	?	?	?	0	0	0	0	2	0	0	1	0	0	0	1	0	0	0	0	0	0	0	1	0	0
†*Protoclaviger trichodens*	1	0	0	1	1	1	0	0	0	0	0	1	1	0	0	0	0	?	?	?	0	0	2	1	-	-	-	-	-	-	-	-	-	-	-	-	-	?	?	?
†*Protopselaphus thayerae*	0	0	0	0	0	0	1	0	0	0	0	0	0	0	0	0	0	?	?	0	0	0	0	0	0	0	0	0	0	0	0	0	0	0	0	0	0	0	-	-
Pyxidion ufv-07	1	0	1	0	1	0	1	0	0	0	1	0	1	0	0	0	1	1	0	0	0	0	0	0	0	0	0	0	0	0	0	0	0	0	0	0	0	1	0	0
Rhinoscepsis ufv-30	1	0	0	0	1	0	1	0	1	1	1	0	1	0	0	0	1	1	0	0	0	0	0	0	0	0	0	1	0	1	0	0	0	0	0	0	0	1	0	0
Sagola poortmani	1	0	0	0	0	0	1	0	0	0	0	0	1	1	0	0	0	?	?	?	0	0	0	0	?	?	0	?	0	?	0	0	0	0	0	0	0	1	0	0
Syrraphesina agostii	1	0	0	1	1	1	0	0	1	0	1	1	1	0	1	-	-	?	?	?	0	1	-	1	-	-	-	-	-	-	-	-	-	-	-	-	-	?	?	?
Tmesiphorus ufv-116	1	1	1	0	1	1	0	0	0	0	1	0	1	0	0	0	1	1	0	0	0	0	0	0	0	1	1	1	0	0	1	0	0	0	0	0	0	1	0	0
Tuberoplectus ufv-06	1	0	1	0	0	0	1	0	0	0	0	0	1	0	0	1	1	0	-	0	0	0	0	0	0	0	0	1	0	0	0	0	0	0	0	0	0	1	0	0

	0	0	0	0	0	0	0	0	0	0	0	0	0	0	0	0	0	0	0	0	0	0	0	0	0	0	0	0	0	0	0	0	0	0	0	0	0	0	0	0
	4	4	4	4	4	4	4	4	4	4	5	5	5	5	5	5	5	5	5	5	6	6	6	6	6	6	6	6	6	6	7	7	7	7	7	7	7	7	7	8
	1	2	3	4	5	6	7	8	9	0	1	2	3	4	5	6	7	8	9	0	1	2	3	4	5	6	7	8	9	0	1	2	3	4	5	6	7	8	9	0
Anotylus CELC000244	-	-	1	0	0	0	0	0	-	0	0	0	0	1	0	0	1	1	1	0	0	2	0	-	0	0	0	-	1	0	0	-	0	0	0	0	-	0	0	0
Arthmius ufv-16	1	0	0	0	1	0	0	1	0	0	0	0	0	1	1	1	0	1	1	0	0	2	-	-	0	0	0	-	0	0	1	1	0	1	-	0	-	0	0	0
Barrojuba ufv-03	0	1	0	0	0	0	0	1	2	0	0	0	0	1	0	0	0	1	0	-	-	2	0	-	0	0	0	-	0	0	1	0	0	0	0	1	1	0	0	0
†*Boreotethys caii*	0	0	1	1	0	0	0	1	0	0	0	0	?	?	1	?	0	1	1	?	0	2	-	-	0	0	?	?	0	0	?	?	0	0	0	0	-	0	?	?
†*Boreotethys* cf. *grimaldii*	0	0	1	0	0	0	0	1	0	0	0	0	?	0	1	?	0	1	1	?	?	2	-	-	0	0	?	?	?	0	1	0	0	0	?	0	-	0	?	0
†*Burmagluta rougemonti*	0	0	0	0	0	0	0	1	0	0	0	0	?	0	?	?	0	1	1	1	-	2	-	-	1	0	?	?	0	?	1	1	0	0	0	0	-	1	0	0
†*Burmalogasa* CELC002162	0	0	0	0	0	0	0	0	-	0	0	1	?	0	?	?	0	1	1	0	-	1	1	-	1	0	?	?	1	?	1	0	0	0	1	?	?	?	?	?
†*Burmalogasa perisi*	?	0	0	1	0	0	0	0	-	0	1	1	?	0	1	?	0	1	1	0	-	1	1	-	0	0	?	?	?	?	1	1	0	0	1	?	?	?	?	?
†*Cretobrachygluta laurasiensis*	0	0	0	0	0	0	0	1	0	0	1	0	?	0	1	1	0	1	0	-	-	2	-	-	0	0	?	?	?	1	1	0	0	0	0	0	-	1	0	0
†*Cretobythus yini*	0	0	0	1	0	0	0	1	0	0	0	0	?	0	1	?	0	1	1	2	0	2	-	-	1	1	?	?	-	?	1	0	0	1	-	0	-	0	1	1
†*Cretobythus excavatus*	0	0	1	0	0	0	0	1	0	0	0	0	?	?	?	?	0	1	1	2	0	2	-	-	1	1	?	?	0	?	1	0	0	1	-	0	-	?	?	0
†*Cretobythus parkeri*	0	0	1	1	0	0	0	1	0	0	1	0	?	0	1	1	0	1	1	2	0	2	-	-	1	1	?	?	0	?	1	0	0	1	-	0	-	0	1	-
Curculionellus ufv-57	0	0	0	0	0	0	0	1	2	0	0	1	1	0	0	0	0	1	1	1	-	0	1	1	0	0	0	-	0	0	1	0	0	0	1	0	-	0	0	0
Durbos ufv-117	0	0	0	0	0	0	0	0	1	0	0	0	0	0	0	0	0	0	1	1	0	-	2	-	-	0	0	0	-	0	0	1	0	0	0	0	0	-	0	0	0
Euphalepsus ufv-107	0	0	0	0	0	0	0	0	0	0	0	0	0	0	-	0	1	0	1	1	0	0	2	0	-	?	0	1	0	0	0	1	1	0	0	1	0	-	1	0	0
Eurhexius ufv-11	0	1	1	0	0	0	0	1	0	0	0	0	0	1	?	1	0	1	1	2	0	2	0	-	1	0	0	-	0	0	1	0	0	0	1	0	-	0	0	0
Fustiger ufv-27	1	1	0	0	0	0	1	-	-	1	-	0	0	0	0	0	0	0	1	2	1	-	1	0	-	0	0	0	-	0	0	1	1	0	0	0	0	-	0	0	0
Fustiger ufv-41	1	1	0	0	0	0	1	-	-	1	-	0	0	0	0	0	0	0	1	0	-	-	1	0	-	0	0	0	-	0	0	1	1	0	0	0	0	-	0	0	0
†Gen-nov-1 CELC003040	0	0	0	0	0	0	0	1	0	0	1	?	?	0	?	?	0	1	2	1	-	1	0	-	0	0	?	?	0	?	1	0	0	0	1	0	-	0	0	0
Hamotus ufv-05	1	0	1	0	0	0	0	1	0	0	0	0	0	0	0	0	0	1	1	0	-	1	1	-	0	0	0	-	0	1	1	0	0	0	0	0	-	0	0	0
Listriophorus ufv-29	0	0	1	1	0	0	1	0	-	0	0	0	1	?	0	0	0	1	1	1	0	0	1	0	0	0	0	-	0	0	1	1	0	0	1	0	-	0	0	0
Mareeba storeyi	0	0	0	0	0	0	0	1	2	0	0	0	1	0	0	0	0	1	1	0	-	1	1	-	0	0	0	-	0	0	1	0	0	0	0	0	-	0	0	0
Mayetia atlantica	0	1	0	0	0	0	0	1	1	0	0	0	0	1	1	1	0	1	1	0	-	1	0	-	0	0	0	-	0	0	1	0	0	0	1	0	-	0	0	0
†*Megabythinus spinitibialis*	0	0	1	1	0	0	0	1	0	0	0	0	?	?	?	?	0	1	1	0	-	2	-	-	0	0	?	?	?	?	?	?	0	0	0	0	-	0	0	0
Megarafonus sp.	0	0	0	0	0	0	0	0	-	0	?	?	?	1	?	?	0	1	1	0	-	1	?	-	0	0	?	?	?	1	1	1	0	0	1	0	-	0	?	?
Metopiellus emavieirae	1	1	1	1	0	0	0	1	0	0	0	1	1	0	0	0	0	1	1	1	0	0	1	1	0	0	0	-	0	0	1	1	0	0	1	0	-	0	0	0
Peckiella ufv-60	0	0	0	0	0	0	0	0	1	0	0	0	0	0	1	0	0	0	1	1	2	0	1	1	-	0	0	0	-	0	0	1	0	0	0	1	0	-	0	0	0
Phalepsus ufv-103	1	0	0	0	0	0	0	0	1	0	0	0	0	0	0	0	0	0	0	1	1	1	0	1	1	-	0	0	0	-	0	0	1	0	0	0	0	0	-	0	0	0
Praeruptifrons arnhemensis	0	0	0	0	0	0	0	0	1	0	0	0	0	0	-	0	1	0	1	1	0	-	1	0	-	1	0	0	-	1	1	1	0	0	0	1	0	-	0	0	0
†*Priscaplectus carinatus*	0	0	0	0	0	0	0	0	1	0	0	0	0	?	0	1	?	0	1	1	2	0	2	-	-	1	1	?	?	-	?	1	1	0	1	-	0	0	0	1	0
†*Priscaplectus grandiceps*	0	0	0	0	0	0	0	0	1	0	0	0	0	?	0	1	?	0	1	1	2	0	2	-	-	1	1	?	?	-	?	1	0	0	1	-	0	0	0	?	0
†*Protoclaviger trichodens*	?	?	0	0	0	0	0	-	-	1	-	?	?	0	0	0	0	1	1	1	-	1	0	-	0	0	?	?	0	?	?	?	0	0	0	0	-	0	0	0
†*Protopselaphus thayerae*	-	-	0	0	0	0	0	1	0	0	0	0	?	?	0	?	0	1	0	-	-	2	-	-	0	0	0	-	1	0	0	-	0	0	0	0	-	0	1	0
Pyxidion ufv-07	0	0	1	0	0	1	0	1	1	0	0	0	1	1	0	0	0	1	0	-	-	0	1	0	1	0	0	-	0	0	1	0	1	0	0	0	-	0	0	0
Rhinoscepsis ufv-30	1	0	1	0	0	0	0	1	0	0	0	1	1	0	0	1	0	1	1	1	0	0	1	1	0	0	0	-	1	0	1	1	0	0	1	0	-	0	0	0
Sagola poortmani	0	0	0	0	0	0	0	0	-	0	0	0	0	0	0	0	0	0	1	1	0	-	2	-	-	0	0	?	?	0	1	1	1	0	0	1	0	-	0	0	1
Syrraphesina agostii	?	?	0	0	0	0	1	-	-	1	-	0	0	0	0	0	0	1	1	1	-	2	-	-	0	0	0	-	0	0	1	1	0	0	0	0	-	0	0	0
Tmesiphorus ufv-116	0	0	1	0	0	0	0	1	0	0	0	0	0	0	0	0	0	1	1	0	-	1	1	-	0	0	1	1	0	1	1	0	0	0	0	0	-	0	0	0
Tuberoplectus ufv-06	0	1	0	0	0	0	0	1	0	0	0	0	0	?	1	1	0	1	1	0	-	1	0	-	0	0	0	-	0	1	1	0	0	0	1	0	-	0	0	0

	0	0	0	0	0	0	0	0	0	0	0	0	0	0	0	0	0	0	0	1	1	1	1	1	1	1	1	1	1	1	1	1	1	1	1	1	1	1
	8	8	8	8	8	8	8	8	8	9	9	9	9	9	9	9	9	9	9	0	0	0	0	0	0	0	0	0	0	1	1	1	1	1	1	1	1	2
	1	2	3	4	5	6	7	8	9	0	1	2	3	4	5	6	7	8	9	0	1	2	3	4	5	6	7	8	9	0	1	2	3	4	5	6	7	8	9	0
Anotylus CELC000244	0	0	0	0	0	0	0	0	0	0	0	0	0	0	1	0	1	0	0	0	0	0	0	0	0	0	0	-	0	0	1	0	0	0	1	0	0	0	0	0
Arthmius ufv-16	1	1	0	1	0	0	0	0	1	0	0	0	0	1	1	0	0	0	0	0	0	0	0	0	0	1	1	1	0	0	1	0	0	0	?	0	0	0	0	0
Barrojuba ufv-03	1	1	0	0	0	0	0	0	1	0	0	0	0	1	0	0	0	0	0	0	0	0	-	0	0	0	?	?	?	0	0	0	0	0	0	0	0	0	0	0
†*Boreotethys caii*	1	0	0	0	0	0	0	0	0	0	0	0	0	1	?	0	0	0	0	0	0	0	-	0	?	?	1	?	?	0	1	0	0	0	?	0	0	0	0	?
†*Boreotethys* cf. *grimaldii*	1	0	0	?	0	0	0	0	0	0	0	0	0	1	0	0	0	0	0	0	0	0	-	0	0	?	1	?	?	0	1	1	0	0	?	1	0	0	0	?
†*Burmagluta rougemonti*	?	?	0	0	0	0	0	0	0	0	0	0	0	1	1	0	0	1	0	1	0	-	0	1	1	1	0	0	0	1	1	1	0	0	1	0	0	0	0	?
†*Burmalogasa* CELC002162	?	?	0	0	0	0	0	0	0	0	1	0	0	1	0	0	0	1	1	0	1	0	0	0	1	1	?	0	1	1	0	1	0	0	0	0	?	0	0	0
†*Burmalogasa perisi*	?	?	0	0	0	0	0	0	0	1	?	0	0	1	0	0	0	1	1	0	0	-	0	1	1	1	?	?	1	0	0	1	0	0	0	0	?	0	0	0
†*Cretobrachygluta laurasiensis*	1	0	0	0	0	0	0	0	0	0	0	0	0	0	1	0	0	0	0	0	0	0	-	0	1	1	1	0	1	0	1	0	0	0	0	1	0	0	0	0
†*Cretobythus yini*	1	?	0	1	0	0	-	1	0	0	0	0	0	1	0	0	0	0	1	0	1	0	1	0	1	1	0	?	0	1	0	1	1	1	1	0	0	0	0	?
†*Cretobythus excavatus*	?	?	0	?	0	0	-	1	0	0	0	0	0	1	0	0	0	0	1	0	1	0	1	0	?	1	?	?	0	1	0	1	1	1	1	0	0	0	0	0
†*Cretobythus parkeri*	?	?	0	?	0	0	0	0	1	0	0	0	0	1	0	0	0	0	1	0	1	0	1	0	1	1	0	?	0	1	1	1	0	0	1	0	0	0	0	0
Curculionellus ufv-57	1	0	1	0	0	0	0	0	1	1	0	0	0	1	0	0	0	0	0	0	0	0	-	0	0	1	1	0	0	0	1	0	0	1	1	0	0	0	0	0
Durbos ufv-117	1	0	0	0	0	0	0	0	1	1	0	0	0	1	0	1	0	0	1	0	0	-	0	0	0	1	1	0	0	1	0	1	0	0	0	0	0	1	0	0
Euphalepsus ufv-107	1	0	0	0	1	0	0	0	1	0	0	0	0	1	1	0	0	1	0	1	1	0	1	0	1	1	0	1	0	1	1	0	0	1	0	0	0	1	0	0
Eurhexius ufv-11	1	1	0	0	0	0	1	-	0	0	0	0	1	1	1	0	1	0	0	0	0	-	0	1	1	1	0	0	0	0	1	0	0	1	0	1	1	0	0	0
Fustiger ufv-27	1	0	0	0	0	0	0	0	0	0	0	0	0	0	2	0	0	0	0	0	0	0	-	0	0	0	0	-	0	0	1	0	0	1	1	0	0	0	0	0
Fustiger ufv-41	1	0	0	0	0	0	0	0	0	0	0	0	0	0	2	0	0	0	0	0	0	0	-	0	0	0	0	-	0	0	1	0	0	1	1	0	0	0	0	0
†Gen-nov-1 CELC003040	1	1	0	0	0	0	0	0	0	0	0	0	0	1	1	0	?	0	0	0	0	-	0	?	1	1	?	1	?	?	1	?	?	?	?	0	0	0	0	0
Hamotus ufv-05	1	1	1	0	0	0	0	0	1	0	1	0	0	1	0	0	0	0	0	0	0	-	0	1	1	1	1	0	0	1	0	1	0	1	0	0	0	1	0	0
Listriophorus ufv-29	1	0	0	1	0	0	1	-	1	0	0	0	0	2	0	0	1	0	0	1	0	-	0	0	0	0	-	0	0	1	1	0	1	1	0	0	0	1	0	0
Mareeba storeyi	1	0	0	0	0	0	0	0	1	1	0	1	0	1	0	0	0	1	0	0	0	-	0	0	1	1	0	0	0	1	0	0	1	1	0	0	0	0	1	0
Mayetia atlantica	1	1	0	0	0	0	0	0	0	0	0	0	0	1	1	0	1	0	0	0	0	-	0	0	0	1	1	0	0	1	0	0	0	1	0	0	0	0	1	0	0	0
†*Megabythinus spinitibialis*	?	?	0	0	0	0	0	0	0	0	0	0	0	1	0	0	0	0	0	0	0	-	0	?	?	?	?	?	?	1	0	1	0	?	?	0	0	0	0	0
Megarafonus sp.	?	?	0	0	0	0	0	0	0	0	0	0	0	1	0	0	0	1	0	0	0	-	0	?	1	1	?	?	1	1	0	1	0	0	0	0	0	0	0	0
Metopiellus emavieirae	1	0	0	0	0	0	0	0	0	0	0	0	0	1	0	0	0	0	0	0	0	-	0	1	1	1	1	0	0	1	1	1	0	0	0	0	0	0	0	0
Peckiella ufv-60	1	0	1	0	0	0	1	-	0	1	0	0	0	1	1	0	0	1	0	0	0	-	0	0	1	1	1	0	0	1	0	0	1	1	0	0	0	0	1	0
Phalepsus ufv-103	1	0	0	0	0	0	0	0	1	0	0	0	0	1	0	0	0	0	0	0	0	-	0	1	1	1	1	0	0	1	0	0	0	?	0	0	0	0	0	0
Praeruptifrons arnhemensis	1	0	0	1	1	0	1	-	1	0	0	0	0	1	0	0	0	0	0	0	0	-	0	0	0	1	1	0	0	1	0	1	0	1	0	1	0	0	0	0	1
†*Priscaplectus carinatus*	1	1	0	?	0	1	-	1	0	0	0	0	0	1	0	1	0	0	0	0	1	1	1	1	1	1	0	1	0	1	1	1	2	1	1	0	0	0	0	0
†*Priscaplectus grandiceps*	1	?	0	0	0	1	0	0	0	0	0	0	0	1	0	1	1	0	0	0	1	1	1	1	1	1	0	1	0	1	1	1	1	1	1	0	0	0	0	0
†*Protoclaviger trichodens*	?	?	0	0	0	0	0	0	0	0	0	0	0	1	?	0	0	0	0	0	0	-	0	?	?	1	?	?	0	1	?	?	1	1	0	0	?	0	0	?
†*Protopselaphus thayerae*	0	-	0	0	0	0	0	0	0	1	0	0	0	1	0	0	0	0	0	0	0	-	0	0	0	0	-	0	0	0	0	0	0	0	0	0	0	0	0	0	0
Pyxidion ufv-07	1	1	0	1	0	0	0	0	1	0	0	0	0	1	0	0	0	0	0	0	0	-	0	0	1	0	1	0	0	1	0	1	0	0	0	0	1	0	0	0
Rhinoscepsis ufv-30	1	0	0	0	0	0	1	-	0	0	0	0	0	1	1	0	1	0	0	0	0	-	0	1	1	1	1	1	0	1	1	0	0	0	1	0	1	0	0	0
Sagola poortmani	?	?	0	0	0	0	0	0	0	0	0	0	0	1	0	0	0	1	0	0	0	-	0	1	1	1	1	?	1	1	0	1	0	0	0	0	0	0	0	?
Syrraphesina agostii	1	0	0	0	0	0	0	0	1	0	0	0	0	2	0	0	0	0	0	0	0	-	0	0	0	0	-	0	0	1	0	0	0	1	0	0	0	0	0	0
Tmesiphorus ufv-116	1	0	0	0	0	0	0	0	1	0	1	1	0	1	0	0	0	0	0	0	0	-	0	1	1	1	1	0	0	1	0	0	0	1	0	0	0	0	1	0
Tuberoplectus ufv-06	1	1	0	0	0	0	0	0	1	0	0	0	0	1	0	0	0	0	1	0	0	-	0	0	1	1	1	?	0	1	1	1	0	0	0	0	0	0	0	1

	1	1	1	1	1	1	1	1	1	1	1	1	1	1	1	1	1	1	1	1	1	1	1	1	1	1	1	1	1	1	1	1
	2	2	2	2	2	2	2	2	2	3	3	3	3	3	3	3	3	3	3	4	4	4	4	4	4	4	4	4	4	5	5	5	5	5
	1	2	3	4	5	6	7	8	9	0	1	2	3	4	5	6	7	8	9	0	1	2	3	4	5	6	7	8	9	0	1	2	3	4
Anotylus CELC000244	0	0	0	0	1	0	0	1	0	0	0	0	0	0	1	0	0	1	0	0	1	0	0	0	0	0	0	0	0	0	0	-	0	1
Arthmius ufv-16	0	0	1	0	1	0	0	0	0	1	1	0	0	0	1	1	1	0	1	0	0	0	2	0	0	0	0	1	1	1	1	0	0	0
Barrojuba ufv-03	0	0	0	0	1	0	1	0	0	0	0	0	0	0	1	1	1	0	1	0	0	0	0	0	0	0	0	0	0	0	0	-	0	0
†*Boreotethys caii*	0	0	?	0	?	0	0	0	0	0	1	0	0	0	1	1	1	0	3	0	0	0	0	0	0	0	0	0	0	0	0	-	0	0
†*Boreotethys* cf. *grimaldii*	0	0	0	0	?	0	0	0	0	0	1	0	0	0	1	1	0	0	4	0	0	0	0	0	0	0	0	0	0	0	0	-	0	0
†*Burmagluta rougemonti*	?	0	0	0	?	0	0	0	0	0	0	0	0	0	1	1	0	0	1	0	0	0	0	?	0	0	0	0	0	0	0	-	0	0
†*Burmalogasa* CELC002162	0	1	0	0	?	0	0	1	0	0	0	0	0	0	1	0	0	1	0	1	1	0	3	0	0	0	0	0	0	0	0	-	0	0
†*Burmalogasa perisi*	0	1	?	0	?	0	0	0	0	0	?	0	0	0	1	0	0	1	0	1	0	0	3	0	0	0	0	0	0	0	0	-	0	0
†*Cretobrachygluta laurasiensis*	0	1	0	0	?	0	0	0	0	0	0	0	0	0	1	1	0	0	3	0	0	0	1	1	0	0	0	0	0	0	0	-	0	0
†*Cretobythus yini*	0	?	?	0	0	0	0	0	0	1	1	0	0	0	1	1	1	0	1	0	0	0	0	0	0	0	0	0	0	0	0	-	0	0
†*Cretobythus excavatus*	0	0	?	0	?	0	0	0	0	1	1	0	0	0	1	1	1	0	2	0	0	0	0	0	0	0	0	0	0	1	0	0	0	0
†*Cretobythus parkeri*	0	0	0	0	0	0	0	0	0	0	0	0	0	0	1	1	1	0	2	0	0	0	0	0	0	0	0	0	0	0	0	-	0	0
Curculionellus ufv-57	1	1	0	0	0	1	0	1	1	1	1	1	0	0	1	1	0	0	3	0	0	0	2	0	1	0	0	0	0	0	1	0	1	0
Durbos ufv-117	0	0	1	0	0	0	0	0	1	1	1	0	0	0	1	1	1	1	0	0	0	0	2	1	1	0	0	1	0	0	1	0	0	0
Euphalepsus ufv-107	0	1	0	0	0	0	0	0	0	1	1	0	0	0	1	1	1	0	0	0	0	0	1	0	0	0	0	1	0	1	1	0	0	0
Eurhexius ufv-11	0	0	0	0	0	0	0	0	0	0	?	0	0	0	1	1	1	0	2	0	0	0	1	0	0	0	0	0	0	0	1	0	0	0
Fustiger ufv-27	0	1	0	0	0	1	0	1	1	1	1	1	0	1	1	-	-	-	3	0	0	1	3	0	0	0	1	0	0	0	1	1	0	0
Fustiger ufv-41	0	1	0	0	0	1	0	1	1	1	1	1	0	1	1	-	-	-	3	0	0	1	0	0	0	0	1	0	0	0	1	1	0	0
†Gen-nov-1 CELC003040	0	1	?	0	?	0	0	0	0	?	0	0	0	1	1	0	0	3	0	0	0	0	0	0	0	0	0	0	0	0	0	-	0	0
Hamotus ufv-05	0	0	1	0	0	0	0	1	1	1	0	0	0	0	1	1	1	1	0	1	0	0	1	0	0	0	0	0	0	0	1	0	0	0
Listriophorus ufv-29	0	1	1	1	0	0	0	1	0	1	0	0	0	1	1	1	1	0	3	0	0	0	0	0	0	0	0	0	0	0	1	0	0	0
Mareeba storeyi	1	1	0	0	1	1	0	1	1	1	1	1	1	0	1	1	1	1	0	3	0	0	1	2	0	1	0	0	0	0	0	1	0	1	0
Mayetia atlantica	0	1	0	0	0	0	0	0	0	0	0	0	0	0	1	-	0	0	3	0	1	0	0	0	0	0	0	0	1	0	0	0	-	0	1
†*Megabythinus spinitibialis*	0	0	?	0	?	0	0	0	0	0	?	0	1	0	1	1	0	0	1	0	0	0	0	?	0	0	0	0	0	0	0	-	0	0
Megarafonus sp.	0	0	0	0	0	1	0	0	0	0	0	0	0	0	?	1	0	0	?	0	?	?	0	3	0	0	0	0	1	0	0	0	-	0	0
Metopiellus emavieirae	0	0	1	0	0	0	1	1	0	0	0	0	0	0	1	1	1	0	2	0	0	0	0	0	0	0	0	0	0	0	0	-	0	0
Peckiella ufv-60	1	1	0	0	0	0	0	1	1	1	1	1	0	0	1	1	1	0	3	0	0	0	2	0	1	0	0	0	0	0	1	0	1	0
Phalepsus ufv-103	0	0	1	0	0	0	0	0	1	1	0	0	0	0	1	1	1	0	0	0	0	0	0	0	0	0	0	0	1	0	0	1	0	0	0
Praeruptifrons arnhemensis	0	0	1	0	0	0	0	0	0	0	1	0	0	0	1	1	1	0	3	0	0	0	1	1	0	0	0	0	0	0	1	0	0	1
†*Priscaplectus carinatus*	0	0	0	0	?	0	0	0	0	0	0	0	0	0	1	1	0	0	4	0	0	0	0	0	0	0	0	0	0	0	1	0	0	0
†*Priscaplectus grandiceps*	0	0	0	0	?	0	0	0	0	0	0	0	0	0	1	1	0	0	4	0	0	0	0	0	0	0	0	0	0	0	1	-	0	0
†*Protoclaviger trichodens*	0	1	?	?	0	1	0	?	1	1	?	1	0	?	1	-	-	-	3	?	0	1	0	0	0	0	0	0	0	0	?	?	0	0
†*Protopselaphus thayerae*	0	0	0	0	0	0	0	0	0	0	0	0	0	0	1	1	0	1	0	1	0	0	3	0	0	0	0	0	0	0	0	-	0	0
Pyxidion ufv-07	0	1	0	0	0	0	0	0	0	0	0	0	0	0	1	-	-	-	3	0	0	0	3	0	1	1	0	1	0	0	1	0	0	0
Rhinoscepsis ufv-30	0	0	0	0	1	0	1	0	0	0	0	0	0	0	1	1	1	0	2	0	0	0	0	0	0	0	0	0	0	0	0	-	0	1
Sagola poortmani	0	0	0	?	0	0	0	0	0	0	0	0	0	0	1	0	0	1	0	1	0	0	3	0	0	0	0	?	0	0	?	?	0	0
Syrraphesina agostii	0	1	0	0	0	1	0	1	1	1	1	1	0	?	1	-	-	-	3	0	0	1	2	0	0	0	1	1	0	0	?	?	0	0
Tmesiphorus ufv-116	1	0	0	0	0	0	0	1	1	1	1	0	0	0	1	1	0	0	1	0	0	0	0	0	0	0	0	0	0	0	1	0	0	0
Tuberoplectus ufv-06	0	1	0	0	0	0	0	0	0	0	0	0	0	0	1	-	-	-	3	0	0	0	0	0	0	0	0	1	0	0	?	1	0	0

Appendix 2

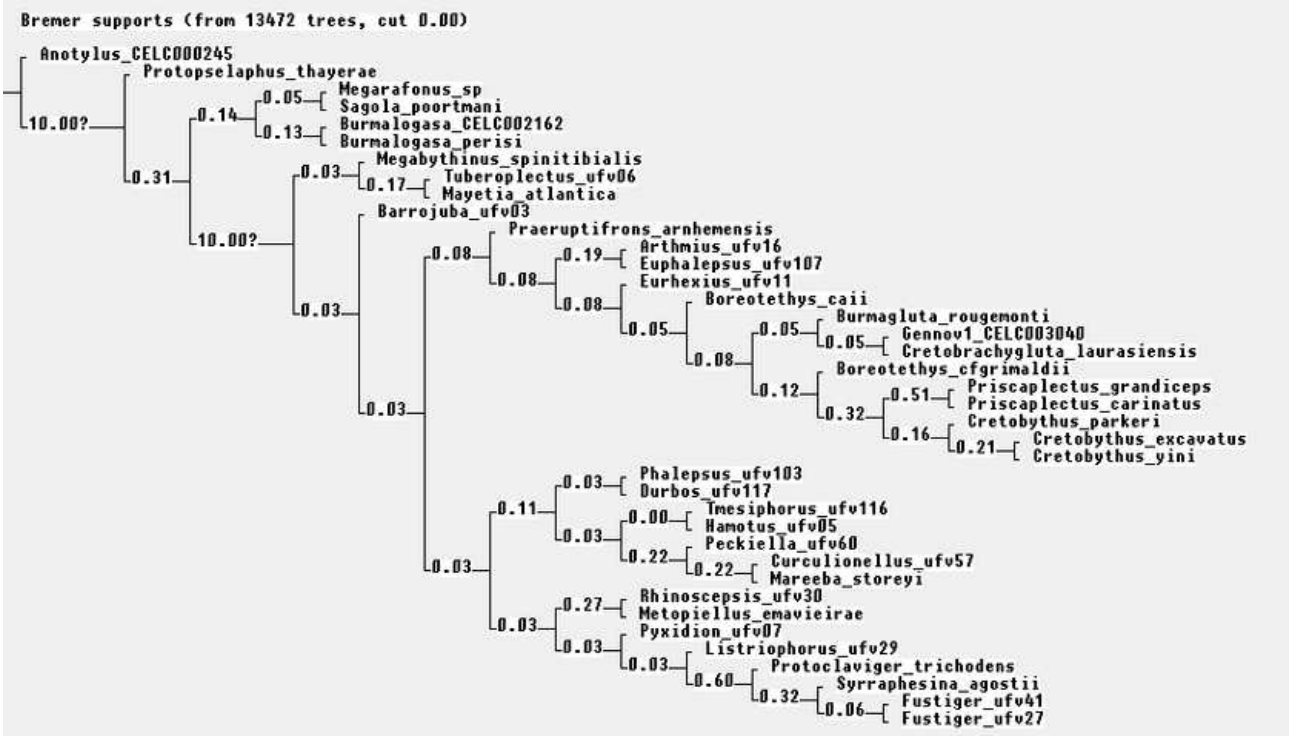

Bremmer support for the tree presented in Figure 1Bootstrap values for the tree presented in

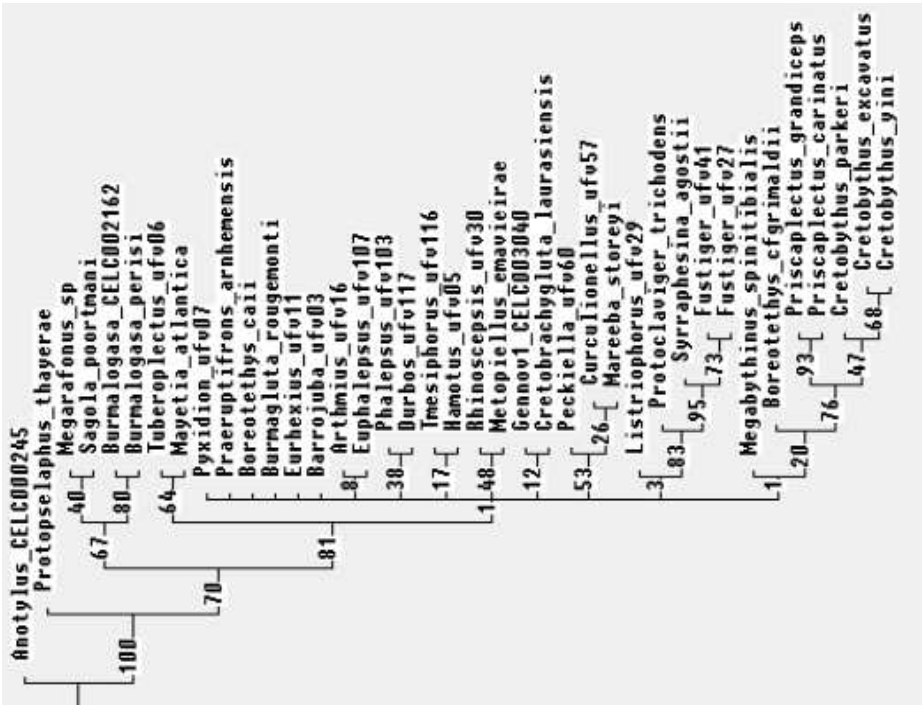

Figure 1. GC values, 1000 replicates, cut=1 (tree 0) - Symmetric Reampling (P=33)

VI. CONCLUSÕES GERAIS

Em decorrência do estudo das espécies viventes para a comparação com os fósseis, se estabeleceu na Coleção Entomológica do Laboratório de Sistemática de Coleoptera (CELC), uma coleção representativa para a subfamília, com no mínimo 200 espécies, muitas das quais ainda não identificadas no nível específico. A maioria dos espécimes da CELC provém de fragmentos florestais ou unidades de conservação da Mata Atlântica de Minas Gerais, Espírito Santo e Santa Catarina, mas também há um bom número de espécies amazônicas (região de Manaus, AM, e Belém, PA), espécimes do Pantanal (MT) e dos pampas (RS), além de que há inúmeros exemplares australianos, do norte e leste do país (NT e QLD).

Esta tese somou ao conhecimento dos pselafíneos fósseis do período Cretáceo e, através da comparação destes com as espécies viventes, propôs uma nova hipótese filogenética que contempla uma maior parte da diversidade conhecida desta fauna do que as hipóteses filogenéticas anteriores. A diversidade dos Pselaphinae cretácicos ainda é subestimada e certamente irá aumentar nos próximos anos, dada a grande quantidade de estudos com âmbar de Kachin. Espera-se que esta tese, principalmente o seu último capítulo, contribua para que as relações entre os fósseis e as espécies viventes sejam reveladas.

Os avanços ópticos dos últimos anos apontam para um futuro promissor, antes imaginado como impossível, para se desvendar as relações de parentesco entre os artrópodes viventes e extintos. As técnicas ópticas e outras tecnologias (como as microtomografias) nos permitem alcançar grande detalhamento na descrição destes organismos extintos, de modo que apenas limitações impostas pela incompletude do registro fóssil parecem ser incontornáveis.